

**The Effects of Novel
Xenooestrogens on the BK Channel**

Jacqueline Maher

**A thesis submitted in partial
fulfilment of the requirements
of the
University of Brighton
for the degree of
Doctor of Philosophy**

2014

ABSTRACT:

Novel steroidal oestrogens, that incorporate some of the structural motifs of non-steroidal antioestrogens, were synthesised and tested for their actions on the BK channel. These novel compounds were first checked for purity and structure using, where appropriate, ^1H NMR, ^{13}C NMR, IR spectroscopy, mass spectroscopy, thin layer chromatography, melting point analysis, elemental analysis and X-ray crystallography. Using Oestrone as the starting compound, the following five novel compounds were synthesised; DME-Oestrone, Quat-DME-Oestrone, DME-Oestradiol, Quat-DME-Oestradiol and Oestrone-Oxime. Two of the derivatives, Quat-DME-Oestrone and Quat-DME-Oestradiol, incorporated a quaternary ammonium side-chain making them membrane impermeable.

These compounds were tested in a range of assays for their ability to modulate BK activity. These BK assays were; aortic ring relaxation assays; whole cell patch-clamp recordings, using HEK 293 cells over-expressing BK channels; and planar lipid bilayer experiments.

Apart from Quat-DME-Oestrone, all compounds demonstrated relaxant activity in pre-contracted aortic rings. However, only relaxations by Quat-DME-Oestradiol were consistently iberiotoxin sensitive. These data suggest that oestrogen can relax aortic rings using a range of mechanisms in addition to BK activation.

The compounds DME-Oestrone, Quat-DME-Oestrone, Quat-DME-Oestradiol, Oestrone and Oestrone-Oxime were selected for further investigation on BK channels expressed in HEK 293 cells. None of these compounds could activate BK currents in cells expressing BK α subunits; however, Oestrone-Oxime, Oestrone, and Quat-DME-Oestradiol were able to activate BK currents in cells expressing both α and β_1 subunits.

These observations in whole cell patch-clamp experiments were fundamentally confirmed in single channel recordings made in planar lipid bilayers using DME-Oestrone, Quat-DME-Oestrone, Oestrone and Oestrone-Oxime.

These data are consistent with an extracellular site of action and a requirement for an associated β_1 subunit for BK activation by oestrogens. In addition, the data point to the importance of the 17β -hydroxyl group in BK activation by steroidal oestrogens.

CONTENTS:

ABSTRACT	2
CONTENTS	3
LIST of TABLES	11
LIST of FIGURES	13
ABBREVIATIONS	23
PREFACE	28
ACKNOWLEDGEMENTS	29
DECLARATION	30
CHAPTER 1	
GENERAL INTRODUCTION	31
1.1 INTRODUCTION	32
1.1.1 The BK channel.....	32
1.1.2 The BK channel and vascular tone.....	35
1.1.3 The BK channel and hypertension.....	37
1.1.4 Cardiovascular disease and hypertension - epidemiology.....	38
1.1.5 Oestrogens - genomic or non-genomic pathway.....	41
1.1.5.1 Genomic effects of oestrogen.....	41
1.1.5.2 Non-genomic effects of oestrogen.....	42
1.1.5.3 Non-genomic indirect and direct activation of BK channels.....	
by oestrogens	43
1.1.6 The BK channel as a therapeutic target for oestrogens.....	46
1.2 HYPOTHESES	49
1.3 AIMS	49
CHAPTER 2	
SYNTHESIS OF XENOOESTROGENS	51
2.1 INTRODUCTION	52
2.1.1 BK channel as therapeutic target.....	52
2.1.2 BK modulators.....	53
2.1.3 Sex-steroids as endogenous BK modulators and their.....	
structural analogues.....	58
2.1.4 Synthesis of vasodilators from known BK activators.....	61

2.1.4.1 Chemical starting points.....	61
2.1.5 AIMS.....	64
2.2 METHODS.....	65
2.2.1 Chemicals, reagents and analytical apparatus.....	65
2.2.2 Synthesis of DME-Oestrone.....	65
2.2.3 Synthesis of Quat-DME-Oestrone.....	69
2.2.4 Synthesis of DME-Oestradiol.....	71
2.2.5 Synthesis of Quat-DME-Oestradiol.....	72
2.2.6 Synthesis of Oestrone-Oxime (17-hydroximino-estra-3-ol).....	73
2.3 RESULTS.....	74
2.3.1 ¹³ C NMR of starting compound, Oestrone, and novel derivatives.....	74
2.3.2 Analysis and identification of compounds.....	74
2.3.2.1 Analytical assessment DME-Oestrone.....	76
2.3.2.2 Analytical assessment Quat-DME-Oestrone.....	76
2.3.2.3 Analytical assessment DME-Oestradiol.....	77
2.3.2.4 Analytical assessment Quat-DME-Oestradiol.....	77
2.3.2.5 Analytical assessment Oestrone-Oxime.....	77
2.4 PROOF of COMPOUNDS.....	79
2.4.1 Structural determination of DME-Oestrone.....	79
2.4.1.1 Crystallographic structure determination of DME-Oestrone.....	79
2.4.2 Structural determination of Quat-DME-Oestrone.....	82
2.4.3 Structural determination of DME-Oestradiol.....	82
2.4.4 Structural determination of Quat-DME-Oestradiol.....	83
2.4.5 Structural determination of Oestrone-Oxime.....	83
2.4.6 Summary - Proof of compounds.....	84
2.5 DISCUSSION.....	86
CHAPTER 3	
EX VIVO VASCULAR STUDIES.....	89
3.1 INTRODUCTION.....	90
3.1.1 Vascular smooth muscle: physiology and mechanics.....	90
3.1.2 Signalling of contraction in smooth muscle.....	92
3.1.2.1 Gap junctions.....	92
3.1.2.2 The role of Ca ²⁺ in smooth muscle contraction.....	93

3.1.2.3 The role of Ca ²⁺ in smooth muscle relaxation.....	95
3.1.2.4 Vascular tone and the role of the endothelium.....	97
3.1.2.5 BK _{Ca} channels in vascular smooth muscle and.....	
endothelium cells.....	100
3.1.2.6 Vasodilatory effects of 17β-oestradiol and other oestrogens.....	102
3.1.5 AIMS.....	104
3.2 METHODS.....	105
3.2.1 Preparation of isolated rat thoracic aorta rings.....	105
3.2.2 Statistical analysis.....	106
3.3 RESULTS.....	108
3.3.1 The effect of novel steroidal oestrogens on isolated rat thoracic.....	
aorta rings.....	108
3.3.2 Comparison of vascular responses to increasing concentrations	
of Oestrone on pre-contracted rat aortic rings.....	110
3.3.3 Comparison of vascular responses to increasing concentrations.....	
of DME-Oestrone on pre-contracted rat aortic rings.....	111
3.3.4 Comparison of vascular responses to increasing concentrations of...	
Quat-DME-Oestrone on pre-contracted rat aortic ring.....	112
3.3.5 Comparison of vascular responses to increasing concentrations.....	
of Oestrone-Oxime on pre-contracted rat aortic rings.....	113
3.3.6 Comparison of vascular responses to increasing concentrations.....	
of DME-Oestradiol on pre-contracted rat aortic rings.....	115
3.3.7 Comparison of vascular responses to increasing concentrations of...	
Quat-DME-Oestradiol on pre-contracted rat aortic rings.....	116
3.3.8 Toxin reversal of oestrogen-induced relaxation of aortic rings.....	118
3.3.9 Summary of results.....	119
3.4 DISCUSSION.....	122
3.4.1 Structure-activity relationships for novel oestrogens.....	125
3.5 SUMMARY.....	130
CHAPTER 4	
EFFECTS of OESTROGENS on BK CURRENTS in HEK 293 CELLS.....	132
4.1 INTRODUCTION.....	133
4.1.1 Expression systems.....	133

4.1.1.1 HEK 293 cells as an expression system for BK channels.....	135
4.1.2 The patch clamp technique.....	140
4.1.3 Topography and structure of BK channel (hS/o).....	143
4.1.3.1 BK alpha subunit (S/o1).....	146
4.1.3.2 BK α transmembrane segment.....	148
4.1.3.3 BK α intracellular C-terminus segment: RCK domains, Ca ²⁺ sensors and Ca ²⁺ activation.....	151
4.1.3.4 BK Auxiliary β subunits.....	152
4.1.3.5 Effects of ancillary β subunits on the BK α channel.....	156
4.1.3.6 Stoichiometry of BK α and β subunits.....	158
4.1.3.7 BK β_1 subunit function and physiology.....	159
4.1.4 AIMS.....	163
4.2 METHODS.....	165
4.2.1 Molecular biology of HEK 293 expressing the α alone and..... α plus β_1 subunit of the BK channel.....	165
4.2.2 Culture of HEK 293 cells solely expressing the α subunit of the..... BK channel.....	166
4.2.3 Culture of HEK 293 cells expressing the α plus β_1 subunits of the..... BK channel.....	166
4.2.4 Whole cell patch clamp experimental methods.....	167
4.2.5 Data Analyses of whole cell patch clamp recordings.....	169
4.2.5.1 Statistical analysis of run-up and run-down	169
4.2.5.2 Analysis of activation rates.....	170
4.2.5.3 Statistical analysis of G-V relationships.....	170
4.2.5.4 Statistical analysis of the effects of oestrogens on..... evoked current.....	171
4.2.5.5 Non-stationary noise analysis (fluctuation analysis).....	171
4.3 RESULTS.....	173
4.3.1 Characterisation of the evoked BK currents of HEK 293 cells..... expressing the α subunit alone.....	173
4.3.2 Effects of Oestrone on HEK 293 cells expressing BK α subunits.....	179
4.3.3 Effects of DME-Oestrone on HEK 293 cells expressing..... BK α subunits.....	180

4.3.4 Effects of Quaternary-DME-Oestrone on HEK 293 cells expressing... BK α subunits.....	182
4.3.5 Effects of Oestrone-Oxime on HEK 293 cells expressing..... BK α subunits.....	184
4.3.6 Effects of Quaternary-DME-Oestradiol on HEK 293 cells..... expressing BK α subunits.....	186
4.3.7 Comparison of the effects of oestrogens on BK α peak currents..... with control data.....	188
4.3.8 Characterisation of the evoked BK currents from HEK 293..... cells expressing α plus β_1 subunits.....	190
4.3.9 Effects of Oestrone on HEK 293 cells expressing..... BK α plus β_1 subunits.....	194
4.3.10 Effects of DME-Oestrone on HEK 293 cells expressing..... BK α plus β_1 subunits.....	195
4.3.11 Effects of Quaternary-DME-Oestrone on HEK 293 cells expressing BK α plus β_1 subunits.....	197
4.3.12 Effects of Oestrone-Oxime on HEK 293 cells expressing..... BK α plus β_1 subunits.....	199
4.3.13 Effects of Quaternary-DME-Oestradiol on HEK 293 cells..... expressing BK α plus β_1 subunits.....	202
4.3.14 Comparison of the effects of oestrogens on BK α plus β_1 peak..... currents with control data.....	204
4.3.15 Summary of results.....	206
4.4 DISCUSSION.....	208
4.4.1 Comparison of α control data with $\alpha+\beta_1$ control data.....	209
4.4.1.1 Run-up/run-down.....	209
4.4.1.2 Ca ²⁺ sensitivity.....	214
4.4.1.3 Activation rates and toxin blockade.....	216
4.4.2 Effects of Oestrone and novel compounds (5 μ M) on HEK 293..... cells expressing BK α subunits and BK α plus β_1 subunits.....	217
4.5 SUMMARY.....	225

CHAPTER 5

SINGLE CHANNEL RECORDINGS in LIPID BILAYERS	227
5.1 INTRODUCTION	228
5.1.2 Cell membranes and the lipid bilayer.....	228
5.1.3 Reconstitution of a planar lipid bilayer.....	232
5.1.4 Planar lipid bilayers (BLMs) and ion channel reconstitution.....	235
5.1.5 Advantages/disadvantages of the BLM as a model..... for biomembranes.....	238
5.1.6 AIMS	240
5.2 METHODS	242
5.2.1 Production of HEK 293 cells for lipid bilayer experiments.....	242
5.2.2 Planar lipid bilayer experimental methods.....	244
5.2.2.1 Choice of lipids.....	245
5.2.2.2 Preparation of lipid bilayer and bilayer set-up.....	246
5.2.2.3 BK channel insertion into planar lipid bilayers.....	248
5.2.2.4 Channel orientation in the bilayer.....	249
5.2.2.5 Preparation and use of stock solutions.....	250
5.2.3 Data analysis of single channel BK current kinetics recorded in..... planar lipid bilayers.....	250
5.2.3.1 Measuring open probability (NP_o).....	251
5.2.3.2 Measuring single-channel current amplitudes.....	253
5.2.3.3 Measuring dwell time observations.....	253
5.2.4 Statistical analysis of the effects of oestrogens on BK..... channel activity.....	254
5.2.4.1 BK channel open probability (NP_o) during 450s recordings.....	254
5.2.4.2 BK single channel current amplitude analysis.....	254
5.3 RESULTS	255
5.3.1 Characteristics of bilayer recording of BK α and BK α + β_1 channels....	255
5.3.2 Effects of Oestrone and novel derivatives on BK channels recorded in planar lipid bilayers.....	258
5.3.2.1 Effects of Oestrone (5 μ M) on the BK α channels in..... lipid bilayers.....	259
5.3.2.2 Effects of Oestrone (5 μ M) on BK channels comprising..... α plus β_1 subunits in planar lipid bilayers.....	262

5.3.2.3 Effects of high concentrations of Oestrone (50 μ M) on BK α channels in lipid bilayers.....	267
5.3.2.4 Effects of high concentrations of Oestrone (50 μ M) on BK channels comprising both α plus β_1 subunits in lipid bilayers.....	270
5.3.3 Effects of DME-Oestrone on BK channels recorded in lipid bilayers.....	273
5.3.3.1 Effects of DME-Oestrone (5 μ M) on BK α channels in lipid bilayers.....	274
5.3.3.2 Effects of DME-Oestrone (5 μ M) on the NP _o of BK α plus β_1 channels in lipid bilayers.....	277
5.3.3.3 Effects of high concentrations of DME-Oestrone (50 μ M) on BK α channels in lipid bilayers.....	280
5.3.4 Effects of Quaternary-DME-Oestrone on BK channels recorded in lipid bilayers.....	284
5.3.4.1 Effects of Quaternary-DME-Oestrone (5 μ M) on BK α channels in lipid bilayers.....	285
5.3.4.2 Effects of Quaternary-DME-Oestrone (5 μ M) on BK channels comprising α plus β_1 subunits in lipid bilayers.....	288
5.3.4.3 Effects of high concentrations of Quaternary-DME-Oestrone (50 μ M) on the NP _o of BK α channels in lipid bilayers.....	291
5.3.5 Effects of Oestrone-Oxime on BK channels recorded in lipid bilayers.....	295
5.3.5.1 Effects of Oestrone-Oxime (5 μ M) on BK α channels in lipid bilayers.....	296
5.3.5.2 Effects of Oestrone-Oxime (5 μ M) on BK channels comprising α plus β_1 subunits in lipid bilayers.....	299
5.3.6 Results summary.....	303
5.4 DISCUSSION.....	306
5.4.1 Effects of Oestrone and novel derivative xenoestrogens on NP _o of BK channels recorded in lipid bilayers.....	307
5.4.2 Effects of Oestrone and novel derivative xenoestrogens on single channel current of BK channels recorded in lipid bilayers.....	309
5.4.3 The planar bilayer as a system for investigating direct activation of BK channels.....	310

5.5 SUMMARY.....	313
 CHAPTER 6	
GENERAL DISCUSSION.....	314
6.1 GENERAL DISCUSSION.....	315
6.1.1 Synthesis of novel xenoestrogens from known BK activators.....	315
6.1.2 <i>Ex vivo</i> vascular studies.....	317
6.1.3 Whole cell patch-clamp studies.....	319
6.1.4 Planar lipid bilayer studies.....	322
6.2 SUMMARY.....	325
6.3 FURTHER WORK.....	326
6.4 CONCLUSIONS.....	332
 REFERENCES and BIBLIOGRAPHY.....	
	334
 APPENDICES.....	
	405
APPENDIX 1 (Published Papers).....	406
APPENDIX 2 (Published Abstracts).....	420
APPENDIX 3 (Poster presentations).....	424

LIST OF TABLES:

Table 1.1.5.3.1 Phosphorylation sites on BK subunits and consequences of phosphorylation on BK channel.....	46
Table 2.3.1.1 ¹³ C NMR of starting compounds.....	75
Table 2.4.6.1 Summary table depicting proof of structure and purity.....	85
Table 2.5.1 Comparison of advantages/disadvantages of..... oestradiol-bovine serum albumin (BSA) conjugates vs quaternary tagging.....	87
Table 3.1.2.4.1 Mediators of vascular tone regulation in the endothelium.....	97
Table 3.3.9.1 Comparison of concentration thresholds of oestrogen..... and derivatives on rat aortic rings.....	120-1
Table 3.4.1 Some potential mechanisms for oestrogen-induced relaxation of vascular smooth muscle.....	124
Table 4.1.1.1.1 Examples of proteins, receptors and ion channels detected in native untransfected HEK 293 cells.....	138
Table 4.1.2.1 Summary of advantages and disadvantages of..... patch-clamp configurations.....	142
Table 4.1.3.1 The <i>Slo</i> family of channels.....	144
Table 4.1.3.4.1 BK regulatory β subunits, their tissue expression and effect on BK α channels.....	154
Table 4.3.1.1 Summary of shifts in the $V_{0.5}$ for the voltage-conductance..... curve of BK α channels due to increasing free intracellular..... concentrations of Ca ²⁺	177

Table 4.3.7.1 Comparison of control (run-up) with normalised peak..... current in the presence of oestrogens in HEK 293 cells expressing..... BK α channels.....	188
Table 4.3.8.1 Summary of shifts in the $V_{0.5}$ for the voltage-conductance..... curve of BK α + β_1 channels due to increasing free intracellular..... concentrations of Ca ²⁺	193
Table 4.3.14.1 Comparison of control (run-down) with normalised peak..... current in the presence of oestrogens in HEK 293 cells expressing..... BK α + β_1 channels.....	204
Table 4.4.1.1.1 Potential diffusible factors that may be responsible for..... run-up/down.....	211
Table 4.4.2.1 Summary of effects of oestrogen and novel derivatives on.... BK whole cell currents in HEK 293 cell over-expressing BK channels.....	219
Table 5.1.5.1 Advantages and disadvantages of artificial bilayer systems... as a model for ion channel investigation and characterisation.....	239
Table 5.3.6.1 Effects of oestrogens and novel derivatives on BK..... channels reconstituted in lipid bilayers.....	305
Table 6.2.1 Summary of main findings of compounds on smooth..... muscle relaxation and BK channel currents.....	325

LIST OF FIGURES:

Figure 1.1.1.1 Schematic depicting the 7-transmembrane domains of a..... BK α subunit, the 2-transmembrane domains of an associating β_1 subunit.... and the tetrameric formation of a native BK channel.....	34
Figure 1.1.2.1 Schematic diagram of cross section of arteriolar smooth..... muscle cell showing regulation of smooth muscle tone <i>via</i> BK channel..... activity in response to changes in membrane potential and intracellular..... Ca ²⁺ concentrations.....	36
Figure 1.1.3.1 Histogram showing difference in degree of contraction..... between KCl-treated thoracic aortic rings taken from wild type mice..... (BK $\beta_1^{+/+}$) and gene-targeted (BK $\beta_1^{-/-}$) mice either in the presence or absence of iberiotoxin.....	37
Figure 1.1.4.1 Prevalence of high blood pressure in England (1998 - 2008) by age and gender.....	39
Figure 1.1.4.2 Flow chart showing post-menopausal hypertension risk..... factor algorithm.....	40
Figure 1.1.5.3.1 Cartoon of indirect cyclic nucleotide-dependent relaxatory and contractile stimulation of BK channels in a smooth muscle cell.....	44
Figure 1.1.6.1 Histograms showing inside-out patch recordings of..... mouse colonic smooth muscle cell BK channels (wild type and $\beta_1^{-/-}$) in..... the presence and absence of 17 β -oestradiol or tamoxifen.....	47
Figure 2.1.2.1 Chemical structures of BK modulators withdrawn from..... clinical trials (NS-8 and BMS204352).....	53
Figure 2.1.2.2 Chemical structure of a BK modulator of bronchial..... smooth muscle, Andolast™.....	54

Figure 2.1.2.3 Chemical structures of synthetic openers of the BK channel (NS-004; NS-1619; NS-1608).....	55
Figure 2.1.2.4 Chemical structures of naturally-derived openers of the BK channel (maxikdiol; primaric acid; dihydrosoyasaponin-1).....	56
Figure 2.1.2.5 Chemical structures of flavonoids and isoflavonoids with purported BK-activating properties.....	57
Figure 2.1.2.6 Chemical structure of lithocholate, a purported BK β_1 subunit-dependent vasorelaxant in smooth muscle.....	58
Figure 2.1.3.1 Chemical structures of steroidal BK modulators and non-steroidal structural derivatives.....	60
Figure 2.1.4.1.1 Structures of chemical starting points involved in the synthesis of novel xenoestrogens as possible BK activators.....	62
Figure 2.1.4.1.2 Chemical mechanisms for the synthesis of five oestrogen derivatives from the parent compound oestrone.....	63
Figure 2.2.2.1 The synthesis of DME-Oestrone from Oestrone.....	68
Figure 2.2.3.1 Compound synthesis and characterisation of Quat-DME-Oestrone.....	70
Figure 2.2.4.1 Compound synthesis and characterisation of DME-Oestradiol.....	71
Figure 2.2.5.1 Compound synthesis and characterisation of Quat-DME-Oestradiol.....	72
Figure 2.2.6.1 Compound synthesis and characterisation of Oestrone-Oxime	73
Figure 2.4.1.1.1 X-ray crystal structure of DME-Oestrone.....	81

Figure 3.1.1.1 Schematic of blood vessel structure shown in cross-section	91
Figure 3.1.2.2.1 Regulatory pathways leading to smooth muscle contraction	95
Figure 3.1.2.3.1 Regulatory pathways leading to smooth muscle relaxation	96
Figures 3.1.2.4.1 and 3.1.2.4.2 Schematics of known effectors..... and endothelium-derived relaxation/contracting factors in vascular..... smooth muscle.....	98/100
Figure 3.2.1.1 Measurement of relaxation / contraction of rat aortic..... rings mounted in an organ bath.....	105
Figure 3.3.1.1 Representative traces showing effects of DMSO and..... compound (Oestrone-Oxime) on relaxation of PE-contracted rat aorta.....	109
Figure 3.3.2.1 Comparison of vascular responses of rat aorta to..... increasing concentrations of Oestrone.....	110
Figure 3.3.3.1 Comparison of vascular responses of rat aorta to..... increasing concentrations of DME-Oestrone.....	111
Figure 3.3.4.1 Comparison of vascular responses of rat aorta to..... increasing concentrations of Quat-DME-Oestrone.....	112
Figure 3.3.5.1 Comparison of vascular responses of rat aorta to..... increasing concentrations of Oestrone-Oxime.....	114
Figure 3.3.6.1 Comparison of vascular responses of rat aorta to..... increasing concentrations of DME-Oestradiol.....	115
Figure 3.3.7.1 Comparison of vascular responses of rat aorta to..... increasing concentrations of Quat-DME-Oestradiol.....	117

Figure 3.3.8.1 An example trace of cumulative additions of..... Quat-DME-Oestradiol on pre-contracted aortic rings followed by iberiotoxin (100 nM).....	118
Figure 4.1.1.1.1 Transmitted light images of non-transfected HEK 293..... cells illustrating morphology and processes.....	136
Figure 4.1.2.1 Schematic illustration of the four different methods of..... patch clamp technique.....	141
Figure 4.1.3.1.1 Schematic of <i>Slo1</i> α subunits.....	147
Figure 4.1.3.2.1 Cartoon of the BK α subunit illustrating the voltage..... sensor domain (VSD), RCK domains and Ca ²⁺ bowl.....	148
Figure 4.1.3.2.2 Model of putative location of SO relative to S1-S6..... consistent with the disulfide cross-linking technique.....	149
Figure 4.1.3.4.1 Schematic showing a proposed topography of BK α subunit with an associating β subunit.....	155
Figure 4.1.3.4.2 Schematic of <i>hSlo</i> KNCM β genes encoding the BK..... β subunits.....	156
Figure 4.1.3.5.1 Plot illustrating the BK conductance-voltage relationship in presence/absence of auxiliary β subunits at different Ca ²⁺ levels.....	157
Figure 4.1.3.7.1 Comparison of single BK α + β_1 currents (WT) and BK $\beta^{-/-}$ taken from recordings of isolated mouse aorta at different [Ca ²⁺]..... and voltages.....	160
Figure 4.1.3.7.2 Recordings illustrating how the BK β_1 subunit stabilises BK channel conductance.....	161
Figure 4.2.4.1 Cartoon illustrating voltage protocol for activating BK currents	168

Figure 4.2.5.2.1 Example of single exponential fit of evoked BK currents in the rising phase of BK channel activation.....	170
Figure 4.3.1.1 Control BK peak currents (run-up) and activation time..... constant in HEK 293 cells expressing BK α subunits.....	174
Figure 4.3.1.2 The properties of BK currents in HEK 293 cells expressing BK α subunits.....	175
Figure 4.3.1.3 Non-stationary noise analysis on control BK channel currents in a HEK 293 cell expressing α subunits.....	178
Figure 4.3.2.1 The effect of Oestrone (5 μ M) on evoked currents in..... HEK 293 cells expressing BK α subunits.....	179
Figure 4.3.3.1 The effect of DME-Oestrone (5 μ M) on evoked currents in HEK 293 cells expressing the BK α subunits.....	181
Figure 4.3.4.1 The effect of Quat-DME-Oestrone (5 μ M) on evoked currents in HEK 293 cells expressing the BK α subunits.....	183
Figure 4.3.5.1 The effect of Oestrone-Oxime (5 μ M) on evoked currents in HEK 293 cells expressing the BK α subunits.....	184
Figure 4.3.6.1 The effect of Quat-DME-Oestradiol (5 μ M) on evoked currents in HEK 293 cells expressing the BK α subunits.....	186
Figure 4.3.7.1 Dunn's Multiple Comparison test of control (run up)..... with normalised peak current in the presence of oestrogens from..... BK α recordings.....	189
Figure 4.3.8.1 Control BK peak currents (run-down) and activation..... time constant in HEK 293 cells expressing BK α and β_1 subunits.....	191
Figure 4.3.8.2 The properties of BK currents in HEK 293 cells expressing BK α and β_1 subunits.....	192

Figure 4.3.9.1 The effect of Oestrone (5 μ M) on evoked currents in..... HEK 293 cells expressing BK α and β_1 subunits.....	194
Figure 4.3.10.1 The effect of DME-Oestrone (5 μ M) on evoked currents in HEK 293 cells expressing BK α and β_1 subunits.....	197
Figure 4.3.11.1 The effect of Quat-DME-Oestrone (5 μ M) on evoked currents in HEK 293 cells expressing BK α and β_1 subunits.....	199
Figure 4.3.12.1 The effect of Oestrone-Oxime (5 μ M) on evoked currents in HEK 293 cells expressing BK α and β_1 subunits.....	201
Figure 4.3.13.1 The effect of Quat-DME-Oestradiol (5 μ M) on evoked..... currents in HEK 293 cells expressing BK α and β_1 subunits.....	203
Figure 4.3.14.1 Dunn's Multiple Comparison test of control (run up)..... with normalised peak current in the presence of oestrogens from..... BK α and β_1 recordings.....	205
Figure 4.4.2.1 Chemical structures of quaternary ammonium cations.....	221
Figure 4.4.2.2 A putative pathway for redox conversion and..... metabolic regeneration of A ring oestrogens through quinols.....	222
Figure 4.4.2.3 Mechanism showing the conversion of Oestrone-Oxime... to Oestrone.....	224
Figure 5.1.2.1 Cartoons of a cell membrane structure based on the..... Singer-Nicolson fluid mosaic model.....	229
Figure 5.1.2.2 Structure and classification of mammalian cell membrane lipids.....	231
Figure 5.1.3.1 Illustrations of equipment and set-up of vertical painted..... bilayers.....	232

Figure 5.1.3.2 Schematic illustrating two principle techniques for the formation of a planar lipid bilayer.....	233
Figure 5.1.3.3 Cross-section of cup and septum illustrating the process of bilayer thinning.....	234
Figure 5.1.4.1 Schematic of the fusion process of ion channel protein with the planar lipid bilayer.....	236
Figure 5.2.1.1 A cell disruption vessel, “cavitation bomb”, used for processing cell suspensions by the nitrogen decompression method.....	242
Figure 5.2.1.2 Bursting cells into membrane fragments by nitrogen gas delivered under pressure (1000-1500 psi) into the cavity of the cell disruption vessel.....	243
Figure 5.2.2.1.1 Models and chemical structures of 1-palmitoyl-2-oleoyl-sn-glycero-3-phospho-L-serine (POPS) and 1-palmitoyl-2-oleoyl-sn-glycero-3-phosphoethanolamine (POPE).....	245
Figure 5.2.2.2.1 Schematic of chamber and cup for the formation of painted bilayers.....	246
Figure 5.2.2.2.2 A cross-section schematic of a voltage clamped bilayer set-up depicting the two separate chambers.....	248
Figure 5.2.2.3.1 An example trace recording before and after BK α plus β_1 channel insertion into the prepared phospholipid bilayer.....	249
Figure 5.3.1.1 An example trace showing a control recording of BK α channel activity in a lipid bilayer reconstituted from POPS and POPE.....	256
Figure 5.3.1.2 An example trace showing a control recording from BK α plus β_1 channel activity in a lipid bilayer reconstituted from POPS and POPE.....	256

Figure 5.3.1.3 Sample dwell time histograms of control closed times vs.... number of events from the BK α + β_1 trace in Figure 5.3.1.2.....	257
Figure 5.3.1.4 Sample dwell time histograms of control open times vs..... number of events from BK α + β_1 trace in Figure 5.3.1.2.....	258
Figure 5.3.2.1.1 The effect of Oestrone (5 μ M) on the NP _o of the BK α channel.....	260
Figure 5.3.2.1.2 The effect of Oestrone (5 μ M) on the single channel current of the BK channel consisting of α subunits alone.....	261
Figure 5.3.2.2.1 The effect of Oestrone (5 μ M) on the NP _o of the..... BK α plus β_1 channel.....	264
Figure 5.3.2.2.2 The effect of Oestrone (5 μ M) on the single channel current of the BK α plus β_1 channel.....	265
Figure 5.3.2.3.1 The effect of Oestrone (50 μ M) on the NP _o of the..... BK α channel.....	268
Figure 5.3.2.3.2 The effect of Oestrone (50 μ M) on the single channel..... current of the BK α channel.....	269
Figure 5.3.2.4.1 The effect of Oestrone (50 μ M) on the NP _o of the..... BK α plus β_1 channel.....	271
Figure 5.3.2.4.2 The effect of Oestrone (50 μ M) on the single channel..... current of the BK α plus β_1 channel.....	272
Figure 5.3.3.1.1 The effect of DME-Oestrone (5 μ M) on the NP _o of the..... BK α channel.....	275
Figure 5.3.3.1.2 The effect of DME-Oestrone (5 μ M) on the single..... channel current of the BK α channel.....	276

Figure 5.3.3.2.1 The effect of DME-Oestrone (5 μ M) on the NP _o of the.... BK α plus β_1 channel.....	278
Figure 5.3.3.2.2 The effect of DME-Oestrone (5 μ M) on the single..... channel current of the BK α plus β_1 channel.....	279
Figure 5.3.3.3.1 The effect of DME-Oestrone (50 μ M) on the NP _o of the... BK α channel.....	282
Figure 5.3.3.3.2 The effect of DME-Oestrone (50 μ M) on the single..... channel current of the BK α channel.....	283
Figure 5.3.4.1.1 The effect of Quat-DME-Oestrone (5 μ M) on the NP _o of.. the BK α channel.....	286
Figure 5.3.4.1.2 The effect of Quaternary-DME-Oestrone (5 μ M) on the.... single channel current of the BK α channel.....	287
Figure 5.3.4.2.1 The effect of Quat-DME-Oestrone (5 μ M) on the NP _o of.. the BK α plus β_1 channel.....	289
Figure 5.3.4.2.2 The effect of Quat-DME-Oestrone (5 μ M) on the single.. channel current of the BK α plus β_1 channel.....	290
Figure 5.3.4.3.1 The effect of Quat-DME-Oestrone (50 μ M) on the NP _o of the BK α channel.....	293
Figure 5.3.4.3.2 The effect of Quat-DME-Oestrone (50 μ M) on the..... single channel current of the BK α channel.....	294
Figure 5.3.5.1.1 The effect of Oestrone-Oxime (5 μ M) on the NP _o of the... BK α channel.....	297
Figure 5.3.5.1.2 The effect of Oestrone-Oxime (5 μ M) on the single..... channel current of the BK α channel.....	298

Figure 5.3.5.2.1 The effect of Oestrone-Oxime (5 μ M) on the NP _o of the... BK α plus β_1 channel.....	301
Figure 5.3.5.2.2 The effect of Oestrone-Oxime (5 μ M) on the single..... channel current of the BK α plus β_1 channel.....	302
Figure 6.3.1 Schematic description of possible BK β_1 - β_2 subunit..... chimeric constructs.....	329

ABBREVIATIONS:

AA - *Arachidonic acid*

AC – *Adenylate cyclase*

AChR - *Acetylcholine receptor*

Ad 5 DNA - *Sheared adenovirus type 5 DNA*

AgII (ATII) - *Angiotensin II*

ASIC - *Acid sensing ion channel*

ATII (AgII) - *Angiotensin II*

ATP - *Adenosine triphosphate*

bbTBA - *N-(4-[benzoyl]benzyl)-N,N,N-tributylammonium bromide*

Bk - *Bradykinin*

BK_α - *Large potassium channel comprising α subunits only*

BK_{α+β1} - *Large potassium channel comprising α plus β subunits combined*

BK_{Ca} - *Large calcium-activated potassium channel*

BLM - *Black lipid membrane (Planar lipid bilayer)*

BSA – *Bovine serum albumin*

cAMP - *Cyclic adenosine monophosphate*

ceSlo - *Caenorhabditis elegans slopote*

cGMP - *Cyclic guanosine monophosphate*

Ca²⁺_i - *Intracellular calcium*

CHD - *Coronary heart disease*

CHO - *Chinese hamster ovary*

ChTX - *Charybdotoxin*

Cl_{Ca} - *Calcium activated chloride channel*

CDCl₃ – *Deuterated chloroform*

¹³CNMR - *Carbon thirteen nuclear magnetic resonance*

CNS - *Central nervous system*

COPD - *Chronic obstructive pulmonary disease*

COX - *Cyclooxygenase*
CVD - *Coronary vascular disease*
DAG - *Diacylglycerol*
DES - *Diethylstilbestrol*
DG - *Diacylglycerol*
DHS-1 - *Dihydrosoyasaponin*
diCL-DHAA - *12, 14-dichlorodehydroabietic acid*
DMAEC HCl - *Dimethylamine ethyl hydrochloride*
DME-Oestrone - *3-(2-Dimethylamino-ethoxy)-Oestrone*
DMF - *Dimethylformamide*
DMSO - *Dimethyl sulfoxide*
DNA - *Deoxyribonucleic acid*
DRG - *Dorsal root ganglia*
dSLO - *Drosophila melanogaster slopoko*
d₅-pyr - *Pentadeuteropyridine*
EBT - *Ethyl bromide tamoxifen*
ECE - *Endothelin converting enzyme*
ECs - *Endothelial cells*
EDCF - *Endothelium-derived contracting factor*
EDHF *Endothelium-derived hyperpolarising factor*
EDRF - *Endothelium-derived relaxation factor*
EGTA - *Ethylene glycol tetraacetic acid*
EIM - *Excitability inducing material*
ER - *Oestrogen receptor*
ET - *Endothelin*
EtOAc - *Ethyl acetate*
EtOH – *Ethanol*
5-HT - *Serotonin*
FBS - *Foetal bovine serum*

GC – *Guanylate cyclase*

G418 - *Geneticin*

GPER - *G-protein coupled Oestrogen receptor*

H1HR - *H1 histamine receptor*

HEK 293 cells - *Human embryonic kidney cells*

¹HNMR - *Proton nuclear magnetic resonance*

HRE - *Hormone response element*

hSLO - *Human slopoko*

IbTX - *Iberiotoxin*

IK_{Ca} - *Intermediate calcium-activated potassium channel*

I_{ks} - *Delayed-rectifier K⁺ channel*

IP₃ - *Inositol 1,4,5-triphosphate*

IR. - *Infra-red*

I.u - *Unitary current*

IUPAC - *International Union of Pure and Applied Chemistry*

K_{Ca} channel - *Calcium-activated potassium channel*

KCNMA1 - *Potassium large conductance calcium-activated channel, subfamily M(ammalian), alpha member 1*

K_{IR} - *Inward rectifier K⁺ channel*

KO (^{-/-}) - *Knock-out*

Ktxs - *The α-, β-, and γ-scorpion toxins*

K_V - *Voltage-gated potassium channel*

MEM - *Minimum Essential Medium*

MeOH - *Methanol*

MLCK - *Myosin light chain kinase*

Na_v - *Voltage-gated sodium channel*

NaH - *Sodium hydride*

NAD/NADH - *Nicotinamide adenine dinucleotide (oxidising)/Nicotinamide adenine dinucleotide (reducing)*

NCX - *Sodium/calcium exchanger*

NF - *Neurofilament*

nNOS – *Neuronal nitric oxide isoform*

NO - *Nitric oxide*

NOS - *Nitric oxide synthase*

NP₀ - *Open probability*

NSC - *Non selective channel*

O₂⁻ - *Superoxide anions reactive oxygen species*

Oestrone-Oxime - *17-hydroximino-estra-3-ol*

PE - *Phenylephrine*

PGI₂ - *Prostacyclin (also called prostaglandin I2)*

PiMA - *Pimaric acid*

PKA – *Protein kinase A*

PKC - *Protein kinase C*

PLC - *Phospholipase C*

PMCA - *Plasma membrane Ca²⁺-ATPase*

POPE - *Palmitoyl-oleoyl-phosphatidylethanolamine*

POPS - *Palmitoyl-oleoyl-phosphatidylserine*

PPM - *Parts per million*

Quat-DME-Oestradiol - *Quaternary-3-(2-Dimethylamino-ethoxy)-oestradiol*

Quat-DME-Oestrone - *Quaternary-3-(2-Dimethylamino-ethoxy)-oestrone*

RBC - *Red blood cell*

RCK - *Potassium regulating domains*

RNA - *Ribonucleic acid*

RT - *Room temperature*

RyR - *Ryanodine receptor*

SEM - *Standard error of the mean*

SERM - *Selective oestrogen receptor modulator*

SHR - *Spontaneously hypertensive rat*

SK - *Small-conductance potassium channel*

SOC - *Store operated channel*

SR - *Sarcoplasmic reticulum*

SR/ER - *Sarco/endoplasmic reticulum*

STOC - *Spontaneous transient outward currents*

STX - *Stotoxin*

T, TH and Thr - *Thrombin*

TEA - *Tetraethylammonium*

TLC - *Thin layer chromatography*

TM - *Transmembrane*

TRPC - *Transient receptor potential channels*

TX - *Tamoxifen*

TxA₂ - *Thromboxane A₂*

VGCC - *Voltage gated calcium channel*

V_m - *Membrane potential*

VOCC - *Voltage operated calcium channels*

VP - *Vasopressin*

VRAC - *Volume regulated ion channel*

VSD - *Voltage sensor domain*

VSMCs - *Vascular smooth muscle cells*

WKY - *Wistar Kyoto (rat)*

WT - *Wild type*

“Sedulously eschew obfuscatory hyperverbosity and prolixity”

Roedy Green.

ACKNOWLEDGEMENTS:

It would have been next to impossible to write this thesis without the help and support that I have received from many quarters throughout this period of my doctoral studies. My first thanks should go to my undergraduate project supervisors for introducing me to the wonders and joy of scientific research; to Cinzia Dedi who convinced me to throw caution to the wind and embark on such a venture and who has been a wonderful support; and to Flavia Fucassi and Anna Blunden for being there for me.

To Dr Christy Hunter, my second supervisor, I will forever be in his debt. His intelligence, patience and wicked sense of humour nurtured this non-chemist throughout the early days of organic synthesis and I thank him from the bottom of my heart.

It is difficult to overstate my gratitude to my principal supervisor, Dr. Marcus Allen. With his enthusiasm, his intelligent wit, and his great efforts to explain things clearly and simply, he helped to make electrophysiology fun for this '*Sheila*'. Throughout my thesis-writing period, he has provided encouragement, sound advice, good teaching and good company. He has been a tower of strength and I would have been lost without him. A special mention must go to Hilary who had to put up with the late nights at the office when bilayers misbehaved (which happened quite a lot). Thank you for all your support.

To my husband and sons, thank you all so much for your support and encouragement, what can I say? You are my inspiration. Finally, thank you to my father William Joseph Devaney, a highly intelligent and meticulous scientist, the cleverest person I know, to him I dedicate this thesis.

DECLARATION:

I declare that the research contained in this thesis, unless otherwise formally indicated within the text, is the original work of the author. The thesis has not been previously submitted to this or any other university for a degree and does not incorporate any material already submitted for a degree.

Signed:

Date:

CHAPTER 1

General Introduction

1.1 INTRODUCTION

Pharmacological targeting of ion channels is an exciting field for possible therapeutic intervention and novel drug development. Previous ion channel research into potential novel targets has mainly concentrated on sodium and calcium blockers [1]. However, with increasing numbers of channelopathies being identified, other cation selective channels, and potassium channels in particular, are being investigated as potential targets in a number of pathologies [2-5]. Dysregulation of potassium channels is a known feature in diverse pathologies such as cardiovascular disease, hypertension, incontinence and even epilepsy and many researchers have attempted to produce various chemical and natural potassium channel openers with a view to producing therapeutically relevant compounds [6, 7]. This study will concentrate on the large conductance, calcium-activated potassium channel (BK channel) found in the vasculature which may be a promising target for treating smooth muscle disorders. Indeed, it is well documented that oestrogens such as 17β -oestradiol are able to relax vascular smooth muscle and can interact directly with membrane receptors and channels including BK vascular channels [8-14]. Here, novel oestrogen derivatives were synthesised by the author and their potential acute vasorelaxant effects investigated to obtain an insight into their mode of action and selectivity for BK channels.

1.1.1 The BK channel

The BK (big potassium) channel, also known as the Maxi-K potassium channel, is a large conductance, calcium and voltage-sensitive potassium channel. BK

channels are found in the majority of excitable and non-excitable tissues with the heart being an anomaly [15]. The channels have functional roles in vascular smooth muscle, skeletal muscle, neurons, kidney and secretory cells.

The existence of a calcium-activated potassium channel was first reported by Elkins and co-workers in the early 1980s from work involving the *Drosophila* slowpoke mutant [16]. Thereafter, the α subunit, encoded by the *KCNMA1/Slo1* gene, was cloned from *Drosophila* and various mammalian species [17-20]. Subsequent investigations revealed a typical tetrameric, voltage-regulated channel [21, 22] with a unique additional transmembrane segment (S0), that places the NH₂ terminus at the extracellular side of the membrane, and two large intracellular regions designated S7-S8 and S9-S10 [23]. The exoplasmic S0 segment is essential for regulatory β -subunit interaction [24], while S7-S10 allow for Ca²⁺ regulation. S7 and S8 contain the low affinity Ca²⁺ and Mg²⁺ binding sites and S9 and S10, the high affinity Ca²⁺ bowl (Figure 1.1.1.1).

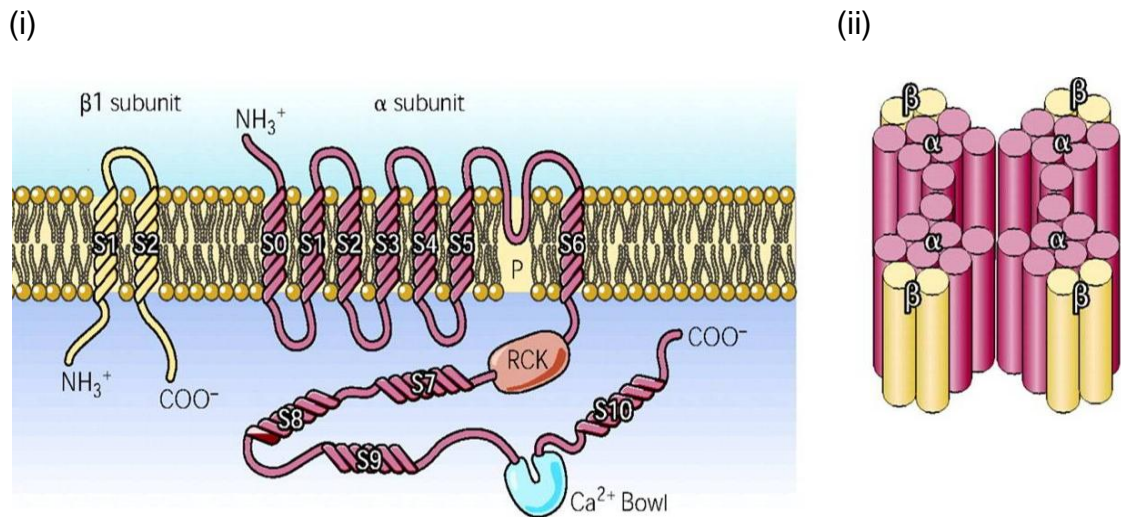


Figure 1.1.1.1 Cartoon of BK channel (i) depicting the BK β_1 subunit with its two transmembrane domains, and the seven-transmembrane segments of the α subunit (ubiquitous to the BK channel. Also illustrated are the hydrophobic S7-S8 and S9-S10 intracellular regions, incorporating Mg^{2+} and Ca^{2+} binding sites and professed calcium bowl (segments S7 – S10. (ii) Depicts a tetramer of α subunits and their regulatory β subunits, forming the native BK channel [25].

BK channels comprise four α proteins and are ubiquitously distributed among most tissues. However, the molecular diversity of the channel is due to the association of its various β subunits. Alpha and beta subunits are usually expressed together in a 1:1 stoichiometry [26-30]. The tissue specific regulatory β subunits 1, 2, 3 and 4 were cloned shortly after the discovery of the BK channel [26, 31-34] and revealed the mechanisms underlying the previously unexplained tissue specific behaviour of the BK channel [35]. The pore-forming four α subunits can associate with more than one type of β subunit which uniquely, alters the characteristics of the BK channel [35]. For example, the β_1

subunit, in addition to enhancing the channel's sensitivity to voltage and calcium [36-38], is a key factor in vascular tone homeostasis [39-41], whereas, co-expression of the β_4 subunit with the α subunit decreases the calcium sensitivity of the channel [31, 35]. The β_2 subunit is associated with BK channels present in chromaffin cells located in the adrenal medulla [42]. An association between the β_3 subunit and BK channels is found in secreting beta cells of the pancreas and also within the testes. The β_4 subunit is associated with BK channels of the brain and kidney [43].

1.1.2 The BK channel and vascular tone

Vascular tone can be described as a sustained state of contraction of the blood vessel wall [44]. Indeed, the status quo of resistance arteries is to exist in a mode of partial constriction which responds to various stimuli e.g. a rise in intracellular calcium concentrations and / or shifts in membrane potential according to the perfusion and metabolic wants of a particular tissue [45]. In vascular smooth muscle tissue, under normal conditions i.e. pressurised arteries; physiological membrane potentials of around -40 mV; intracellular calcium concentrations of no more than 200 nM, BK channels have a very low open probability [46]. However, the BK regulatory β_1 subunit, ubiquitous in vascular smooth muscle tissue, couples BK activation to calcium sparks (a sharp local rise in calcium due to opening of L-type Ca^{2+} channels and ryanodine receptor channels). This serves to regulate vascular tone and protect against membrane depolarisation and pressure-induced vasoconstrictions by providing a negative feedback mechanism [43, 47, 48]. When $\text{BK}\beta_1$ channels are open there is an efflux of potassium ions from the cell causing the

membrane to hyperpolarise which, in turn, leads to vasodilation. Closure of these channels causes cell depolarisation thereby, opening voltage-gated L-type calcium channels and increasing intracellular calcium leading to vasoconstriction (Figure 1.1.2.1). Accordingly, it seems that the BK channel, co-expressing both α and β_1 subunits, assumes the role of a molecular tuner of vasoregulation.

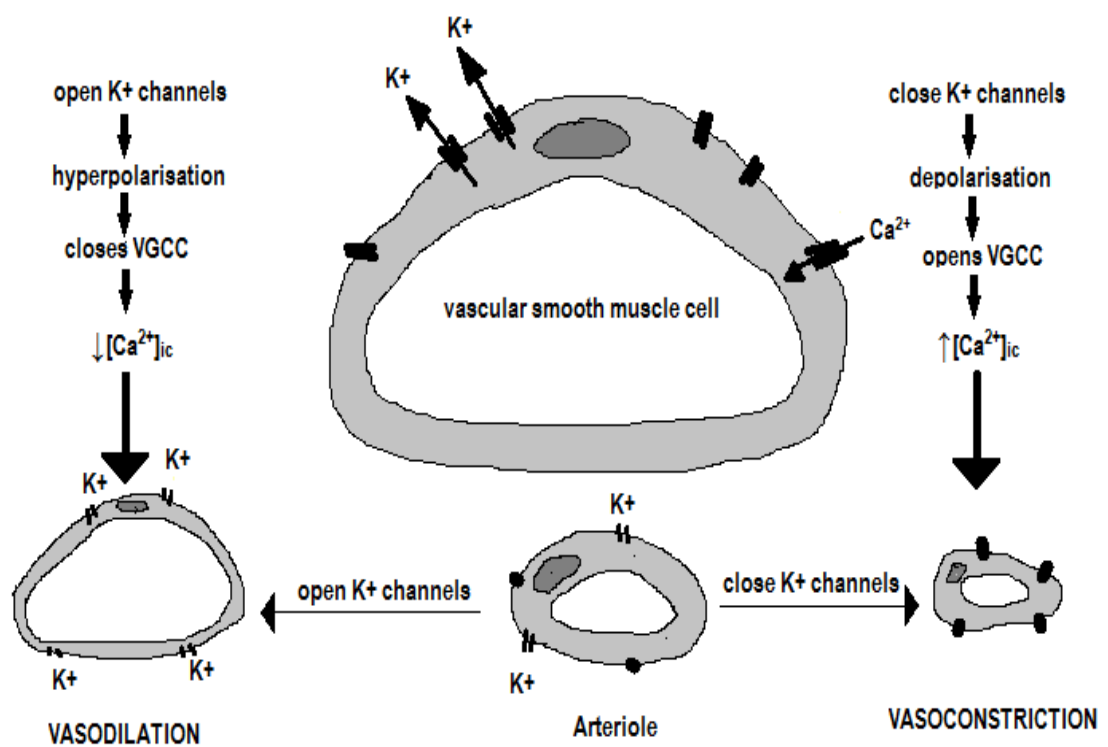


Figure 1.1.2.1 Schematic cross section of arteriolar smooth muscle cell showing regulation of smooth muscle tone. It illustrates the negative feedback mechanism of potassium channels in response to changes in membrane potential and intracellular Ca^{2+} concentrations. A rise in intracellular Ca^{2+} results in K^+ efflux that is sufficient to hyperpolarise the membrane potential by up to 20 mV. This induces closure of voltage-gated calcium channels (VGCCs) and a reduction in intracellular calcium levels and subsequent vasodilation [46, 49].

1.1.3 The BK channel and hypertension

Increased vascular tone is a hallmark of hypertension and various studies have reported the physiological importance of the association of the BK β_1 subunit in non-hypertensive systems. Indeed, in comparison with their β_1 subunit-expressing counterparts, studies with animals with gene-targeted ablation of the β_1 subunit (β_1 knockout mice), show an impaired BK function leading to increased arterial tone associated with symptoms of hypertension [43, 50, 51]. Work done by Plüger *et al.*, has demonstrated the importance of associating regulatory BK β_1 subunits, in maintaining resting blood pressure homeostasis (Figure 1.1.3.1) [51].

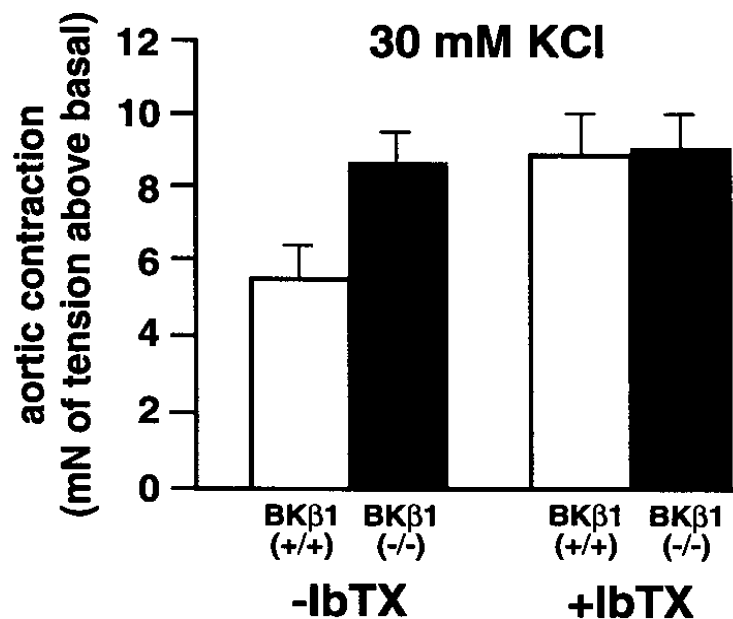


Figure 1.1.3.1 Histogram showing difference in degree of contraction between KCl-treated thoracic aortic rings taken from wild type mice ($+/+$) and gene-targeted ($BK\beta_1^{-/-}$) mice either in the presence or absence of the BK blocker, iberiotoxin (IbTX). These data demonstrate that the lack of associating BK β_1 subunits evokes an increased contractile response of mouse thoracic aortic rings to KCl which is significantly ameliorated by application of IbTX (10^{-7} M) [51].

Conversely, a polymorphism of the β_1 subunit that promotes a gain in function, is associated with low prevalence of diastolic hypertension in humans [52]. Furthermore, spontaneously hypertensive rats (SHR), which display severe hypertension, and the Wistar-Kyoto rats (WKY), which suffer borderline hypertension, show a down-regulation of the BK β_1 subunit [53]. Consequently, animal models of hypertension based on BK dysfunction are firmly established.

1.1.4 Cardiovascular disease and hypertension - epidemiology

Coronary vascular disease (CVD) is the commonest cause of mortality in Europe and at present accounts for over thirty *per cent* of all deaths and in the UK alone, mortality rates are the highest worldwide [54, 55]. According to statistics released by the British Heart Foundation, UK mortality rates from cardiovascular disease (CVD) reached nearly 200,000 in 2008 [56, 57]. Remarkably, the latest research suggests that 1:3 adults in England and Scotland are hypertensive, fifty *per cent* of whom receive no prophylactic treatment [57].

Nonetheless, there is much to indicate a gender difference in the development of coronary heart disease. Epidemiological studies suggest that the observed discrepancy in the pathogenesis of hypertensive disease between the sexes may be ascribed to hormonal status [58]. From menarche to the onset of menopause, female populations have a much lower incidence of high blood pressure than in age-matched male populations. However, post-menopause, the incidence of hypertension in females matches that of males of the same age

and indeed, in old age (>75 years), females are more vulnerable to the condition than their male counterparts (Figure 1.1.4.1) [58].

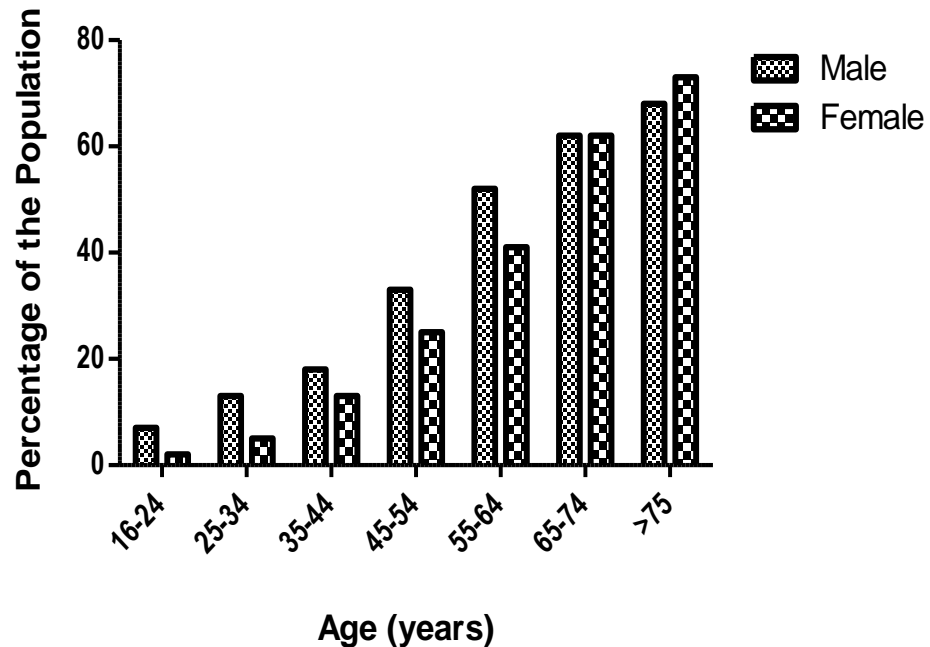


Figure 1.1.4.1 Prevalence of high blood pressure in England (1998 - 2008) by age and gender. For these data, high blood pressure was classified as ≥ 140 mmHg (systolic) and/or ≥ 90 mmHg (diastolic) or currently taking prescribed anti-hypertensive medication. (Graph constructed by author using data derived from Joint Health Surveys Unit (2009); Health Survey for England 2008; Adult Trend Tables (www.ic.nhs.uk accessed June 2011)).

There are several contributing factors to the pathogenesis of hypertension in post-menopausal women, not least deprivation of circulating oestrogens and a decrease in the oestrogen:androgen ratio. Reduced oestrogen levels may lead to endothelial dysfunction with ensuing increases in endothelin and angiotensin II, in turn, leading to vasoconstriction and subsequent hypertension. The

evidence implies a possible link between post-menopausal hypertension and decreased levels of endogenous circulating oestrogens (Figure 1.1.4.2) [59].

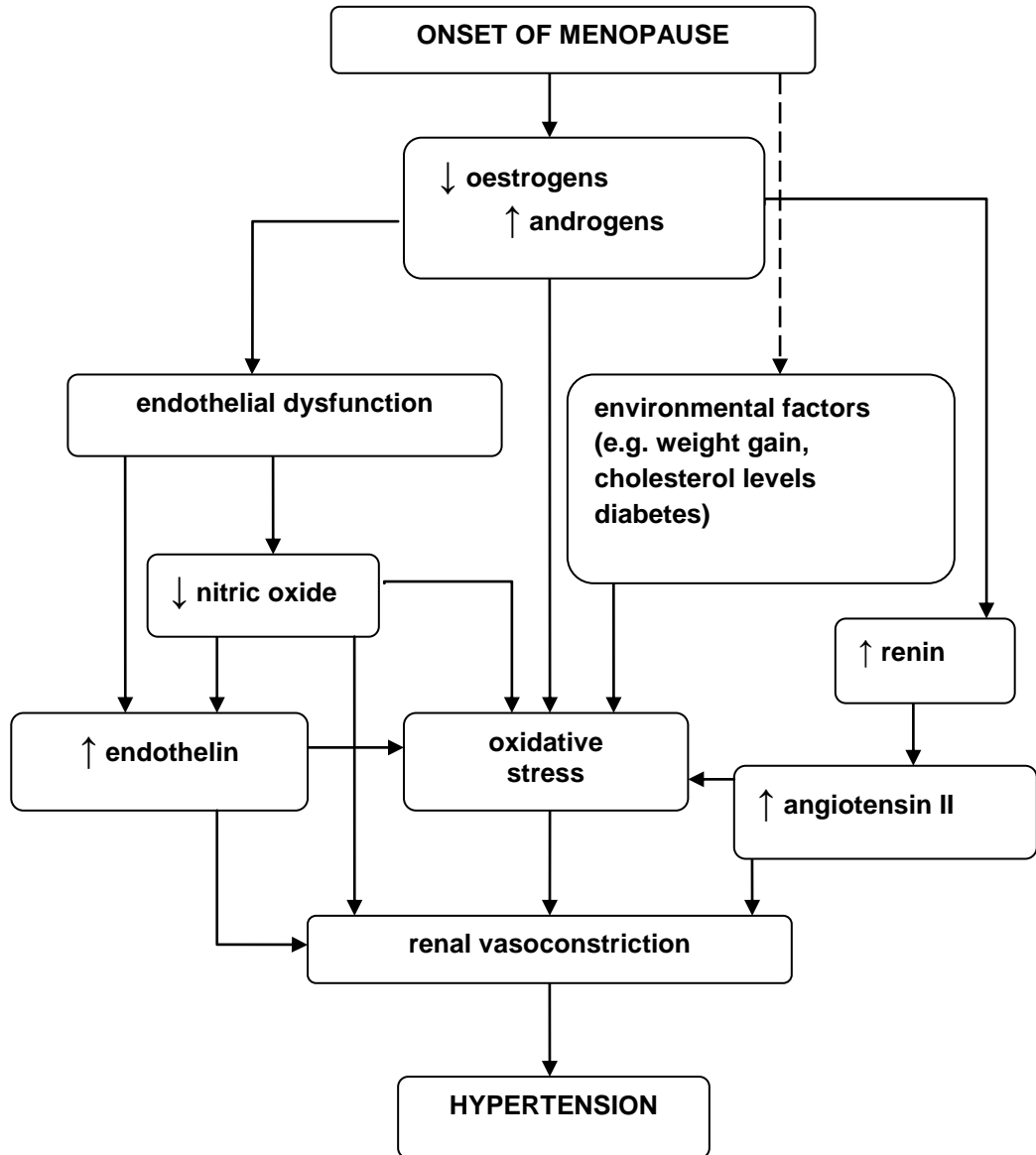


Figure 1.1.4.2 Flow chart showing post-menopausal hypertension risk factor algorithm [59].

1.1.5 Oestrogens - genomic or non-genomic pathway

The circulating endogenous sex hormones are steroid hormones, synthesised by the body. There are three major circulating endogenous oestrogens in women, oestrone, oestradiol and oestriol. Oestrone is the major circulating oestrogen in menopausal and post-menopausal women, whereas, oestradiol is the major oestrogen produced from menarche to menopause. Oestriol is mainly produced during pregnancy by the placenta. The male sex hormone, testosterone, can be converted *in vivo* to oestradiol by the enzyme aromatase.

Steroidal oestrogens are uncharged, lipophilic molecules and as such, readily diffuse across cell membranes. Physiological responses to oestrogen are triggered by altered conformation of receptors post ligand binding which results in activation of cell signalling pathways [60, 61]. Response to oestrogen binding is characterised as genomic or non-genomic.

1.1.5.1 Genomic effects of oestrogen

Genomic effects have a delayed onset and prolonged duration due to transcriptional events, culminating in subsequent modulation of protein expression [62-65]. Endogenous oestrogens bind to intracellular oestrogen receptors to form an oestrogen-receptor complex which triggers various nuclear events eg. transactivation of gene expression in response to oestradiol [66]. Two different nuclear oestrogen receptors to date, have been identified, ER α and ER β , both of which belong to a superfamily of hormone nuclear receptors [67]. These receptors serve as signal transducers and transcription factors modulating target gene expression by recognising palindromic hormone

elements (HREs) [14, 63, 68-71]. Both ER α and ER β are expressed in vascular smooth muscle and endothelial cells, yet research has revealed that ER α expression preponderates over ER β in vascular smooth muscle and *vice versa* in the endothelium [67].

1.1.5.2 Non-genomic effects of oestrogen

Non-genomic steroid action may be characterised by its rapid onset and short duration (seconds - minutes compared with hours for a genomic response). Non-genomic responses also lack the necessity for translation and transcription and consequently, do not act on the genome. In addition, non-genomic steroid action is mediated by receptor proteins other than the nuclear ER α and ER β [72, 73]. Convention dictates that rapid cellular response signalling is frequently linked to such cell surface receptors as G-protein-coupled receptors and growth factor receptors which generate non-genomic signalling events such as Ca²⁺ mobilisation, kinase activation and synthesis of nitric oxide [74, 75]. Oestrogens have been shown to trigger rapid intracellular signalling through second messengers *via* GPR30/GPER, a G protein-coupled receptor belonging to the family of 7-transmembrane receptors [61, 76-78].

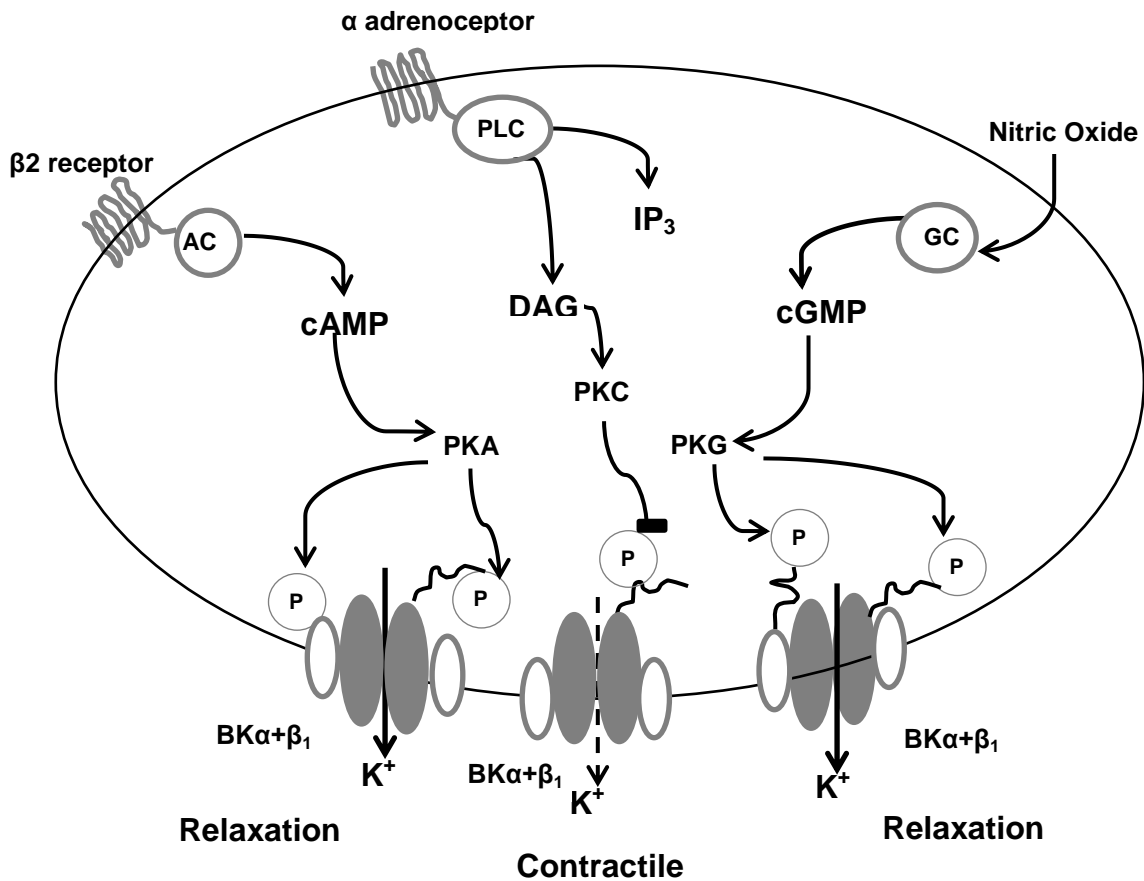
In vascular smooth muscle, oestrogen-induced rapid relaxation is a well-characterised, non-genomic event [79] and is a result of changes in membrane ionic permeability and activation of vasoactive enzymes in the endothelium, such as nitric oxide synthase (eNOS) [63, 80, 81]. Additionally, oestrogen can relax arteries independent of endothelium involvement. Salom *et al.*, have demonstrated non-genomic relaxation of isolated rabbit carotid artery by 17 β -

oestradiol where the relaxant effects were attributed to inhibition of extracellular calcium influx [82]. Moreover, Nakajima and co-workers, showed 17 β -oestradiol inhibits voltage-dependent L-type Ca²⁺ channels in rat aortic smooth muscle cells [83], while Ullrich *et al.*, have reported oestrogen-induced inhibition of L-type Ca²⁺ currents in HEK 293 cells transfected with Ca_v channels *via* direct interaction with the channel protein itself [84]. Conversely, oestrogen is known to engender a rapid increase in intracellular Ca²⁺ in the endothelium of the vasculature which may involve eNOS and nitric oxide release [85]. Indeed, a considerable body of evidence exists demonstrating a role for eNOS in rapid and short-lived vascular actions of oestrogen [79], whereas inducible nitric oxide synthase isoform (iNOS), known to be present in vascular smooth muscle [86] and to a lesser extent endothelial cells [87], has been shown to mediate oestrogen-induced vasodilation *via* a genomic pathway [88].

1.1.5.3 Non-genomic indirect and direct activation of BK channels by oestrogens

It is widely accepted that BK channels play an important role in the regulation of vascular tone *via* oestrogens and there is a wealth of evidence that oestrogens and xenoestrogens are capable of non-genomic activation of BK channels in vascular smooth muscle. This activation may be effected through both direct and indirect pathways. BK channels are regulated by protein kinases and, in smooth muscle, the binding of certain hormones, neurotransmitters and drugs to membrane-bound receptors such as G-protein-coupled receptors, trigger signaling cascades *via* activated protein kinases PKA, PKG and PKC (Figure 1.1.5.3.1). Indeed, Schubert *et al.*, have demonstrated in freshly isolated

vascular smooth muscle cells, that the effect of protein kinase G on K_{Ca} currents is mediated by its direct action on the BK channel [89].



Key: AC (adenylyl cyclase); GC (guanylate cyclase); PKA (protein kinase A);
 PLC (phospholipase C); IP₃ (inositol 1,4,5-triphosphate); PKG (protein kinase G);
 DAG (diacylglycerol); PKC (protein kinase C);
 cAMP (cyclic adenosine monophosphate);
 cGMP (cyclic guanosine monophosphate).

Figure 1.1.5.3.1 Cartoon of indirect cyclic nucleotide-dependent relaxatory and contractile stimulation of BK channels in a smooth muscle cell. The cGMP and cAMP pathways are key regulators of smooth muscle tone and stimulation of BK channels via these pathways contributes to vasorelaxation [90, 91].

In bronchial and vascular smooth muscle, cAMP-dependent PKA and cGMP-dependent PKG contribute to smooth muscle vasodilation and decreased

vascular resistance, respectively, by enhancing BK sensitivity to Ca^{2+} and voltage leading to ion channel activation [91]. Conversely, phosphorylation by PKC actually inhibits BK channels facilitating vasoconstriction [92].

It is also true that oestrogen-induced BK channel activation in smooth muscle is mediated by means both physiological and pharmacological which may promote cAMP or cGMP involvement [93, 94]. For instance, nitric oxide (NO) induces BK channel activation in human pulmonary artery cells which is PKG-mediated [95] whereas, oestrogen is known to relax coronary arteries by activating BK channels through a cGMP-dependent pathway, as demonstrated by White *et al.*, [96].

Cyclic nucleotide-dependent protein kinases are important factors when considering the site of action of BK activators, not least because BK channels have phosphorylation sites on both α and β subunits (Figure 1.1.5.3.1). Cloned BK channels in smooth muscle have been found to have strong phosphorylation sites for PKA and PKG on the α subunit, the majority of which are located in the COOH terminus. Strong phosphorylation sites for these kinases on the β subunit are present in the intracellular NH_2 terminus [97] (Table 1.1.5.3.1).

Table 1.1.5.3.1 Phosphorylation sites on BK subunits and consequences of phosphorylation on BK channel.

Protein Kinases	α subunits alone	β subunits alone	Both α and β subunits	References
PKA	-	-	↑	[30, 92, 97]
PKG	-	-	↑	[30, 92, 98-100]
PKC	↓	-	-	[30, 89, 92, 98]

Key: ↓ (inhibitory effect on BK channel); ↑ (activation of BK channel).

1.1.6 The BK channel as a therapeutic target for oestrogens

The tissue specificity of BK subunits means that BK channels are ideal targets for pharmaceutical therapeutic drug design. The all-important β_1 subunit, ubiquitous in vascular smooth muscle, is known to increase BK activity after application of 17β -oestradiol [101, 102]. Furthermore, for effective activation of the channel by 17β -oestradiol, Allen *et al.*, through Bayesian analysis, describe how at least two subunits must be associating with the BK channel [40]. Work done by Dick and Sanders [103] demonstrated that both the α and β_1 BK subunits can be individually targeted by oestrogens. They discovered that while xenoestrogens activate the BK channel in mouse colonic smooth muscle cells through binding to the β_1 subunit, they also elicit a decrease in unitary current by interaction with the α subunit (Figure 1.1.6.1).

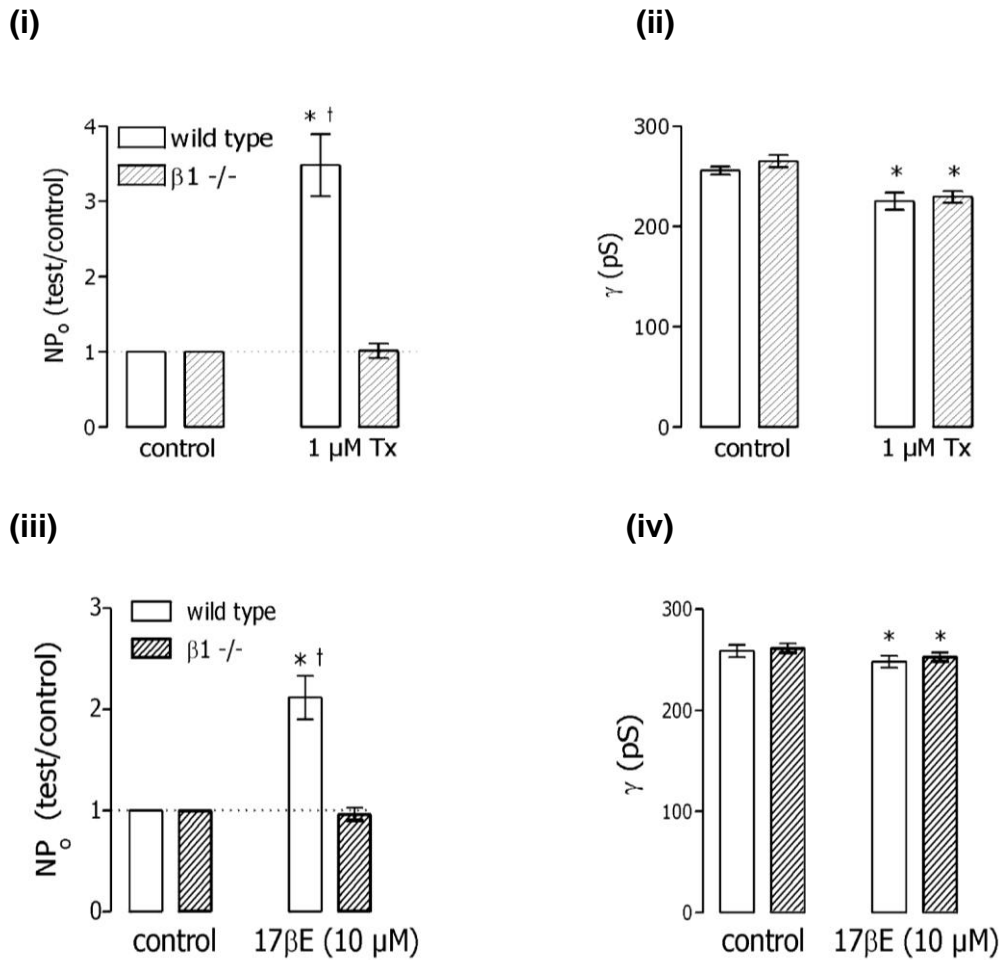


Figure 1.1.6.1 Histograms showing inside-out patch recordings of mouse colonic smooth muscle cell BK channels (wild type and $\beta_1^{-/-}$) in the presence and absence of 17 β -oestradiol (10 μ M) or tamoxifen (1 μ M); (i) and (iii) group data for channel activity (NP_o); (ii) and (iv) group data for conductance (γ); all recordings used symmetrical 140 mM K⁺ and 100 nM free Ca²⁺. These data demonstrate that although, both 17 β -oestradiol (10 μ M) and tamoxifen (1 μ M) activate BK channels only in the presence of its regulatory β_1 subunit, both oestrogens elicit a reduction in unitary conductance in $\beta_1^{-/-}$ channels. Asterisks (i) and (iii) represent a significant difference from control NP_o while the dagger represents a significant difference in normalised NP_o between wild type and $\beta_1^{-/-}$ mice. Asterisks (ii) and (iv) represent a significant difference between control γ and in the presence of either 17 β -oestradiol (10 μ M) or tamoxifen (1 μ M).

Although there have been many studies claiming the beneficial and cardio-protective roles that oestrogens possess, research has also shown that these molecules can act both as agonists and antagonists and thus, lack the desired selectivity of potential therapeutic agents. Indeed, little is known regarding the binding site or mechanism of action of these oestrogen-based BK channel modulators. Previous work using 17β -oestradiol conjugated with an albumin molecule has proposed the BK site of action for oestrogens is located extracellularly [102]. Furthermore, an extracellular site of action for xenoestrogens on the BK channel was demonstrated by Dick and Hunter using the quaternary xenoestrogen, ethylbromide tamoxifen [104].

This study will investigate novel steroidal oestrogens, to be synthesised by the author, and their effects on the BK channel. The idea that oestrogens and novel derivatives act directly on BK channels at the external face of the membrane between the α and β_1 subunits will be explored. If this proves to be correct then the β_1 subunit of the BK channel would be a valuable potential target for pharmacological intervention.

1.2 HYPOTHESES

This study hypothesises that:-

- (i) these novel oestrogens and xenoestrogens can relax vascular smooth muscle by directly activating BK channels;
- (ii) BK activation by these novel oestrogens and xenoestrogens requires the presence of the β_1 subunit;
- (iii) the site of action for these novel oestrogens and xenoestrogens on the BK channel is located on the external interface between the α and β_1 subunits.

1.3 AIMS

This investigation proposes to develop novel BK activators using steroidal oestrogens and non-steroidal antioestrogens as lead compounds. To accomplish this:-

- the N,N-dimethyl-2-phenoxyethanamine motif, found in triphenolic anti-oestrogens such as tamoxifen, will be incorporated into the aromatic ring, found in steroidal oestrogens, with the aim of developing novel BK channel activators.
- To obviate any oestrogenic nuclear effects, the novel compounds will be further developed through alkylation of the nitrogen group, to produce novel membrane-impermeant quaternary amine derivatives.

- The selectivity of these compounds will be further investigated by studying the subunit dependence for BK activation.

This development will be considered successful if these derivatives are able to:-

(i) relax smooth muscle in a BK channel dependent manner

(ii) activate BK channels when expressed in cells

(iii) activate BK channels when reconstituted into lipid bilayers;

It is hoped that the investigations for this study will contribute to the body of information with regards to BK channels as potential pharmacological targets and their site of action.

CHAPTER 2

Synthesis of Xenooestrogens

2.1 INTRODUCTION

Ion channel modulation is an obvious target for drug development and novel compounds are continuously being sought as potential therapeutic treatments for diverse pathologies diseases. In this chapter, novel oestrogen derivatives as potential BK channel modulators were synthesised and tested for purity.

2.1.1 BK channel as therapeutic target

The idea that the large conductance Ca^{2+} -activated potassium channel (BK) is directly implicated in the manifestation of numerous channelopathies is supported by an abundance of scientific evidence [5, 52, 105-108]. The channels are present in excitable cells of the central nervous system (CNS), endocrine tissue and smooth muscle, where they play a demonstrable role as purported guardians of cell membrane potential *via* regulation by intracellular calcium and membrane depolarisation. Consequently, BK channels present an ideal molecular platform for the development of innovative and auspicious drug therapies for an array of pathologies from stroke, epilepsy, bladder and erectile dysfunction to asthma, hypertension and cardiovascular disease. It is, therefore, not surprising that the last decade or so has witnessed the development of a plethora of novel BK modulators such as imidazopyrazine, benzimidazolones and the soyasaponins [109-112]. Nevertheless, nearly all of these compounds have, for the most part, been restricted to investigational and pharmacological research, while the establishment of clinically-approved BK modulators has been elusive [113].

2.1.2 BK modulators

Some BK modulators have, indeed, reached the clinical trial stage of development only to be withdrawn before being granted full clinical approval e.g. NS-8 and BMS204352 (Figure 2.1.2.1) [113].

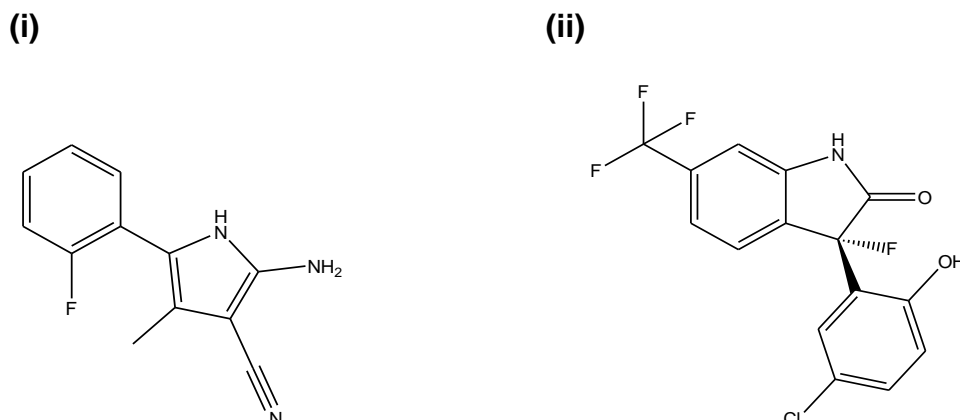


Figure 2.1.2.1 Chemical structures of BK modulators withdrawn from clinical trials (i) NS-8, a pyrrole derivative reported to be a putative treatment for overactive bladder symptoms [114, 115]; (ii) BMS204352, a derivative of NS-004. Substitution of a hydroxyl group in the 3 position with a fluorine atom creates a fluorooxindole compound reported to have possible therapeutic value in the treatment of neuronal ischemia [116-118].

To date, there are no known BK activators in current clinical use with the exception of CR2039 (Andolast™) [119]. This, recently introduced, BK modulator is currently in phase III of clinical trials as an inhalant for the potential relief of asthma and chronic obstructive pulmonary disease (COPD) (Figure 2.1.2.2).

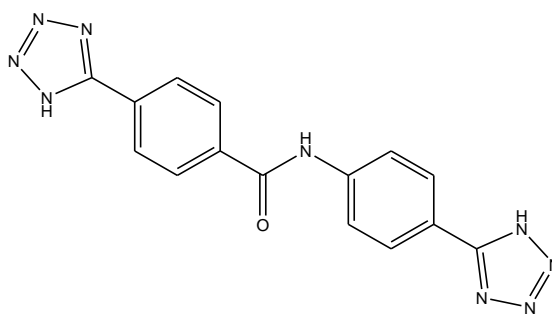
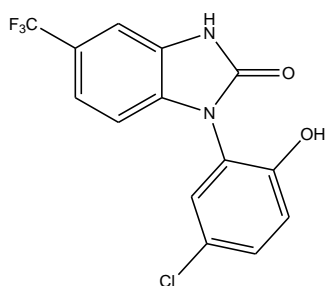


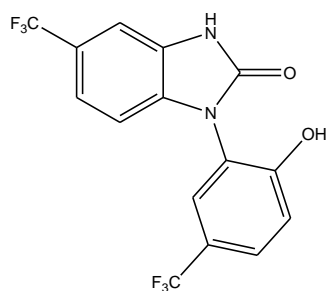
Figure 2.1.2.2 N-4-(1H-tetrazol-5-yl) phenyl-4-(1H-tetrazol-5-yl) benzamide disodium salt, Andolast™ disodium salt (CR2039), currently in Phase III of clinical trials for symptomatic relief of mild asthma, targets bronchial smooth muscle BK channels [6].

As far as is known, there is no data available to suggest this compound targets the β_1 subunit of the BK channel. Rovati *et al.*, have described relaxation in isolated bronchial guinea pig rings which is reversed in the presence of charybdotoxin (ChTX), a general BK channel inhibitor. However, mechanism of action was not explored. Accordingly, most BK modulators are marketed as pharmacological or investigational compounds and encompass such novel compounds as benzimidazolone derivatives e.g. NS-004, NS-1619 and NS-1608 (Figure 2.1.2.3) [109, 110, 112, 120]; naturally-derived modulators such as dihydrosoyasaponin-1(DHS-1), maxikdiol and primaric acid (PiMA) (Figure 2.1.2.4) [121-123]; flavonoids such as apigenine, kaempferol and naringenone (Figure 2.1.2.5) [118, 124]; and endogenous steroidal modulators and their synthetic structural analogues such as 17β -oestradiol, lithocholate, ICI182,780 (*Faslodex*™), diethylstilbestrol (DES), tamoxifen and ethyl bromide tamoxifen (Figure 2.1.2.6 and Figure 2.1.3.1) [102, 104, 125-129].

(i)



(ii)



(iii)

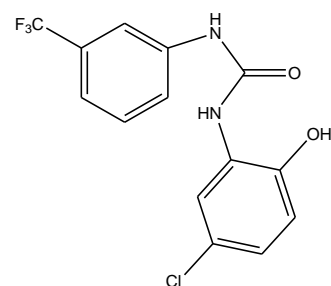
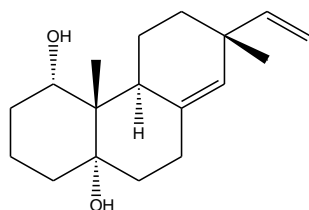
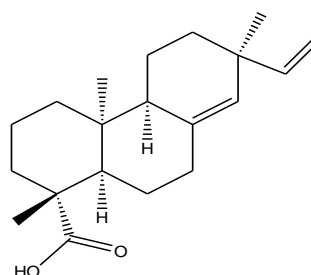


Figure 2.1.2.3 Chemical structures of synthetic openers of the BK channel (i) NS-004, a BK α subunit-selective opener; (ii) NS-1619, a BK α subunit-selective opener; (iii) NS-1608 (a diphenylurea analogue of NS-004) has been reported to activate BK channels in rat and human urinary bladder smooth muscle cells under physiological conditions. Conversely, channel openings are blocked in guinea pig bladder at concentrations $>10 \mu\text{M}$ (NS-1608) [109, 110, 130].

(i)



(ii)



(iii)

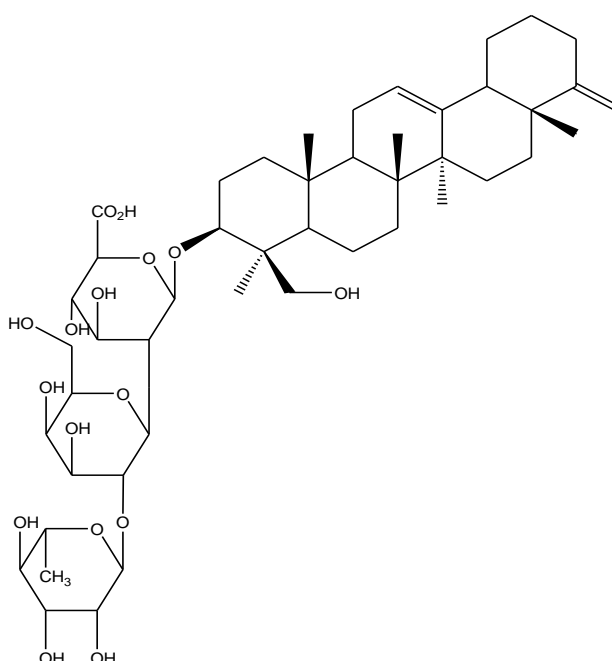
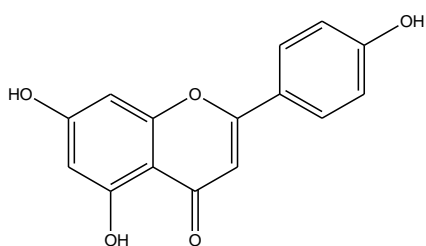
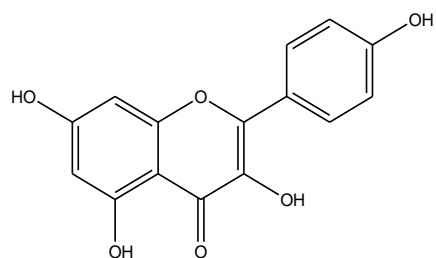


Figure 2.1.2.4 Chemical structures of naturally-derived openers of the BK channel (i) maxikdiol, an isoprimane diterpenoid, is a membrane-impermeable weak activator of BK channels comprising α subunits alone; (ii) primaric acid, a diterpene, can activate BK channels comprising α subunits alone; (iii) dihydrosoyasaponin-1 (DHS-1), a glycosylated triterpene and potent BK activator, derived from the medicinal herb Desmodium adscendens, which increases the open probability of channels co-expressing α plus β subunits. Lipid bilayer experiments have shown DHS-1 is strongly voltage-dependent and increases the open probability of BK channels only when acting from the cytosolic side of the cell membrane [111, 121, 122, 131].

(i)



(ii)



(iii)

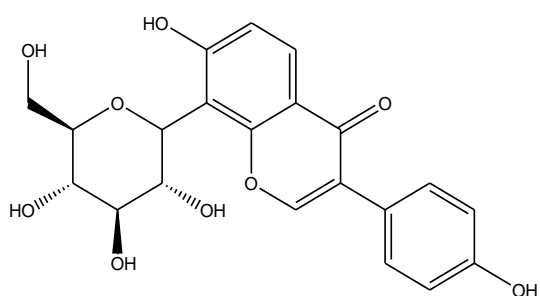


Figure 2.1.2.5 *Flavonoids, and isoflavonoids (phytoestrogens), have been reported to have BK activating properties (i) apigenine and (ii) kaempferol activate BK channels in Xenopus laevis expressing mSlo BK channels [118, 124]. These flavenoids were identified using a 3-D pharmacophore model based on NS-004 [132] (iii) the isoflavonone puerarin is reputed to effect a concentration-dependent vasodilation in rat aorta [133, 134].*

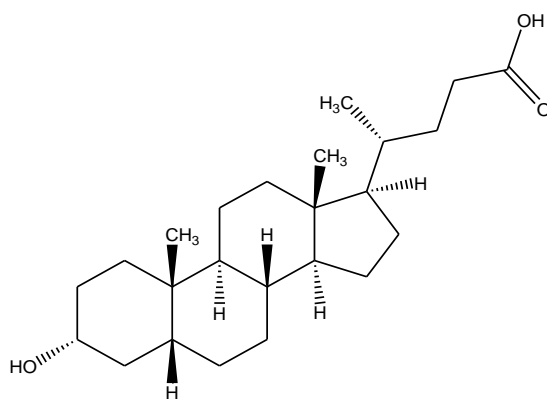


Figure 2.1.2.6 *Lithocholate is an endogenous cholane-derived steroidal BK activator which has been reported to possess β_1 subunit-dependent vasorelaxant properties both in rabbit mesenteric smooth muscle cells and in myocytes isolated from small, resistance-size arteries in rats [126, 135].*

2.1.3 Sex-steroids as endogenous BK modulators and their structural analogues

It is well-documented that oestrogens and their non-steroidal synthetic analogues are able to activate BK channels in smooth muscle cells when in the presence of the β_1 subunit [40, 102, 136]. However, Valverde *et al.*, were the first to report oestrogens bind and activate BK channels, comprising α and β_1 subunits, in a non-genomic way *via* an extra-cellular binding site. These workers coupled the steroid to a membrane-impermeable protein (bovine serum albumin) and applied it, extracellularly, to patches excised from *Xenopus laevis* oocytes expressing both α and β_1 BK subunits [102]. This study prompted other workers to exploit further, possible novel oestrogen-based BK modulators. Indeed, non-steroidal oestrogens (xenoestrogens) such as ICI182,780 (*Faslodex*[™]) [127], toremifene, tamoxifen and its membrane-impermeable analogue, ethylbromide tamoxifen (EBT), are also reported to possess BK

modulating properties alongside compounds containing only partial structures of tamoxifen such as diethylstilbestrol (DES) [104, 128] (Figure 2.1.3.1). Nevertheless, none of these compounds are particularly potent and in reality, some have been found to be promiscuous blockers of a variety of plasma membrane ion channels e.g. voltage-gated sodium channels, delayed rectifier potassium channels and swell-activated chloride channels [137-140]. Zhang *et al.*, for example, demonstrated block of swell-activated chloride channels by tamoxifen [141, 142] and work done by Allen *et al.*, revealed tamoxifen as a non-competitive blocker of 5-HT₃ receptors channels [137]. Furthermore, this group established that EBT inhibits 5-HT₃ receptors in NG108 cells which supports the accepted paradigm of an extracellular binding site for antioestrogens [104, 143].

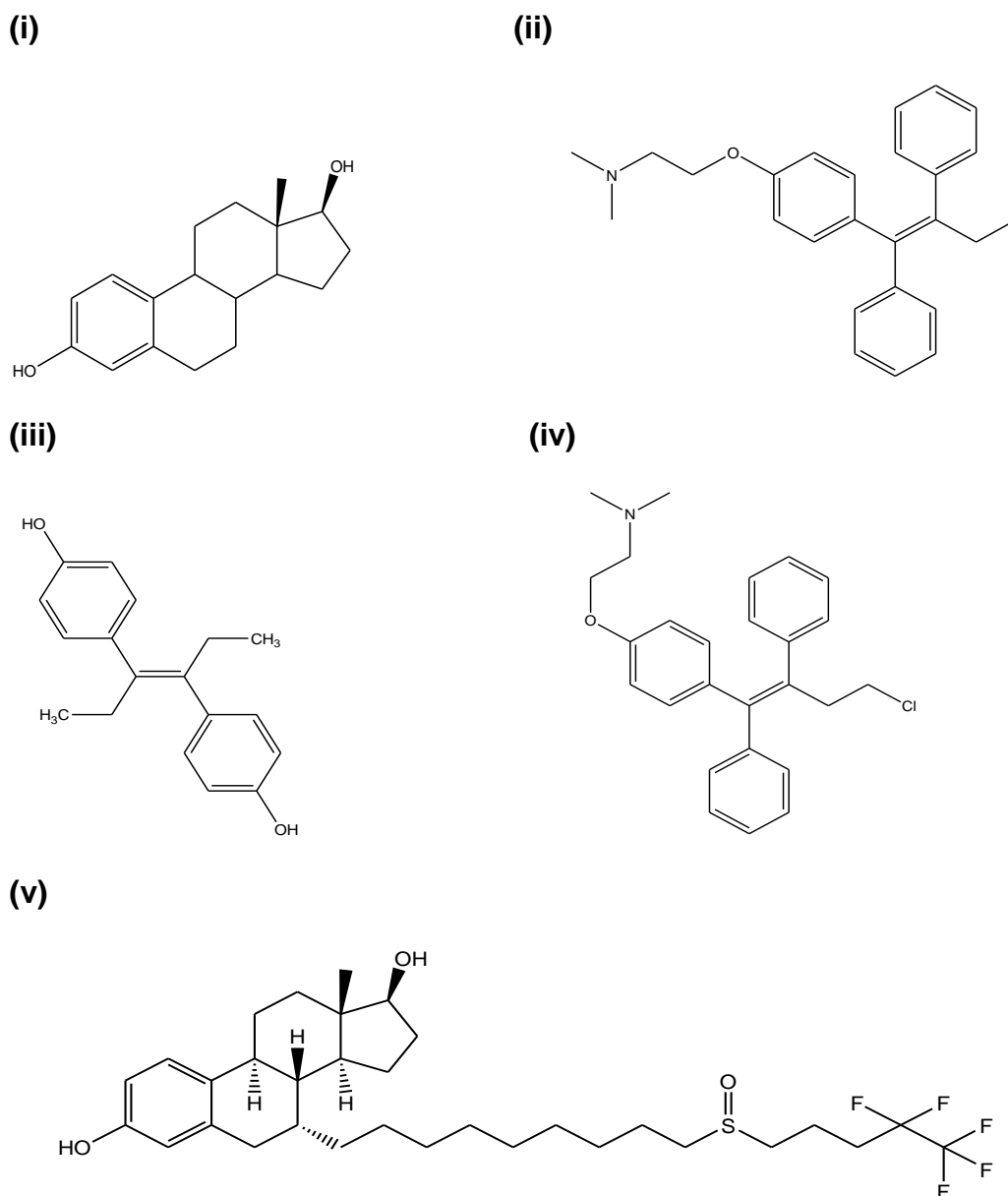


Figure 2.1.3.1 Chemical structures of steroidal BK modulators and structural derivatives. (i) 17β-oestradiol, a potent BK activator in the presence of β₁ subunits, is the predominant circulating oestrogen in humans and purported as cardio-protective; (ii) the xenoestrogen tamoxifen, an oestrogen receptor antagonist, is able to activate BK channels at therapeutic concentrations when the β₁ subunit is present. Conversely, it is a promiscuous inhibitor of a number of other plasma membrane ion channels [144]; (iii) diethylstilbestrol, a chemical modulator of BK channels incorporating a partial structure of tamoxifen but with more potency than tamoxifen. This compound was used to prevent miscarriages between the 1940s and 1970s [145]; (iv) toremifene, a non-steroidal xenoestrogen structurally related to tamoxifen; (v) ICI182,780 (Faslodex™), a synthetic antagonist of oestrogen receptors, suppresses Ca²⁺ current and stimulates BK activity in vascular smooth muscle cells but conversely inhibits BK activity in endothelial cells [127, 146].

2.1.4 Synthesis of vasodilators from known BK activators

The BK channel in vascular smooth muscle with its associated regulatory β_1 subunit is thought to be a valid chemotherapeutic target for the possible treatment of hypertension. Nonetheless, any BK activator would need to be BK selective and activate through a non-genomic pathway. Consequently, the synthesis of novel steroidal oestrogenic compounds, which incorporate some of the structural motifs of the non-steroidal antioestrogens class of drugs, may facilitate structure optimisation which may preclude oestrogenic genomic effects.

2.1.4.1 Chemical starting points – Oestrone, tamoxifen, ethylbromide tamoxifen and novel xenoestrogens derivatives

Oestrone was chosen as the parent compound because of its ketone structure which makes it an ideal starting compound for the etherification reaction during synthesis. Alternative endogenous oestrogens such as oestradiol or oestriol, would lead to a mixture of etherification products whereas Oestrone guarantees a single reaction product as etherification can only take place on the phenolic group.

Using Oestrone as a parent compound, novel xenoestrogens were synthesised retaining the *N,N*-dimethylethanamine functional group of the known BK activator tamoxifen and the quaternary ammonium group of its membrane-impermeant derivative, ethyl bromide tamoxifen (EBT) (Figure 2.1.4.1.1).

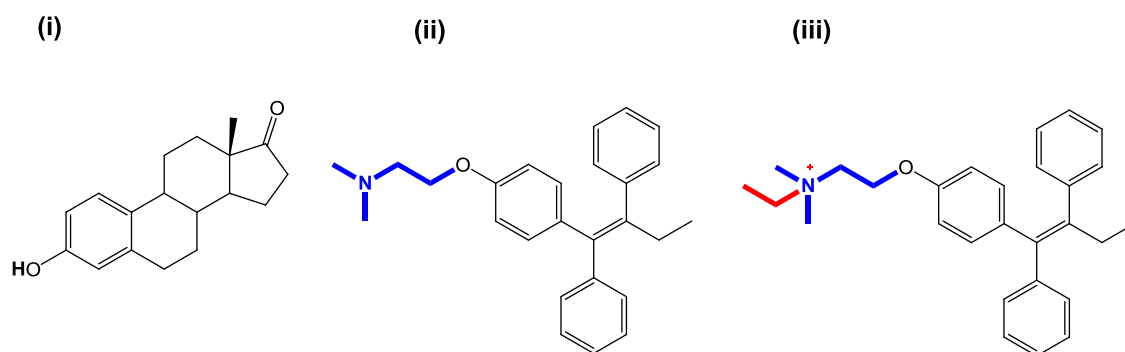


Figure 2.1.4.1.1 Structures of chemical starting points involved in the synthesis of novel xenoestrogens as possible BK activators and subsequent novel xenoestrogens (i) Oestrone, an endogenous steroidal oestrogen used in this study as the parent compound; (ii) tamoxifen is a partial agonist to the nuclear oestrogen receptor. The N,N -dimethylethanamine group, highlighted in blue, will be incorporated into the novel xenoestrogens; (iii) ethylbromide tamoxifen, the quaternary analogue of tamoxifen, has a positively charged side chain quaternary ammonium group, highlighted in red, which renders the compound membrane-impermeant, thus, providing potential activation of the BK channel via a non-genomic pathway.

Five compounds were synthesised in all, 3-(2-Dimethylamino-ethoxy)-Oestrone (DME-Oestrone); Quaternary-DME-Oestrone (Quat-DME-Oestrone); 3-(2-Dimethylamino-ethoxy)-Oestradiol (DME-Oestradiol); Quaternary-DME-Oestradiol (Quat-DME-Oestradiol) and Oestrone-Oxime. All novel derivatives incorporated the steroidal backbone of Oestrone comprising 20 carbon atoms formed in the classic arrangement of four conjoined cycloalkane rings, designated by the *International Union of Pure and Applied Chemistry* (IUPAC) as A, B, C and D. The three cyclohexane rings are A, B and C, and the cyclopentane ring is designated as D (Figure 2.1.4.1.2).

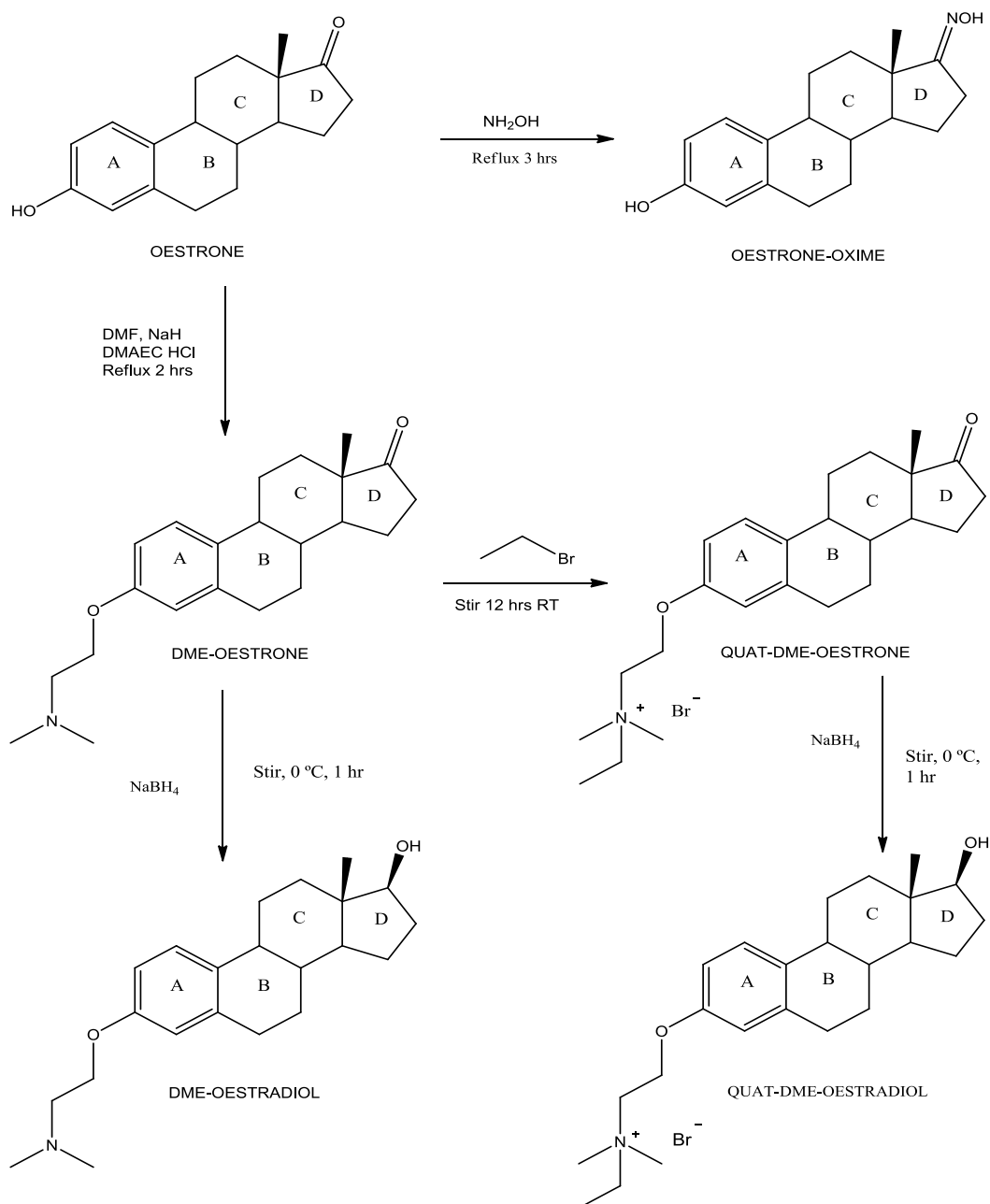


Figure 2.1.4.1.2 Chemical mechanisms for the synthesis of five oestrogen derivatives from the parent compound Oestrone. The derivatives incorporate the steroidal backbone of Oestrone, comprising the four characteristic conjoined cycloalkane rings designated A, B, C, D by the International Union of Pure and Applied Chemistry (IUPAC), and, with the exception of Oestrone-Oxime, the N,N-dimethyl-2-phenoxyethanamine side chain present in the tamoxifen molecule. Employing an etherification reaction based on the Williamson Ether Synthesis [147], 3-(2-Dimethylamino-ethoxy)-Oestrone (DME-Oestrone) was synthesised and used as a starting point for three other novel xenoestrogens - Quaternary-DME-Oestrone; 3-(2-Dimethylamino-ethoxy)-Oestradiol (DME-Oestradiol); Quaternary-DME-Oestradiol. The Oestrone-Oxime was also synthesised.

2.1.5 AIMS

The aim of this chapter is to synthesise novel xenoestrogens which incorporate some of the structural motifs of two known BK activators, tamoxifen and ethylbromide tamoxifen, and the steroidal back-bone of the endogenous oestrogen, Oestrone.

The starting compound Oestrone will undergo etherification and the 3-(2-dimethylaminoethoxy) (DME) group will substitute for the phenolic group on the A ring. Oestrone is the ideal starting compound for this reaction because the use of an alternative endogenous oestrogen such as oestradiol or oestriol, would lead to a mixture of etherification products. With Oestrone, a ketone, etherification can only take place on the A ring, helping to guarantee a single reaction product. This key substitution will produce the first compound which can be further alkylated to produce quaternary derivatives, or reduced to produce oestradiol analogues. Reduction of the ketone in the 17 position will produce the secondary alcohol group found in oestradiol.

Alkylation of the nitrogen to produce novel quaternary ammonium derivatives of compounds is a classical technique for studying the mode of action of tertiary amine type ligands. For example, the quaternary analogues of lignocaine will only inhibit sodium channels if injected directly into the cytoplasm, being completely inactive if applied to the outside of the neuron [148]. The parent compound lignocaine being a tertiary amine can cross the cell membrane and can work from either side of the membrane. Thus, quaternary amines are valuable in determining which side of the cell membrane amine drugs work. This technique has been applied to the study of non-steroidal oestrogens by the

Hardy research group [143]. They demonstrated that antioestrogens such as tamoxifen and quaternary antioestrogens such as ethylbromide tamoxifen could inhibit ligand-gated ion channels such as nicotinic and 5HT₃ receptors from the extracellular side of NG108 cell membranes whereas, in the same cell, only the cell-permeable tamoxifen could inhibit delayed rectifier potassium channels which requires access to the intracellular side of the channel [143].

In this study, the development of novel steroidal oestrogens and xenoestrogens aims to extend previous valuable work in the field of non-steroidal oestrogens done by the Hardy research group which supports the idea that the binding site for antioestrogens is extracellular and not mediated through genomic/transcriptional activity [143].

2.2 METHODS

2.2.1 Chemicals, reagents and analytical apparatus

- All chemicals and reagents used were supplied by the *Aldrich Chemical Company (UK)* and were of analytical grade.
- A spray of 50% sulphuric acid and 50% methanol was used to develop the thin layer chromatography plates.
- Silica for chromatography was *Merck 9385*.
- Thin layer chromatography (TLC) was performed with *Macherey-Nagel Alugram® SIL G/UV₂₅₄* plates.
- For ¹H NMR, ¹³C NMR, compounds were analysed in deuteriochloroform using tetramethylsilane or deuteriopyridine as an internal standard.
- ¹H NMR and ¹³C NMR spectra were recorded on a *Bruker WM 360* Spectrometer at 360 and 90 MHz, respectively.
- Infra-red absorption spectra were recorded on a *Nicolet Avatar 320 FT-IR* fitted with a *Smart Goldengate®*.
- Melting points were determined on an electrothermal melting point apparatus and uncorrected for temperature and pressure.

2.2.2 Synthesis of DME-Oestrone

The etherification pathway, based on the Williamson ether synthesis, was a two stage process (see Figure 2.2.2.1) using Oestrone as a starting material, and is described after a method of Auger *et al.*,[147]. A mixture of Oestrone (18.5 mmol), dimethylformamide (DMF 60 ml), and sodium hydride (3.75 mmol of NaH 60% dispersion in mineral oil) was stirred at 40°C for 2 hours. The mixture

was then cooled to 25°C and 2-dimethylamine ethyl-chloride (12.5 mmol) was added. A condenser was fitted and the mixture was left stirring at 40°C for 12 hours. The reaction was cooled to 0°C on ice, after which, the reaction was quenched by adding water and a saturated sodium hydrogen carbonate (NaHCO₃) solution. The aqueous phase was extracted with ethyl acetate (EtOAc). The solvent was evaporated using rotary evaporation, after which, the collected compound was attached to a high-powered vacuum pump for 12 hours to dry out. The compound was isolated by column chromatography (solid phase - silica gel, eluent – ethyl acetate: methanol (80: 20)). The isolated compound was confirmed using thin layer chromatography (TLC, by appearance of a single spot on silica gel *ALUGRAM* pre-coated TLC sheets. The TLC bath contained MeOH: EtOAc (20:80) (40 ml) and the spots were visualised using a spray of MeOH and sulphuric acid (5%). Isolated yield from starting compound (5g) - DME-Oestrone 3.94g (79%). Crystals were formed by dissolving the product in MeOH, after which, EtOAc was added drop wise. This was left overnight to crystallise at room temperature.

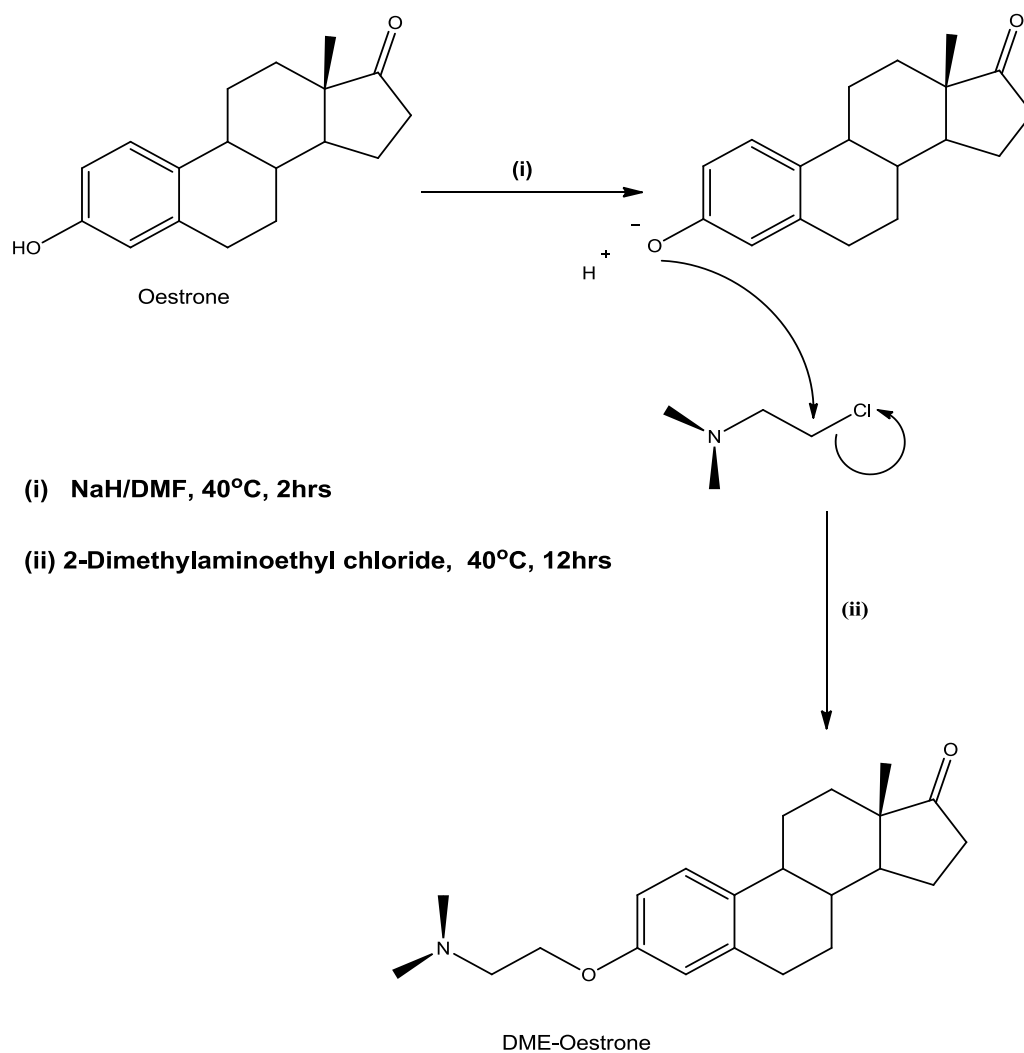


Figure 2.2.2.1 The synthesis of DME-Oestrone from Oestrone. The synthesis is based on the Williamson Ether Synthesis. Sodium hydride (NaH) is basic enough to deprotonate the alcohol function (OH) i.e. it facilitates removal of the phenolic proton to produce the alkoxide or conjugal base. Molecular hydrogen (H₂) is generated from this reaction (so it is necessary to avoid any source of ignition). Then, a bimolecular nucleophilic substitution (S_N2) occurs with 2-dimethylaminoethyl chloride to form the novel compound 3-(2-Dimethylamino-ethoxy)-Oestrone (DME-Oestrone).

2.2.3 Synthesis of Quat-DME-Oestrone

To synthesise the quaternary amino form of DME-Oestrone, the compound (DME-Oestrone) was prepared as described previously in section 2.2.2. The prepared compound was reacted with ethylbromide by stirring overnight at room temperature. The solvent was evaporated using rotary evaporation after which, the collected compound was attached to a high-powered vacuum pump for 12 hours to dry out. The compound was isolated by column chromatography (solid phase - silica gel, eluent - EtOAc: methanol (80: 20). The isolated compound was confirmed, using thin layer chromatography (TLC), by appearance of a single spot on silica gel *ALUGRAM* pre-coated TLC sheets. The TLC bath contained MeOH: EtOAc (20:80) (40 ml) and the spots were visualised using a spray of MeOH and sulphuric acid (5%). In this reaction, the lone pair of electrons around the nitrogen attacks the polarised carbon on the ethylbromide. In order to attain optimal energetic stability the electron pair goes to form Br⁻ and hence becomes a leaving ion, so as the quaternary is generated, Br⁻ becomes a counter-ion balancing the charge (Figure 2.2.3.1).

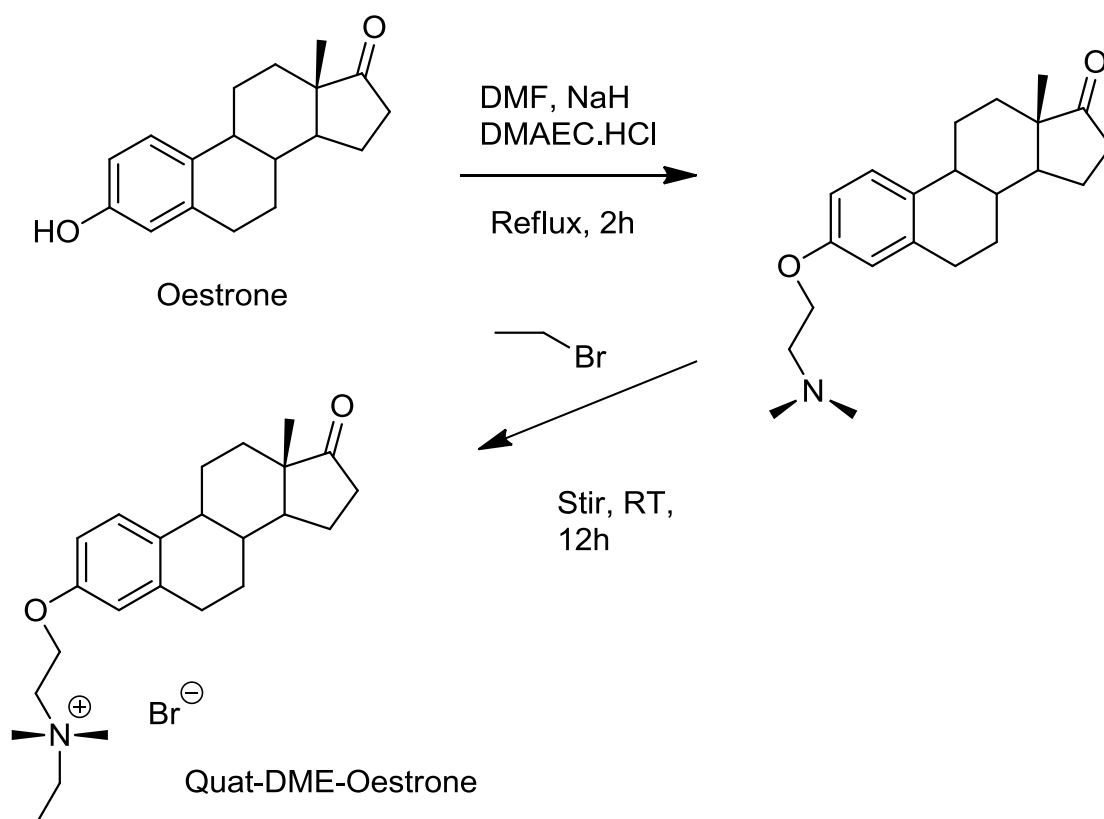


Figure 2.2.3.1 Compound synthesis and characterisation of the quaternary form of DME-Oestrone (Quat-DME-Oestrone). In order to attain optimal energetic stability, the electron pair goes to form Br^- and hence becomes a leaving ion, so as the quaternary is generated, Br^- becomes a counter-ion balancing the charge.

2.2.4 Synthesis of DME-Oestradiol

The reduction of DME-Oestrone was effected to form the compound, DME-Oestradiol (Figure 2.2.4.1). The compound (DME-Oestrone) was prepared as described previously in section 2.2.2. Compound 1 (2g) was dissolved in dry methanol (80 ml) and treated with sodium borohydride (500 mg) at 0°C. The reaction mixture was stirred for 1 hour when thin layer chromatography showed that the reaction was complete. Acetic acid (1 ml) was added and the solvent removed *in vacuo* to afford compound 2, the reduced DME-Oestrone, 3-(2-Dimethylamino-ethoxy)-Oestradiol (DME-Oestradiol).

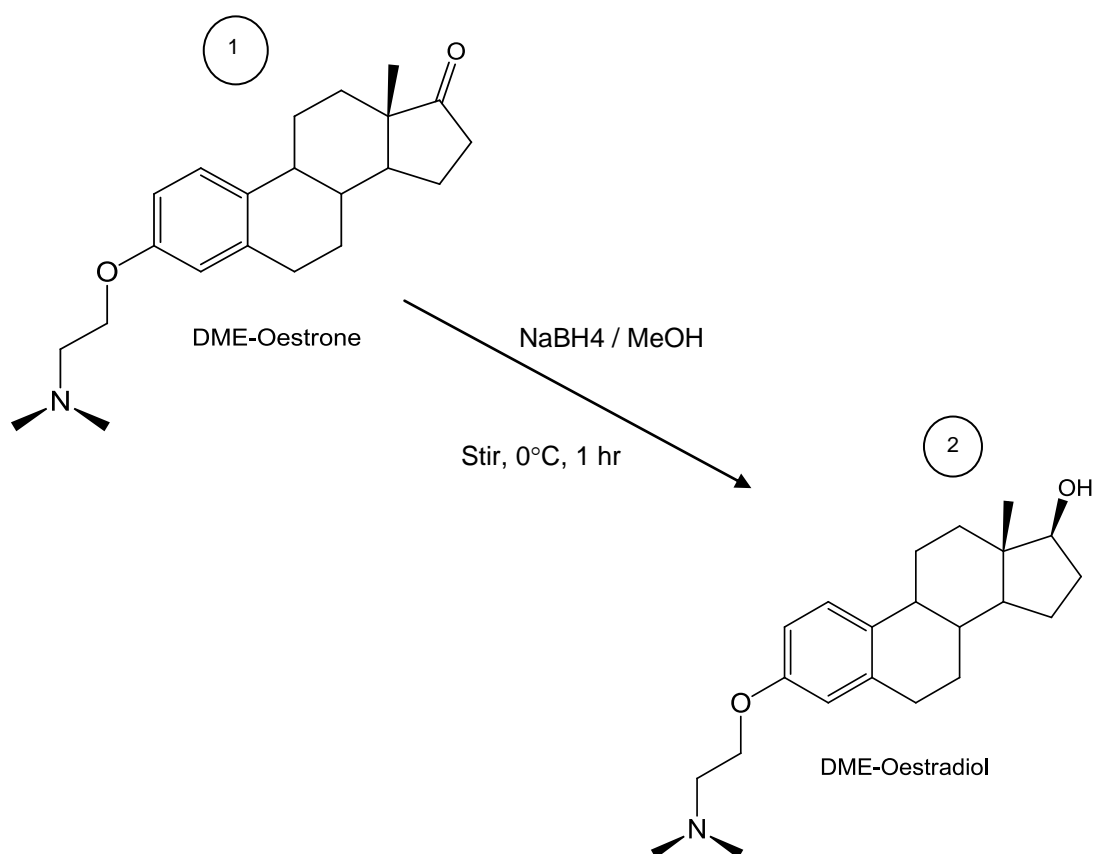


Figure 2.2.4.1 Compound synthesis and characterisation of the reduction of DME-Oestrone (compound 1) to afford 3-(2-Dimethylamino-ethoxy)-Oestradiol (compound 2), (DME-Oestradiol).

2.2.5 Synthesis of Quat-DME-Oestradiol

The reduction of the quaternary amino form of DME-oestrone was effected to form the compound Quat-DME-oestradiol (Figure 2.2.5.1). The compound 1, Quat-DME-Oestrone, was prepared as described previously in section 2.2.3. Compound 1 (2g) was dissolved in dry methanol (80 ml) and treated with sodium borohydride (500 mg) at 0°C. The reaction mixture was stirred for 1 hour when thin layer chromatography showed that the reaction was complete. Acetic acid (1 ml) was added and the solvent removed *in vacuo* to afford compound 2, the reduced Quat-DME-Oestrone (Quat-DME-Oestradiol).

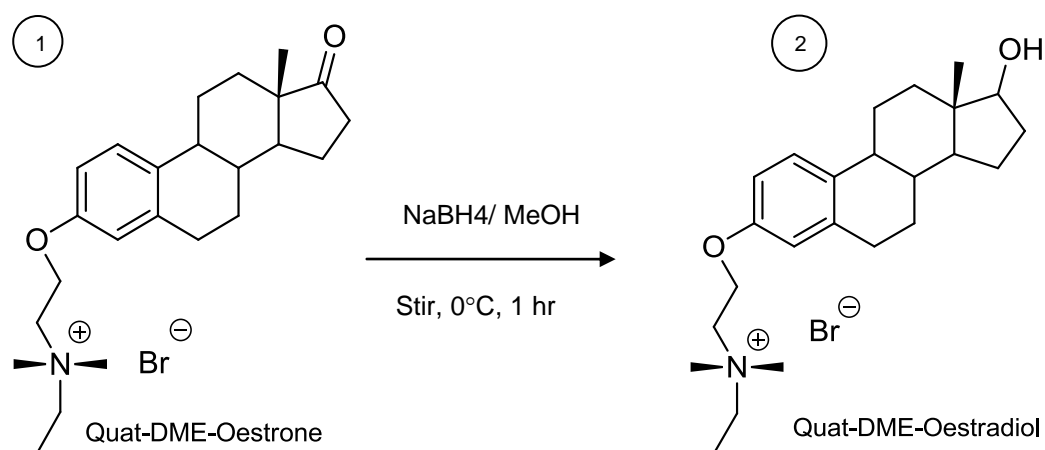


Figure 2.2.5.1 Compound synthesis and characterisation of the reduction of Quat-DME-Oestrone (compound 1) to afford Quat-DME-Oestradiol (compound 2).

2.2.6 Synthesis of Oestrone-Oxime (17-hydroximino-estra-3-ol)

A solution of oestrone (2 g) in ethanol (60 ml), hydroxylamine hydrochloride (1 g) and pyridine (6 ml) was refluxed for 2 hours. The mixture was then poured into ice which caused the formation of a white precipitate. The precipitate was filtered through a sintered funnel and washed with water. The compound was dissolved in ethanol and stirred for 12 hours at room temperature. The solvent was evaporated using rotary evaporation after which, the collected compound was attached to a high-powered vacuum pump for 12 hours to afford 17-hydroximino-estra-3-ol as clear, needle-like crystals (Figure 2.2.6.1).

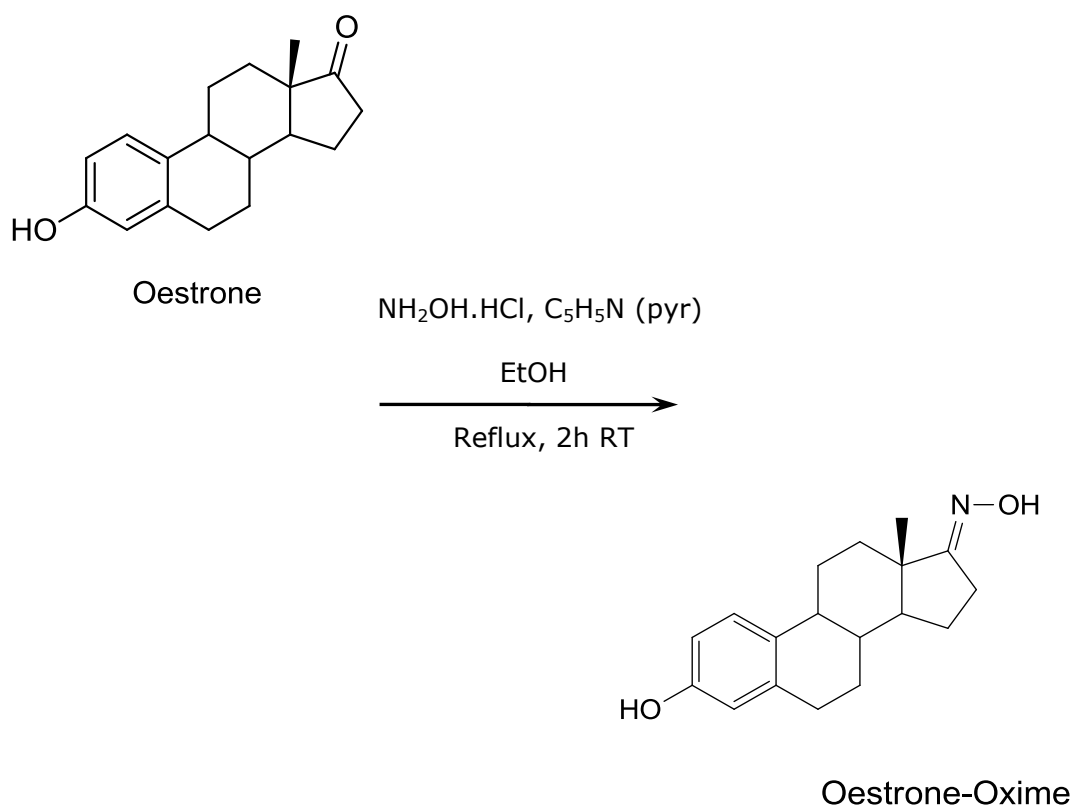


Figure 2.2.6.1 Compound synthesis and characterisation of the Oestrone-Oxime (17-hydroximino-estra-3-ol) from the starting material Oestrone.

2.3 RESULTS

To provide confirmation of structure, functionality and purity of the compounds, the following analytical assessments were implemented

- thin layer chromatography
- characteristic shift values in the ^{13}C NMR [149] in combination with DEPT (distortion enhancement by polarisation transfer) analysis
- characteristic shift values in the ^1H NMR [150]
- infra-red absorption spectroscopy
- melting point
- crystallography and elemental analysis.

2.3.1 ^{13}C NMR of starting compound, Oestrone, and novel derivatives

The ^{13}C NMR is used as an analytical tool in organic chemistry to elucidate the carbon skeleton of an organic molecule. Each peak identifies a carbon atom in a different environment within the molecule thus revealing how many different carbons are present. The splitting of a signal reveals the amount of protons attached to each carbon, and the chemical shift demonstrates the hybridisation of atomic orbitals (sp^3 , sp^2 , sp) for each carbon atom.

Distortion enhancement by polarisation transfer analysis (DEPT) determines the presence of primary (CH), secondary (CH_2) and tertiary (CH_3) carbon atoms present in the analyte. Quaternary carbons typically produce no DEPT signal due to their lack of protons. A full presentation of the results gained from ^{13}C NMR and DEPT analysis are shown in Table 2.3.1.1. Full interpretation of these signals is reported in Section 2.4.

Table 2.3.1.1 ^{13}C NMR of starting compound (Oestrone and derivatives in deuterated chloroform (CDCl_3) or pentadeuteropyridine ($d_5\text{-pyr}$) in ppm.

Carbon atom	Compounds					
	(a)	(b)	(c)	(d)	(e)	(f)*
1	115.28	111.09	113.27	112.10	112.00	116.78
2	126.53	113.55	115.57	114.60	114.82	127.39
3	132.11	155.77	156.86	155.04	156.65	131.71
4	112.82	125.17	127.65	126.33	126.81	114.38
5	138.06	136.59	139.39	136.26	138.17	138.58
6	29.47	28.54	30.66	29.80	27.56	28.13
7	26.49	25.46	27.64	27.27	26.79	27.23
8	38.35	37.26	39.81	38.86	37.41	39.12
9	43.96	42.88	45.33	43.27	42.00	45.00
10	153.48	131.00	134.71	131.09	131.00	157.23
11	25.92	24.81	27.08	43.98	23.41	26.14
12	31.57	30.49	32.80	30.61	30.03	30.41
13	48.03	46.91	48.30	43.98	44.34	44.59
14	50.41	49.32	49.01	50.07	44.42	53.80
15	21.59	20.48	22.51	21.48	22.00	23.67
16	35.88	30.49	36.73	28.33	30.91	35.58
17	221.10	219.80	219.80	81.84	81.20	169.41
18	13.86	12.75	14.28	11.08	11.67	18.09
19		64.84	63.78	65.91	66.55	
20		57.26	62.84	58.34	58.53	
21		44.79	48.77	44.21	45.88	
22		44.79	48.54	44.21	45.85	
23			62.84		50.24	
24			8.61		39.22	

Key: (a) Oestrone; (b) DME-Oestrone; (c) Quat-DME-Oestrone; (d) DME-Oestradiol; (e) Quat-DME-Oestradiol; (f) Oestrone-Oxime ($\star = d_5\text{-pyr}$). See structure obtained from x-ray crystallography for position of numbered carbons (Figure 2.4.1.1.1).

2.3.2 Analysis and identification of compounds

Nuclear magnetic resonance (^{13}C NMR and ^1H NMR) determines the carbon-hydrogen framework of an organic compound. To determine the purity and structure of a compound, a variety of additional analytical assessments can be carried out, including elemental analysis, melting point, x-ray crystallography, infra-red (IR) and high resolution mass spectroscopy (HRMS ESI). The following sections detail the data collected for the novel synthesised compounds using these techniques.

2.3.2.1 Analytical assessment DME-Oestrone

The melting point was determined as 113 - 115°C. The purity of DME-Oestrone was greater than 99% as determined by elemental analysis. Elemental analysis found C, 77.25; H, 9.07; N, 4.08; O, 9.37; $\text{C}_{22}\text{H}_{31}\text{NO}_2$ requires C, 77.38; H, 9.15; N, 4.10; O, 9.37%; ^1H NMR spectrum was δH (360MHz; CDCl_3): 0.90 (3H, s, 18-H₃), 2.33 (6H, s, N-(CH₃)₂), 4.04 (4H, t, J 5.6 Hz, 19-H₂), 6.66 (1H, s, 4-H), 6.72 (1H, d, J 2.3 Hz, 1-H), 7.20 (1H, d, J 2.3 Hz, 2-H); IR_{max} cm⁻¹: 1736, 1604, 1304 and 854; HRMS ESI: calc. for $\text{C}_{22}\text{H}_{32}\text{NO}_2$: 342.24276; observed 342.24214 m/z.

2.3.2.2 Analytical assessment Quat-DME-Oestrone

Due to the deliquescent nature of quaternary compounds, melting point and elemental analysis could not be implemented. ^1H NMR spectrum was δH (360MHz; CDCl_3): 0.93 (3H, s, 18-H₃), 1.45 (3H, t, J brs, 24-H₃), 3.26 (6H, s, N(CH₃)₂), 3.57 (2H, q, J 7Hz, 19-H), 3.81 (2H, m, $w/2$ 4.6 Hz 20 H), 4.44 (2H, s,

23-H), 6.75 (1H, s, 4-H), 6.78 (1H, d, J 8.6 Hz, 1-H), 7.25 (1H, d, J 8.6 Hz, 2-H); IR_{vmax} cm⁻¹: 1730, 1607, 1304 and 847; HRMS ESI: calc. for C₂₄H₃₆NO₂: 370.274; observed 370.275 *m/z*.

2.3.2.3 Analytical assessment DME-Oestradiol

The melting point and elemental analysis could not be implemented as compound was deliquescent and not crystalline. ¹H NMR spectrum was δ_H (360MHz; CDCl₃): 0.77 (3H, s, 18-H₃), 2.32 (6H, s, N-(CH₃)₂), 2.71 (2H, t, J 5.8 Hz, 20-H₂), 3.71 (1H, t, J 8.5 Hz, 17α-H), 4.05 (1H, t, J 5.8 Hz, 19-H₂), 6.65 (1H, d, J 8.5 Hz, 1-H), 7.20 (1H, d, J 8.5 Hz, 2-H); IR_{vmax}: 3407, 3339, 3046 cm⁻¹; HRMS ESI: calc. for C₂₂H₃₄NO₂: 344.25841; observed 344.25835 *m/z*.

2.3.2.4 Analytical assessment Quat-DME-Oestradiol

The melting point was determined as 237 - 243°C. ¹H NMR spectrum was δ_H (360MHz; ds - pyr): 0.77 (3H, s, 18-H₃), 1.48 (3H, s, 24-H₃), 3.40 (2H, s, 23-H), 3.75 (1H, t, J 8.5Hz), 4.28 (1H, brs, 20-H), 4.46 (1H, brs, 21-H), 6.82 (1H, s, 4-H), 6.94 (1H, d, J 8.5 Hz, 1-H), 7.30 (1H, d, J 8.5 Hz, 2-H) ; IR_{vmax} 3341, 3047cm⁻¹ HRMS ESI: calc. for C₂₄H₃₈NO₂: 372.289706; observed 372.288527 *m/z*.

2.3.2.5 Analytical assessment Oestrone-Oxime

The melting point was determined as 249-251°C. ¹H NMR spectrum was δ_H (360MHz; ds - pyr): 0.95 (3H, s, 18 H₃), 6.98 (1H, d, J 2.4 H₃, 4-H), 7.06 (1H, d,

J 2.4H₃, 1-H), 7.08 (1H, d, J 2.4H₃, 2-H); IR_{νmax}: 3414, 3212, 1681; cm⁻¹HRMS

ESI: calc. for C₁₈H₂₄N₂O: 286.181; observed 286.180 m/z .

2.4 PROOF OF COMPOUNDS

The structural determination and ensuing proof of each novel compound were verified by comparing chemical shifts in conjunction with appearances and disappearances of significant signals in the spectra of the ^1H NMR, ^{13}C NMR, infra-red and mass spectroscopy data. All compounds ran as a single spot on TLC plates demonstrating a lack of contamination by the starting material.

2.4.1 Structural determination of DME-Oestrone

Etherification of oestrone at the 3-alcohol position was confirmed following comparison of its spectra to that of oestrone. The ^1H NMR spectrum contained new resonance signals for the N-dimethyl and ethyl side chain at 2.33 ppm (6H) and 4.04 ppm (4H, t, $J = 5.6$ Hz). This structure was further supported by new signals in the ^{13}C NMR spectrum at 44.79 ppm (N-dimethyl), 57.26 ppm (C-20) and 64.84 ppm (C-19) (see Table 2.3.1.1). Attachment of this functionality was fully supported by accurate mass determination where HRMS ESI found 370.275, $\text{C}_{22}\text{H}_{31}\text{NO}_2$ requires 370.274. In addition, the lack of a phenolic OH stretch within the IR spectra demonstrates complete etherification of Oestrone. Absolute proof of structure was provided by single x-ray crystallography.

2.4.1.1 Crystallographic structure determination of DME-Oestrone

$\text{C}_{22}\text{H}_{31}\text{NO}_2$, Mr 341.48: triclinic space group P1 (No 1), $a = 7.0115(3)$, $b = 7.7771(3)$, $c = 8.9911(4)$ Å, $\alpha = 79.365(3)^\circ$ $\beta = 82.760(2)^\circ$ $\gamma = 83.184(2)^\circ$, $V = 475.72(3)$ Å³, $Z = 1$, $D = 1.19$ Mg/m³, $u = 0.08$ mm⁻¹, $F(000)$ 186. Data were collected using a crystal of dimension 0.4 x 0.4 x 0.4 mm³ on a KappaCCD

diffractometer. A total of 5,898 reflections were collected for $3.55 < \theta < 26.01$. There were a total of 1,836 independent reflections and 1,799 reflections with $I > 2\sigma(I)$ used in the refinement. No absorption correction was applied. The structure was solved by direct methods and refined using SHELXL-97. The diagrams used ORTEP-3 for *Windows*. The final R indices were $R_1 = 0.034$, $wR_2 = 0.093$ and R indices (all data) $R_1 = 0.036$, $wR_2 = 0.095$. The goodness-of-fit on F^2 was 0.999 and the largest difference peak and hole was 0.19 and -0.17 e. \AA^{-3} (Figure 2.4.1.1.1).

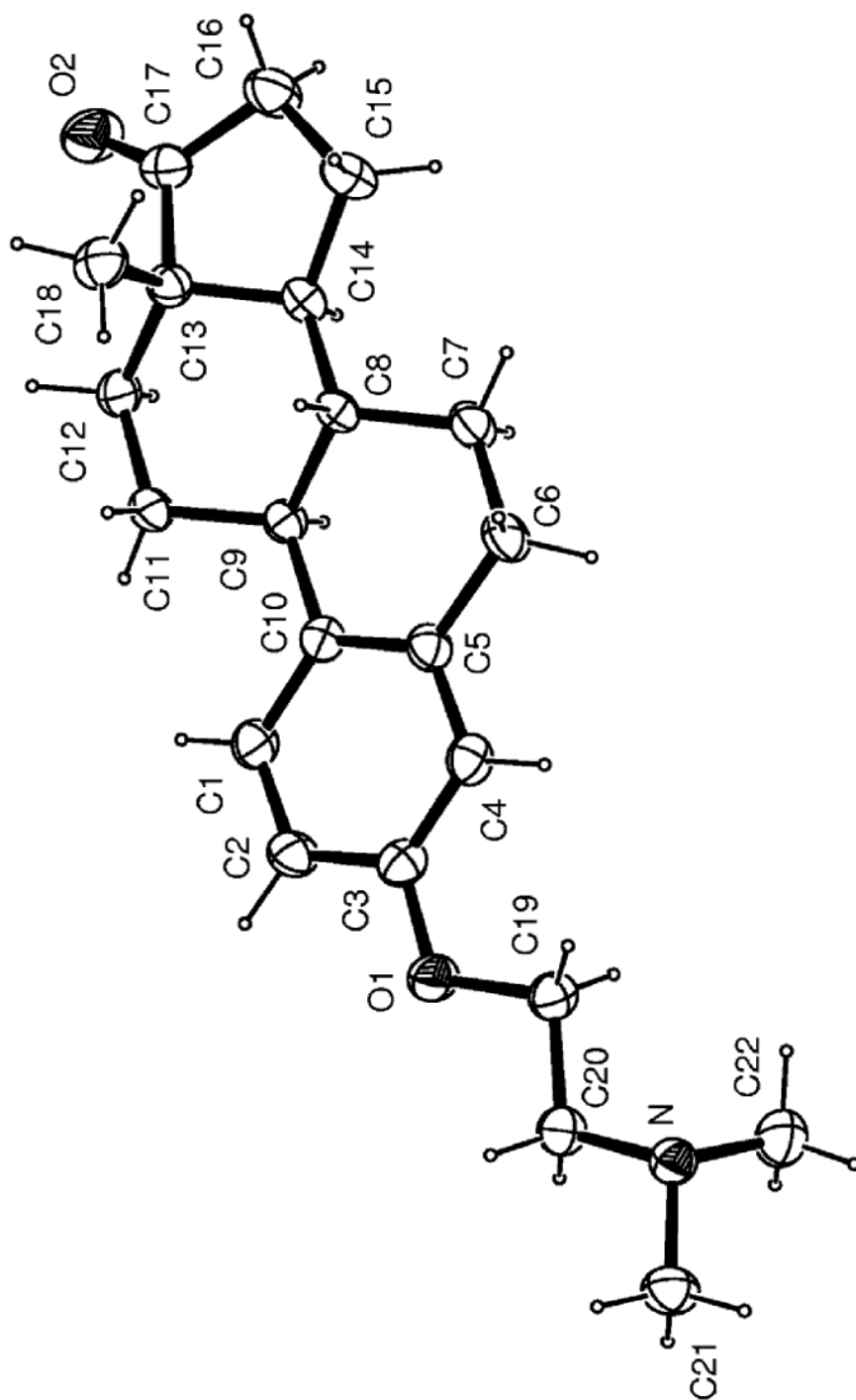


Figure 2.4.1.1.1 X-ray crystal structure of DME-Oestrone. Data collection KappaCCD. Program package WinGX. Refinement using SHELXL-97. Drawing using ORTEP-3 for Windows. (Data collected 06/03/2007).

2.4.2 Structural determination of Quat-DME-Oestrone

Comparison of the product spectra following quaternisation of DME-Oestrone revealed two new signals in the ^1H spectra consistent with the presence of a new methyl group (1.45 ppm, 3H, s, 23-H₃) and methylene (4.44 ppm, 2H, s, 23-H) in the ^1H NMR spectrum. This finding was reflected in the ^{13}C NMR spectrum with new resonance signals at 8.61 ppm (23-H₃) and 62.84 ppm (22-H) (see Table 2.3.1.1). Addition of the ethyl functionality to the starting material was confirmed by accurate mass determination. HRMS ESI found 370.275, $\text{C}_{24}\text{H}_{36}\text{NO}_2$ requires 370.274.

2.4.3 Structural determination of DME-Oestradiol

Reduction of the C-17 ketone, present in the starting material, was confirmed by NMR. The ^1H NMR spectrum of the product contained a new signal at 3.71 ppm (1H,t) fully consistent with the presence of a C-17 β alcohol. This was further supported in the ^{13}C NMR spectrum of the product, which was devoid of the 5 ring quaternary resonance ketone signal at 219.80 ppm (see Table 2.3.1.1). This had been replaced with a CHOH resonance signal at 81.84 ppm, which is fully consistent with the C-17 β alcohol, as was the infra-red absorption signal at 3339.14 cm^{-1} . The structure was also fully supported by accurate mass measurement with a signal at 344.25835 m/z consistent with the $\text{M}+\text{H}^+$ ($\text{C}_{22}\text{H}_{34}\text{NO}_2$) (344.25841). Finally, the loss of a ketone stretch within IR spectra demonstrated complete conversion of the C-17 ketone to C17 OH. In addition an OH stretch appeared in the IR spectra due to the production of the required secondary alcohol at position 17.

2.4.4 Structural determination of Quat-DME-Oestradiol

Formation of the quaternary ammonium bromide was confirmed by comparison of the product ^1H and ^{13}C spectra with that of DME-oestradiol. A new signal present in the ^1H NMR spectrum of the product at 1.48 ppm (3H, s) was fully supportive of the C-24 methyl group, as was the resonance signal at 39.22 ppm in the ^{13}C NMR spectrum. Presence of the C-23 methylene group was observed with a resonance signal in the ^1H NMR spectrum of the product at 3.40 ppm (2H, s) and at 50.24 ppm in the ^{13}C NMR spectrum consistent with the presence of the adjacent quaternary positively charged nitrogen (see Table 2.3.1.1). These data fully support the addition of the ethyl group, as did the accurate mass determination where HRMS ESI found: 372.289, $\text{C}_{24}\text{H}_{38}\text{NO}_2$ requires 372.289706. Further, the presence of the salt afforded improvement in the physicochemical properties of the molecule as witnessed by a much improved aqueous solubility profile.

2.4.5 Structural determination of Oestrone-Oxime

Oestrone was readily converted to the C-17 oxime derivative, the spectra of which were devoid of the carbonyl on the 5-membered ring-D (220.18 ppm) in the ^{13}C NMR spectrum of the product and the carbonyl absorption signal in the starting material infra-red spectrum at 1715 cm^{-1} . These were replaced with a new C-17 quaternary resonance signal at 169.41 ppm demonstrating an upfield shift of $\Delta 50.77$ ppm consistent with the reduction in the electronegative environment with the oxime (see Table 2.3.1.1). Molecular weight determination fully supported the proposed structure where HRMS ESI $\text{M}+\text{H}^+$ found 286.181, $\text{C}_{18}\text{H}_{24}\text{NO}_2$ requires 286.180.

2.4.6 Summary - Proof of compounds

Purity of compound is normally checked with 2 or 3 purity checks, the usual being chromatographic, a sharp melting point and ^{13}C or ^1H NMR. Structure is checked by a combination of IR, ^{13}C , ^1H NMR and mass spectroscopy. All the novel compounds were subjected to at least 3 purity and 4 structural tests. Table 2.4.6.1 illustrates that these compounds can be deemed pure with the correct structure and functional group.

Table 2.4.6.1 Summary table depicting proof of structure and purity.

TECHNIQUES USED TO CHECK PRODUCT PURITY											
Compound	TLC	Elemental analysis	mp range	Crystal structure	¹³ C NMR	¹ H NMR	IR	MS	Conclusion	No. of purity checks	No. of structure checks
Oestrone	Single spot ∴ precursor compound not present	-	258-260°C as per data sheet	commercially acquired	as expected	as expected	as expected	as data sheet	commercially acquired parent compound from Aldrich	4	4
DME-Oestrone	Single spot ∴ precursor compound not present	>99% purity	113-115°C	successfully attained	no evidence of any phenolic groups on carbon 3 ∴ precursor compound not present	as predicted	no evidence of any phenolic groups on carbon 3 ∴ precursor compound not present	MW consistent with presence N-dimethyl and ethyl side chain	>99% pure	6	4
Quat-DME-Oestrone	Single spot ∴ precursor compound not present	-	deliquescent	deliquescent compound	no evidence of any phenolic groups on carbon 3 ∴ precursor compound not present	as predicted	no evidence of any phenolic groups on carbon 3 ∴ precursor compound not present	MW consistent with presence of ethyl functionality	pure no contamination with parent compound Oestrone	3	4
Oestrone-Oxime	Single spot ∴ precursor compound not present	-	249-251°C	amorphous compound	devoid of ketone resonance. ∴ precursor compound not present	as predicted	Oxime group present no ketone stretch	MW consistent with presence of C-17 oxime quaternary functionality	pure no contamination with parent compound Oestrone	4	4
DME-Oestradiol	Single spot ∴ precursor compound not present	-	liquid	liquid compound	devoid of ketone resonance ∴ precursor compound not present	as predicted	presence of secondary C-17β-alcohol	MW consistent with presence of C-17β-alcohol	pure no contamination with parent compound DME-Oestrone	3	4
Quat-DME-Oestradiol	Single spot ∴ precursor compound not present	-	237-243°C	amorphous compound	devoid of ketone resonance ∴ precursor compound not present	as predicted	presence of secondary C-17β-alcohol	MW consistent with presence of ethyl group and C-17β-alcohol	pure no contamination with parent compound Quat-DME-Oestrone	4	4

TECHNIQUES USED TO CHECK PRODUCT STRUCTURE

Key: TLC (thin layer chromatography); mp (melting point); ¹³C NMR (carbon nuclear magnetic resonance); ¹H NMR (proton nuclear magnetic resonance); IR (infra-red spectroscopy); MS (mass spectroscopy); MW (molecular weight).

2.5 DISCUSSION

Oestrone is an endogenous circulating oestrogen in humans which, *in vivo*, is inter-convertible with oestradiol. Five novel xenoestrogens, DME-oestrone, Quat-DME-Oestrone, DME-Oestradiol, Quat-DME-Oestradiol and Oestrone-Oxime were successfully synthesised by the author utilising Oestrone as the parent compound. The novel compounds were designed to incorporate select structural motifs of known oestrogenic BK activators:-

- the steroidal structure of 17β -oestradiol
- the amine side chain of tamoxifen
- the positively charged side chain of ethyl bromide tamoxifen, a membrane-impermeant quaternary analogue of tamoxifen

The specific design of these novel xenoestrogens was intended to activate BK channels through a non-genomic pathway. Valverde *et al.*, successfully demonstrated oestrogens can activate $BK\alpha+\beta_1$ channels through a non-genomic pathway by coupling 17β -oestradiol to an albumin molecule (BSA) to afford cell impermeability [102]. However, this technique has been called into question as other workers have found that the relative binding efficiency of oestradiol-BSA conjugates is low and, thus, these molecules do not compete for oestradiol binding to oestrogen receptors *in vitro* [151]. Furthermore, oestradiol-BSA conjugates easily disassociate and leaching of free oestrogen invariably occurs [152]. In this study, the incorporation of the amine side chain motif of tamoxifen or the quaternary amine of EBT to oestrone, to afford DME-Oestrone and Quat-DME-Oestrone respectively, may offer an elegant alternative and negate the disadvantages of the addition of a large albumin

molecule while ameliorating any unwanted side-effects generated by tamoxifen (see Table 2.5.1).

Table 2.5.1 Comparison of advantages/disadvantages of oestradiol-bovine serum albumin (BSA) conjugates versus quaternary tagging.

Advantages Oestradiol-Bovine Serum Albumin conjugates	Advantages Quaternary tagging	Disadvantages Oestradiol-Bovine Serum Albumin conjugates	Disadvantages Quaternary tagging	
No expert organic chemical synthesis required	Small low molecular weight tag.	Between 5 – 10 oestradiol attached per molecule therefore stoichiometry variable	Requires organic chemical synthesis experience	
	Precise molecular weight and structure	Reported to leach free oestradiol during experiments [152]		
	Water soluble	Huge bulky 48 kDa tag		
		Unable to bind to oestrogen receptors after removal by filtration of free oestradiol [151]		
		Additional cross linking between more than one albumin to form albumin aggregates.		

However, the phenolic proton present in oestrogens may prove to be important in the activation of BK channels. If this phenolic proton is, indeed, important, then Oestrone and Oestrone-Oxime would be active while DME-Oestrone, DME-Oestradiol, Quat-DME-Oestradiol and Quat-DME-Oestrone would all be inactive as the phenolic proton at position three is lost or converted to an ether linkage in these compounds.

Five xenoestrogens were successfully synthesised and tested for purity before being pharmacologically evaluated in:-

- aortic rings in order to investigate selectivity for BK channels and other potential oestrogen targets
- HEK 293 cells expressing either α or $\alpha+\beta_1$ subunits to investigate the subunit dependence of BK activation
- in planar lipid bilayers to investigate the molecular and functional effects on reconstituted BK channels.

CHAPTER 3

***Ex Vivo* Vascular Studies**

3.1 INTRODUCTION

In the previous chapter, novel oestrogens were synthesised incorporating structural motifs of known oestrogenic BK activators. The aim of drug discovery is to synthesise novel and selective molecules that influence cellular processes with the view to developing possible therapeutic treatments. Part of this process is to endeavour to identify the mechanism of action of the compounds and to achieve this, it is necessary to test compounds using different assays.

The isolated organ bath is an effective *in vitro* pharmacological screening tool used to assess the efficacy, potency and selectivity of a novel compound at a defined target. In contrast to other molecular assays, the effects of compounds with uncertain molecular targets may be explored. In this study, aortic ring assays bridge the gap between *in vivo* and *in vitro* models and afford the opportunity to observe the effects of the novel compounds when applied to smooth muscle tissue which is rich in BK β_1 expression. The assay was implemented in this study primarily to investigate selectivity of the novel synthesised compounds for BK channels and other potential oestrogen targets in vascular smooth muscle tissue.

3.1.1 Vascular smooth muscle: physiology and mechanics

The vasculature is a network of blood vessels of varying size and shape perfectly adapted to facilitate shifting blood flow rates and pressure throughout the body. Characteristically, blood vessels have a universal structural

organisation, typified by that of the aorta and vena cava, arranged in three discreet layers: the *tunica intima*, *media* and *adventitia*. The *tunica intima* comprises a monolayer lining of macrovascular endothelial cells on the surface of the lumen wall. This is surrounded by the medial layer (separated by a continuous basement membrane) mainly containing a complex of vascular smooth muscle made up of spindle-shaped, non-striated cells with some collagen and elastin. The outer adventitial layer comprises loose connective tissue and extra cellular matrix alongside other cell types such as fibroblasts, nerves and perivascular cells (pericytes - thought to be precursors of smooth muscle) (Figure 3.1.1.1). The combination of all these cellular components comprises the vascular tissue and creates tight junctions facilitating transmembrane transport.

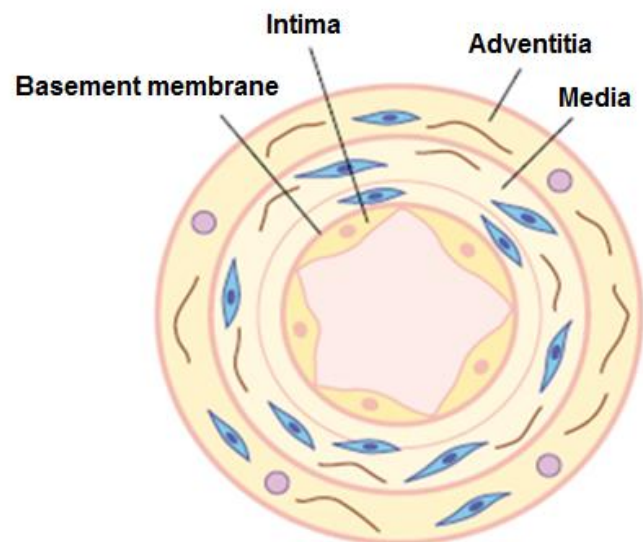


Figure 3.1.1.1 Schematic of blood vessel structure shown in cross-section. Large blood vessels such as arteries (and veins) have three distinct layers: the intima comprises endothelial cells which line the luminal surface; the media consists of several sheets of vascular smooth muscle; and a thin covering of connective tissue that makes up the adventitial layer. The intima and the media are separated by a basement membrane [153].

3.1.2 Signalling of contraction in smooth muscle

Contraction and dilation of vascular smooth muscle is an involuntary process, principally regulated by receptor and stretch (mechanical) activation of proteins myosin and actin. The process is generally controlled by the sympathetic nervous system and can be either phasic or tonic [154]. When smooth muscle cells contract, they shorten in length altering the diameter of the vessel lumen, thereby regulating blood flow [154]. However, alongside neuronal stimuli, smooth muscle is regulated by an array of transduction signalling molecules e.g. noradrenalin, angiotensin II, endothelin, histamine and a variety of hormones, as well as a range of intracellular mechanisms including myosin light chain kinase (MLCK) and myosin phosphatase. These pathways initiate smooth muscle responses via modulation of intracellular Ca^{2+} concentrations [Ca^{2+}]_i [155, 156].

3.1.2.1 Gap junctions

Intercellular, electrical communication between individual smooth muscle and endothelial cells is made possible by the presence of gap junctions. Gap junctions facilitate the passage of electrical current and small molecules and ions e.g. Ca^{2+} , cAMP, ATP and possibly nitric oxide, leading to co-ordinated lengthening or shortening of the individual smooth muscle cells, necessary for regulating vascular tone [157-161]. Gap junctions are zones of paired hexameric assemblages of connexin that act as intercellular pores or channels known as hemi-channels [162]. Two of these hemi-channels link to form a gap junction which creates a signalling pathway between cells within the same tissue or commonly, heterocellularly at junctions between VSMCs, ECs, renal

juxtaglomerular cells and pericytes. To date there have been only three connexin isoforms found to associate with VSMCs and ECs, explicitly C37, C40 and C43, named in relation to their molecular weight [160, 163, 164]. Interestingly, expression levels of these particular connexins, varies according to location and size of vessels. Typically, all three connexins are abundant in endothelial cells whereas, only C43 is common in VSMCs [165-167]. The point at which VSMCs and ECs make contact is called the myoendothelial junction (MEJ). This is a putative location for the presence of connexins in the hypertensive system [168-171]. Vascular smooth muscle and endothelial cells are a functionally coupled syncytium i.e. changes in membrane potential in one cell type can alter the function of voltage-gated Ca^{2+} channels in the other cell type [172-176]. Gap junctions are vital to the coordination of $[\text{Ca}^{2+}]_i$ variations in neighbouring VSMCs, and the maintenance of vascular tone in general [176, 177].

3.1.2.2 The role of Ca^{2+} in smooth muscle contraction

The principal stimulus for contraction of vascular smooth muscle is an increase in $[\text{Ca}^{2+}]_i$, derived from an influx of extracellular Ca^{2+} through voltage-sensitive and receptor-activated Ca^{2+} channels (membrane depolarisation can be triggered in response to mechanical stretch of the smooth cells causing these channels to open), or from intracellular Ca^{2+} stores i.e. sarcoplasmic reticulum (SR). Store operated Ca^{2+} release creates a rapid phasic response and is initiated by the binding of a variety of transduction signalling molecules and hormones and neurotransmitters such as noradrenalin, angiotensin and endothelin, leading to a cascade of potent

second messenger pathways (diacylglycerol – DG and inositol 1,4,5-triphosphate – IP₃) [154] (Figure 3.1.2.2.1). However, the SR in smooth muscle cells is sparse and not well developed, hence much of the increase in [Ca²⁺]_i is acquired *via* the voltage-gated and receptor-activated Ca²⁺ channels and generates a slow sustained vasoconstrictor response.

Contraction is regulated *via* myosin thick filaments triggered by Ca²⁺ binding to the acidic protein, calmodulin. The Ca-calmodulin complex binds to myosin light chain kinase (MLCK) which leads to phosphorylation of a serine residue on two of the myosin light chains, enabling interaction of myosin with actin (Figure 3.1.2.2.1). This phosphorylation is very often sustained at low levels without mechanical or receptor stimuli, thus, creating a dynamic state of vasoconstriction, the basis of smooth muscle tone [178-180]. Contraction of smooth muscle is maintained by activation of Rho kinase and RhoA pathways [181], which serve as Ca²⁺-sensitising mechanisms (Figure 3.1.2.2.1) [154]. Increased levels of [Ca²⁺]_i are transitory and thus, maintenance of muscle tone is a dynamic process. Rho kinase inhibits myosin phosphatase activity (concomitant with the activation of phospholipase C), initiated by activation of the protein RhoA. In this way, the myosin light chain remains phosphorylated and upholds a state of contraction [182].

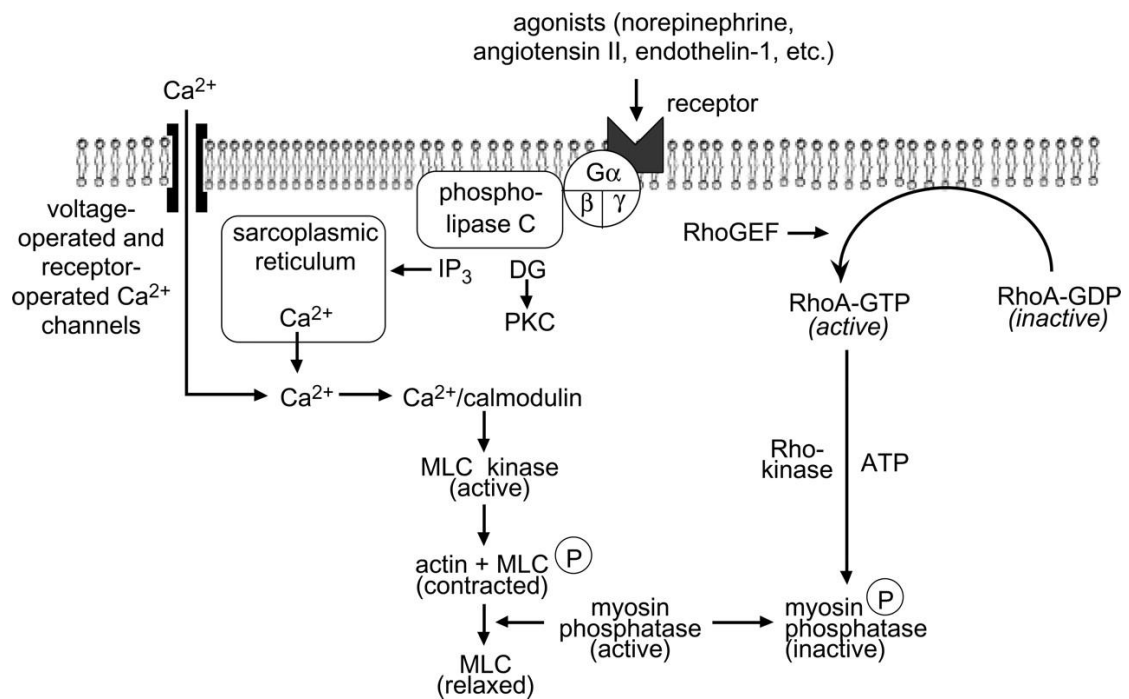


Figure 3.1.2.2.1 Regulatory pathways leading to smooth muscle contraction. A variety of agonists e.g. noradrenalin, angiotensin, endothelin etc. initiate smooth muscle contraction by binding to specific receptors. This instigates increased levels of phospholipase C activity through G protein coupling. Phospholipase C generates the second messengers DG and IP₃. The latter binds to SR receptors triggering the release of Ca²⁺. Ca²⁺ then binds to calmodulin to activate MLCK which in turn phosphorylates myosin light chain so that cross-bridging in juxtaposition with actin can take place, causing the smooth muscle cell to shorten and contract. DG activates protein kinase C (PKC) which in turn can promote contraction via phosphorylation of voltage-sensitive Ca²⁺ channels located in the cell membrane. Activation of Rho kinase is initiated by activation of RhoA and leads to the phosphorylation of the myosin light chain resulting in inhibition of myosin light chain phosphatase (MLCP) and a contractile state [154].

3.1.2.3 The role of Ca²⁺ in smooth muscle relaxation

Smooth muscle relaxation is initiated by a decrease in [Ca²⁺]_i and involves reuptake of calcium ions into the SR facilitated by ATP hydrolysis. Calcium,

magnesium ATPases are present in the SR and when phosphorylated, bind to two calcium ions which are sequestered back into the SR (Figure 3.1.2.3.1) [154]. Calcium, magnesium ATPases are also present in the plasma membrane. However, the activity of these proteins differs from those of the SR as they can be bound by calmodulin leading to activation of the plasma membrane calcium pump. Other $[Ca^{2+}]_i$ -reducing mechanisms involve the presence of Na^+/Ca^{2+} exchange pumps in the plasma membrane and the inhibition of receptor and voltage-sensitive Ca^{2+} channels.

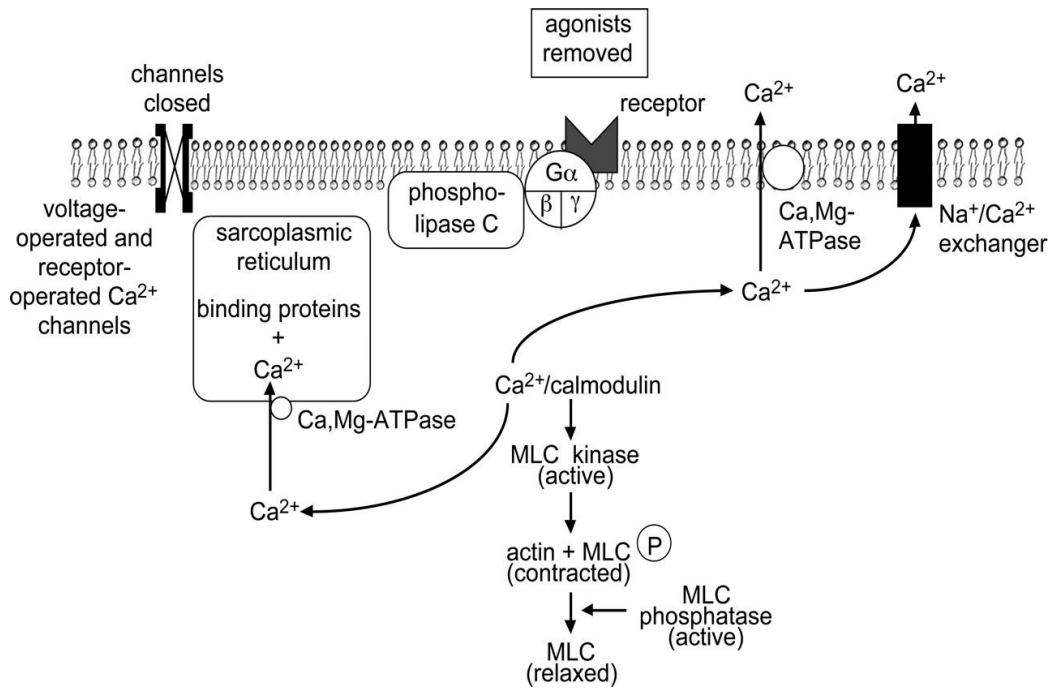


Figure 3.1.2.3.1 Regulatory pathways leading to smooth muscle relaxation. For smooth muscle relaxation to occur, there has to be a decrease in the levels of $[Ca^{2+}]_i$ and subsequent increase of myosin light chain activity. $[Ca^{2+}]_i$ is reduced via a number of mechanisms involving the SR and cell membrane, which contain calcium, magnesium ATPases. These enzymes are instrumental in the removal of cytosolic calcium ions [154].

3.1.2.4 Vascular tone and the role of the endothelium

It is now well known that the endothelium is involved in the maintenance of vascular tone [183-185]. The entire vascular system is lined with endothelial cells which not only act as a protective layer for the vessel but also, operate as a dynamic, signal transducing organ, involved in diverse physiological functions. These functions include expression of a remarkable range of signalling chemicals, some constitutively expressed such as anticoagulant factors to aid blood flow [186, 187], and others released in response to various mechanical (shear stress and tension) and biochemical stimuli, including a variety of vasoactive effectors (Table 3.1.2.4.1).

Table 3.1.2.4.1 Mediators of vascular tone regulation in the endothelium

Blood flow regulation / anticoagulation factors	Vasorelaxation	Vasoconstriction
Thrombomodulin (TM)	Nitric oxide (NO)	Endothelin (ET)
Antithrombin	Prostacyclin(PGI) ₂	Angiotensin II (AgII)
Plasminogen activator	Endothelium-Derived Hyperpolarising Factor (EDHF)	Thromboxane A ₂ (TxA ₂)
Heparin		

There are a diverse range of receptors located on the luminal surface of functionally-intact endothelium (Figure 3.1.2.4.1) and stimulation of these receptors by various neurohumoral agents and physical stimuli such as shear stress, serotonin, catecholamines, acetylcholine (ACh) and adenosine diphosphate (ADP), triggers release of endogenous, endothelial-derived vasoactive substances.

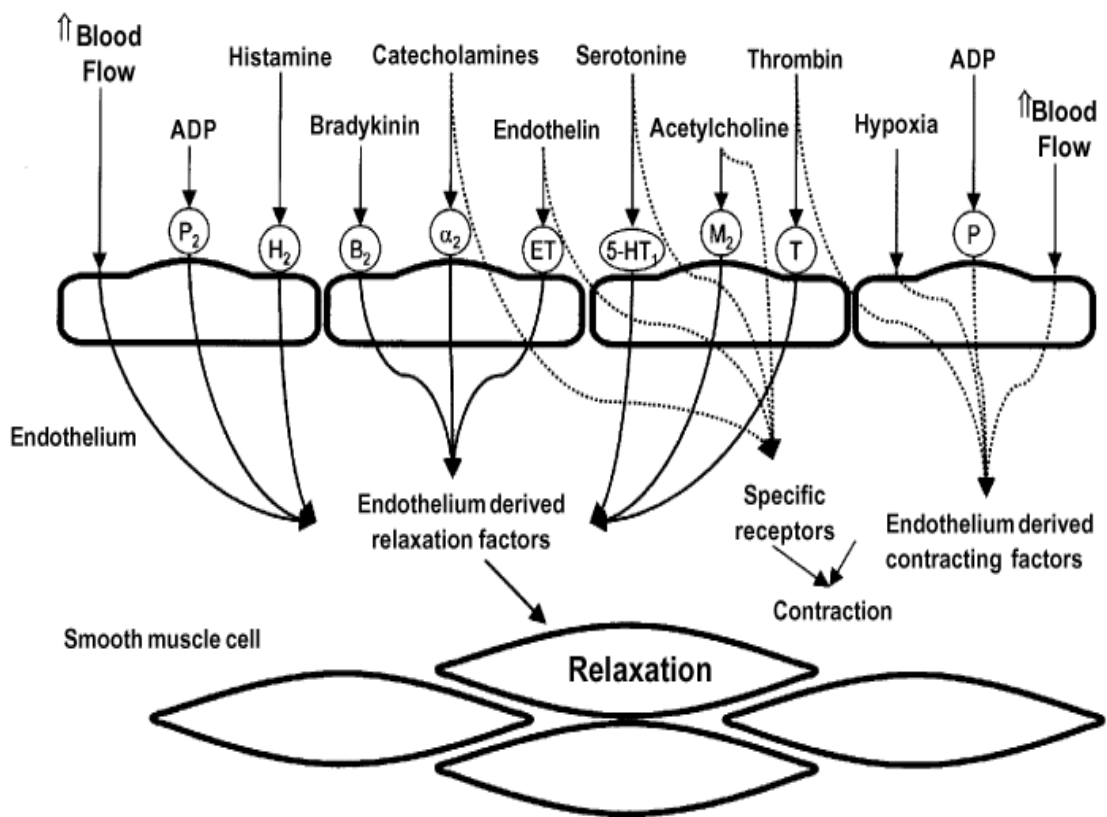


Figure 3.1.2.4.1 Schematic of known effectors on vascular endothelium receptors stimulating the release of endothelium-derived relaxation factor (EDRF) and endothelium-derived contracting factor (EDCF) leading to vascular smooth muscle relaxation and contraction, respectively [188].

In an early study (1980), Furchgott and Zawadzki reported that relaxation of vascular smooth muscle by acetylcholine in isolated rat aortic rings is endothelium-dependent. This relaxation was perceived to be due to an endogenous mediator which they termed endothelium-derived relaxing factor (EDRF) [183, 189]. This was subsequently identified as nitric oxide (NO) [184, 185], a product of L-arginine-NO-synthase pathway [190, 191]. There are three known NO synthase (NOS) isoforms all of which are involved in the regulation of vascular tone: eNOS - expressed in the endothelium, nNOS – a neuronal isoform, both constitutively expressed, and an inducible isoform, iNOS, which is expressed in the presence of certain pathologies typically involving an immune response [192]. NO is a labile short lived ($t_{1/2} < 4$ seconds) powerful vasodilator which acts in a paracrine fashion by directly stimulating cytosolic soluble guanylate cyclase [190, 193]. This leads to an increase in cGMP levels and decreased intracellular Ca^{2+} resulting in vasorelaxation [194] (Figure 3.1.2.4.2).

Prostacyclin (PGI_2), a member of the eicosanoid family of signaling molecules, has since been revealed to be another important endothelium-derived relaxing factor, initiating vasodilation in VSMCs by stimulation of adenylate cyclase and the formation of cAMP [195] (Figure 3.1.2.4.2).

Endothelium-dependent relaxations are also associated with the hyperpolarisation of endothelial and smooth muscle cells via endothelium dependent hyperpolarising factor (EDHF), of which there is an abundance of

putative candidates e.g. carbon monoxide, C-type natriuretic peptide, short-lived arachidonic acid metabolites (via cytochrome P450) [169, 171, 196, 197].

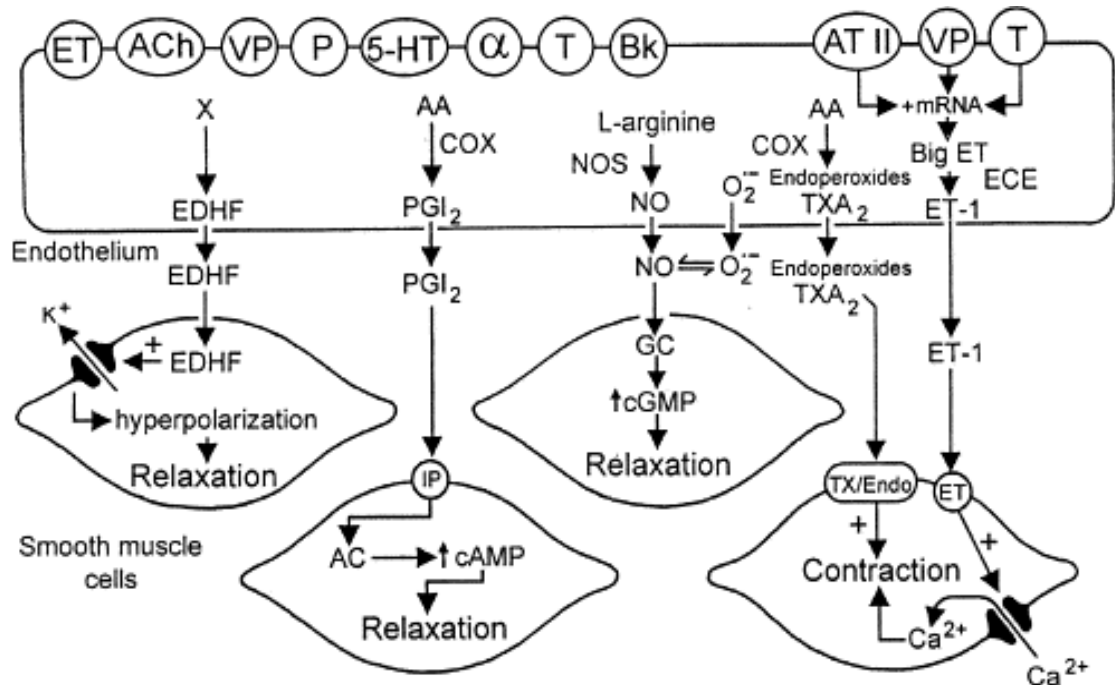


Figure 3.1.2.4.2 A Schematic of endothelium-derived relaxing and contracting factors. KEY AA (arachidonic acid); Ach (acetylcholine); α (alpha-adrenergic); ATII (angiotensin II); Bk (bradykinin); COX (cyclooxygenase); ECE (endothelin converting enzyme); EDHF (endothelium-derived hyperpolarizing factor); ET (endothelin1); NO (nitric oxide); NOS (NO synthase); O_2^- (superoxide anions reactive oxygen species); P (purines); PGI_2 (prostacyclin); T (thrombin); TXA_2 (thromboxane A_2); VP (vasopressin); 5-HT (serotonin) [198].

3.1.2.5 BK_{Ca} channels in vascular smooth muscle and endothelium cells

There are a multiplicity of ion channels involved in endothelium-derived and VSMC vasoreactivity [199]. EDHF-mediated vasodilatory responses entail activation of endothelial K_{Ca} channels, fundamental to the control of membrane potential in both endothelial cells and VSMCs and subsequent vascular tone

[93, 187, 197, 200, 201]. All vascular K_{Ca} channels can be activated by calcium and to date there are three known sub-types i.e. the small (SK_{Ca}), the intermediate (IK_{Ca}) and the large (BK_{Ca}) conductance potassium channel [25, 49, 93]. However, expression of these channels varies within the vasculature i.e SK_{Ca} channels are expressed mainly on ECs, while IK_{Ca} and BK_{Ca} channels are found in both endothelial and smooth muscle cells, albeit BK_{Ca} is preferentially expressed in smooth muscle tissue [202-207]. Moreover, in the case of the BK_{Ca} , different combinations of α with β subunit associations exist within the tissue [187, 208]. There is evidence to suggest that while β subunits (constitutively expressed in VSMCs as the β_1 form) are not expressed in endothelial cells at the mRNA and protein level [36, 187, 208, 209], the BK_{Ca} channel comprising α subunits alone are fully expressed in vascular endothelial cells and have a functional role [202, 210]. Consequently, in the absence of associating β_1 subunits, BK_{Ca} channels in the endothelium are less sensitive to Ca^{2+} than in VSMC channels and activate at more positive potentials [211, 212]. Interestingly, activation of BK_{Ca} channels in VSMCs can be induced by various endogenous effectors including nitric oxide, arachidonic acid metabolites such as dihydroxyeicosatrienic acids, and also reactive oxygen species (ROS) [213-216]. However, recent studies have demonstrated that low concentrations of the BK_{Ca} activators, compound NS1619 and resveratrol (a phytoestrogen), applied to isolated rat aortic rings, induce vasodilation via endothelial $BKCa$ channel activation and not through VSMC $BKCa$ involvement [217].

3.1.2.6 Vasodilatory effects of 17 β -oestradiol and other oestrogens

The vasodilatory effects of steroidal and non-steroidal oestrogens have been extensively studied in the rat aorta and it is now widely established that 17 β -oestradiol can induce reversible relaxation in vascular smooth muscle in a genomic or non-genomic manner *via* both endothelium-dependent and endothelium-independent pathways [218, 219]. Endothelium-independent vasorelaxation by oestrogens acutely increases vascular relaxation in a non-genomic manner [218, 220] and is mediated, in part, by activation of the BK_{Ca} channel in association with its β_1 subunit [9, 221]. Vasorelaxation to 17 β -oestradiol has also been shown to occur in the presence of NOS inhibitors, N^G-nitro-L-arginine and N ^{ω} -nitro-L-arginine [219, 222, 223]. These studies offer further evidence that oestrogen-evoked relaxation is due to interactions with vascular smooth muscle ion channels directly. Previous studies by Zhang *et al.*, White *et al.*, and Tep-Areenan *et al.*, have demonstrated that 17 β -oestradiol interacts with ion channels within the plasma membrane of vascular smooth muscle cells [96, 224, 225]. They showed that micromolar concentrations of 17 β -oestradiol inhibit Ca²⁺ channels and activate BK_{Ca} channels.

Other endogenous oestrogens such as 17 α -oestradiol, oestriol and oestrone have been shown to produce vasorelaxant effects, albeit less marked (17 β -oestradiol >> oestrone > oestriol > 17 α -oestradiol) [40, 102, 226]. Studies have reported tamoxifen, a non-steroidal xenoestrogen, to induce vasodilation *via* inhibition of mitogen-activated protein kinase in rat aortic smooth muscle [227] and raloxifene, a selective oestrogen receptor modulator

(SERM), to induce vasorelaxation in porcine coronary arteries by the inhibition of Ca^{2+} channels and the activation of BK_{Ca} channels in an endothelium-independent manner [228]. Here, the vasodilatory effects of Oestrone and its derivatives, DME-Oestrone, Quaternary-DME-Oestrone, Oestrone-Oxime, DME-Oestradiol and Quaternary-DME-Oestradiol were compared on endothelium intact and endothelium denuded rat aortic rings, pre-contracted with phenylephrine (1 μM).

3.1.5 AIMS

If the compounds synthesised in the previous chapter are novel BK activators then they should demonstrate smooth muscle relaxant activity in arterial smooth muscle. This relaxation should not be dependent on nitric oxide release from an intact endothelium. In addition, the relaxation should be reversed by specific BK channel blockers. The aim of the chapter is to test the ability of these compounds to relax pre-contracted aortic smooth muscle in preparations which have their endothelium left intact and preparations which have had the endothelium removed; novel BK activators should be able to relax pre-contracted aorta independent of nitric oxide release from the endothelium.

Objectives:–

1. To determine which compounds relax aorta independent of the endothelium.
2. To determine which compounds can have the relaxant properties reversed by iberiotoxin.
3. To determine the relative potencies and selectivity of these compounds in order to select compounds for further investigations.

3.2 METHODS

3.2.1 Preparation of isolated rat thoracic aorta rings

Adolescent male Sprague-Dawley rats, supplied by Charles River (weight approximately 180 g–240 g), were sacrificed by cervical dislocation. Thoracic aortae were removed and cleared of periadvential fat and then dissected into 4 rings (3-4 mm width). To obviate the effects of nitric oxide (NO) release, the endothelial layer was removed mechanically in half of the rings by gently rubbing the intimal surface of the artery lumen with a matchstick. All rings were then mounted in organ baths (AD Instruments, DMT) which were filled with warmed (37°C) and gas-equilibrated (95% O₂, 5% CO₂) Krebs' solution containing (in mMol/L) CaCl₂ 1.6, MgSO₄ 1.17, EDTA 0.026, NaCl 130, NaHCO₃ 14.9, KCl 4.7, KH₂PO₄ 1.18, and glucose 11 (Figure 3.2.1.1).

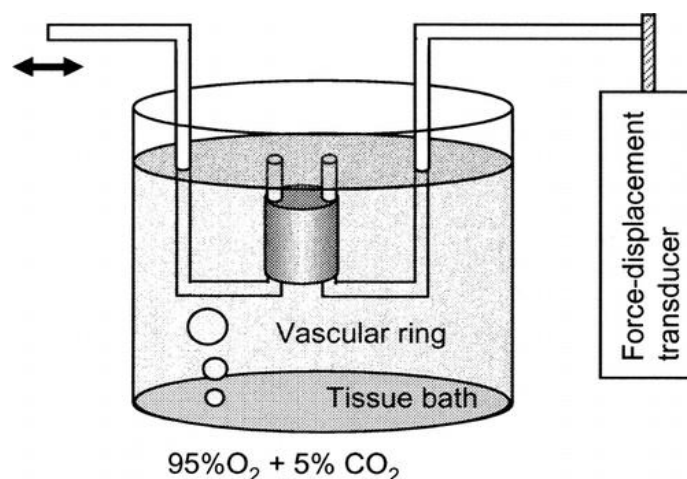


Figure 3.2.1.1 Measurement of relaxation/contraction of rat aortic rings mounted in organ baths filled with warmed (37°C), gas equilibrated (95% O₂, 5% CO₂) Krebs' solution using isometric transducers with an applied pre-load tension of 1.5 g.

Isometric tension was measured with isometric transducers (AD Instruments DMT), digitised using a MacLab A/D converter (AD Instruments) and stored and displayed on a MacIntosh computer. A pre-load tension of 1.5 g was applied and the rings were equilibrated for 60 minutes, changing the Krebs' solution fully every 15 minutes. Relaxation is expressed as a percentage of the steady-state tension (100%). Phenylephrine (1 nM-100 μ M) was used to induce vasoconstriction of the aortic rings and dose response curves were generated. Following pre-contraction with phenylephrine (1 μ M), the cumulative effect of oestrone and derivatives at 0.3 μ M, 1.0 μ M, 3.0 μ M, 10.0 μ M and 30.0 μ M concentrations at 8 minute intervals on percentage relaxation of aortic rings was recorded. For these experiments, 10 mM and 1mM stock solutions of all compounds were made using dimethyl sulfoxide (DMSO) (Figure 3.3.1.1). DMSO is an ideal choice of vehicle as it is a known aprotic solvent which is miscible in water. The stock was further diluted in HEPES buffer to the appropriate concentrations (Figure 3.3.1.1). The artery endothelium viability and integrity were confirmed by dilatory response of the ring to acetylcholine (1 nM -100 μ M).

3.2.2 Statistical analysis

All data throughout this chapter were analysed using GraphPad Prism version 5.03 and are presented as the mean \pm the standard error of the mean (SEM) unless otherwise stated. The level of significance between means was taken at $p < 0.05$. The effect of the oestrogens was expressed as the percentage relaxation with 100% relaxation occurring when baseline is reached. In all

experiments, n equals the number of rats from which thoracic aortae were obtained.

Statistical comparison between the concentration response for rubbed and denuded aortic rings was made using two-way ANOVA with a *Bonferroni post hoc* test for multi-comparison of individual means associated with each concentration.

The threshold relaxation concentration was determined using the Wilcoxon signed rank test, a non-parametric equivalent of the one sample t-test. The lowest concentration that produced a relaxation significantly different from zero determined the upper limit for the threshold concentration.

3.3 RESULTS

3.3.1 The effect of novel steroidal oestrogens on isolated rat thoracic aorta rings

The effects of steroidal oestrogens on the vasculature are diverse depending on the target vessel and even across species [96, 229-232]. *Ex vivo*, experiments using isolated rat aorta are a useful and well-established tool for investigating the mechanisms of action of novel and endogenous modulators of ion channels within tissue [13, 189, 219, 233, 234]. Here, the vascular responses to Oestrone and its novel derivatives were investigated in isolated rat aorta with regard to the role of the BK channel in vascular smooth muscle and the ubiquitous endothelium. Increasing concentrations (0.3 μM ; 1.0 μM ; 3.0 μM ; 10 μM ; 30 μM) of Oestrone, DME-Oestrone, Quat-DME-Oestrone, Oestrone-Oxime, DME-Oestradiol or Quat-DME-Oestradiol were cumulatively added to rat aortic rings pre-contracted with phenylephrine (PE) (1 μM), all at eight minute intervals. The aortic rings were either endothelium-denuded or endothelium intact.

Percentage relaxation and threshold concentrations were duly recorded. An example of a typical trace recording of the percentage relaxation in a pre-contracted and endothelium-intact rat aortic ring is shown in Figure 3.3.1.1(B). The trace illustrates a relaxation in the tissue that is concomitant with the cumulative concentrations of Oestrone-Oxime when applied at 8 minute intervals. Figure 3.3.1.1(A) is an example trace of a control experiment illustrating the relaxant effect on phenylephrine-contracted rat aorta of

increasing concentrations of dimethyl sulfoxide (DMSO). DMSO was used throughout this study as the vehicle solvent for preparation of 1 mM and 10 mM stock solutions of the test compounds. DMSO was chosen as a solvent due to its aprotic properties, dissolves both polar and non-polar compounds, and is miscible in water. As expected, DMSO had no effect on percentage relaxation in the pre-contracted aortic rings.

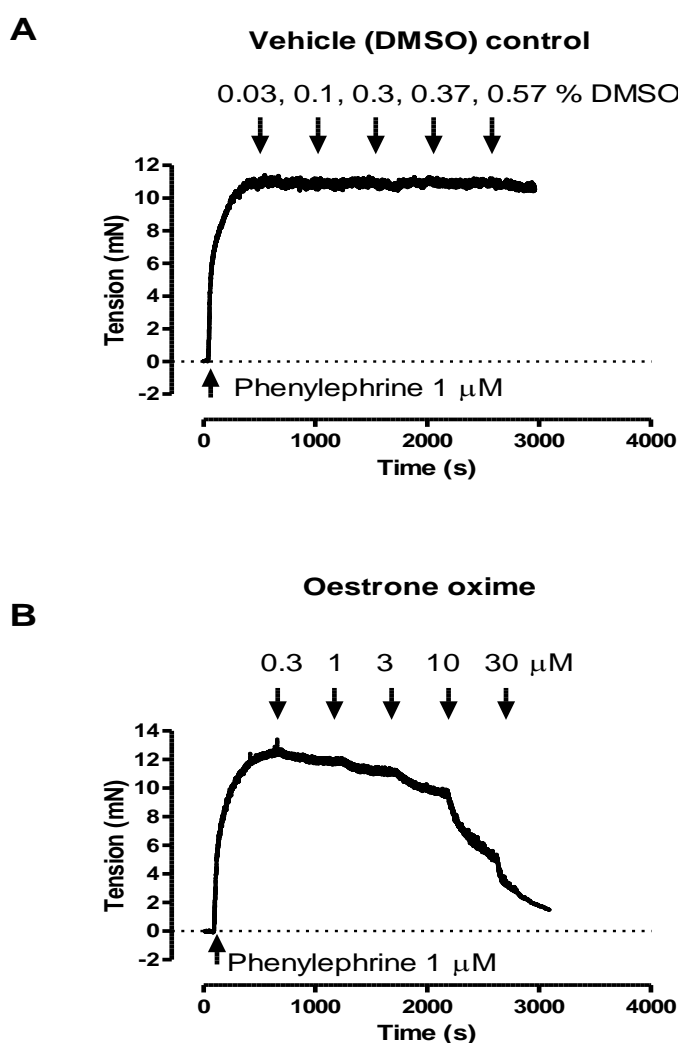


Figure 3.3.1.1 (A) a typical trace of a representative experiment showing relaxation of phenylephrine-contracted (1 μ M) in the presence of increasing concentrations of dimethyl sulfoxide (DMSO) over time (50 minutes); **(B)** a typical trace of a representative experiment showing relaxation of phenylephrine-contracted (1 μ M) and endothelium-intact rat aortic ring after 40 minutes exposure to Oestrone-Oxime at increasing concentrations.

3.3.2 Comparison of vascular responses to increasing concentrations of Oestrone on endothelium-intact and endothelium-denuded, pre-contracted rat aortic rings

The cumulative administration of Oestrone (0.3 μ M; 1.0 μ M; 3.0 μ M; 10 μ M; 30 μ M) at eight minute intervals to PE-contracted (1 μ M) rat aortic rings resulted in relaxation of both endothelium-intact and endothelium-denuded tissue. However, no significant difference to the percentage relaxation between rings with endothelium-intact and endothelium-denuded rings was revealed ($n=11$, $p>0.05$) (Figure 3.3.2.1). Additionally, there was no statistically significant difference in threshold concentrations of Oestrone between endothelium-intact and endothelium-denuded aorta ($p>0.05$). This indicates that the relaxant effect of Oestrone on rat aortic rings is not endothelium-dependent.

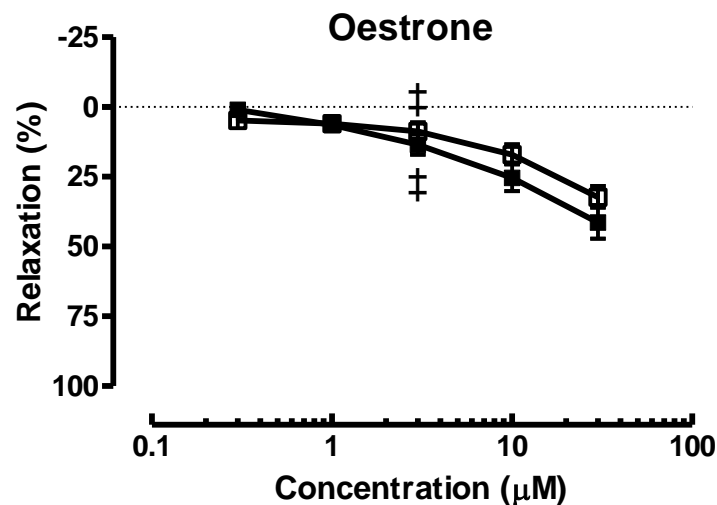


Figure 3.3.2.1 Comparison of vascular responses to increasing concentrations of Oestrone (0.3 - 30 μ M). The graph depicts a complete concentration-response relationship for Oestrone-induced relaxation of endothelium-intact (unrubbed) (\square) and endothelium-denuded (rubbed) (\blacksquare) rat aortic rings over 40 minutes. The effect of Oestrone was expressed as the percentage relaxation with 100% relaxation occurring when baseline is reached. Each point represents the mean \pm SEM ($n=11$, $p>0.05$). \ddagger represents the threshold concentration.

3.3.3 Comparison of vascular responses to increasing concentrations of DME-Oestrone on endothelium-intact and endothelium-denuded, pre-contracted rat aortic rings

The cumulative administration of DME-Oestrone (0.3 μM ; 1.0 μM ; 3.0 μM ; 10 μM ; 30 μM) at eight minute intervals to PE-contracted (1 μM) rat aortic rings resulted in relaxation of both endothelium-intact and endothelium-denuded tissue. However, no significant difference to the percentage relaxation between rings with endothelium-intact and endothelium-denuded rings was revealed ($n=6$, $p>0.05$) (Figure 3.3.3.1). There was no statistically significant difference in threshold concentrations of DME-Oestrone between endothelium-intact and endothelium-denuded aorta ($p>0.05$). This indicates that the relaxant effect of DME-Oestrone on rat aortic rings is not endothelium-dependent.

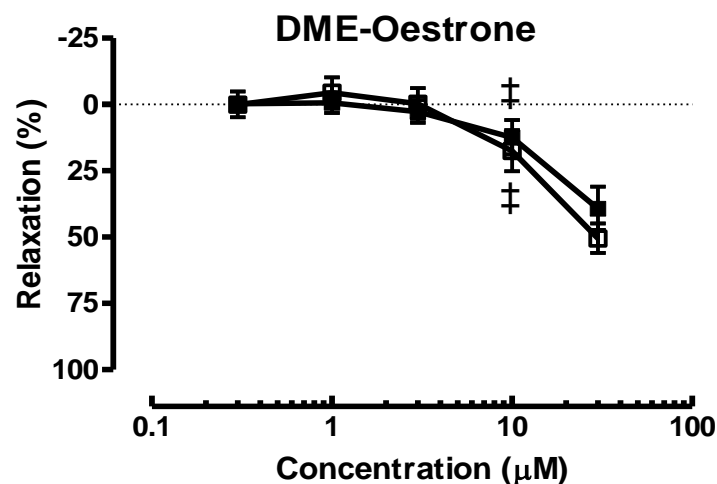


Figure 3.3.3.1 Comparison of vascular responses to increasing concentrations of DME-Oestrone (0.3 - 30 μM). The graph depicts a complete concentration-response relationship for DME-Oestrone-induced relaxation of endothelium-intact (unrubbed) (\square) and endothelium-denuded (rubbed) (\blacksquare) rat aortic rings over 40 minutes. The effect of DME-Oestrone was expressed as the percentage relaxation with 100% relaxation occurring when baseline is reached. Each point represents the mean \pm SEM ($n=6$, $p>0.05$). ‡ represents the threshold concentration.

3.3.4 Comparison of vascular responses to increasing concentrations of Quat-DME-Oestrone on endothelium-intact and endothelium-denuded, pre-contracted rat aortic rings

The cumulative administration of Quat-DME-Oestrone (0.3 μM ; 1.0 μM ; 3.0 μM ; 10 μM ; 30 μM) at eight minute intervals to PE-contracted (1 μM) rat aortic rings resulted in no significant difference to the percentage relaxation between rings with endothelium-intact and endothelium-denuded rings ($n=7$, $p>0.05$) (Figure 3.3.4.1). Relaxation of the rings was not observed and consequently, threshold concentrations of Quat-DME-Oestrone could not be recorded in either endothelium-intact or endothelium-denuded rings. This suggests that Quat-DME-Oestrone possesses limited, if any, relaxant properties.

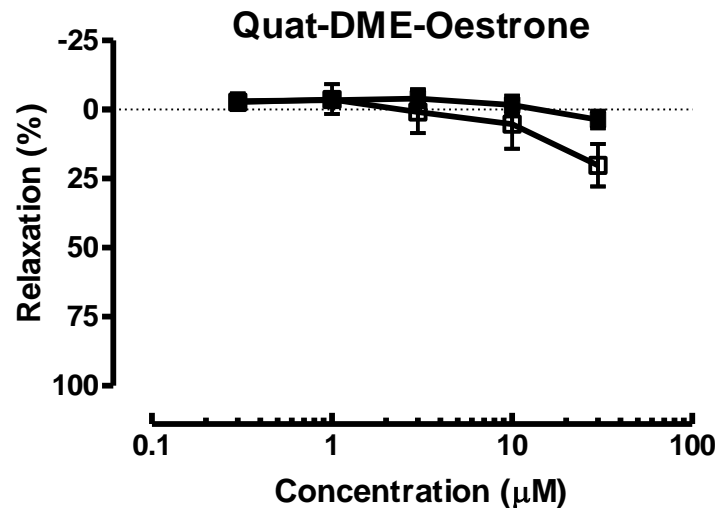


Figure 3.3.4.1 Comparison of vascular responses to increasing concentrations of Quat-DME-Oestrone (0.3 - 30 μM). The graph depicts a complete concentration-response relationship for Quat-DME-Oestrone-induced relaxation of endothelium-intact (unrubbed) (□) and endothelium-denuded (rubbed) (■) rat aortic rings over 40 minutes. The effect of Quat-DME-Oestrone was expressed as the percentage relaxation with 100% relaxation occurring when baseline is reached. Each point represents the mean \pm SEM ($n=7$, $p>0.05$). For Quat-DME-Oestrone no significant relaxation was observed at any of the concentrations tested.

3.3.5 Comparison of vascular responses to increasing concentrations of Oestrone-Oxime on endothelium-intact and endothelium-denuded, pre-contracted rat aortic rings

The cumulative administration of Oestrone-Oxime (0.3 μM ; 1.0 μM ; 3.0 μM ; 10 μM ; 30 μM) at eight minute intervals to PE-contracted (1 μM) rat aortic rings resulted in a significant difference ($p=0.0001$, $n=7$) to the percentage relaxation between rings with endothelium-intact and endothelium-denuded rings (Figure 3.3.5.1). Endothelium-intact rings achieved 100% relaxation with increasing concentrations of Oestrone-Oxime after 40 minutes in comparison with rings from which the endothelium had been removed. Additionally, there was a statistically significant difference in threshold concentrations of Oestrone-Oxime between endothelium-intact and endothelium-denuded aorta ($p<0.05$). Endothelium-intact aortic rings had a lower threshold concentration (1 μM \gg 3 μM) than rings without endothelium (3 \gg 10 μM). This indicates that the relaxant effect of Oestrone-Oxime is endothelium-dependent, in contrast to the actions of Oestrone.

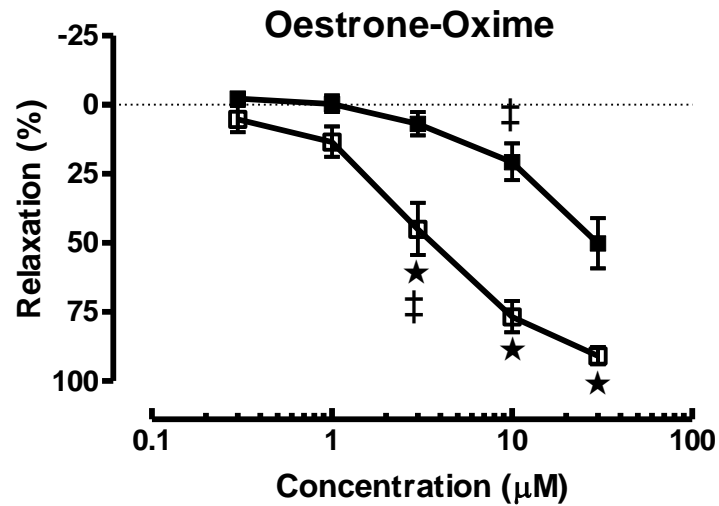


Figure 3.3.5.1 Comparison of vascular responses to increasing concentrations of Oestrone-Oxime (0.3 - 30 µM). The graph depicts a complete concentration-response relationship for Oestrone-Oxime induced relaxation of endothelium-intact (unrubbed) (□) and endothelium-denuded (rubbed) (■) rat aortic rings over 40 minutes. The effect of Oestrone-Oxime was expressed as the percentage relaxation with 100% relaxation occurring when baseline is reached. Each point represents the mean ± SEM (n=7, ★p<0.05 post hoc test). ‡ represents the threshold concentration.

3.3.6 Comparison of vascular responses to increasing concentrations of DME-Oestradiol on endothelium-intact and endothelium-denuded, pre-contracted rat aortic rings

The cumulative administration of DME-Oestradiol (0.3 μM ; 1.0 μM ; 3.0 μM ; 10 μM ; 30 μM) at eight minute intervals to PE-contracted (1 μM) rat aortic rings resulted in relaxation of both endothelium-intact and endothelium-denuded tissue. However, no significant difference to the percentage relaxation between rings with endothelium-intact and endothelium-denuded rings was revealed ($n=6$, $p>0.05$) (Figure 3.3.6.1). There was no statistically significant difference in threshold concentrations of DME-Oestradiol between endothelium-intact and endothelium-denuded aorta ($p>0.05$). This indicates that any relaxant properties of DME-Oestradiol are not endothelium-dependent.

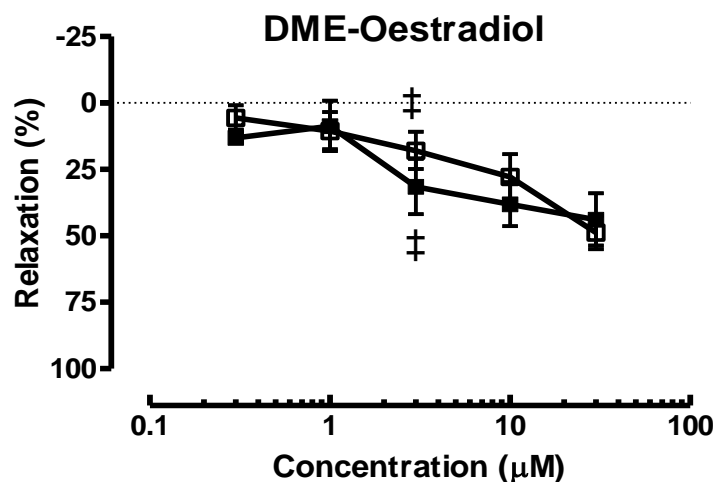


Figure 3.3.6.1 Comparison of vascular responses to increasing concentrations of DME-Oestradiol (0.3 - 30 μM). The graph depicts a complete concentration-response relationship for DME-Oestradiol induced relaxation of endothelium-intact (unrubbed) (\square) and endothelium-denuded (rubbed) (\blacksquare) rat aortic rings over 40 minutes. The effect of DME-Oestradiol was expressed as the percentage relaxation with 100% relaxation occurring when baseline is reached. Each point represents the mean \pm SEM ($n=6$, $p>0.05$). ‡ represents the threshold concentration.

3.3.7 Comparison of vascular responses to increasing concentrations of Quat-DME-Oestradiol on endothelium-intact and endothelium-denuded, pre-contracted rat aortic rings

The cumulative administration of Quat-DME-Oestradiol (0.3 μM ; 1.0 μM ; 3.0 μM ; 10 μM ; 30 μM) at eight minute intervals to PE-contracted (1 μM) rat aortic rings resulted in a significant difference to the percentage relaxation between rings with endothelium-intact and endothelium-denuded rings ($n=6$, $p<0.05$) (Figure 3.3.7.1). Denuded rat aortae afforded rings which exhibited a significantly higher percentage relaxation after application of increasing concentrations of Quat-DME-Oestradiol than rings with endothelium intact. Additionally, there was a statistically significant difference in threshold concentrations of Quat-DME-Oestradiol between endothelium-intact and endothelium-denuded aorta ($p<0.05$). Endothelium-denuded aortic rings had a lower threshold concentration (3 μM \gg 10 μM) than rings with intact endothelium (10 μM \gg 30 μM). This indicates that the relaxant effect of Quat-DME-Oestradiol is endothelium-independent.

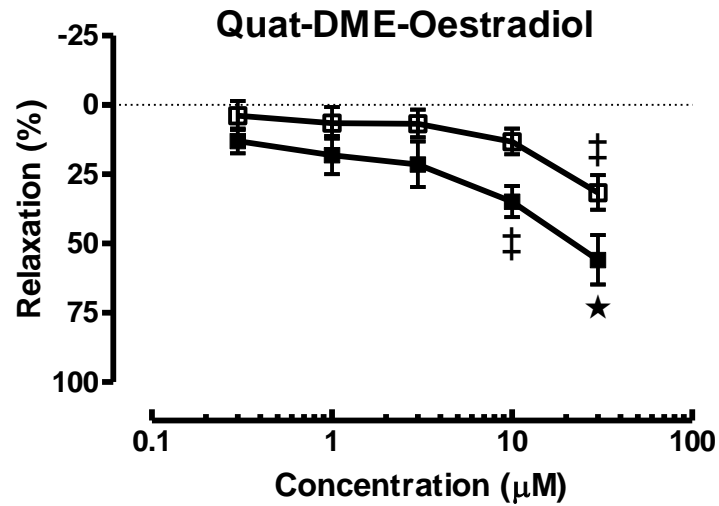


Figure 3.3.7.1 Comparison of vascular responses to increasing concentrations of Quat-DME-Oestradiol (0.3 - 30 μM). The graph depicts a complete concentration-response relationship for Quat-DME-Oestradiol induced relaxation of endothelium-intact (unrubbed) (\square) and endothelium-denuded (rubbed) (\blacksquare) rat aortic rings over 40 minutes. The effect of Quat-DME-Oestradiol was expressed as the percentage relaxation with 100% relaxation occurring when baseline is reached. Each point represents the mean \pm SEM ($n=6$, $\star p<0.05$). ‡ represents the threshold concentration.

3.3.8 Toxin reversal of oestrogen-induced relaxation of aortic rings

After 40 minutes of increasing concentrations of compound exposure, the relaxed rings were then treated with iberiotoxin (IbTX) (100 nM), a BK-specific channel blocker. Only rings treated with Quat-DME-Oestradiol showed reversibility of tissue relaxation (Figure 3.3.8.1) which supports a BK association with the relaxant properties of this compound but correspondingly may be indicative of a weak or a lack of BK involvement in the mechanism of action of the other compounds.

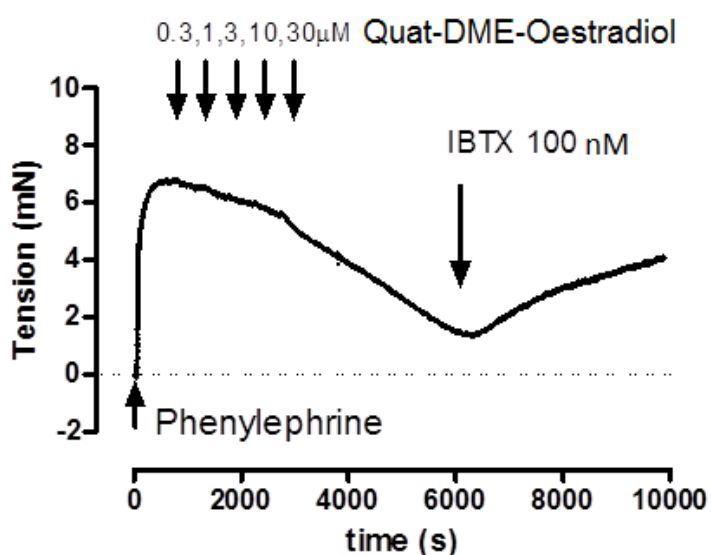


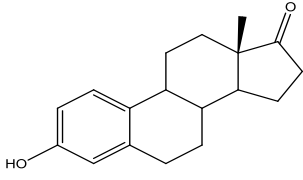
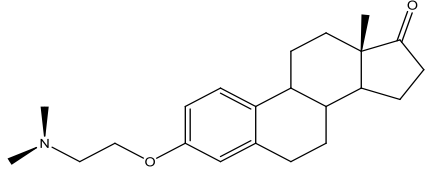
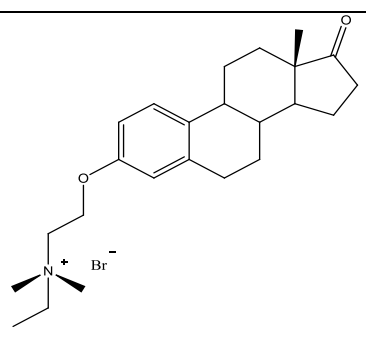
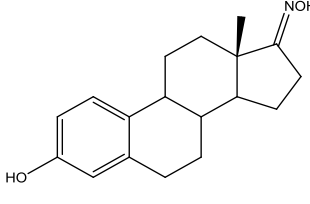
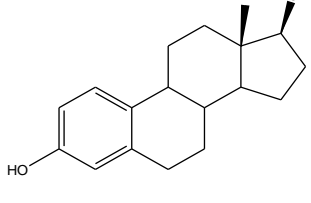
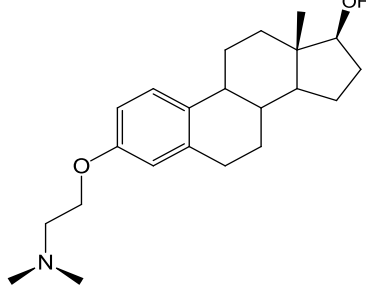
Figure 3.3.8.1 An example trace of cumulative additions of Quat-DME-Oestradiol on pre-contracted aortic rings followed by 100 nM of iberiotoxin, a known BK channel blocker. Quat-DME-Oestradiol was the only compound to show sensitivity to iberiotoxin implying that the other compounds tested can induce relaxation independent of BK channels.

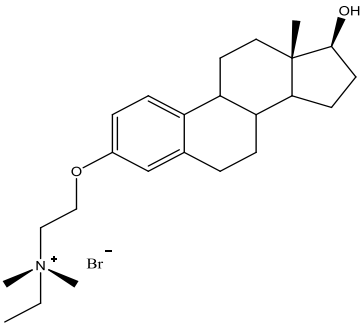
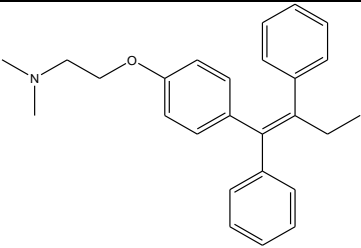
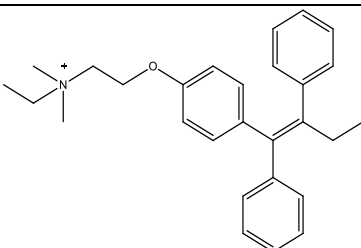
3.3.9 Summary of results

The concentration relationship between compound and tissue relaxation revealed that the threshold concentration was the same for endothelium-intact and endothelium-denuded aortic rings, the exceptions being rings treated with Oestrone Oxime and Quat-DME-Oestradiol. Oestrone-Oxime and Quat-DME-Oestradiol had differing threshold concentrations when applied to denuded aorta and intact aorta with Oestrone-Oxime being more potent with endothelium-intact tissue whereas, Quat-DME-Oestradiol was more potent with endothelium-denuded rings. Table 3.3.9.1 summarises these data and included other compounds from previous work for comparison. The compounds have been categorised according to chemical structure:-

- 17-Keto Oestrogens (incorporation of a ketone at the 17 position)
- 17-Oxime(incorporation of the divalent group C=NOH)
- 17 β -Hydroxy Oestrogens (incorporation of an hydroxyl group at the 17 position)
- Non-steroidal antioestrogens

Table 3.3.9.1 Comparison of concentration thresholds (μM) of oestrogen and antioestrogen derivatives on rat aortic rings with and without intact endothelium.

COMPOUNDS		ENDOTHELIUM (+)	ENDOTHELIUM (-)	STRUCTURE	REFS
17-Keto oestrogens	OESTRONE (⊗)	1 > 3 μM	1 > 3 μM		PS [235]
	DME-OESTRONE (⊗)	3 > 10 μM	3 > 10 μM		PS [235]
	QUAT-DME-OESTRONE (⊗)	> 30 μM	> 30 μM		PS [235]
17 Oxime	OESTRONE-OXIME (⊕)	1 > 3 μM	3 > 10 μM		PS [235]
17 β -hydroxy oestrogens	17 β -OESTRADIOL (⊕)	0.3 > 1 μM	1 > 3 μM		UD
	DME-OESTRADIOL (⊗)	1 > 3 μM	1 > 3 μM		PS [235]

17 β -hydroxy oestrogens (cont.)	QUAT-DME-OESTRADIOL (\emptyset)	10 \gg 30 μ M	3 \gg 10 μ M		PS [235]
	TAMOXIFEN (\otimes)	3 \gg 10 μ M	3 \gg 10 μ M		UD
Non-steroidal antioestrogens	ETHYLBROMIDE TAMOXIFEN	3 \gg 10 μ M	NDA		UD

(Continued from previous page). Table 3.3.9.1 Comparison of concentration thresholds (μ M) of oestrogen and antioestrogen derivatives on rat aortic rings with and without intact endothelium.

Key: \otimes = not endothelium dependent;

\oplus = increased potency in aorta with endothelium;

\emptyset = increased potency in aorta without endothelium;

\boxtimes = compound inactive at concentrations \leq 30 μ M;

NDA (no data available); PS (present study); UD (unpublished data Allen et al.).

Referring to Table 3.3.9.1, it can be seen that for 17-keto steroids, substitution in the three position leads to decreased relaxation ability (see Figure 2.5.1.1.1 for carbon positions). Similarly, for 17 β -hydroxysteroids, substitution in the three position leads to decreasing potency, however, Quat-DME-Oestradiol was the only analogue that demonstrated sensitivity to iberiotoxin.

3.4 DISCUSSION

The vasodilatory effects of oestrogen derivatives were investigated in rat aortic rings. Comparisons were made between endothelium intact and endothelium denuded preparations. Although all oestrogen derivatives, saving Quat-DME-Oestrone, induced a relaxation, only one of the compounds, Quat-DME-Oestradiol, was sensitive to the specific BK channel blocker, iberiotoxin. This suggests that most have relaxant effects in addition to or independent of BK channel activation. This was anticipated as there is ample evidence of oestrogens relaxing vascular smooth muscle by a variety of processes [8, 236-239]. Here, the endothelium was removed to investigate direct effects on smooth muscle and simplify the interpretation of these studies.

That oestrogens have a protective effect on the vasculature has been known for many years from extensive epidemiological studies [58, 240, 241] and there have been numerous investigations into the underlying mechanisms of oestrogenic vasorelaxation. Both genomic and non-genomic pathways are thought to be involved [67, 71, 101, 102, 219, 242, 243] and these studies have highlighted how complex and dynamic these mechanisms are.

Some of the potential mechanisms implicated in oestrogen-induced relaxation involve binding to extracellular components of membrane receptors and ion channels. Previously, the vasorelaxant effect of oestrogens such as 17β -oestradiol was thought to be indirect due to release of vasoactive endothelium-generated relaxing factors, the principle one of which is nitric oxide (NO). However, it is now well-documented that oestrogens can also interact directly

with membrane receptors and ion channels of vascular smooth muscle [8, 239, 244].

Potential ways in which these oestrogen derivatives could relax aortic rings is summarised in Table 3.4.1. Many of these proposed mechanisms could be due, in part, to activating BK channels and thus, may be sensitive to iberiotoxin. Removal of the endothelium and checking the reversibility of vasorelaxation by iberiotoxin helps to narrow down potential mechanisms.

Referring to Table 3.4.1, the reported effects of 17β -oestradiol is consistent with most of the proposed mechanisms (numbers 1-25). Indeed, it has been reported that 17β -Oestradiol can inhibit L-type voltage-gated calcium channels [10, 245, 246], modulate GPR 30 receptors [61, 76-78, 247] and ER α and ER β receptors [72, 73, 79], mediate eNOS [236-238], and nNOS [248-250] while causing increased levels of cGMP [96, 221] to name but a few potential oestrogenic targets. Most of the derivatives are unlikely to involve mediators released from endothelial cells as removing the endothelium did not reduce the ability of these ligands to relax the aortic rings. Oestrone-Oxime was an exception and is a potent vasorelaxant when the endothelium is intact. Quat-DME-Oestradiol-induced relaxations are unlikely to involve intracellular effects on aortic smooth muscle due to its quaternary structure, but mechanisms numbers 20, 21, 24 and 25 are still potential explanations for the vasorelaxation observed after the addition of this compound.

Table 3.4.1 Some potential mechanisms for oestrogen-induced relaxation of vascular smooth muscle.

	Mechanism	Intracellular site	Extracellular site	IBTX sensitivity
ENDOTHELIIUM DEPENDENT	1. Activate cytosolic eNOS	✓		possible - due to indirect effects of NO on BK channels
	2. Muscarinic receptor agonist		✓	possible - due to indirect effects of NO on BK channels
	3. ADP receptor agonist		✓	x
	4. Bradykinin receptor agonist		✓	possible - due to indirect effects of NO on BK channels
	5. Prostacyclin synthase activation	✓		x
	6. GPR30 ligand		✓	not unless GPR30 receptors couple to BK channels
	7. Nuclear ER α receptors	✓		x
	8. Nuclear ER β receptors	✓		x
	9. Membrane ER α receptors		✓	possible - if BK channels are coupled to membrane ER receptors
	10. Membrane ER β receptors		✓	possible - if BK channels are coupled to membrane ER receptors
ENDOTHELIIUM INDEPENDENT	11. α_1 adrenoceptor blocker		✓	x
	12. G protein inhibitor	✓		x
	13. Inhibition phospholipase C	✓		x
	14. Inhibition of phosphodiesterase to \uparrow cGMP and \uparrow cAMP concentrations	✓		possible - due to indirect effects of second messengers on BK channels
	15. Cytosolic nNOS activation	✓		possible - due to indirect effects of NO on BK channels
	16. L type calcium channel blocker	✓	✓	x
	17. Calcium release from SR	✓		x
	18. Calmodulin modulation	✓		x
	19. Inhibition of contractile proteins	✓		x
	20. BK channel	✓	✓	✓
	21. GPR30 ligand		✓	possible - due to coupling with BK channels
	22. Nuclear ER α receptors	✓		x
	23. Nuclear ER β receptors	✓		x
	24. Membrane ER α receptors		✓	possible - if BK channels are coupled to membrane ER receptors
	25. Membrane ER β receptors		✓	possible - if BK channels are coupled to membrane ER receptors

3.4.1 Structure-activity relationships for novel oestrogens

Cumulative concentrations (0.3 μM – 30 μM) of Oestrone and the novel derivatives, with the exception of Quat-DME-Oestrone which was inactive, were able to produce a relaxant response in pre-contracted aortic rings with or without intact endothelium (Figures 3.3.(2.1), (3.1), (4.1), (5.1), (6.1) and (7.1)). Yet, some compounds exhibited higher potency than others and differing threshold concentrations (Table 3.3.9.1). For instance, the potency of Quat-DME-Oestradiol notably increased in rings in which the endothelium had been removed (Figure 3.3.7.1). The difference in percentage relaxation between endothelium-intact or denuded aortic rings was significant, indicating that the endothelium inhibited the relaxation induced by this compound. This was further substantiated by the lower threshold concentration observed in denuded rings (Table 3.3.9.1).

The enhanced relaxation observed in denuded rings in the presence of Quat-DME-Oestradiol may, in part, be attributable to improved diffusion into the vascular smooth muscle. This is entirely in accord with previous studies reporting on the ability of oestrogens to relax vascular smooth muscle in an endothelium-independent manner [218, 221]. Tight junctional endothelium is more likely to be a diffusional barrier to compounds that cannot penetrate across cell membranes, whereas, compounds that can diffuse freely through lipid bilayers are less likely to be impeded by such barriers. Thus, compounds such as Oestradiol and Oestrone can gain ready access to vascular smooth muscle, whereas, quaternary ammonium compounds, which are confined to the extracellular space, may have difficulty in penetrating into the smooth

muscle of the aortic ring preparation from the luminal side. Removing this barrier, thus, increases tissue penetration and response to quaternary ammonium compounds. However, a pharmacological action on the vascular endothelium by Quat-DME-Oestradiol, which can inhibit background NO modulation, cannot be ruled out.

Interestingly, the other quaternary xenoestrogen, Quat-DME-Oestrone, was remarkably unresponsive in denuded rings and proved to be inactive (Figure 3.3.4.1). This incongruity may simply be ascribed to the chemical structure of the compounds. Unlike Quat-DME-Oestradiol and the known vasorelaxant 17β -oestradiol, Quat-DME-Oestrone lacks a β -OH group on position 17 of the D ring. Additionally, 17β -Oestradiol has been reported to be stereospecific with the position of the β -hydroxyl group seemingly critical for substrate-receptor interaction [40, 102, 251]. In support of this, separate investigations carried out by de Wet and co-workers [40] and White *et al.*, [96] have detailed the lack of potency of the stereoisomer, 17α -oestradiol on the BK channel.

Aortic rings challenged with increasing and cumulative concentrations (0.3 μ M - 30 μ M) of Oestrone, DME-Oestrone or DME-Oestradiol showed relaxation, however, the percentage relaxation was similar in both denuded and intact endothelium rings (Figures 3.3.(1.1.1), (1.2.1), and (1.5.1) respectively). Hence, the underlying mechanism of action is not endothelium-dependent. It might have been expected that the efficacy of Oestrone, an endogenous oestrogen in humans, as an inhibitor of PE-induced smooth muscle contraction, would be high. Nevertheless, this was not the case with only

approximately half maximal percentage relaxation of the PE-contracted tissue realised. This observation is not, however, at variance with previous findings. Work done by Kitawaza *et al.*, and Freay *et al.*, demonstrates that Oestrone (5 μ M) is a much less potent relaxant than 17β -oestradiol, of pre-contracted rat femoral artery smooth muscle [226].

In the same way, the efficacy of DME-Oestrone to relax smooth muscle might be expected to parallel that of tamoxifen, a known relaxant of vascular smooth muscle. The structure of the novel xenoestrogen, DME-Oestrone, by design incorporates some of the structural motifs of tamoxifen, specifically the tertiary amine side group. Kitazawa *et al.*, have previously shown 5 μ M tamoxifen was able to reduce the control PE-induced contraction of rat femoral artery smooth muscle by 99% in a time course similar to that of 17β -oestradiol [226]. However, a key point not to be overlooked is that tamoxifen is a non-steroidal antioestrogen, in contrast to the steroidal DME-Oestrone, and is known to relax smooth muscle in both an endothelium-dependent [252, 253] and independent manner [227, 254, 255]. Additionally, DME-Oestrone incorporates a ketone rather than an hydroxyl group in the 17β position.

Correspondingly, the structure of DME-Oestradiol lends it to be a strong smooth muscle relaxant. It is not only steroidal but possesses the putatively important hydroxyl group in the 17β position, alongside the incorporation of a tertiary amine side group, again mimicking the structure of tamoxifen. Surprisingly, although relaxation was indeed achieved, and independent of endothelium, the addition of a 17β -OH group did not confer any more potency

than did the parent compound, Oestrone, which only realised approximately half maximal percentage relaxation. Of course, this is not an unknown response for oestrogens possessed of a 17β -OH group. For instance, Kitazawa *et al.*, report the relative potency of oestriol for relaxing pre-contracted rat femoral arterial smooth muscle is much less than 17β -oestradiol but no more than Oestrone [226].

Oestrone-Oxime is structurally similar to Oestrone but with the substitution of an oxime group in place of the carbonyl group at position 17 of the D ring. Given that tamoxifen is a vasorelaxant in possession of a tertiary amine group, it was postulated that the nitrogen component of the oxime group may enhance the activation of the BK channel by strengthening the interaction between drug and channel. It was previously shown by Cui *et al.*, [256] that addition of a short chain oxime ether to 12, 14-dichlorodehydroabiatic acid (diCl-DHAA), a novel BK channel opener, significantly increased activation of the BK channel

Here, Oestrone-Oxime appeared to be the most potent analogue of Oestrone, but this potency was dependent on the presence of an intact endothelium (Figure 3.3.5.1). This suggests that this compound acts *via* endogenous, endothelial-derived vasoactive substances. This is not to say compounds bearing a C=NOH function cannot elicit an endothelium-independent vasorelaxant response. Indeed, previous work has established that such compounds can relax vascular smooth muscle by acting as efficient NOS-independent nitric oxide donors and activators of the cGMP pathway.

Furthermore, it has been reported that oximes are prone to metabolise to NO *via* cytochrome-P450 [257-260]. These studies have substantiated that oxidative cleavage of the C=NOH functional group is characteristic of a NOS-independent pathway for NO production in the rat aorta [258, 261]. Chalupsky *et al.*, also established that in isolated rat aorta, some oxime derivatives increase NO levels and induce an endothelium-independent relaxant effect suggesting that metabolism of oximes to NO occurs within the smooth muscle cells themselves [261].

The recordings from this study, which show that Oestrone-Oxime is a more effective relaxant when the endothelium is left intact, indicate that the Oestrone-Oxime may act as a nitric oxide donor, principally, within the endothelial cells of the vasculature. This also implies that this is a potential site for oxime metabolism and nitric oxide release. An alternative explanation is that Oestrone-Oxime is an agonist at one of the vasorelaxant receptors found on vascular endothelium. For example, Oestrone-Oxime could be a muscarinic, bradykinin or substance-P receptor agonist. Whatever the mechanism involved, when the endothelium is removed, Oestrone-Oxime has a similar potency to the other derivatives.

3.5 SUMMARY

The principal findings in this chapter are:-

1. With the exception of Quat-DME-Oestrone, all compounds could relax the aortic rings in a concentration-dependent manner.
2. Oestrone-Oxime was the most potent derivative provided that the endothelium was intact, thus demonstrating an endothelium-dependent relaxation and that the oxime functional group may afford a conduit for NO donation.
3. Quat-DME-Oestradiol was the only derivative that demonstrated significant IbTX sensitivity implying that BK channels are important in its mode of action.
4. With the exception of Quat-DME-Oestrone, all the compounds demonstrated a relaxation in the aortic rings with or without endothelium. Apart from Quat-DME-Oestradiol, this relaxation was not reversed by IbTX, implying a mechanism of action for these compounds that is independent of BK channels.

The fact that BK channels are known to be activated by nitric oxide [262, 263] and regulated by second messengers such as cGMP [91, 264], it would be premature to claim the reversal by IbTX is proof of direct action on BK channels by Quat-DME-Oestradiol and further experimental investigation was essential to preclude a delineated membrane receptor mechanism.

These data have highlighted the intricacy of the underlying mechanisms of BK involvement in smooth muscle vasorelaxation. In addition, the long

established modulatory effects of oestrogens on endothelial NOS, and neuronal NOS more recently discovered to be present in vascular smooth muscle [265-268], generate a complicated picture which is not conducive to the direct investigation of novel BK activators. It was, therefore, essential to explore the effects of Oestrone and the novel xenoestrogens in a simpler system capable of isolating the BK channel from some of these cellular events.

The next chapter investigates the compounds *in vitro* with HEK 293 cells over-expressing BK proteins using the whole cell-patch-clamping technique. This technique allows control of the extra and intracellular environments and in addition, HEK 293 cells are not known to express some endogenous membrane bound receptors such as ER α or ER β [269, 270] or GPR30/GPER [271]. Thus, the effects of the compounds on BK channel activity and subsequently, their mode of action can be studied in more detail and free from confounding factors.

CHAPTER 4

Effects of Oestrogens on BK Currents

in

HEK 293 Cells Expressing

BK Channels

4.1 INTRODUCTION

In the previous chapter (Chapter 3), relaxation of pre-contracted rat aortic rings was demonstrated after application of the novel oestrogenic compounds. However, because this technique is an assessment of these compounds as relaxants and not a test for direct activation of the BK channel, it is at best a proxy marker for BK channel involvement. It is possible that some of these compounds are, for example, inhibitors of the spasmogenic α_1 receptor which could explain some of the relaxations observed in Chapter 3. In addition, these compounds could be activating the BK channel indirectly *via* membrane oestrogen receptors such as GPR30. Thus, reversal of relaxation by iberiotoxin is only an indication of BK channel involvement and not proof of direct binding to the channel. It is for these reasons that a more direct approach was required. The patch-clamp technique affords the opportunity to test the compounds on BK channels over-expressed in an appropriate expression system devoid of these confounding factors.

4.1.1 Expression systems

Expression systems are carefully selected as vehicles designed for the specific reproduction of a particular gene product of interest. Expression systems are not new in nature, indeed viruses successfully utilise this platform, replicating viral proteins and genetic material *via* a host cell. Prokaryotic e.g. *Escherichia coli* and eukaryotic systems e.g. yeast, insect cells and mammalian cells, are the favoured expression systems, although no system is deemed to be a universal expression system for heterologous

proteins [272]. However, many eukaryotic proteins experience various post-translational modifications such as protein-folding, glycosylation and phosphorylation, therefore, it is logical that these proteins be expressed in a eukaryotic system [272]. Other known advantages of eukaryotic protein expression systems include very high expression levels of the protein of interest, purification of the proteins is easier and protein tagging can be implemented. Two commonly used heterologous systems of choice being *Xenopus* oocytes and mammalian cell lines.

Oocytes, taken from the South African clawed toad (*Xenopus laevis*), have been extensively employed to express mammalian proteins for ion channel characterisation. Various pioneering experiments by Miledi and co-workers in the early 1980s illustrated that different ion channels, receptor and transporter proteins could be successfully expressed in *Xenopus* oocytes [273-279]. Indeed, this was very quickly adopted as a preferred technique for the study of ion channel properties by electrophysiologists. The oocyte's ease of manipulation, due to its substantial girth (≤ 1.1 mm), is a great advantage, alongside very high levels of channel expression in the plasma membrane, achieved through proficient translation of cRNA [274]. However, various pharmacological agents have been deemed less potent on channels expressed in oocytes, compared with those expressed in mammalian cell lines or native tissue [280]. In addition, interaction with endogenous proteins, leading to upregulation of endogenous channels, is a possible disadvantage of heterologous exogenous protein expression in *Xenopus* oocytes. This was successfully demonstrated by Sanguinetti *et al.*, (1996) who hypothesised that

the slowly activating delayed-rectifier K⁺ channel (I_{Ks}) forms from co-expression of KvLQT1 and minK, a constitutively expressed subunit [274, 281]. Additionally, differences in lipid organisation and structure between *Xenopus* cell membranes and those of the native cells may cause modification of the channel of interest [274, 282, 283].

These multifarious cellular events are not unique to *Xenopus* oocytes; various workers have demonstrated altered ion channel characteristics depending on the particular expression system employed [284-287]. For example, work done by Zhang *et al.*, showed that the TRPC4 channel instigates expression of inward rectifier (Kir) subunits when expressed in HEK 293 cells [287]. Experiments, carried out by Petersen and Nerbonne (1999), included a comparison of the voltage-dependent properties of Kv4.2 currents expressed in HEK 293 cells and cardiac myocytes with *Xenopus* oocytes and Chinese hamster ovary cells (CHO) [285]. They showed that Kv4.2-induced currents diverge depending on which expression system is used. They were able to demonstrate activation/inactivation rates and recovery from steady-state inactivation are significantly slower (x 5-10) in *Xenopus* oocytes compared to mammalian HEK 293, CHO and neonatal rat ventricular cells. However, despite their functional variance, expression systems are considered to successfully mimic ion channel behaviour [288].

4.1.1.1 HEK 293 cells as an expression system for BK channels

Human embryonic kidney (HEK 293) cells, since their inception more than 30 years ago, are a well-known expression system for the study of exogenous ion

channels, exchangers and transporters [289, 290]. This human cell line is a heterogeneous population generated by transformation of primary cultures of kidney epithelial cells through the incorporation of sheared adenovirus (Ad)5 DNA into chromosome 19 of the host genome [289-291]. For this study, HEK 293 cells were the preferred ion channel expression system for patch-clamp recordings of BK currents. These cells are well suited to the whole cell patch clamp technique due to their morphology and electrical properties. A viable HEK 293 cell has a typical flattish polygonal or rhomboid appearance with elongated processes and have a distinct epithelial appearance when confluent (Figure 4.1.1.1.1) [291]. With a resting membrane potential of about -40 mV and, at about 20 - 30 μm in length, the cells are an ideal size to sustain voltage clamping and accommodate the patch electrode [291].

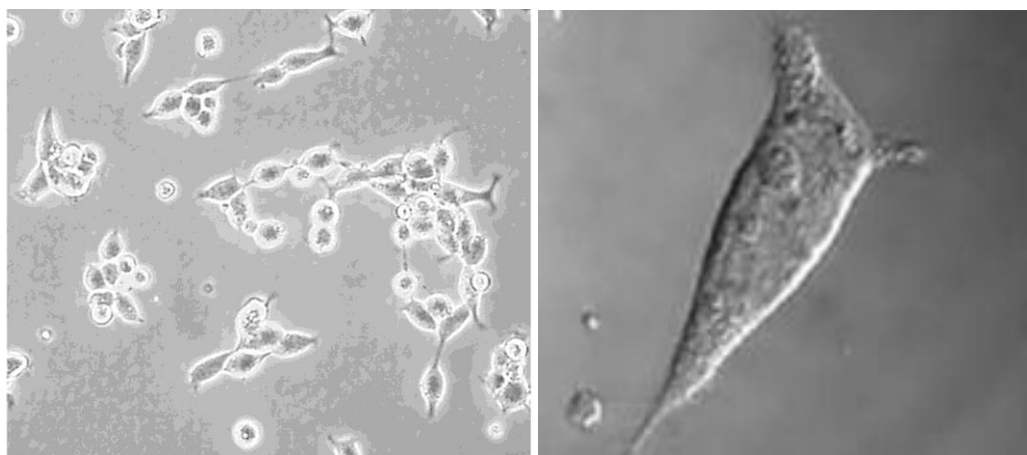


Figure 4.1.1.1.1 Transmitted light images of non-transfected HEK 293 cells illustrating morphology and processes [291]

While HEK 293 cells are epithelial in origin, they are not typical kidney cells and have been shown to possess proteins e.g. neurofilament (NF) subunits which have neuronal heritage [290, 291]. There have been numerous other

studies showing the presence of a variety of endogenous ion channels in HEK 293 cells [284, 292-299] (Table 4.1.1.1.1) and, as with *Xenopus* oocytes, there is evidence for cross-talk between constitutively-expressed and exogenous proteins [281].

Table 4.1.1.1.1 Examples of proteins, receptors and ion channels (non-exhaustive) detected in native untransfected HEK 293 cells.

Endogenously expressed proteins	Type		Refs
Potassium channels	Voltage-gated	Kv(α) 1.1; 1.2; 1.3; 1.4; 1.6; 3.1; 3.3; 3.4; 4.1 and Kv(β) SK1	[284, 292, 293, 300]
Sodium channels	Subunits Voltage-gated	BNaC2; β 1A Na _v 1.7	[294, 295]
Ca²⁺ channels	Voltage-gated	α 2 β ; α 2 δ isoforms I and β	[296]
Chloride channels	Voltage-independent		[292]
Acid sensing ion channel	ASIC	1 a	[297]
Protein Kinase A	Subunits	Catalytic and regulatory (R) II α and β	[301, 302]
Protein Kinase C		α and δ	
Store operated Ca²⁺ entry		Transient receptor potential channels (Trp)1, 3, 4, 6, 7	[298, 303]
Receptors	Ryanodine		[304]
	G-protein coupled	Histamine (H1HR)	[305]
	Ligand-gated	Muscle AchR δ	[291]
		nAchR α 7 and α 5	[291]
Neuronal proteins	Neurofilament Subunits (NF)	NF-L, NF-M, NF-H and α -internexin	[290]

It is well documented native HEK 293 cells possess endogenous voltage-gated potassium channels [284, 292, 293]. Work carried out by Yu and Kerchner [292], using whole cell voltage clamp recordings, confirmed the presence of outward potassium currents in non-transfected HEK 293 cells. Their experiments indicated that the potassium sensitivity and reversal potential of the outward current were commensurate with *Nernst* equation predictions and implicated the involvement of delayed rectifier channels. However, it is important to emphasise, that these observed endogenous potassium currents are insignificant and overwhelmed by currents engendered from the over-expression of the exogenous channel gene of interest [306]. Cloned BK genes have been successfully expressed in HEK 293 cells facilitating single-channel analysis of BK currents [307, 308]. To date, no constitutively expressed BK channels have been observed in non-transfected HEK 293 cells [292, 300, 309-311].

Also, there are no known endogenous membrane oestrogen receptors in HEK 293 cells, such as ER α and ER β or GPR30s [271, 312]. This is a key advantage for this study as any observed modulation of BK channels in the presence of the novel oestrogens is unlikely to be due to involvement of these receptors.

Another important advantage of HEK 293 cells is their lack of endogenous eNOS, nNOS, and iNOS [313-317], making them an ideal expression system for this study. In aortic rings, nitric oxide synthase involvement could not be discounted as a contributory factor in the observed relaxation of the tissue

after adding synthesised compounds. Moreover, eNOS and other NOS isoforms (nNOS and iNOS) are activated by transient increases in intracellular Ca^{2+} which triggers Ca^{2+} -calmodulin binding causing subsequent release of nitric oxide [316, 318]. Using the HEK 293 expression system and the patch-clamp technique, the effects of NOS activity can be precluded due to - a) a lack of endogenous NOS and b) control of intracellular Ca^{2+} concentrations. Since NOS is activated by intracellular Ca^{2+} , recordings made with zero Ca^{2+} in the pipette guarantee a lack of NO involvement.

The HEK 293 cell is a stable, well used cell line which possesses an immense capacity for effective transfection [306] and remains an expression system of choice for the investigation of BK channels using the patch clamp technique. For this study, the patch clamp technique will be used to examine the effects of the novel oestrogens on the function, kinetics and pharmacological activity of BK channels. For this reason, an expression system which is stable and can accommodate high expression levels of the cloned channel of interest is essential and HEK 293 cells are an ideal option.

4.1.2 The patch clamp technique

Patch clamping, first introduced by Neher and Sakmann during the 1970s, is a modification of the voltage clamp technique and has become a principal procedure for studying the properties of ion channel. The patch clamp method revolutionised electrophysiology and has facilitated the direct recording of both single and whole cell ion channel currents across the cell membrane in real time [319]. Due to the high sensitivity and high time resolution of the

technique, it is now possible to examine and characterise the biophysics and pharmacological properties of specific ion channels expressed in different cell lines. Various patch clamp configurations have been developed which have facilitated the recording of ionic activity from different surfaces of the plasma membrane. Specifically, outside out, inside out, cell attached, whole cell and perforated whole cell techniques (Figure 4.1.2.1) [319].

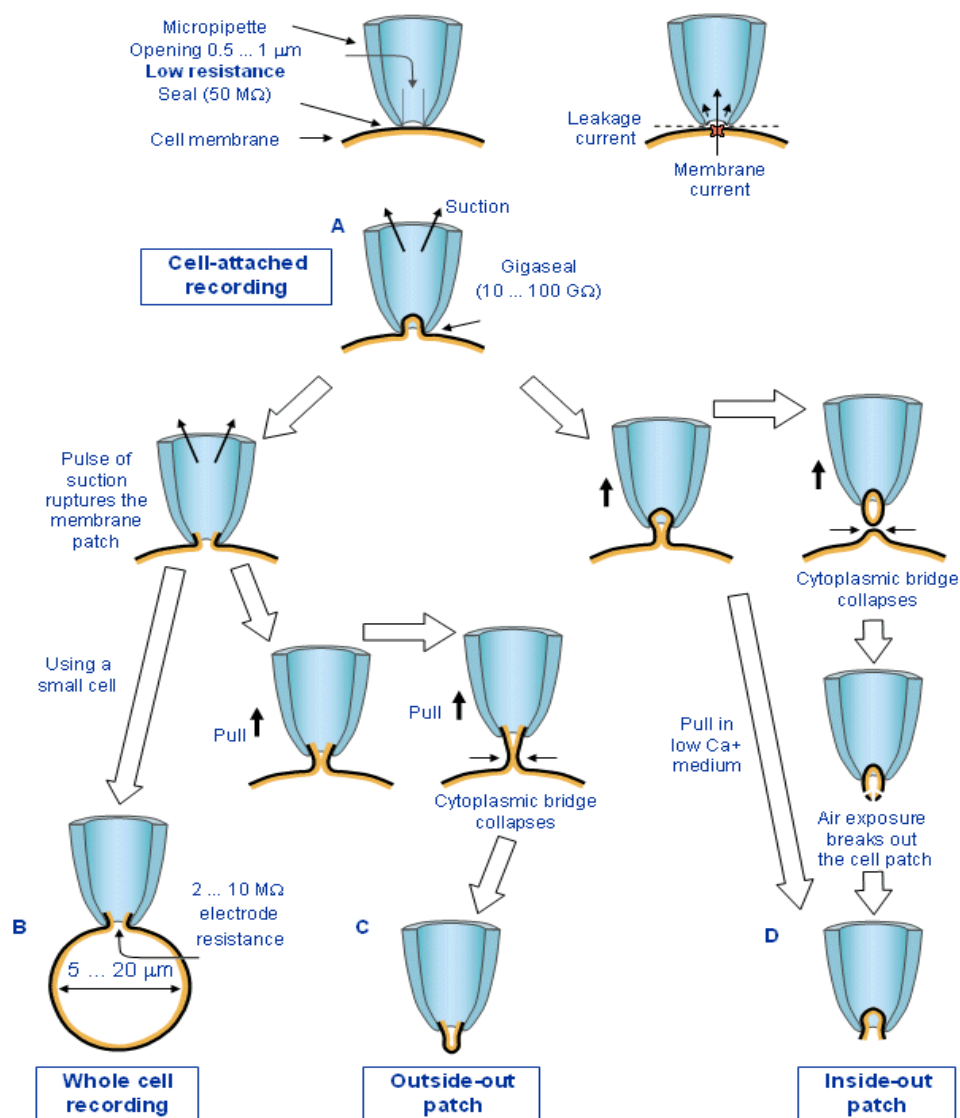


Figure 4.1.2.1 Schematic illustration of the four different methods of patch clamp: (A) cell-attached recording; (B) whole cell configuration; (C) outside-out configuration; (D) inside-out configuration [319]

There are intrinsic advantages and disadvantages associated with each of these configurations but the versatility of the patch-clamping technique is such that disadvantages may be overcome by using a different configuration. For example, a paucity of active channels present in a small patch of cell-membrane may be overcome by using whole-cell method (Table 4.1.2.1).

Table 4.1.2.1 Summary of advantages and disadvantages of patch-clamp configurations.

Configuration	Recording	Advantages	Disadvantages
Cell-attached	Single-channel	Cytosolic side intact (physiological). Easy to obtain.	Exact patch potential unknown. No easy superfusion possible. Possible paucity of active channels in patch.
Outside-out	Single-channel	Extracellular side can be superfused. Cytosolic environment is controlled.	Wash-out of cytosolic factors leading to possible run-up/down of observed currents. Disruption of cytoskeletal structure. Possible paucity of active channels in patch.
Inside-out	Single-channel	Cytosolic side can be superfused. Extracellular environment is controlled.	Bath solution must be replaced by intracellular solution. Relatively difficult to obtain Disruption of cytoskeletal structure. Possible paucity of active channels in patch.
Whole cell	Macro-current	Quick assertion of ion channel populations. Cytosolic environment is controlled. Extracellular side can be superfused.	Wash-out of cytosolic factors leading to possible run-up/down of observed currents.
Perforated whole cell	Macro-current	Cytosolic ionic environment can be controlled. No wash-out of organic factors. Extracellular side can be superfused.	No control over organic cytosolic factors. Relatively difficult to obtain.

Patch clamping is, thus, a powerful tool to investigate the actions of hormones and novel channel modulators in a cellular environment where intracellular Ca^{2+} and membrane potential can be regulated.

4.1.3 Topography and structure of BK channel (*hSlo*)

The BK channel is encoded by a single mammalian gene (KCNMA1) and belongs to the multigene *Slowpoke* family that includes *Slo1*, *Slo2.1* (Slick) and *Slo2.2* (Slack) and *Slo3* [98, 320-323] (See Table 4.1.3.1).

Table 4.1.3.1 The Slo family of channels [324].

Channel	Alternative names	Gene (human)	Chromosome location	Conductance	Blockers	Openers	Auxiliary Subunits
<i>Slo1</i>	BK, K _{Ca} , Maxi-K, KCa1.1	<i>KCNMA1</i>	10q22.3	150–350 pS	Slotoxin ^[325] Iberiotoxin ^[326, 327] , Charybdotoxin ^[327-330] , Tubocurarine ^[331-334] , Kaliotoxin ^[335] , Penitrem A ^[336] , TEA ^[308, 337-340] Paxilline	NS004 ^[120] , NS1619 ^[341] DHS1 ^[209]	β ₁ (KCNMB1) β ₂ (KCNMB2) β ₃ (KCNMB3) β ₄ (KCNMB4)
<i>Slo 2.1</i>	Slick, K _{Na} , KCa4.2	<i>KCNT2</i>	1q31.3	60–140 pS	Intracellular ATP, Quinidine,	Fenamates e.g.niflumic acid [342]	Not known
<i>Slo 2.2</i>	Slack, K _{Na} , KCa4.1	<i>KCNT1</i>	9q34.3	100–180 pS	Bepridil [343]	Loxipine [344]	Not known
<i>Slo 3</i>	K ⁺ large conductance pH sensitive channel, KCa5.1	<i>KCNU1</i>	8p11.2	70–100 pS	Quinidine	Not characterised [345]	LRRC52 (testis-specific <i>mSlo3</i> auxiliary subunit) [345]

The single gene (*Slo1 locus*; 10q22.3) encoding the BK channel is highly conserved and was first cloned from *Drosophila melanogaster* (*dSlo*) [17, 20, 346]. Mutations of the *dSlo* locus were discovered to eliminate rapid Ca²⁺-activated K⁺ currents in *Drosophila* muscle and neuronal tissue [16, 347]. Since then, orthologues of the *Slo* gene have been isolated and cloned from organisms including the nematode *Caenorhabditis elegans* (*ceSlo*) as well as smooth muscle, skeletal muscle, cochlea and brain from a variety of mammals e.g. *mSlo*, *rSlo*, *hSlo* (mouse, rat and human respectively) [19, 20, 34, 98, 348].

Although it is highly conserved, Lagrutta *et al.*, demonstrated that expression of the *Slo* gene is concomitant with multiple alternate splice variants which give rise to wide-ranging and complex mRNA expression patterns and functional differences between the encoded channels [17, 19, 324, 346, 349, 350]. Their findings suggest the presence of interactive functional domains of *Slo* subunits which influence unitary conductance, calcium sensitivity and gating [350-352]. Alongside alternate splicing, other mechanisms have been found to modify *Slo* channel properties, including heteromeric assembly with other subunits e.g. *Slo/Slack* channels [353], intracellular phosphorylation/dephosphorylation [354, 355] and redox states, which have been shown to alter activation kinetics and shift channel activation to more negative potentials without altering conductance or voltage dependence [356]. Indeed, DiChiara and Reinhart used cloned *hSlo* and *dSlo* channels expressed in HEK 293 cells and *Xenopus laevis* oocytes to investigate the redox modulation of Ca²⁺-activated potassium channels [356]. Interestingly, while changes to the redox

ratio in the cytoplasm of *dSlo* channels had no effect on channel modulation, they established that the oxidising agent, H₂O₂, caused a shift in voltage sensitivity towards a more positive direction in *hSlo*, thereby, decreasing the activity of the channel over time. They also suggested that the observed *hSlo* channel run-down in patch excision configurations might be explained by the gradual oxidation of cysteine residues usually exposed to the relatively reduced state within the cell [356]. This was borne out in a later study carried out by Tang *et al.*, [357] who established that cysteine oxidation generally inhibits *hSlo* channel activity.

4.1.3.1 BK alpha subunit (*Slo1*)

Slo1 encodes for the pore-forming α subunit which, as a typical tetrameric assemblage, comprises a functional BK channel [17-19, 21, 22, 358]. Although, included in the voltage-dependent potassium (Kv) channel superfamily as a consequence of the presence of a positively charged fourth transmembrane segment (S4) and sequence analysis [24, 359], the presence of an extra hydrophobic seventh transmembrane segment at the NH₂ terminus (S0) [23, 24] lends individuality to this BK α protein (most members of this family comprise just six transmembrane segments S1 to S6) [23, 35] (see Figure 4.1.3.1.1 for comparison).

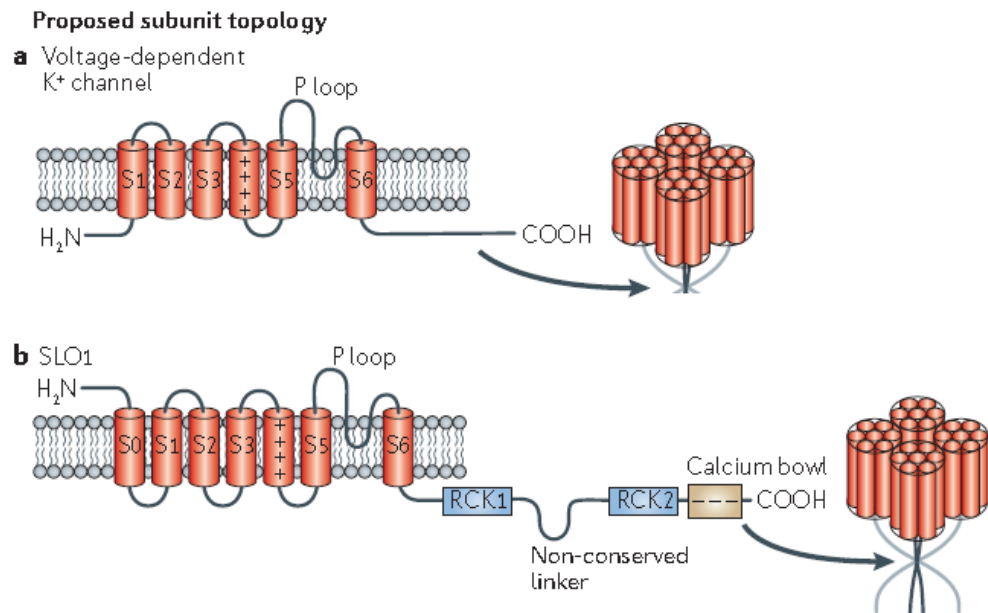


Figure 4.1.3.1.1 Schematic of Slo1 α subunits. The structural properties of Slo1 (b) are compared to the α subunit of a voltage-dependent ion channel (a). Both channels have membrane-spanning domains S1-S6 but the Slo1 channel has an extra S0 membrane-spanning domain. Slo1 also has an extended intracellular carboxyl C-terminal incorporating the Ca²⁺ bowl and RCK potassium regulating domains which modify channel gating. Four α subunits of each channel come together to form the pore of the individual channel. Taken from Salkoff et al., (2006) [324].

The modular structural characteristics of the BK (Slo1) channel are testament to its unique physiological property, viz. dual regulation through membrane depolarisation and varying levels of intracellular Ca²⁺ concentrations [324, 360-362]. Effectively, BK α can be considered to consist of two parts - the transmembrane segments and the intracellular C-terminus region. This can further be categorised into three distinct structural domains, specifically the voltage sensor domain (VSD) which senses voltage (S1-S4); the C-terminal cytoplasmic domain which senses intracellular signalling compounds and

ligands; and the pore domain which controls ion permeation (S5-S6 spanning domains) (Figure 4.1.3.1.1 b) [363].

4.1.3.2 BK α transmembrane segment

The BK α transmembrane segments comprise the S0, the voltage sensor domain (VSD S1-S4) and the pore domain (S5-S6) (Figure 4.1.3.2.1). The S0 segment places the NH₂-terminus extracellularly and is essential for β subunit association and modulation [23, 24].

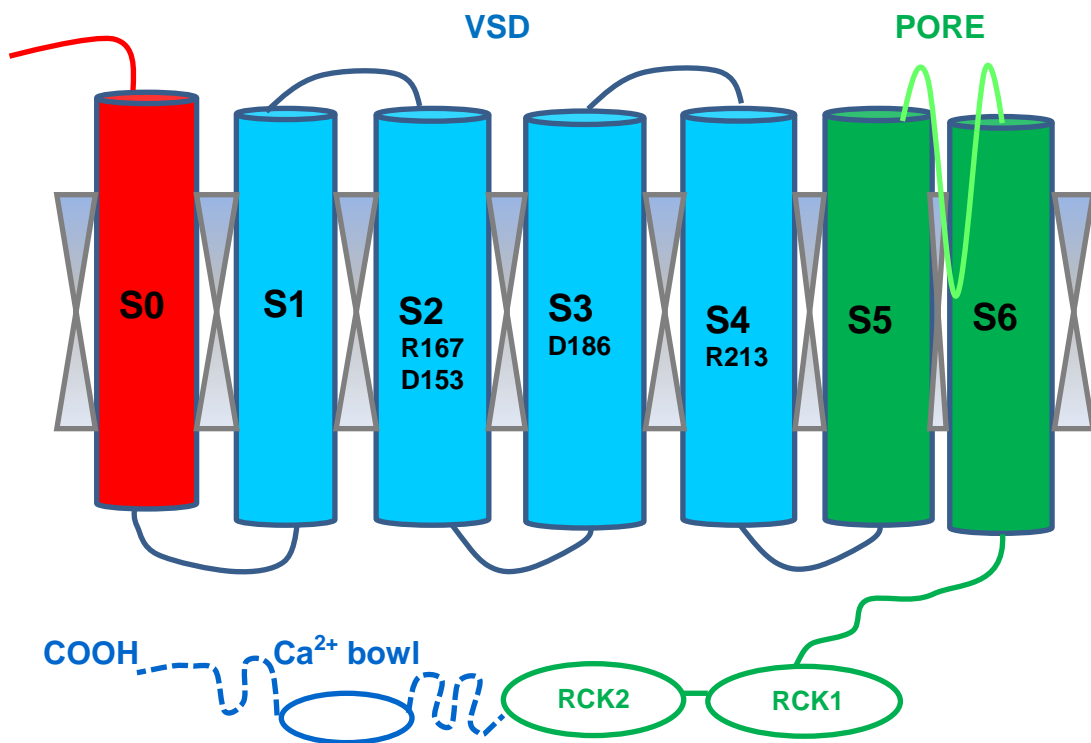


Figure 4.1.3.2.1 Cartoon of the BK α subunit illustrating the voltage sensor domain (VSD), located within S1 – S4. Four charged residues within the VSD, D153 and R167 on S2, D186 on S3 and R213 on S4, play a major role in the channel's voltage membrane sensitivity [364]. The intracellular location of BK RCK domains and Ca²⁺ bowl are also shown. Each BK α subunit possesses two tandem RCK domains, designated RCK1 and RCK2 which form the gating ring. For each α subunit in a functional tetramer, addition of a calcium bowl causes a stepwise increase in calcium sensitivity [365]. Key: VSD = Voltage sensor domain; COOH = carboxylic end.

Work done by Liu *et al.*, using disulfide cross-linking experiments, indicates the extracellular end of S0 to be in close proximity to the S3 and S4 in the VSD loop but interestingly, not to S1 and S2 [366-369]. In this experiment, double residues, one next to S0 and the other alongside S1, S2, S5, S6 transmembrane segments of the S3 – S4 loop, were mutated to cysteines (Figure 4.1.3.2.2). Given the propinquity of the S0 region to the voltage sensor, it is possible that this segment plays a role in the stabilisation of the voltage sensor in the resting state relative to other voltage-gated K⁺ channels [364, 366].

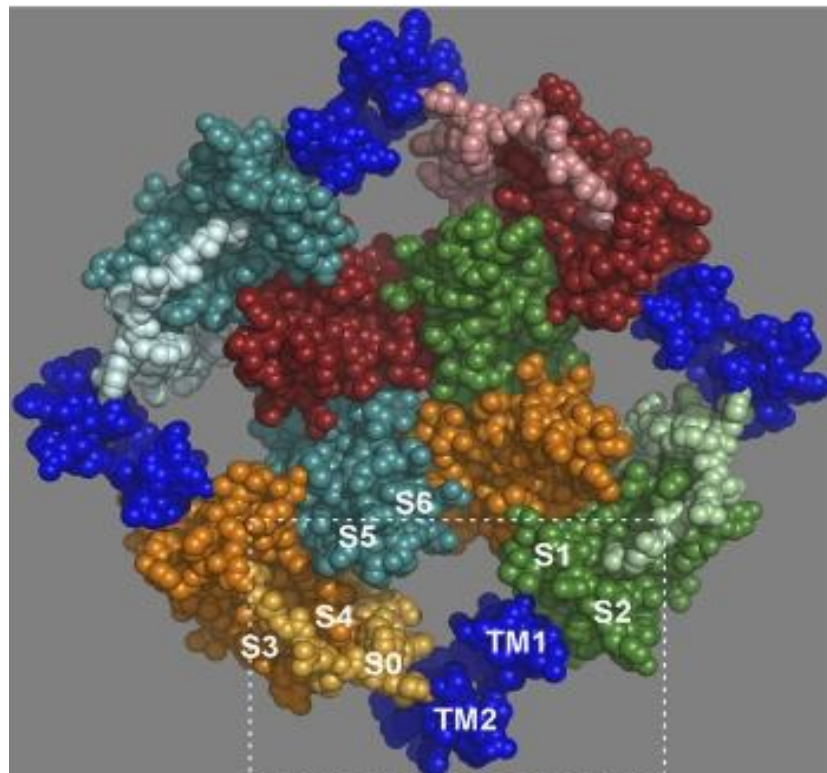


Figure 4.1.3.2.2 Model of putative location of S0 (extracellular end) relative to S1-S6 consistent with the disulfide cross-linking technique according to Liu *et al.*. This was achieved by taking a model of a Kv1.2/Kv2.1 chimera as a model for the structure of S1-S6 (BK). In this model, each of the four α subunits are represented by different colours (orange, green, red and light blue)[367]. β_1 subunits are represented by TM1 and TM2 (dark blue) with TM2 next to S0.

Voltage regulation and hence, the voltage-dependent gating kinetics of the BK channel is powerfully linked with the core region of the VSD and S0 [23, 24, 370, 371]. There are four charged amino acid residues associated with the VSD (D153 and R167 in S2; D186 in S3 and R213 in S4) (Figure 4.1.3.2.1), some of which play a role in the voltage sensitivity of the channel membrane [21, 364, 372]. S4 is reported to be the primary voltage sensor of the majority of voltage-gated channels and is certainly the most highly charged of all the transmembrane segments. However, work done by Ma *et al.*, illustrating that while S4 and in particular R213, contributes $\geq 50\%$ of the overall gating charge of the BK channel, suggests that this region may not be the primary voltage sensor [371].

Ion conduction in all potassium channels is similar and, invariably, involves interaction with amino acid residues within the pore domain or P-region, located between the S5 and S6 segments which also include a signature sequence of the potassium channel – TVGYG [373]. Many workers have demonstrated the involvement of these residues with pore-blocking toxins (the α -, β -, and γ -scorpion toxins abbreviated KTx), K^+ channel blockers and conducting ions [374-377]. However, BK and other voltage-dependent potassium channels diverge in their affinity and specificity for the diverse subfamilies of α -KTx. Indeed, only one α -KTx subfamily (α -KTx 1.x) has high affinity for BK α subunits while other voltage-gated K^+ channels display high affinity with a variety of α -KTx subfamilies [374]. However, Gross *et al.*, using site-directed mutagenesis, have demonstrated that the S5-S6 linker (pore) is probably the only part of the ion channel that directly interacts with bound toxin

[378]. The external face of the channel pore governs the blocking characteristics of tetraethylammonium (TEA) and the scorpion toxins, iberiotoxin (IbTx) and charybdotoxin (ChTx) [364, 379-381]. The turret and loop regions of the subunits' outer pore, believed to influence the binding of α -KTx, possess high sequence variability between different potassium channels. This has been mooted to be a factor in the observed variability of α -KTx specificity [374]. Additionally, work done by Carvacho *et al.*, suggests that the BK turret has 18 amino acids and an assemblage of polar residues that are strictly conserved at the N-terminal side of the turret. This implies that there are six extra residues compared to other voltage-gated potassium channels which uniquely present a site for interaction resulting in the observed exclusive BK selectivity for α -KTx 1.x [382].

4.1.3.3 BK α intracellular C-terminus segment: RCK domains, Ca²⁺ sensors and Ca²⁺ activation

Members of the *Slo* family α subunits, including the BK channel, have specialised regions that regulate potassium conductance known as RCK domains which are located in the intracellular C-terminal region between the pore-lining inner helix and the Ca²⁺ binding region [383]. The four intracellular subunits each have two tandem RCK domains (RCK1 and RCK2), where the Ca²⁺ and Mg²⁺ binding sites are located, and form the structure of the so-called gating ring (Figure 4.1.3.2.1) [364, 384]. An individual RCK domain can be divided into three sections: the N-terminal which fashions the central core of the gating ring; an intermediate domain which connects the RCK1 and RCK2 domains; and the C-terminal domain which associates with the

neighbouring RCK domain [384]. The RCK domains have been proposed to undergo a conformational change upon binding calcium which mechanically pulls the channel open [383, 385, 386].

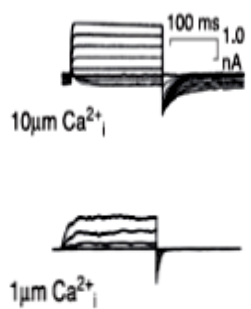
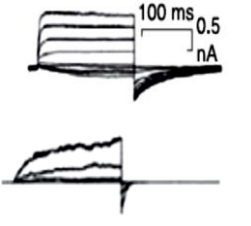
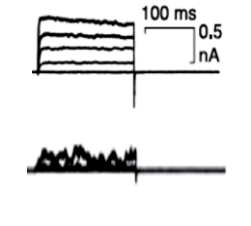
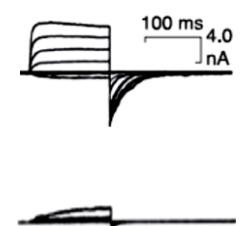
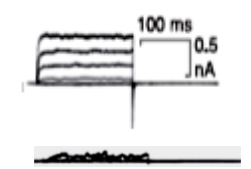
Calcium sensitivity is conferred by the region termed the 'calcium bowl' which is formed by the cytoplasmic carboxyl ends of the four α subunits located between the S9 and S10 regions of the tail (Figure 4.1.3.2.1). This region is thought to be made up of five aspartate residues and is unique to BK channels [387-389]. Wu *et al.*, have demonstrated that there may be more than one site of calcium sensitivity associated with the RCK domains. Furthermore, for each α subunit in a functional tetramer, addition of a calcium bowl causes a stepwise increase in calcium sensitivity showing an inter-subunit cooperation [365].

4.1.3.4 BK Auxiliary β subunits

It is well documented that auxiliary subunits fine tune the functioning of ion channels and the BK channel is no exception [24, 31-33, 390-392]. As fully functional ion channels, BK α convey both Ca²⁺ sensitivity and a large single-channel conductance indicative of the channel's genre (~250 pS) [358, 370, 393-397]. Most BK α tetramers, present in vertebrate cell membranes, construct protein complexes with one of four known regulatory β subunits (KCNM β 1-4) [26, 31, 32, 35, 392, 398-401]. A fifth β subunit has been proposed [402] and Uebele and co-workers have confirmed the existence of β_3 (a-d) variants which have evolved from alternate splicing of a single gene [32]. Although BK α mRNA has ubiquitous tissue distribution (except for cardiac

myocytes) BK β_{1-4} have been described as being tissue specific, furnishing channel phenotypic diversity within highly conserved structures (Table 4.1.3.4.1) [31-33, 35, 42, 390-392, 403].

Table 4.1.3.4.1 BK regulatory β subunits, their tissue expression and effect on BK α channels.

BK Subunit (Gene)	Typical waveform trace (mV)	Ca ²⁺ sensitivity and activation $V_{0.5}$ kinetics	Affinity to Scorpion Toxins (i) ChTX (ii) IbTX (iii) Slotoxin	Tissue expression	Refs
$\alpha + \beta_1$ (KCNMA1 KCNM β 1)		Increased Ca ²⁺ sensitivity; Slowed activation; Slowed deactivation; Negative shift	(i) High (ii) Reduced (iii) Irreversible	Smooth muscle Trachea Coronary aorta	[15, 34, 37, 39, 42, 43, 212, 328, 404, 405]
$\alpha + \beta_2$ (KCNMA1 KCNM β 2)		Increased Ca ²⁺ sensitivity; Slowed activation; Slowed deactivation; Inactivation rapid and complete; Negative shift	(i) Low (ii) N/A (iii) None	Brain tissues Chromaffin cells Ovary Kidney	[15, 32, 35, 39, 390, 404, 406]
$\alpha + \beta_3$ (KCNMA1 KCNM β 3)		Low Ca ²⁺ sensitivity; Rapid activation; Deactivation – no effect; Inactivation rapid and incomplete; Positive shift (β 3a,c)	(i) No effect (ii) No effect (iii) No effect	Testes Spleen Pancreas	[15, 31, 32, 42, 106]
$\alpha + \beta_4$ (KCNMA1 KCNM β 4)		Low Ca ²⁺ sensitivity; Inhibits channel at \downarrow [Ca ²⁺]; Activates channel at \uparrow [Ca ²⁺]; Slowed deactivation; Negative shift	(i) Reduced in \downarrow [Ca ²⁺] (ii) Reduced in \downarrow [Ca ²⁺] (iii) Low	Central nervous system, mainly brain	[15, 31, 33, 392, 407, 408]
α alone (KCNMA1)		4 x subunits form functional channel	(i) High (ii) High (iii) High reversible	Ubiquitous, most abundant in brain tissue	[15, 366, 374, 409, 410]

In general, BK β subunits are structurally different from the cytoplasmic β subunits of other Kv channels in so far as they are membrane integral proteins, each comprising two transmembrane domains, attached by an extracellular loop composed of ~120 residues and with both carboxyl and amine termini sited towards the cytoplasm (Figure 4.1.3.4.1). This extracellular loop has four regions of conserved cysteine residues (Figure 4.1.3.4.2) which are thought to form disulfide bridges [409]. Mutagenesis experiments carried out by Hanner *et al.*, suggest that these residues play an important role in conferring a restrictive conformational change in the channel pore, providing a large increase in the binding affinity for ChTX [409].

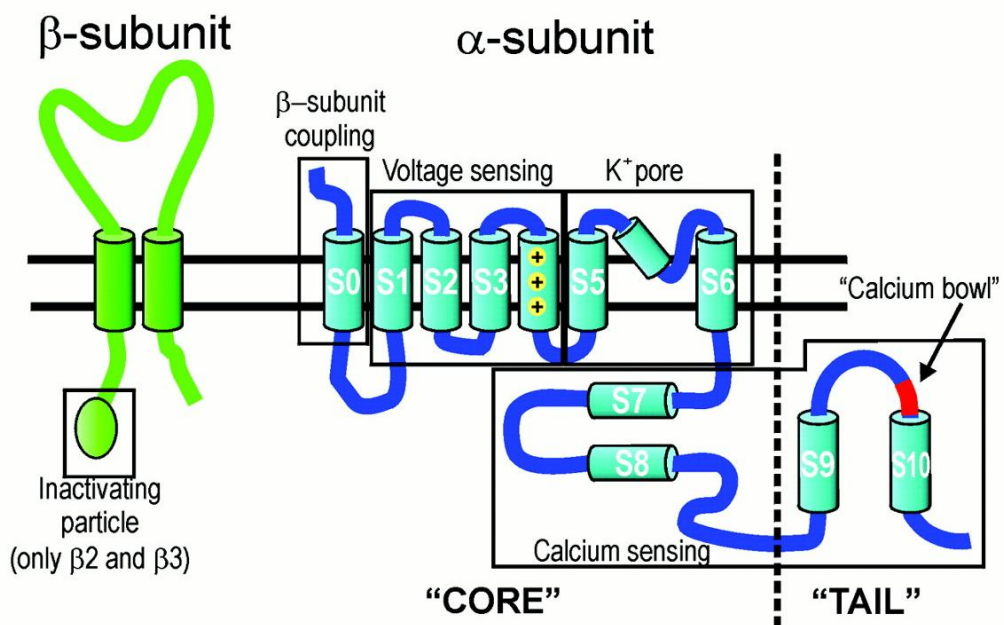


Figure 4.1.3.4.1 Schematic showing a proposed topography of BK α subunit with an associating β subunit. The “ball and chain” peptide purported to be present in β_2 and β_3 subunits is displayed [35]

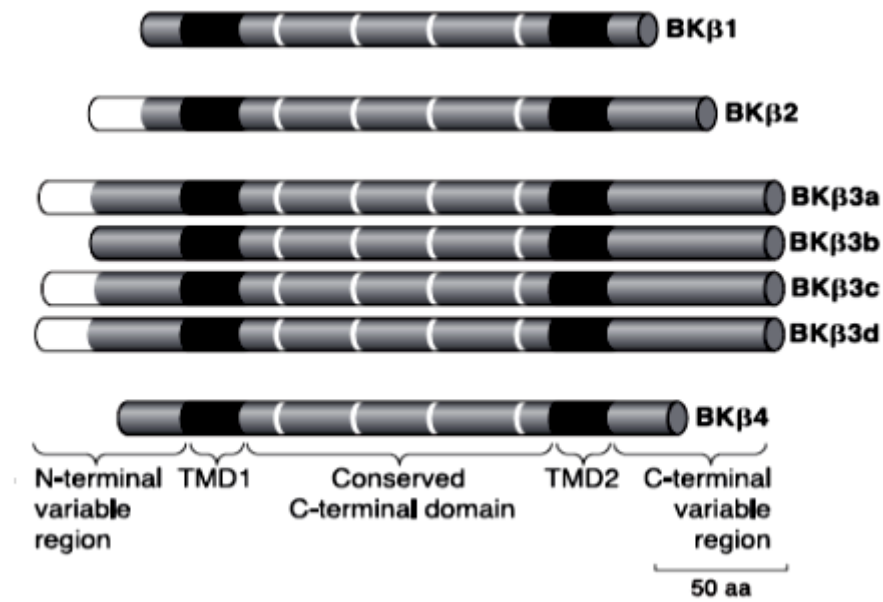


Figure 4.1.3.4.2 Schematic of HSlo KCNM β genes (KCNM β 1; KCNM β 2; KCNM β 3a; KCNM β 3b; KCNM β 3c; KCNM β 3d; KCNM β 4) encoding the pertinent BK β subunits. The diagram shows the highly conserved cysteine residues present in the extracellular domain (shown as white bands) while the two transmembrane domains (TMD1 and TMD2) are highlighted in black. Both the COOH and NH₂ termini have an intracellular orientation.

Homologous sequences are considerable between β_1 and β_2 and also between β_2 and β_3 subunits (Figure 4.1.3.4.2) [35, 401] and to this end, the functional coupling between BK α and one or other of these subunits, not surprisingly, elicits similar effects on channel modulation and kinetics in native BK currents (Table 4.1.3.4.1).

4.1.3.5 Effects of ancillary β subunits on the BK α channel

Modulation of BK α channels by co-expression with ancillary β subunits has been extensively studied and has revealed that channel gating, kinetics and pharmacology are greatly influenced by this association [36, 41, 399]. For

example, Orio *et al.*, illustrate co-expression with β subunits causes a leftward shift in the conductance-voltage relationship, particularly at higher Ca^{2+} concentrations ($>10 \mu\text{M}$) (Figure 4.1.3.5.1) [35].

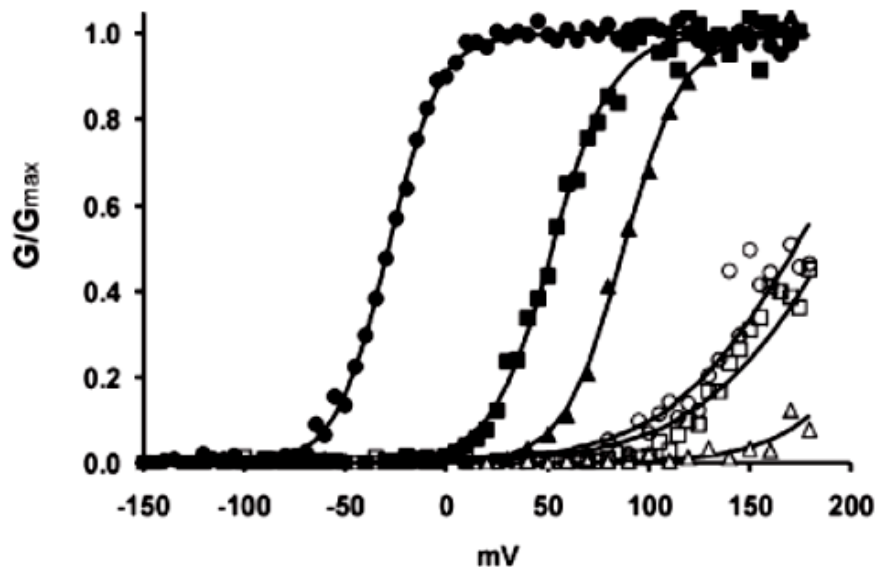


Figure 4.1.3.5.1 Plot showing comparison of G/G_{max} -Voltage at $4 \mu\text{M} [\text{Ca}^{2+}]_i$ (filled-in symbols) and $7 \text{nM} [\text{Ca}^{2+}]_i$ (open symbols) between $\text{BK}\alpha$ alone (square); $\text{BK}\alpha + \beta_1$ (circle); and $\text{BK}\alpha + \beta_4$ (triangle) subunits. The plot illustrates a marked leftward shift at higher $[\text{Ca}^{2+}]_i$ for BK channels co-expressing β_1 subunit in comparison to $\text{BK}\alpha$ alone. At nM concentrations, the leftward shift is less marked. At higher $[\text{Ca}^{2+}]_i$, co-expression with β_1 subunits elicits channel activation, however at $[\text{Ca}^{2+}]_i$ nM, the channel is inhibited [35].

Brenner *et al.*, confirmed similar levels of Ca^{2+} sensitivity enhancement and a negative shift in $V_{0.5}$ activation in $\text{BK}\alpha$ when associated with β_1 or β_2 subunits, and further, noted slower activation kinetics in their presence [31]. Association with β_3 and β_4 subunits, however, induces a low sensitivity to Ca^{2+} but conversely, accelerated activation kinetics with co-expression of the β_{3b} phenotype [404]. Both β_2 and β_3 ancillary subunits can induce rapid inactivation of BK currents, though in the case of β_2 , in comparison with β_3 , the

inactivation is less rapid and complete [391]. This may be explained through work done by Wallner *et al.*, which has suggested the possible presence of a “ball and chain” type peptide attached to the intracellular N terminus on the β_2 subunit which yields inactivating BK currents when co-expressed with BK α [390]. The structure was further illustrated using NMR spectroscopy alongside patch-clamping in work carried out by Bentrop *et al.*, [411]. Of the four known β subunits, β_4 , expressed primarily in brain tissue, displays the least homology to the other three subunits and when co-expressed with BK α , dramatically slows activation and deactivation of the channel [407].

4.1.3.6 Stoichiometry of BK α and β subunits

It is hypothesised that BK α and β subunit stoichiometry is probably a 1:1 ratio [26, 97, 398, 412] and it is generally accepted that the α : β stoichiometry of BK channels has a role to play in channel activation and Ca²⁺ sensitivity [40, 412]. Nevertheless, several workers have suggested that not all four α subunits require coupling to a β subunit to bring about an effect on channel gating, kinetics and pharmacology. For instance, Li *et al.*, report the presence of just three β_2 subunits per BK channel in rat lumbar L4-6 dorsal root ganglia (DRG) [413] and Wang *et al.*, using inactivation as an indicator of the average number of β_2 subunits per BK channel expressed in *Xenopus* oocytes, demonstrated that functional channels are formed with less than a full complement of β_2 subunits [412]. In addition, Wang *et al.*, were able to illustrate that gating properties and inactivation behaviour of the channel correlates incrementally to the number of associating β subunits at any one time. Jones and co-workers also established that BK α + β channels can

function with less than four β subunits and further, that β_1 subunits have an all-or-nothing effect on the voltage dependence of BK α gating [414]. Conversely, the β_2 subunit bestows an incremental effect as each β_2 subunit associates with a BK α tetramer [412, 414].

It is also important to consider that the α : β stoichiometry for BK channels is imperative for pharmacological and endogenous agonists such as oestrogens. Work done by de Wet *et al.*, established, using Bayesian analysis, that at least two β_1 subunits are required for BK channel activation by 17 β -oestradiol [40].

4.1.3.7 BK β_1 subunit function and physiology

The β_1 subunit was the first of the β subunits to be cloned and is most abundant in smooth muscle cells [27, 37, 415, 416]. The β_1 subunit, in particular, has been shown to increase the calcium sensitivity of the channel while at the same time altering gating kinetics, favouring a more open state [34, 36, 37, 41, 211, 417] (Figure 4.1.3.7.1).

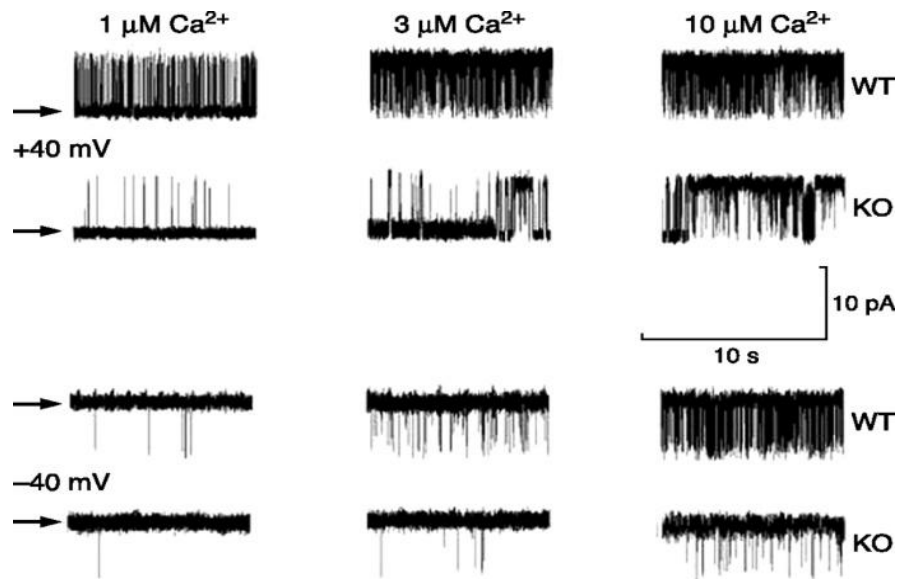


Figure 4.1.3.7.1 Comparison of single $BK\alpha+\beta_1$ currents (wild type (WT) and $BK\beta^{-/-}$ (KO) taken from recordings of isolated mouse aorta at different $[Ca^{2+}]$ and voltages (-40 mV and +40 mV). Closed states are indicated by arrows. The BK current traces pertaining to channels with both α and β_1 subunits present (WT) illustrate that an associating β_1 subunit is more conducive to an open state as opposed to channels expressing just the α -subunit (KO) at any $[Ca^{2+}]$ or selected voltage [43, 401]

These parameters illustrate that β_1 subunits are necessary for normal functioning in VSMCs. Furthermore, Nimigean and Magleby have demonstrated that the β_1 subunit increases burst duration by increasing the mean open time within a bursting state, thus reducing closed times between bursts [211]. Their observations that BK channels expressing both α and β_1 subunits spend less time in sub-conductance states suggests that the β_1 subunit is key in stabilising the full conductance level of the open states of the channel (Figure 4.1.3.7.2).

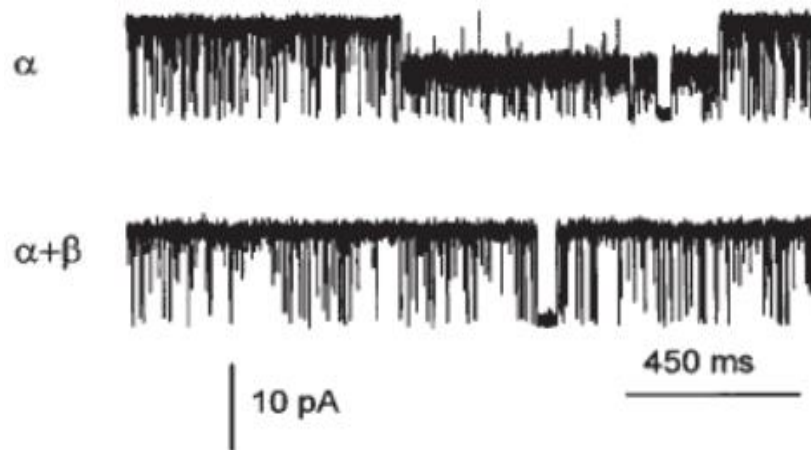


Figure 4.1.3.7.2 Recordings illustrating how the BK β_1 subunit stabilises BK channel conductance. With channels consisting of α subunits alone, sub-conductance states are observed more frequently. Channels which have associating β_1 subunits are more likely to function in the fully open conductance state. The traces show examples with full conductance of ~ 315 pS for $BK\alpha+\beta_1$ channels and sub-conductance of ~ 150 pS (approximately half the amplitude) for $BK\alpha$ alone channels. Membrane potential was held at $+30$ mV; $[Ca^{2+}]_i$ was 18 μ M for $BK\alpha$ and 5.4 μ M for $BK\alpha+\beta_1$, with $[Ca^{2+}]_i$ 3 - 100 μ M [211].

In vascular smooth muscle, the β_1 subunit augments the coupling of Ca^{2+} sparks, caused by a highly localised Ca^{2+} release from ryanodine receptors located in close proximity to the VSMC membrane, to spontaneous transient outward currents (STOC) of the BK channel. This leads to hyperpolarisation of the cell membrane and subsequent inhibition of Ca^{2+} influx via voltage-dependent calcium channels (VDCCs) and eventual relaxation [418]. Work done by Koide has recently shown that after subarachnoid haemorrhage, the frequency of Ca^{2+} sparks coupled with STOC of $BK\alpha+\beta_1$ channels is significantly decreased in cerebral artery myocytes and this contributes to elevated vasoconstriction [419]. Many other channelopathies of the vascular

system, with loss or gain of function polymorphisms of KCNM α_1 and KCNM β_1 have been reported and all are associated with a reduction in BK channel activity even in the presence of Ca²⁺ sparks [419]. For example, in β_1 knock-out mice, arterial tone and systemic blood pressure is increased, Ca²⁺ sensitivity is decreased and coupling of Ca²⁺ sparks to STOCs are disrupted [43, 51]. Furthermore, hyperaldosteronism, asthma, bladder malfunction, hypertension and diabetes are all linked with reduced expression of KCNM β_1 [53, 102, 420-422].

Finally, an additional role for the β_1 subunit has been proposed by Toro *et al.*, [423]. Their research has established that co-expression of the β_1 subunit with the α subunit, enhances surface trafficking of the α subunit. They concluded that β_1 may be a factor in the differential surface expression of BK α subunits required for successful functioning of BK α + β_1 channels expressed in relevant tissues [423].

4.1.4 AIMS

This chapter will examine the effects of oestrogens and xenoestrogens on the activity of BK(*hSlo*) channels expressing α subunits alone and, also, those expressing both $\alpha+\beta_1$ subunits in HEK 293 cells using the whole cell patch-clamp configuration. In the previous chapter, relaxation of vascular smooth muscle was observed in rat aortic rings, the only exception was Quat-DME-Oestrone which was inactive. As relaxation occurred in both endothelium-intact and endothelium-denuded aorta, and only one compound demonstrated reversibility to iberiotoxin, then multiple pharmacological actions in addition to BK activation are likely.

The aim of this chapter is to investigate directly these compounds as novel BK activators in a cellular expression system which may ameliorate some of the disadvantages of whole tissue experiments and thus, confirm effects on BK channels as predicted in Chapter 3. As both non-steroidal antioestrogens and steroidal oestrogens have previously been shown to activate BK channels in a subunit-dependent manner [101, 102, 129] it is hypothesised that these hybrid compounds will show similar subunit dependence.

Objectives:–

1. To demonstrate the presence of functional BK channels comprising either α subunits alone or $\alpha+\beta_1$ subunits in transfected HEK 293 cells. This will be achieved through noise analysis and kinetic observation of the channel in whole cell patch-clamp recordings. In addition, IbTX sensitivity of the two types of channel will be explored.

2. To investigate the activity of the synthesised derivatives on BK channels consisting of α subunits alone, as this is the type of BK channel expressed in the endothelium.
3. To investigate the activity of these compounds on BK channels expressed in HEK cells consisting of α and β_1 subunits, as this is the type of BK channel expressed in vascular smooth muscle.

This approach should:-

- confirm that Quat-DME-Oestrone is inactive as observed in aortic rings
- confirm that Quat-DME-Oestradiol, which relaxed aortic rings in an IbTX reversible manner, is indeed able to enhance BK currents
- reveal which compounds are unable to modulate BK channel function. For example, if DME-Oestrone relaxes aortic rings by a process independent of BK channels, one would expect it to be inactive against BK currents in HEK cells over-expressing BK channels
- demonstrate which compounds require the β_1 subunit of the BK channel in order to modulate BK currents.

4.2 METHODS

To investigate *directly* Oestrone and the xenoestrogen compounds as novel BK activators in a cellular expression system, HEK 293 cells over-expressing BK α alone and α plus β_1 subunits were cultured and subsequently tested using the whole cell patch-clamp electrophysiology technique.

4.2.1 Molecular biology of HEK 293 expressing the α alone and α plus β_1 subunit of the BK channel

This technique was performed by the Ashcroft group (University of Oxford). As previously described [347], the subunit stop codons in constructs pcDNA6-*hSlo α* (as used by [424]) and pcDNA3.1-*hSlo β_1* (J.D. Lippiat, unpublished) were mutated using the *Quikchange* site-directed mutagenesis kit (*Stratagene*) to introduce an in-frame vector sequence encoding V5-His6 and myc-His6 epitope tags, respectively. HEK cells were cultured as described previously [424] and transfected with pcDNA6-*hSlo α -V5* with Fugene 6 reagent, as per manufacturer's instructions. Clones that grew in medium supplemented with 5 μ g/ml blasticidin (*Invitrogen*) were isolated and a line stably expressing the epitope-tagged BK_{Ca} channels was confirmed by electrophysiology [40]. A subculture was transfected with pcDNA3.1-*hSlo β_1 -myc-His6* and a double stable cell line was generated by selection in medium containing 1mg/ml G418 (geneticin) (*Invitrogen*) and 5 μ g/ml blasticidin. A line stably co-expressing *hSlo α -V5-His6* and *hSlo β_1 -myc-His6* was characterised by electrophysiology in the Department of Physiology, University of Oxford by Jon Lippiat (Ashford group).

4.2.2 Culture of HEK 293 cells solely expressing the α subunit of the BK channel

The culture of HEK 293 cells expressing the α subunit alone (tagged at His6 with a V5 tag), was carried out as described previously [347, 425]. The cells were cultured with Minimum Essential Medium (MEM with Earle's salts and L-Glutamine) (*Invitrogen*), 10% v/v heat-inactivated foetal bovine serum (FBS) (*PAA Laboratories*), 1% v/v non-essential amino acids (NEAA) (*PAA Laboratories*) and treated with the antibiotic penicillin / streptomycin (*PAA Laboratories*). Clones, cultivated in a selective medium supplemented with blasticidin (*Invitrogen*) at a concentration of 5 $\mu\text{g/ml}$, were isolated. The cells were incubated for 48 hours at a temperature of 37°C and at a concentration of 95% O₂ and 5% CO₂. The cells were plated at a density of approximately 5 x 10⁴ cells per 35 mm diameter in *nunclon*[®] tissue culture dishes (*Fisher UK*). They were further incubated for 48 hours at a temperature of 37°C and at a concentration of 95% O₂ and 5% CO₂. The presence of BK_{Ca} channels was confirmed by electrophysiological techniques.

4.2.3 Culture of HEK 293 cells expressing the α plus β_1 subunits of the BK channel

The culture of human embryonic kidney 293 (HEK 293) cells expressing both the $\alpha + \beta_1$ subunit (α subunit tagged as before and the β_1 subunit tagged at His6 with the MYC epitope) was described previously [425]. The cells were cultured with MEM (*PAA Laboratories*), 10% v/v heat-inactivated FBS (*PAA Laboratories*) and 1% v/v NEAA (*PAA Laboratories*). Clones, cultivated in a

selective medium supplemented with blasticidin (*Invitrogen*) and geneticin (G418) (*Invitrogen*) at a concentration of 5 µg/ml and 1 mg/ml respectively, were isolated. The cells were incubated for 48 hours at a temperature of 37°C and at a concentration of 95% O₂ and 5% CO₂. The cells were seeded at a density of approx. 5 x 10⁴ cells per 35 mm diameter in *nunclon*[®] tissue culture dishes (*Fisher*). They were further incubated for 48 hours at a temperature of 37°C and at a concentration of 95% O₂ and 5% CO₂. The presence of BKCa channels was confirmed by electrophysiological techniques.

4.2.4 Whole cell patch clamp experimental methods

Macroscopic currents were recorded from single, isolated cells by whole-cell patch clamp technique as described previously [426]. Cultured HEK 293 cells, over-expressing BK α or BK α + β ₁ subunits, were continuously superfused, gravitationally, with an extracellular solution containing (mM): 136 NaCl, 2.6 CaCl₂, 2.4 KCl, 1.2 MgCl₂, 15 HEPES, 10 glucose, titrated with NaOH to pH 7.4 at 21° C. Gravitational superfusion of cells was carried out *via* a Warner Instruments perfusion manifold (model MP-2) at a rate of 2 ml/min and a temperature of 21° C.

Patch electrodes with a resistance of approximately 5 M Ω were forged from borosilicate capillary tubes (*Harvard*), fire-polished and, subsequently, filled with a solution containing (mM): 110 KCl, 3.0 MgCl₂, 40 HEPES, 3 EGTA. In some solutions, calcium concentrations of 2.4 µM and 55 µM were prepared by adding 1.92 and 2.0203 mM CaCl₂ respectively. Free Ca²⁺ in each solution was calculated using the web-based program *Maxchelator* (Bers *et al.*, 1994;

available online at www.stanford.edu/cpatton/maxc.html). Atomic absorption spectroscopy was carried out on the zero μM intracellular calcium solution and was found to contain 7 $\mu\text{moles/L}$ Ca^{2+} which equates to a free calcium concentration of 0.225 nM when in the presence of EGTA (as calculated by *Maxchelator*). All intracellular solutions were titrated with KOH to pH 7.4 at 21° C.

Voltage-gated potassium currents were recorded at 21° C from cultured cells clamped at a holding potential of either -40 or -80 mV and outward K^+ currents were evoked by stepwise 10 mV changes in membrane potential lasting for 50 ms (Figure 4.2.4.1.). This protocol was repeated every 5 seconds and recordings could last up to 400s.

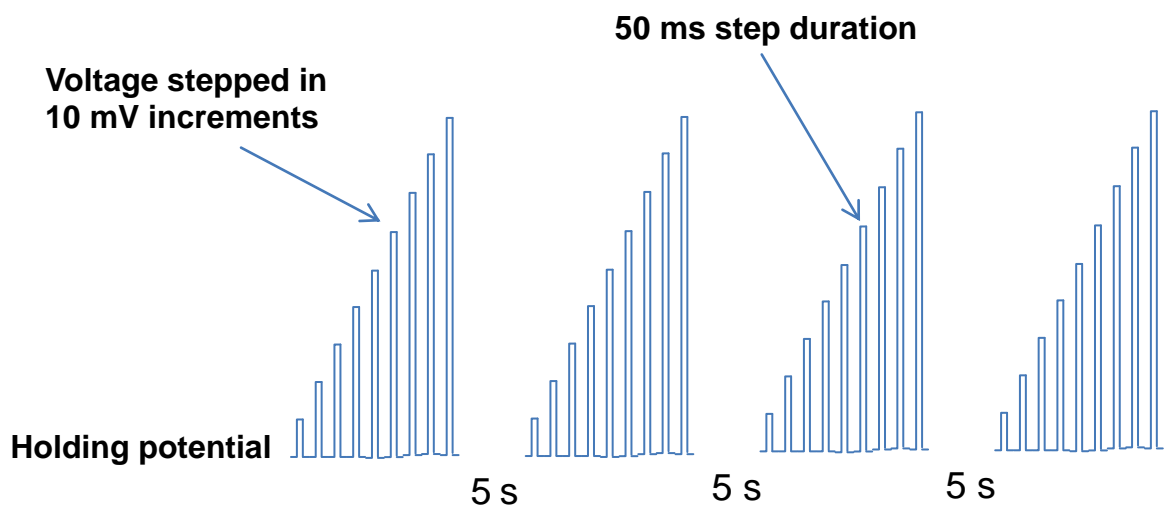


Figure 4.2.4.1 *Cartoon illustrating voltage protocol for activating BK currents. The holding potential was usually -40 mV, and the final step voltage was usually +60 mV. A more extensive range of voltages was used to generate G-V relationships.*

Raw output currents were filtered with a low band pass filter at 5 kHz, and digitised at 25 kHz using a CED 1401 interface connected to a *Pentium*[®] computer running WCP v1.6 patch clamp software. Leak current was <10 pA and did not need compensation. Electrode capacitance was compensated after G Ω seal formation (>2 G Ω). Series resistance was compensated for after obtaining whole cell access. RS compensation required was always less than 30 M Ω .

4.2.5 Data Analyses of whole cell patch clamp recordings

Statistical analyses were carried out using *GraphPad prism* version 5.03. All data are presented as the mean \pm the standard error of the mean (SEM) unless otherwise stated.

4.2.5.1 Statistical analysis of run-up and run-down

The normalised peak current and the activation plots were each analysed for correlation using a Spearman regression. This analysis was undertaken to see if the currents ran up or down with time as reported by other workers [291, 427, 428]. If the currents run up, then a plot of peak currents vs time will have a significant positive correlation. Conversely, if the currents run down, then a plot of peak currents versus time will have a significant negative correlation. No correlation implicates no run up/run down. A similar approach was used to follow changes in the activation rate during the course of the recording.

4.2.5.2 Analysis of activation rates

The activation rates of the channel (τ) were obtained by fitting the early phase of evoked currents to the single exponential function $y(t) = A e^{(-t/\tau)} + Ss$ where t = time, A = amplitude and Ss is the steady state using *winWCP1.6 Strathclyde Electrophysiological* software (Figure 4.2.5.2.1).

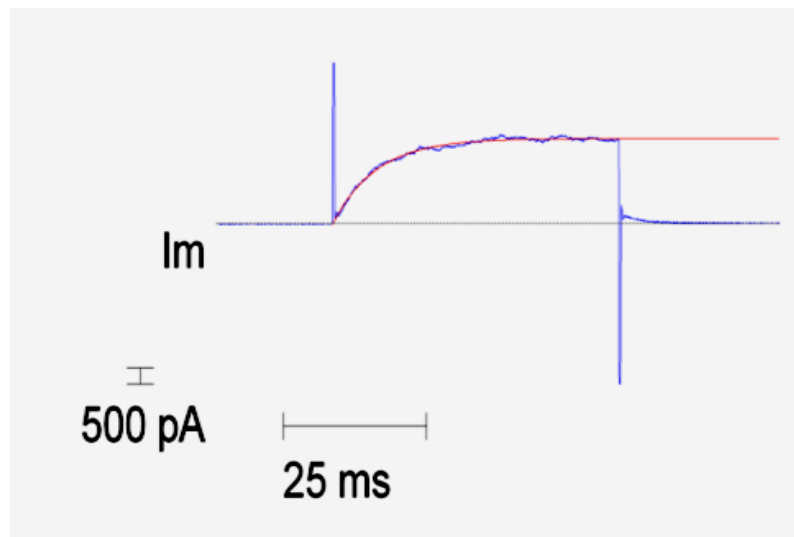


Figure 4.2.5.2.1 Example of single exponential fit of evoked BK currents in the rising phase of BK channel activation

4.2.5.3 Statistical analysis of G-V relationships

The channel conductance was obtained from the whole cell current according to the equation $G_K = I_K / (V_m - V_K)$, where G_K is the conductance and I_K is the potassium channel current, V_m is the membrane potential at which the current was measured and V_K is the equilibrium potential for the potassium current (-97 mV). The conductance data were then normalised (to allow better comparison among cells of different size) and fitted to a Boltzmann function. A

non-parametric one way analysis of variance (Kruskal-Wallis) test was used to assess the statistical significance at $p < 0.05$ of the difference in $V_{0.5}$ and slope values between differing calcium concentrations and channels expressing different subunits. A Tukey's multiple comparison test was used for comparison of multiple sets of data.

4.2.5.4 Statistical analysis of the effects of oestrogens on evoked currents

Normalised peak currents before and after the application of oestrogens were analysed using a Spearman's correlation test. However, to determine genuine effects of drug application to the BK channel currents, these data have to be compared with control data because of the propensity of recorded BK currents to run up/down with time. To address this issue, the data were analysed using a Kruskal-Wallis non-parametric test, followed by a Dunn's *post hoc* multiple comparison test and true significance was determined.

4.2.5.5 Non-stationary noise analysis (fluctuation analysis)

Functional expression of BK channels in HEK 293 cells was confirmed using fluctuation analysis [429, 430]. Fluctuation analysis estimates the single channel conductance underlying the evoked currents by statistically comparing the mean and variance of the current. HEK 293 cells were voltage clamped at -40 mV and voltage jumped to +60 mV. This was repeated 100 times at one second intervals. Using *WinWCP* software, an estimation of the underlying

unitary current (I_u) could be calculated and from this, the single channel conductance was determined.

4.3 RESULTS

Human embryonic kidney cells (HEK 293), since their inception, are a well-known expression system for the study of ion channels [289, 290]. Here, HEK 293 cells, stably transfected with genes expressing BK channel proteins were used for whole cell patch clamp recordings to investigate the effects of Oestrone and the novel xenoestrogens. Initially, the presence of functional BK channels comprising either α subunits alone or $\alpha+\beta_1$ subunits in transfected HEK 293 cells was confirmed through noise analysis and kinetic observation of the channel in whole cell patch-clamp recordings. IbTX sensitivity of the two types of channel was also explored.

4.3.1 Characterisation of the evoked BK currents of HEK 293 cells expressing the α subunit alone

BK currents were identified and recorded from HEK 293 cells over-expressing the α subunit of the BK channel (Figure 4.3.1.1 and Figure 4.3.1.2). An example of evoked currents is illustrated in Ai and Aii.

The averaged peak current versus time (seconds) for HEK 293 cells expressing the BK α subunit is illustrated in Figure 4.3.1.1(B). These currents were evoked by stepping the -40 mV holding potential to +60 mV. A positive correlation with time ($r = 0.89$) and a significant increase in normalised peak current over time ($p < 0.05$, $n = 5$) suggest the occurrence of run-up, also revealed in the recording shown in Ai and Aii. This was a controlled

experiment with no compound added to the bath solution and zero $[Ca^{2+}]_i$ in the pipette.

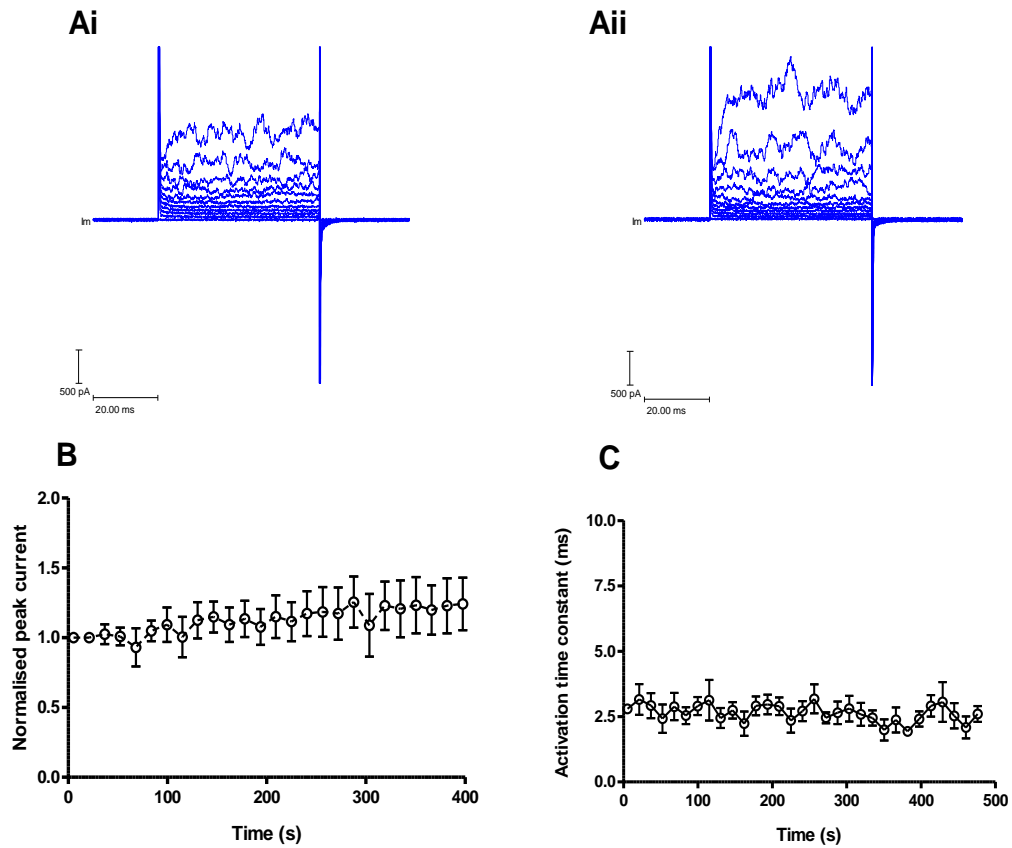


Figure 4.3.1.1 Control BK currents in HEK 293 cells expressing BK α subunits. (Ai) illustrates evoked currents at the beginning of the recording period (0 to 5s) and (Aii) illustrates evoked currents after 350 seconds of recording. Cells were voltage clamped at -40 mV and currents evoked by changing the voltage to a range of test potentials (-40 to +60 mV) in 10 mV steps. (B) illustrates how the peak current changes with time. Currents were evoked by stepping the voltage to +60 mV from -40 mV. A significant increase in the peak current was observed over 400 seconds ($r=0.89$, $p<0.01$, $n=5$). (C) The activation time constant for currents evoked by changing the potential to +60 mV. The activation of the BK current could be fitted to a single exponential ($n=5$). A small but significant difference was observed in the activation time constant over time ($p<0.05$, $r=-0.36$).

BK channels expressing only α subunits characteristically have fast activation rates [31, 431]. These observations are paralleled in Figure 4.3.1.1(C), where rapid activation rates of approximately 2.5 ms are recorded. This activity was maintained throughout the recording period and no inactivation was observed.

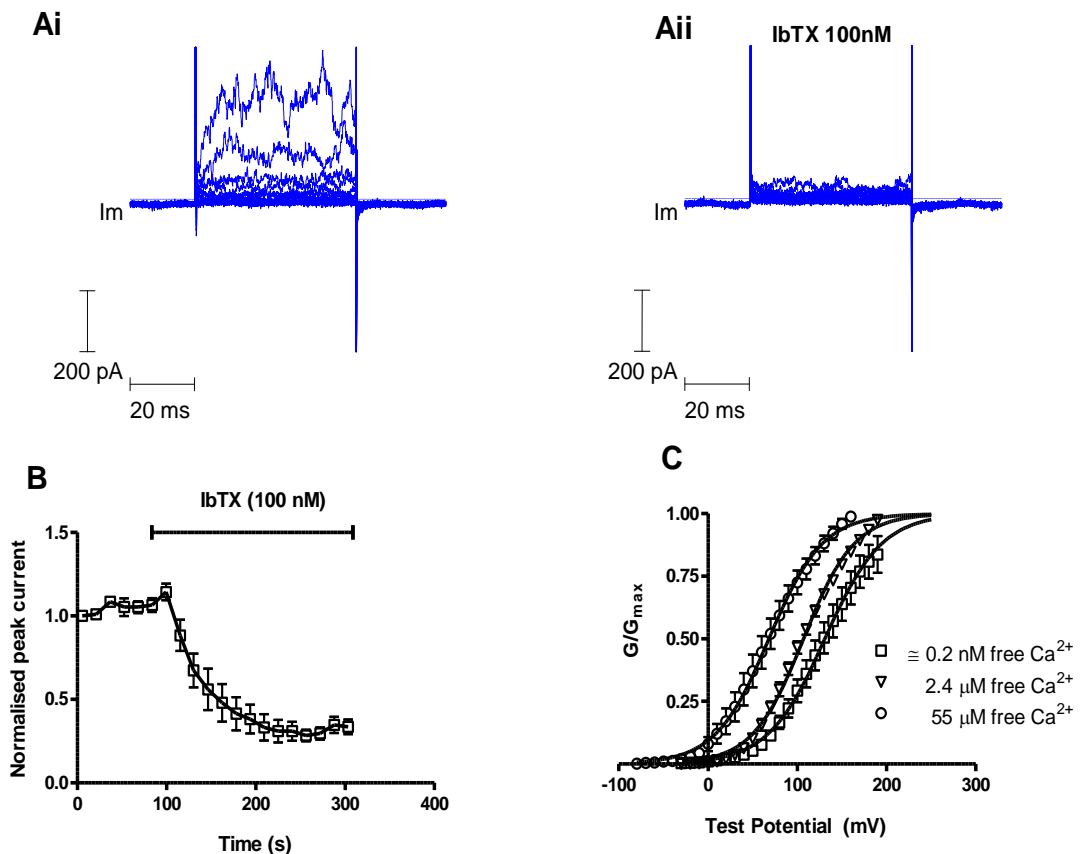


Figure 4.3.1.2 The properties of BK currents in HEK 293 cells expressing the BK α subunit. (A) Cells were held at -40 mV and the voltage changed to a range of potentials up to $+60$ mV in 10 mV increments. (Ai) illustrates evoked currents in a HEK 293 cell at the beginning of the recording period (0 to 5s) and (Aii) illustrates evoked currents after the application of 100 nM iberiotoxin. (B) summarises the blocking properties of IbTX on BK currents ($n=5$). (C) The effects of free intracellular Ca^{2+} on the G-V relationship. Conductance was calculated from current and voltage, normalised to the maximum and plotted error bars represent SEM. Solid curves represent fits to the Boltzmann function.

Consistent with other workers peak BK currents were found to be sensitive to iberiotoxin (IbTX) [432-435] (Figure 4.3.1.2(B)). Appropriate, rapid inhibition of BK current was observed on application of IbTX (100 nM). The current inhibition for this concentration of toxin (100 nM) was fitted to a single exponential with a rate of block of approximately $(2.552 \pm 0.48) \times 10^5 \text{ M}^{-1} \text{ s}^{-1}$ ($k=0.02552 \text{ s}^{-1}$, $\tau = 1/k = 39.185 \text{ s}$; $t_{1/2} = 0.693 \times \tau = 27.16\text{s}$).

The dependence of BK currents on intracellular free calcium was assessed in these preliminary experiments. Figure 4.3.1.2(C) plots normalised membrane conductance against membrane potential for a range of free $[\text{Ca}^{2+}]_i$. Recordings were analysed between a holding potential of -80 or -40 mV, in 10 mV increments up to a potential of 200 mV. BK channel conductance was monitored at 0.2 nM, 2.4 μM and 55 μM concentrations of free $[\text{Ca}^{2+}]_i$ and the $V_{0.5}$ noted (Table 4.3.1.1).

Table 4.3.1.1 Summary of hyperpolarising effects due to increasing free intracellular concentrations of Ca^{2+} ions on shifts in the $V_{0.5}$ for the voltage conductance curve of BK α channels in HEK 293 cells. Significance was determined using a, one-way ANOVA (Kruskal-Wallis) for significance followed by a post hoc Tukey's analysis for multiple comparisons

Free intracellular [Ca^{2+}]	$V_{0.5}$ from the voltage-conductance curves obtained from HEK 293 cells expressing BK α subunits
$\cong 0.2$ nM	130.9 mV ± 1.8 ‡
2.4 μ M	107.0 mV ± 0.7 ‡
55 μ M	68.28 mV ± 1.6 ★ †

Key: ★ = significantly different $V_{0.5}$ ($p < 0.05$) from 0.2 nM free intracellular calcium;
 † = significantly different $V_{0.5}$ ($p < 0.05$) from 2.4 μ M free intracellular calcium;
 ‡ = significantly different $V_{0.5}$ ($p < 0.05$) from 55 μ M free intracellular calcium

Raising the free [Ca^{2+}]_i effected a hyperpolarising shift in the $V_{0.5}$ of the voltage conductance curve (~ 60 mV). Using a one way ANOVA followed by a Tukey's multi comparison test, a significant difference in the $V_{0.5}$ ($p < 0.05$) was revealed between 0.2 nM and 55 μ M and also between 2.4 μ M and 55 μ M free intracellular calcium. While there is a change in voltage sensitive-conductance between virtually zero μ M (0.2 nM) and 2.4 μ M free intracellular calcium, this was not found to be statistically significant ($p > 0.05$).

The expression of BK channels in HEK 293 cells can be confirmed by measuring the single channel conductance of the evoked current. This was done by noise analysis which is a statistical analysis comparing current

variance with mean current and enables the estimation of the underlying unitary current [430]. Figure 4.3.1.3 illustrates this analysis and reveals an appropriate single channel conductance of 272 pS.

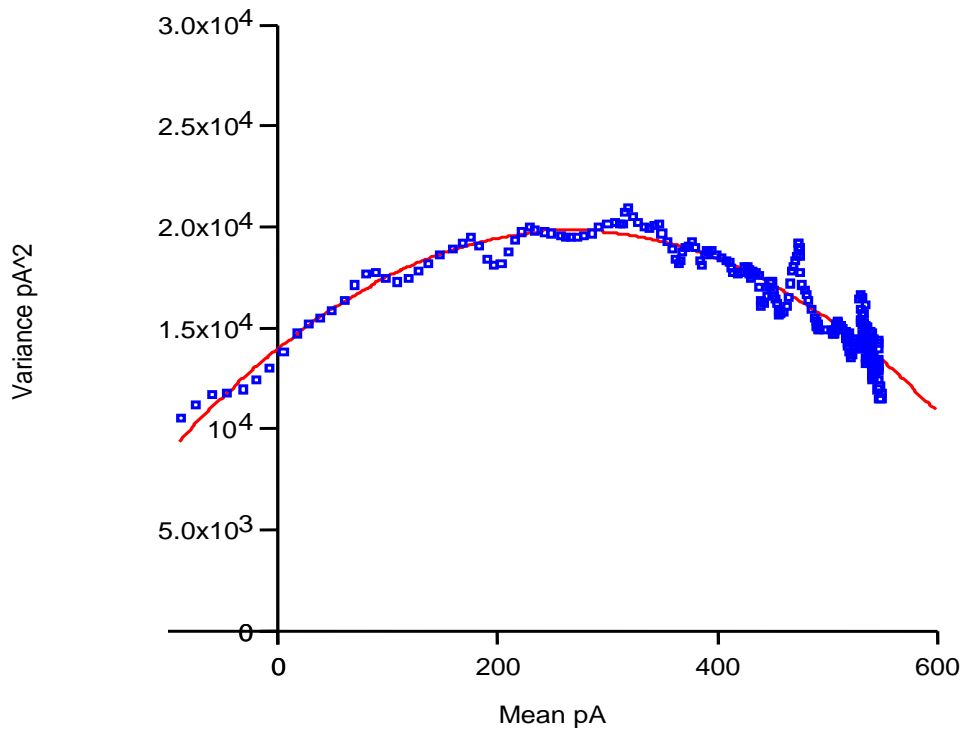


Figure 4.3.1.3 Non-stationary noise analysis on control BK α channel currents, in a HEK-293 cell expressing α subunits alone, with no Ca²⁺ in the pipette. The HEK-293 cell was voltage clamped at -40 mV with a voltage jump to +60 mV. This was repeated 100 times, at one second intervals. Unitary current (I.u) = 43.56 \pm 1.266 (sd) pA. The theoretical line is a fitted parabola. The single channel conductance is 272 pS given by WinWCP software.

4.3.2 Effects of Oestrone on HEK 293 cells expressing BK α subunits

The effect of oestrone on currents in HEK cells expressing BK α subunits is illustrated in Figure 4.3. 2.1.

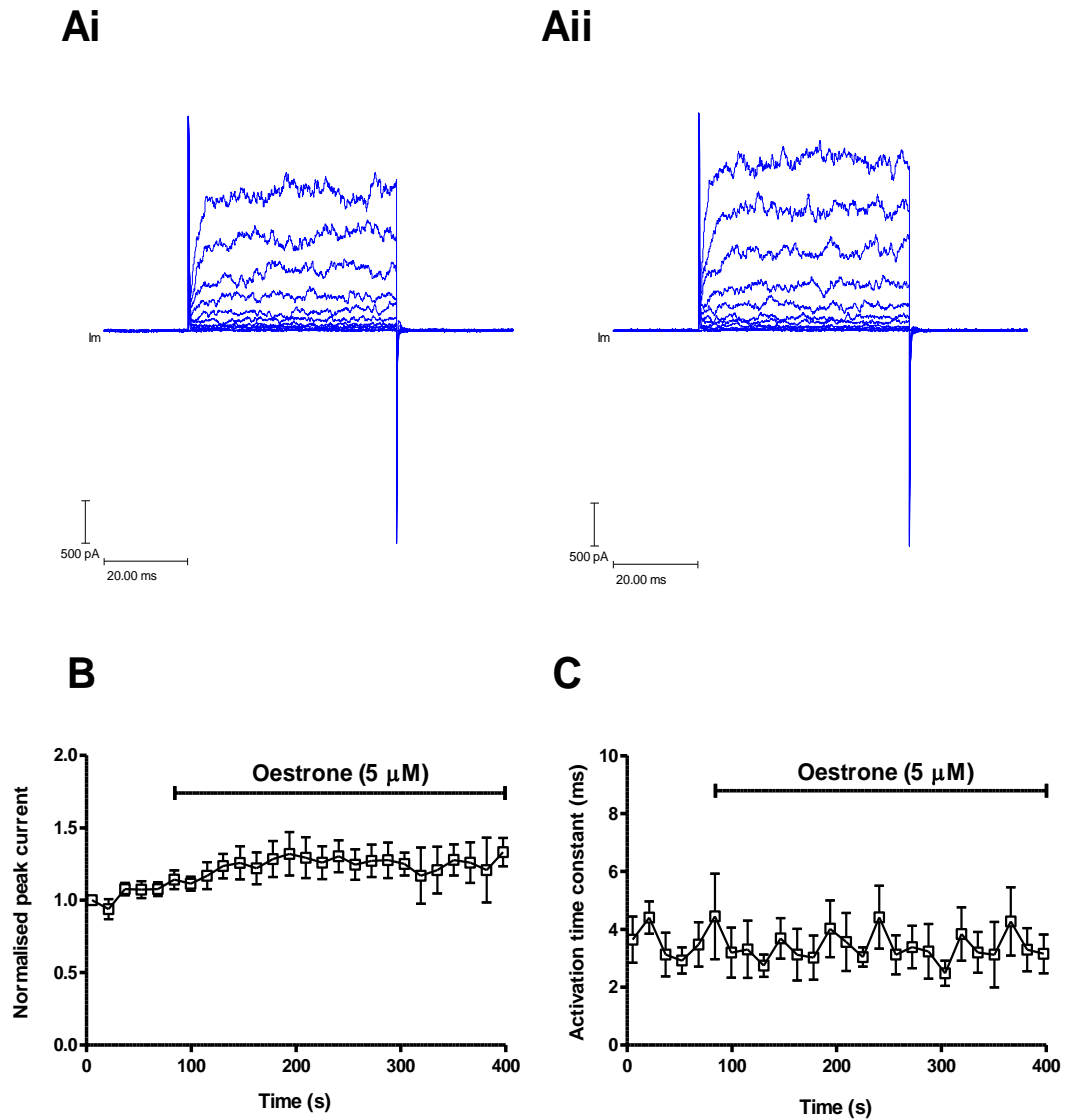


Figure 4.3.2.1 The effect of Oestrone (5 μ M) on evoked currents in HEK 293 cells expressing BK α subunits. (A) Comparison of currents evoked by stepping from -40 mV to +60 mV in 10 mV increments before (Ai) and after (Aii) the applications of Oestrone 5 μ M. (B) Mean data have been normalised and plotted against recording time. Current significantly increased during the application of oestrone ($p < 0.01$, $r = 0.78$, $n = 5$). (C) The activation time constant did not significantly change during the application of drug ($p > 0.05$, $r = -0.08$).

These currents were evoked by stepping the membrane potential from a holding potential of -40 mV to a final potential of +60 mV in 10 mV increments. The internal Ca^{2+} concentration was less than 0.2 nM. The currents before the application of Oestrone are illustrated in Ai and after the application are illustrated in Aii. The normalised mean current data, plotted in B, were generated from the final jump at +60 mV. This illustrates a significant increase in current due to the application of oestrone. However, the pharmacological effects of oestrone can only be determined by comparing its actions with control recordings to take into account the known background run-up observed in Figure 4.3.1.1(B). Thus, a more extensive analysis of the effects of oestrone on BK peak currents is undertaken in Section 4.3.7 to address this issue.

The mean activation rate was obtained by fitting a single exponential curve to the rising phase of the currents evoked at +60 mV. The activation time constant did not significantly change on addition of Oestrone (C) as judged by a Spearman's regression statistical test.

4.3.3 Effects of DME-Oestrone on HEK 293 cells expressing BK α subunits

The effect of DME-Oestrone on BK currents in HEK cells expressing α subunits is illustrated in Figure 4.3.3.1. These currents were evoked by stepping the membrane potential from a holding potential of -40 mV to a final potential of +60 mV in 10 mV increments.

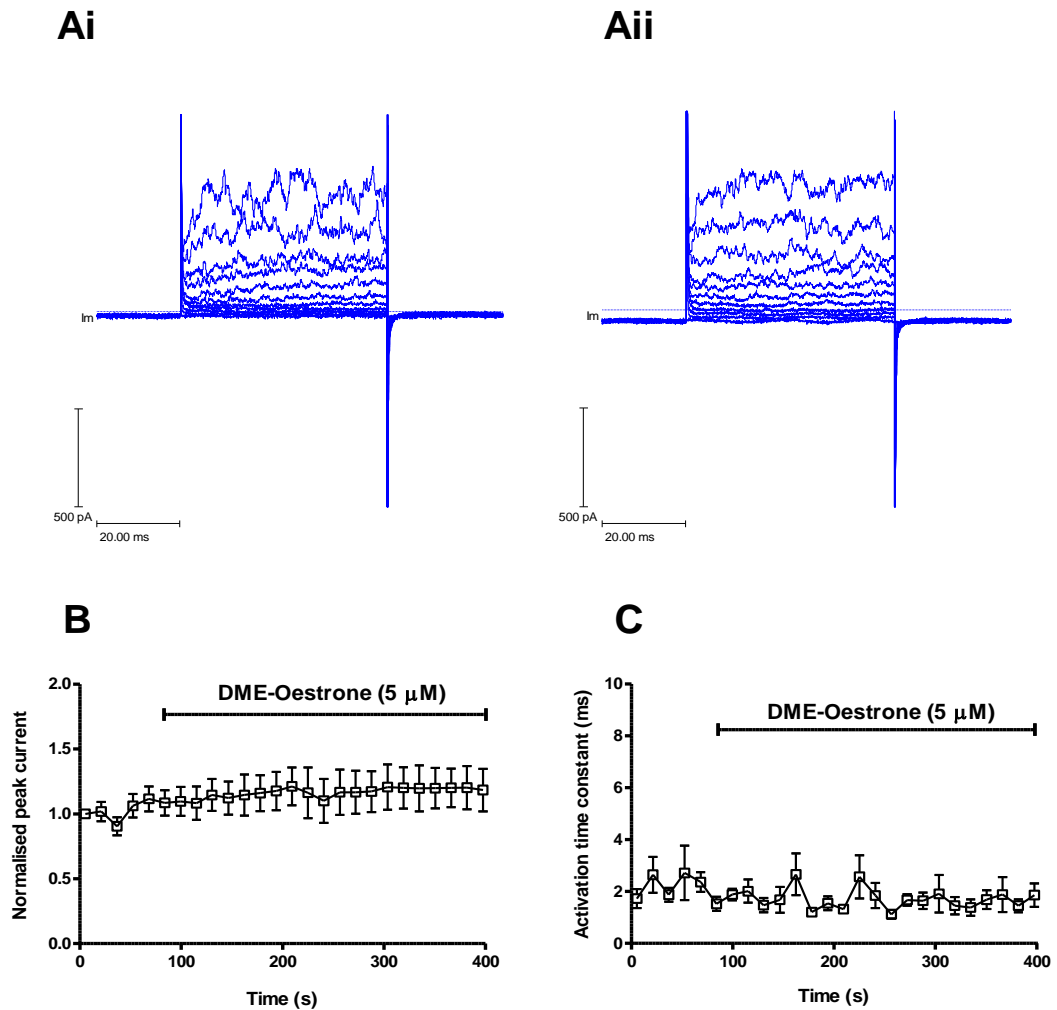


Figure 4.3.3.1 The effect of DME-Oestrone (5 μM) on evoked currents in HEK 293 cells expressing BK α subunits. (A) Comparison of currents evoked by stepping from -40 mV to +60 mV in 10 mV increments before (Ai) and after (Aii) the applications of DME-Oestrone (5μM). (B) Mean data have been normalised and plotted against recording time. Current significantly increased during the application of DME-Oestrone ($p<0.01$, $r=0.92$, $n=5$). (C) The activation time constant did not significantly changed during the application of drug.

As previously, the intracellular Ca^{2+} concentration was <0.2 nM. The currents before the application of DME-Oestrone are illustrated in Ai and after the application are illustrated in Aii. The normalised mean current data, plotted in B, were generated from the final jump at +60 mV. This illustrates a significant

increase in current during the application of DME-Oestrone. As previously, to take into account the observed run-up a more extensive analysis of the actual effects of DME-Oestrone on BK currents is undertaken in Section 4.3.7.

The mean activation rate was obtained by fitting a single exponential curve to the rising phase of the currents evoked at +60 mV. The activation time constant did not significantly change on addition of DME-Oestrone (C).

4.3.4 Effects of Quaternary-DME-Oestrone on HEK 293 cells expressing BK α subunits

The effect of Quaternary-DME-Oestrone (Quat-DME-Oestrone) on currents in HEK cells expressing BK α subunits is illustrated in Figure 4.3.4.1. These currents were evoked by stepping the membrane potential from a holding potential of -40 mV to a final potential of +60 mV in 10 mV increments. Again, the intracellular Ca^{2+} concentration was <0.2 nM. The currents before the application of Quat-DME-Oestrone are illustrated in Ai and after the application are illustrated in Aii. The normalised mean current data, plotted in B, were generated from the final jump at +60 mV. This illustrates a significant increase in current during the application of Quat-DME-Oestrone. However, to take into account the observed run-up, a more extensive analysis of the actual effects of Quat DME-Oestrone on BK currents is undertaken in Section 4.3.7.

The mean activation rate was obtained by fitting a single exponential curve to the rising phase of the currents evoked at +60 mV. There was a small but

significant change in the activation time on addition of Quat-DME-Oestrone (C).

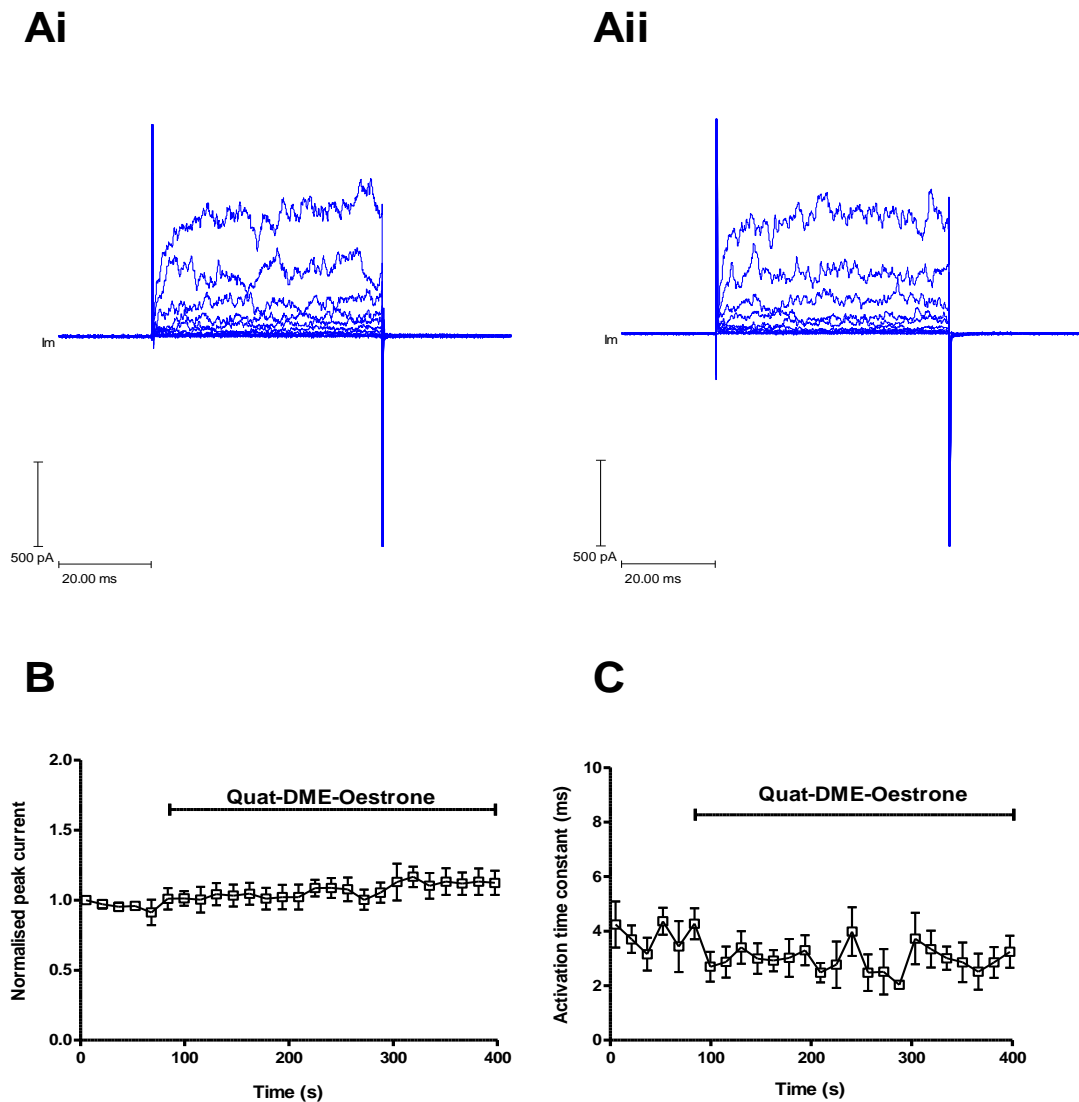


Figure 4.3.4.1 The effect of Quat-DME-Oestrone ($5 \mu\text{M}$) on evoked currents in HEK 293 cells expressing BK α subunits. (A) Comparison of currents evoked by stepping from -40 mV to $+60 \text{ mV}$ in 10 mV increments, before (Ai) and after (Aii) the applications of Quat-DME-Oestrone ($5 \mu\text{M}$). (B) Mean data have been normalised and plotted against recording time. Current significantly increased during the application of Quat-DME-Oestrone ($p < 0.01$, $r = 0.69$, $n = 5$). (C) There is a small but significant change in the activation time constant during the application of compound ($p < 0.05$, $r = -0.45$) as judged by a Spearman correlation test.

4.3.5 Effects of Oestrone-Oxime on HEK 293 cells expressing BK α subunits

The effect of Oestrone-Oxime on currents in HEK cells expressing BK α subunits is illustrated in Figure 4.3.5.1.

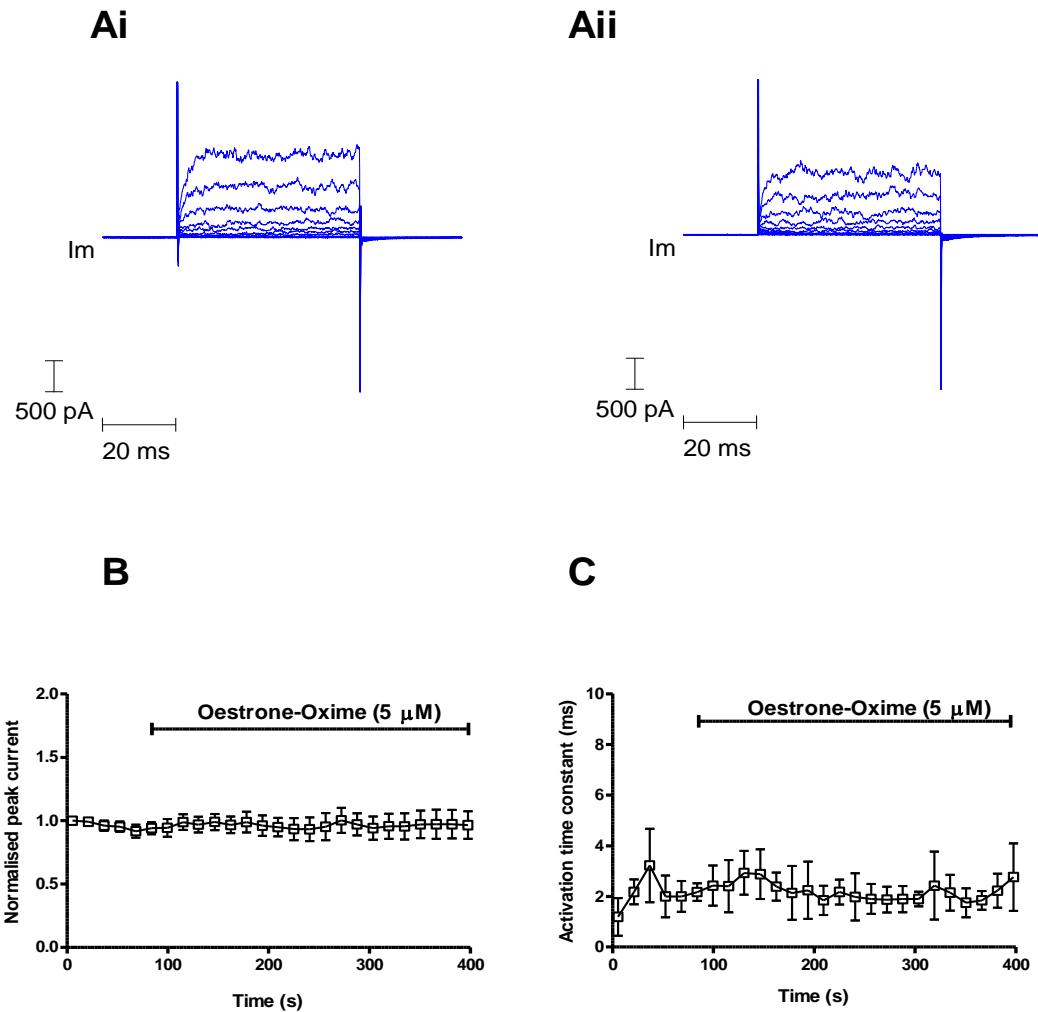


Figure 4.3.5.1 The effect of Oestrone-Oxime (5 μ M) on evoked currents in HEK 293 cells expressing BK α subunits. (A) Comparison of currents evoked by stepping from -40 mV to +60 mV in 10 mV increments, before (Ai) and after (Aii) the applications of Oestrone-Oxime (5 μ M). (B) Mean data have been normalised and plotted against recording time. Current did not significantly change during the application of Oestrone-Oxime ($p>0.05$, $r=0.01$, $n=6$). (C) The activation time constant did not significantly change during the application of drug ($p>0.05$, $r=-0.09$).

These currents were evoked by stepping the membrane potential from a holding potential of -40 mV to a final potential of +60 mV in 10 mV increments and the intracellular Ca^{2+} concentration was <0.2 nM. The currents before the application of Oestrone-Oxime (5 μM) are illustrated in Ai and after the application are illustrated in Aii. The normalised mean current data, plotted in B, were generated from the final jump at +60 mV. There was no significant change in peak current during the application of Oestrone-Oxime. However, to take into account of the observed run-up, a more extensive analysis of the actual effects of Oestrone-Oxime on BK currents is undertaken in Section 4.3.7.

The mean activation rate was obtained by fitting a single exponential curve to the rising phase of the currents evoked at +60 mV. The activation time did not significantly change on application of Oestrone-Oxime (C).

4.3.6 Effects of Quaternary-DME-Oestradiol on HEK 293 cells expressing BK α subunits

The effect of Quaternary-DME-Oestradiol (Quat-DME-Oestradiol) on currents in HEK cells expressing BK α subunits is illustrated in Figure 4.3.6.1.

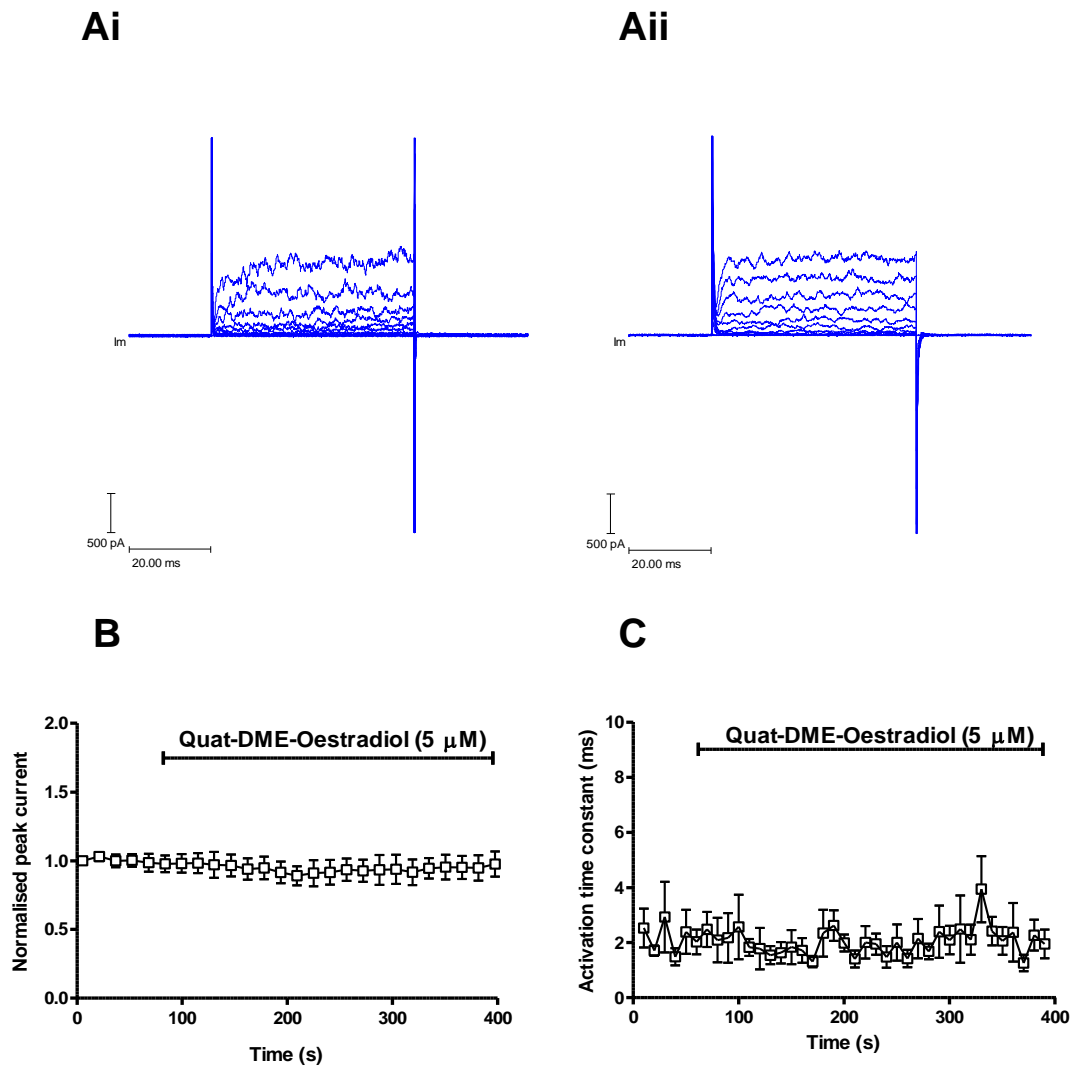


Figure 4.3.6.1 The effect of Quat-DME-Oestradiol (5 μ M) on evoked currents in HEK 293 cells expressing BK α subunits. (A) Comparison of currents evoked by stepping from -40 mV to +60 mV in 10 mV increments, before (Ai) and after (Aii) the applications of Quat-DME-Oestradiol (5 μ M). (B) Mean data have been normalised and plotted against recording time. Current significantly decreased during the application of Quat-DME-Oestradiol ($p < 0.05$, $r = -0.6$, $n = 5$). (C) The activation time constant did not significantly change during the application of drug ($p > 0.05$, $r = -0.02$).

These currents were evoked by stepping the membrane potential from a holding potential of -40 mV to a final potential of +60 mV in 10 mV increments and the intracellular Ca^{2+} concentration was <0.2 nM. The currents before the application of Quat-DME-Oestradiol are illustrated in Ai and after the application are illustrated in Aii. The normalised mean current data, plotted in B, were generated from the final jump at +60 mV. This illustrates a significant decrease in current during the application of Quat-DME-Oestradiol. As previously, to take into account the observed run-up a more extensive analysis of the actual effects of Quat-DME-Oestradiol on BK currents is undertaken in Section 4.3.7.

The mean activation rate was obtained by fitting a single exponential curve to the rising phase of the currents evoked at +60 mV. The activation time did not significantly change on addition of Quat-DME-Oestradiol (C).

4.3.7 Comparison of the effects of oestrogens on BK α peak currents with control data

As can be seen from the graph (Figure 4.3.1.1(B)), the average normalised peak current data reveal a run-up in HEK 293 cells expressing BK α subunits. Consequently, a Kruskal-Wallis analysis followed by a Dunn's *post hoc* multiple comparison test was undertaken to assess the true significance of the observed changes in BK peak current in the presence of oestrogens. These statistical analyses revealed that the application of Oestrone (5 μ M), DME-Oestrone (5 μ M) or Quat-DME-Oestrone (5 μ M) had no significant effect on BK α peak current. However, the application of both Oestrone-Oxime (5 μ M) and Quat-DME-Oestradiol (5 μ M) significantly reduced peak current. These statistical analyses are summarised in Table 4.3.7.1 and illustrated in Figure 4.3.7.1.

Table 4.3.7.1 *Kruskal-Wallis analysis followed by a post hoc Dunn's Multiple Comparison test, comparing control (run-up) with peak current in HEK cell expressing BK α subunits exposed to oestrogens.*

Dunn's Multiple Comparison Test	[ligand]	<i>P</i> value	Significance
Control vs Oestrone	5 μ M	$p > 0.05$	ns
Control vs DME Oestrone	5 μ M	$p > 0.05$	ns
Control vs Quat-DME Oestrone	5 μ M	$p > 0.05$	ns
Control vs Oestrone Oxime	5 μ M	$p < 0.05$	***
Control vs Quat DME-Oestradiol	5 μ M	$p < 0.05$	***

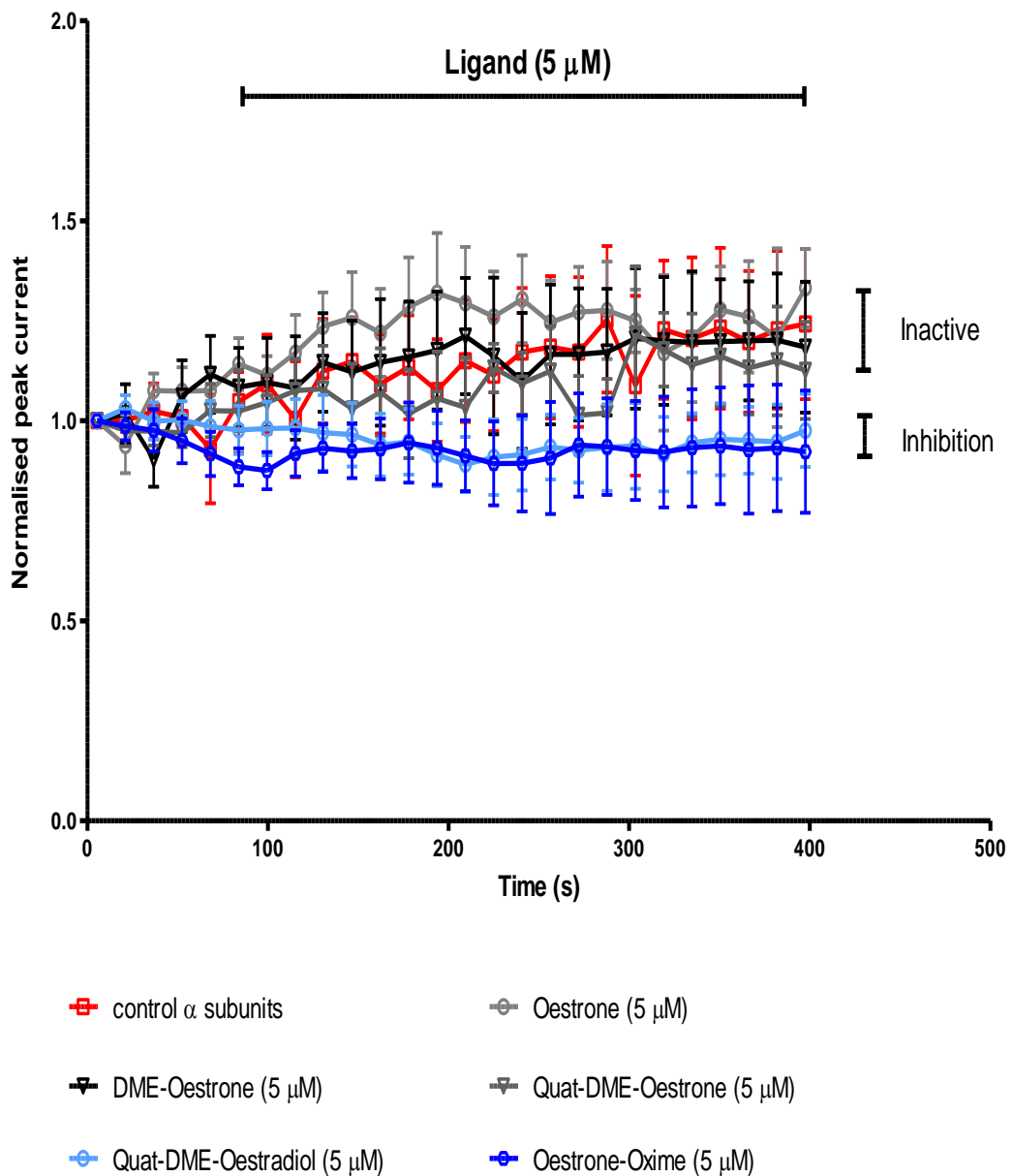


Figure 4.3.7.1 *Dunn's Multiple Comparison test, comparing control (run up) with normalised peak current in the presence of ligands in HEK 293 cells expressing BK channels comprising α subunits alone. No significant difference in channel activity was detected between control peak current flow recordings (no ligands) and those when ligands were applied with the exception of Quat-DME-Oestradiol and Oestrone-Oxime which both displayed evidence of weak inhibition.*

4.3.8 Characterisation of the evoked BK currents from HEK 293 cells expressing α plus β_1 subunits

BK channels are known to be activated by oestrogens and xenoestrogens when associating with their regulatory β_1 subunits. Here, HEK 293 cells, stably transfected with genes expressing BK α and β_1 subunits were used for whole cell patch clamp recordings to investigate the effects of various novel xenoestrogens.

BK currents were recorded from HEK 293 cells over-expressing the BK α + β_1 subunit (Figure 4.3.8.1 and Figure 4.3.8.2). An example of evoked currents is illustrated in Ai and Aii. The averaged normalised peak current versus time (seconds) for HEK 293 cells expressing BK α and β_1 subunits is illustrated in Figure 4.3.8.1 (B). These currents were evoked by stepping the -40 mV holding potential to +60 mV. A negative correlation with time ($r=-0.86$) and a significant decrease in peak current over time ($p<0.01$, $n=7$) suggest the occurrence of run-down, also revealed in the recording shown in Figure 4.3.8.1 (Ai) and (Aii). This was a controlled experiment with no compound added to the bath solution and zero $[Ca^{2+}]_i$ in the pipette.

BK channels expressing both α and β_1 subunits characteristically have slower activation rates than those only comprising α subunits alone [41]. These observations are illustrated in Figure 4.3.8.1(C), where activation rates of approximately 12.5 ms are recorded. This activity was maintained throughout the recording period and no inactivation was observed. Comparison of Figure

4.3.1.1 (Ai) with 4.3.8.1 (Ai) also illustrates the slowing of the activation of the channel when β_1 subunits are associating.

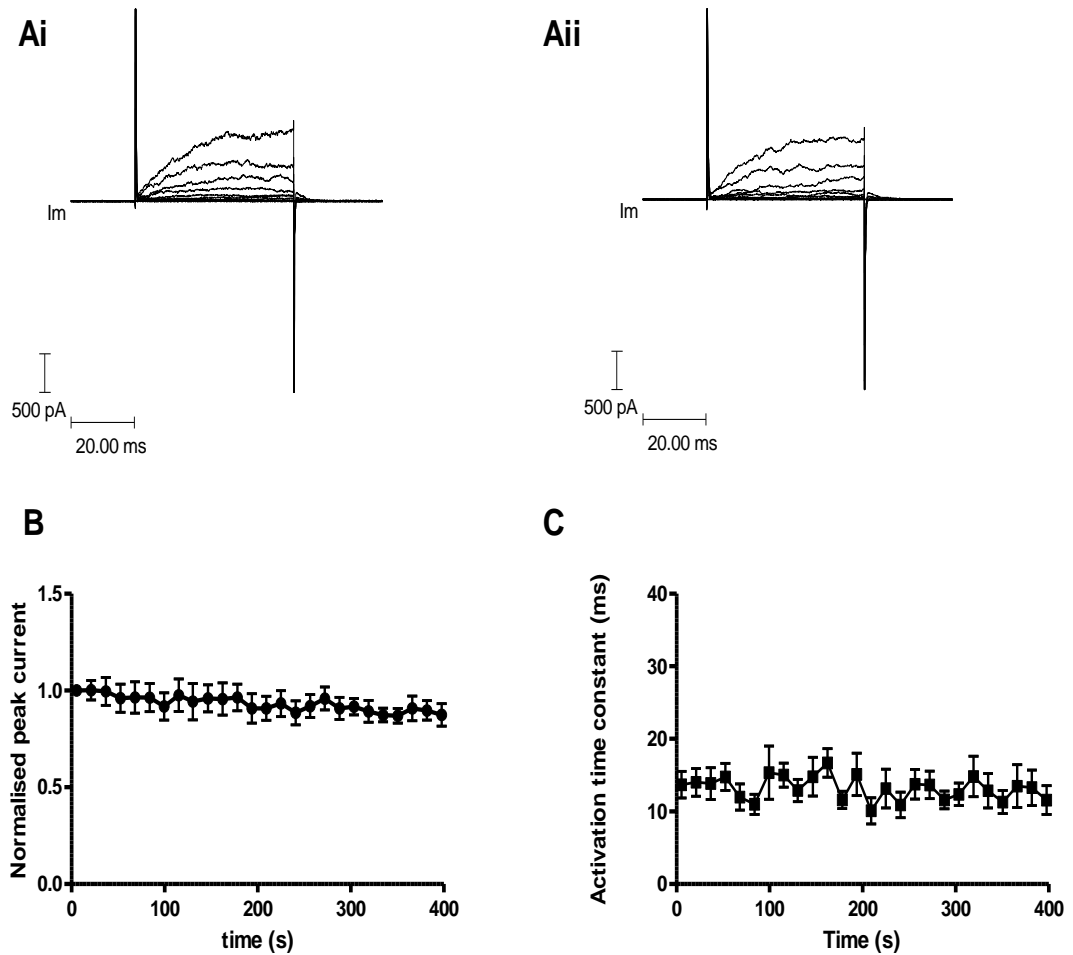


Figure 4.3.8.1 Control BK currents in HEK 293 cells expressing BK α and β_1 subunits. (Ai) illustrates evoked currents at the beginning of the recording period (0 to 5s) and (Aii) illustrates evoked currents after 350 seconds of recording. Cells were voltage clamped at -40 mV and currents evoked by changing the voltage to a range of test potentials (-40 to +60 mV) in 10 mV steps. (B) illustrates how the peak current changes with time. Currents were evoked by stepping the voltage to +60 mV from -40 mV. A significant decrease in the peak current was observed over 400 seconds ($r=-0.86$, $p<0.01$, $n=7$). (C) The activation time constant for currents evoked by changing the potential to +60 mV. The activation of the BK current could be fitted to a single exponential ($n=7$). No significant change in the activation time constant was observed over time.

As expected, peak BK currents were again found to be sensitive to iberiotoxin (IbTX). Appropriate inhibition of BK current was observed on application of IbTX (100 nM). The current inhibition for this concentration of toxin (100 nM) was fitted to a single exponential with a rate of block equal to $2.18 \pm 0.65 \times 10^4 \text{ M}^{-1} \text{ s}^{-1}$. This is slower than that observed in the absence of β_1 subunits (Figure 4.3.1.2(B)).

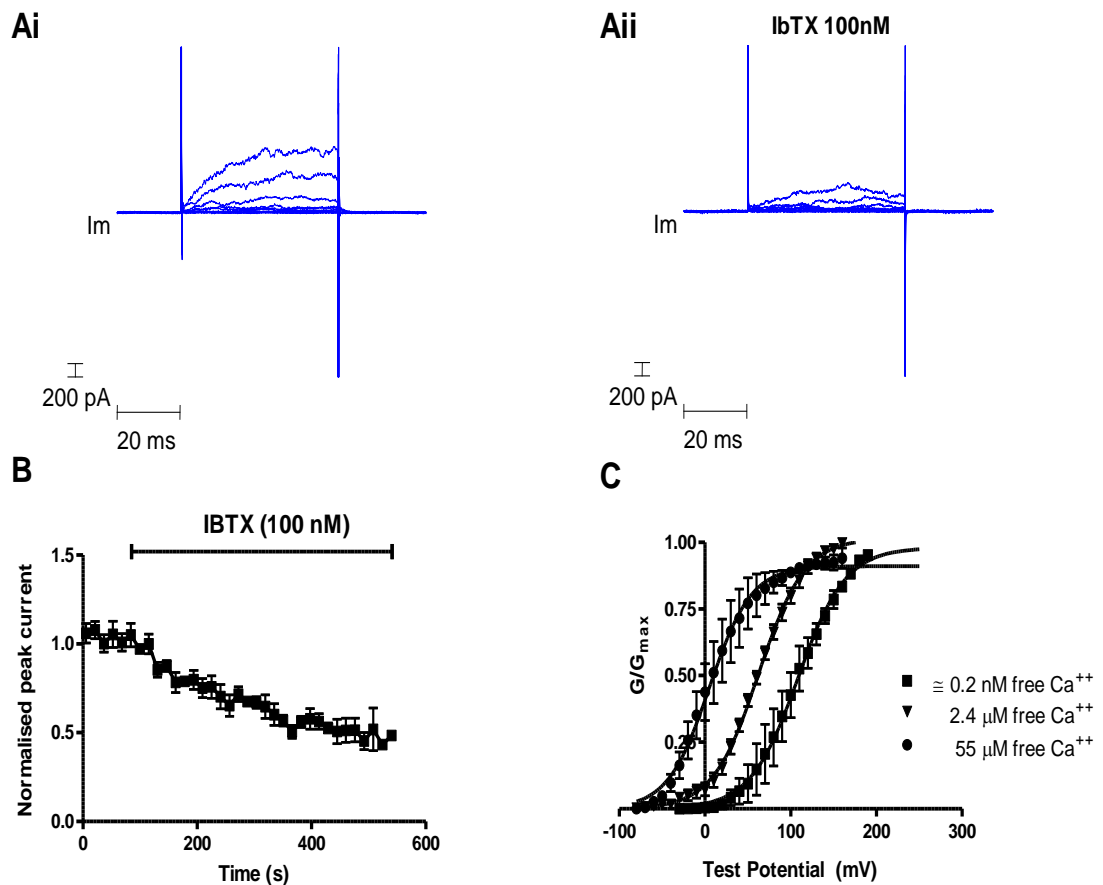


Figure 4.3.8.2 The properties of BK currents in HEK 293 cells expressing the BK α and β_1 subunit. (A) Cells were held at -40 mV and the voltage changed to a range of potentials up to $+60 \text{ mV}$ in 10 mV increments. (Ai) illustrates evoked currents in a HEK 293 cell at the beginning of the recording period (0 to 5s) and (Aii) illustrates evoked currents after the application of 100 nM iberiotoxin. (B) summarises the blocking properties of IbTX on BK currents ($n=6$). (C) The effects of free intracellular Ca^{2+} on the G-V relationship. Conductance was calculated from current and voltage, normalised to the maximum and plotted error bars represent SEM. Solid curves represent fits to the Boltzmann function.

Figure 4.3.8.2(C) gives a comparison of the normalised average membrane conductance versus membrane potential between a range of free intracellular $[Ca^{2+}]$. The membrane potential was held at -40 mV for cells patched with near zero μM intracellular calcium, but to obviate increased basal activity, cell membrane potential was held at -80 mV, increasing in 10 mV increments to +160 mV in the presence of increased intracellular calcium concentrations (2.4 μM and 55 μM $[Ca^{2+}]_{ic}$. BK channel conductance was monitored at 0.2 nM, 2.4 μM and 55 μM concentrations of free intracellular Ca^{2+} and the $V_{0.5}$ noted (Table 4.3.8.1). Raising the free intracellular $[Ca^{2+}]$ effected a hyperpolarising shift in the $V_{0.5}$ of the voltage conductance curve (~ 100 mV). A significant difference in the $V_{0.5}$ ($p < 0.05$) was revealed between all three concentrations of free intracellular calcium.

Table 4.3.8.1 Summary of hyperpolarising effects due to increasing free intracellular concentrations of Ca^{2+} ions on shifts in the $V_{0.5}$ for the voltage conductance curve of BK α plus β_1 subunits in HEK 293 cells. Significance was determined using a, one-way ANOVA (Kruskal-Wallis) for significance followed by a post hoc Tukey's analysis for multiple comparisons

Free intracellular $[Ca^{2+}]$	$V_{0.5}$ from the voltage-conductance curves obtained from HEK 293 cells expressing BK α + β_1 subunits
$\cong 0.2$ nM	108.4 \pm 4.03 †‡
2.4 μM	62.64 \pm 1.33 ★‡
55 μM	5.15 \pm 3.09 ★†

Key: ★ = significantly different $V_{0.5}$ ($p < 0.05$) from 0.2 nM free intracellular calcium;
 † = significantly different $V_{0.5}$ ($p < 0.05$) from 2.4 nM free intracellular calcium;
 ‡ = significantly different $V_{0.5}$ ($p < 0.05$) from 55 μM free intracellular calcium

4.3.9 Effects of Oestrone on HEK 293 cells expressing BK α plus β_1 subunits

The effect of oestrone on currents in HEK cells expressing BK α plus β_1 subunits is illustrated in Figure 4.3.9.1.

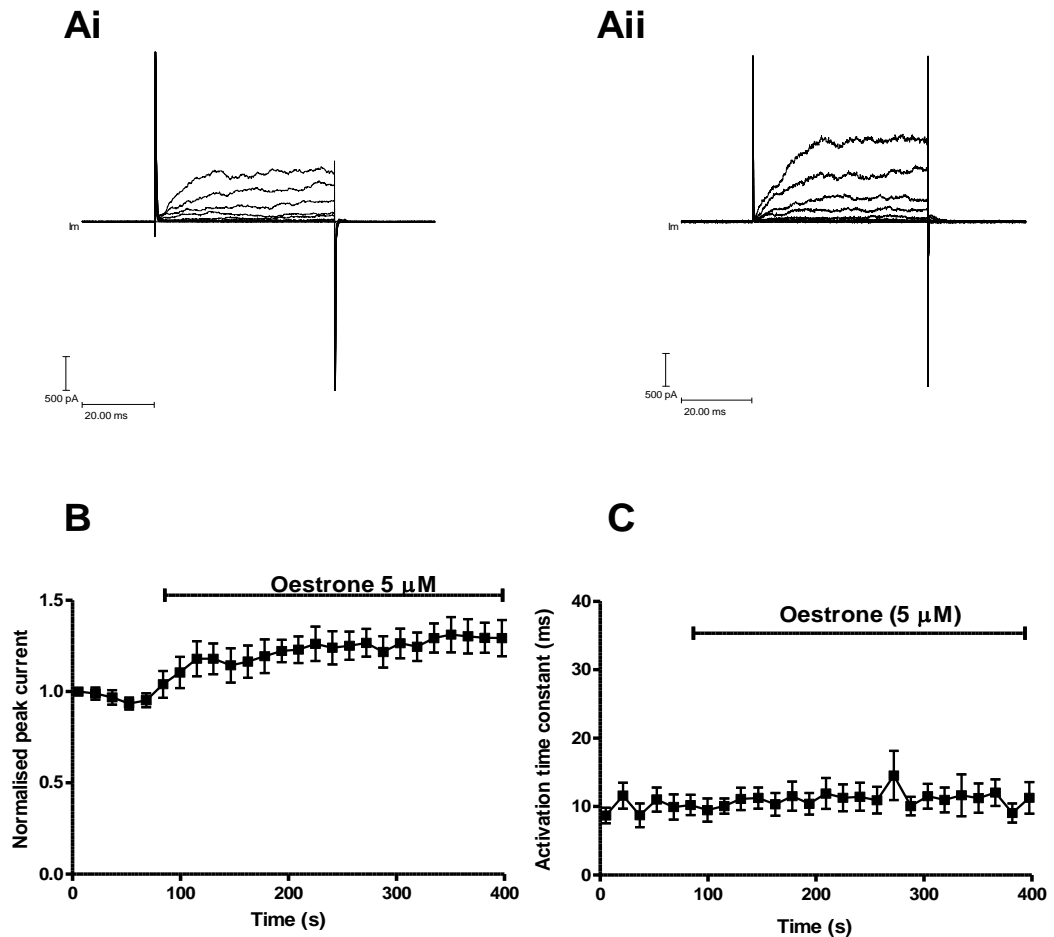


Figure 4.3.9.1 The effect of oestrone (5 μM) on evoked currents in HEK 293 cells expressing BK α and β_1 subunits. (A) Comparison of currents evoked by stepping from -40 mV to +60 mV in 10 mV increments before (Ai) and after (Aii) the applications of oestrone 5 μM . (B) Mean data have been normalised and plotted against recording time. Current significantly increased during the application of oestrone ($p < 0.01$, $r = 0.89$, $n = 8$). (C) The activation time constant did not significantly change during the application of drug ($p > 0.05$ $r = 0.03$).

These currents were evoked by stepping the membrane potential from a holding potential of -40 mV to a final potential of +60 mV in 10 mV increments and the intracellular Ca^{2+} concentration was <0.2 nM. The currents before the application of oestrone are illustrated in Ai, and after the application are illustrated in Aii. The normalised mean current data, plotted in B, were generated from the final jump at +60 mV. This illustrates a significant increase in current during the application of oestrone. However, the true pharmacological effects of oestrone can only be determined by comparing its actions with control recordings to take into account the known background run-down observed in Figure 4.3.9.1(B.). Thus, a more extensive analysis of the effects of oestrone on BK currents is undertaken in Section 4.3.14 to address this issue.

The mean activation rate was obtained by fitting a single exponential curve to the rising phase of the currents evoked at +60 mV. The activation time constant did not significantly change on addition of Oestrone (C).

4.3.10 Effects of DME-Oestrone on HEK 293 cells expressing BK α plus β_1 subunits

The effect of DME-Oestrone on currents in HEK cells expressing BK α plus β_1 subunits is illustrated in Figure 4.3.10.1. These currents were evoked by stepping the membrane potential from a holding potential of -40 mV to a final potential of +60 mV in 10 mV increments and the intracellular Ca^{2+} concentration was <0.2 nM. The currents before the application of DME-Oestrone are illustrated in Ai and after the application are illustrated in Aii.

The normalised mean current data, plotted in B, were generated from the final jump at +60 mV. This illustrates a significant decrease in current during the application of DME-Oestrone. However, to address the issue of run-down a more extensive analysis of the actual effects of DME-Oestrone on BK currents is undertaken in Section 4.3.14.

The mean activation rate was obtained by fitting a single exponential curve to the rising phase of the currents evoked at +60 mV. The activation time constant did not significantly change on addition of DME-Oestrone (C).

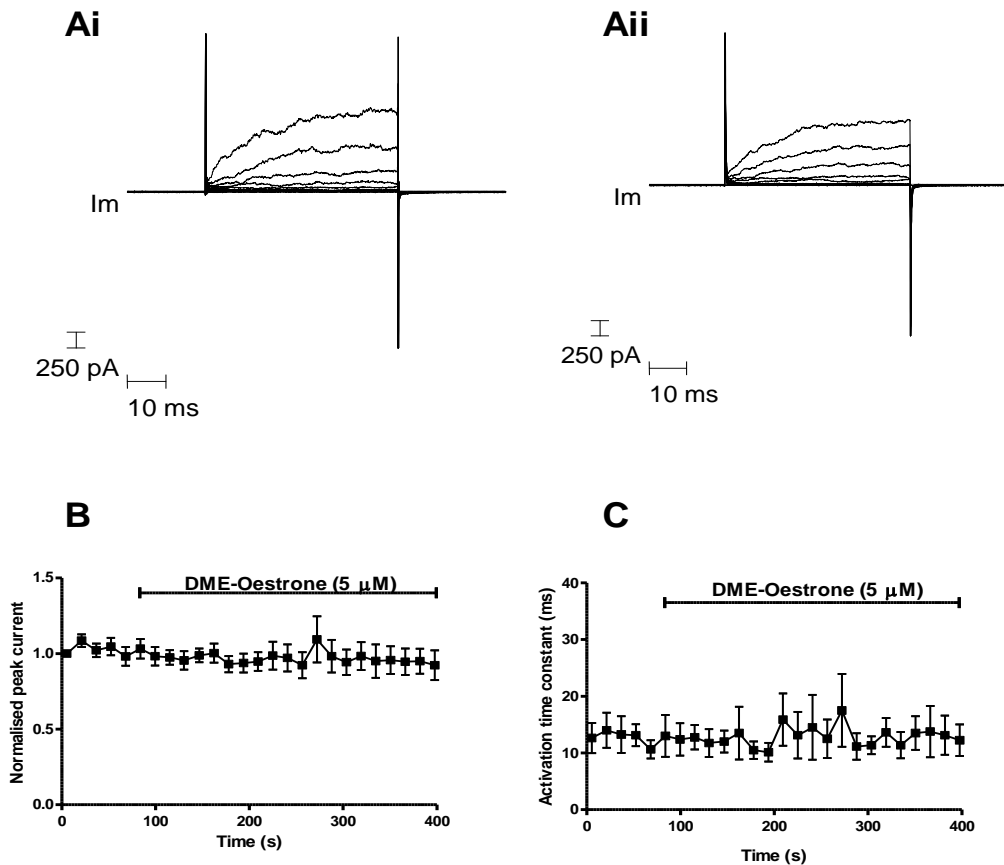


Figure 4.3.10.1 The effect of DME-Oestrone (5 μM) on evoked currents in HEK 293 cells expressing BK α and β₁ subunits. (A) Comparison of currents evoked by stepping from -40 mV to +60 mV in 10 mV increments before (Ai) and after (Aii) the applications of DME-Oestrone 5 μM. (B) Mean data have been normalised and plotted against recording time. Current significantly decreased during the application of DME-Oestrone ($p < 0.05$, $r = -0.57$, $n = 8$). (C) The activation time constant did not significantly change during the application of drug.

4.3.11 Effects of Quaternary-DME-Oestrone on HEK 293 cells expressing BKα plus β₁ subunits

The effect of Quat-DME-Oestrone on currents in HEK cells expressing BK α plus β₁ subunits is illustrated in Figure 4.3.11.1. These currents were evoked by stepping the membrane potential from a holding potential of -40 mV to a

final potential of +60 mV in 10 mV increments and the intracellular Ca^{2+} concentration was <0.2 nM. The currents before the application of Quat-DME-Oestrone are illustrated in Ai and after the application are illustrated in Aii. The normalised mean current data, plotted in B, were generated from the final jump at +60 mV. This illustrates a significant decrease in current during the application of Quat-DME-Oestrone. However, to address the issue of run-down, a more extensive analysis of the actual effects of Quat-DME-Oestrone on BK currents is undertaken in Section 4.3.14.

The mean activation rate was obtained by fitting a single exponential curve to the rising phase of the currents evoked at +60 mV. The activation time did not significantly change on addition of Quat-DME-Oestrone (C).

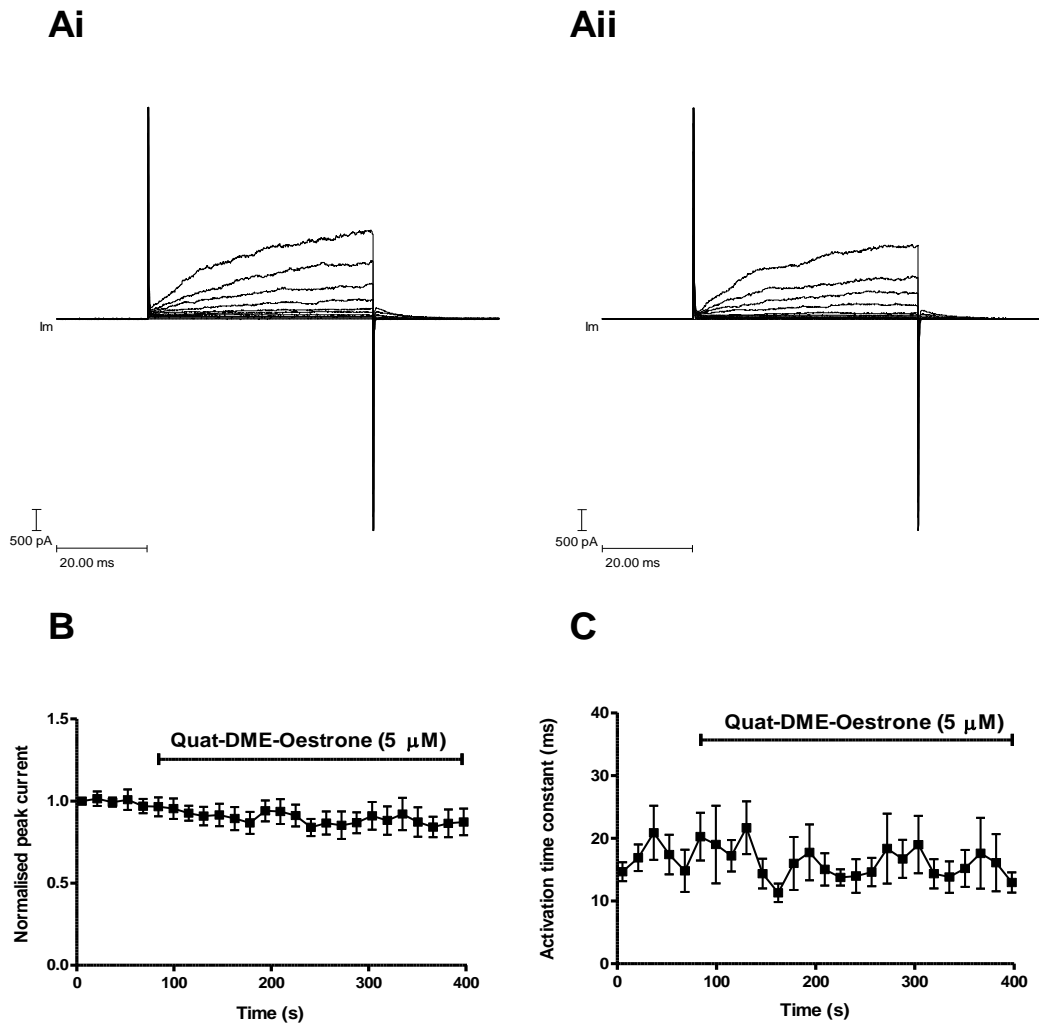


Figure 4.3.11.1 The effect of Quat-DME-Oestrone (5 μM) on evoked currents in HEK 293 cells expressing BK α and β_1 subunits. (A) Comparison of currents evoked by stepping from -40 mV to +60 mV in 10 mV increments, before (Ai) and after (Aii) the applications of Quat-DME-Oestrone (5 μM). (B) Mean data have been normalised and plotted against recording time. Current significantly decreased during the application of Quat-DME-Oestrone ($p < 0.01$, $r = -69$, $n = 8$). (C) The activation time constant significantly changed during the application of drug.

4.3.12 Effects of Oestrone-Oxime on HEK 293 cells expressing BK α plus β_1 subunits

The effect of Oestrone-Oxime on currents in HEK cells expressing BK α plus β_1 subunits is illustrated in Figure 4.3.12.1. These currents were evoked by

stepping the membrane potential from a holding potential of -40 mV to a final potential of +60 mV in 10 mV increments and the intracellular Ca^{2+} concentration was <0.2 nM. The currents before the application of Oestrone-Oxime are illustrated in Ai and after the application are illustrated in Aii. The normalised mean current data, plotted in B, were generated from the final jump at +60 mV. This illustrates a significant increase in current during the application of Oestrone-Oxime. As previously, to address the issue of run-down a more extensive analysis of the actual effects of Oestrone-Oxime on BK currents in these cells is undertaken in Section 4.3.14.

The mean activation rate was obtained by fitting a single exponential curve to the rising phase of the currents evoked at +60 mV. The activation time did not significantly change on addition of Oestrone-Oxime (C).

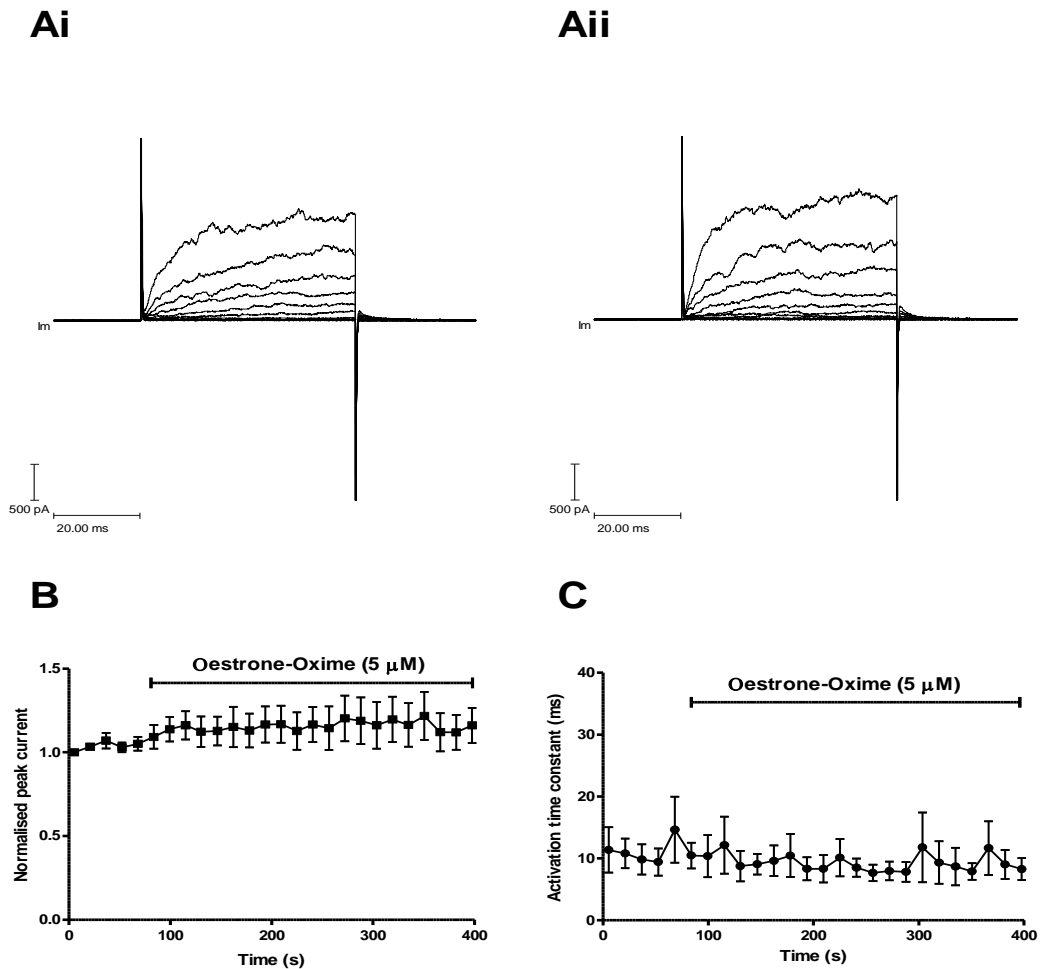


Figure 4.3.12.1 The effect of Oestrone-Oxime ($5 \mu\text{M}$) on evoked currents in HEK 293 cells expressing BK α and β_1 subunits. (A) Comparison of currents evoked by stepping from -40 mV to $+60 \text{ mV}$ in 10 mV increments, before (Ai) and after (Aii) the applications of Oestrone-Oxime ($5 \mu\text{M}$). (B) Mean data have been normalised and plotted against recording time. Current significantly increased during the application of Oestrone-Oxime ($p < 0.01$, $r = 0.62$, $n = 8$). (C) The activation time constant did not significantly change during the application of drug.

4.3.13 Effects of Quaternary-DME-Oestradiol on HEK 293 cells expressing BK α plus β_1 subunits

The effect of Quat-DME-Oestradiol on currents in HEK cells expressing BK α plus β_1 subunits is illustrated in Figure 4.3.13.1. These currents were evoked by stepping the membrane potential from a holding potential of -40 mV to a final potential of +60 mV in 10 mV increments and the intracellular Ca²⁺ concentration was <0.2 nM. The currents before the application of Quat-DME-Oestradiol are illustrated in Ai and after the application are illustrated in Aii. The normalised mean current data, plotted in B, were generated from the final jump at +60 mV. This illustrates a significant increase in current during the application of Quat-DME-Oestradiol. As previously, to address the issue of run-down a more extensive analysis of the actual effects of Quat-DME-Oestradiol on BK currents in these cells is undertaken in Section 4.3.14.

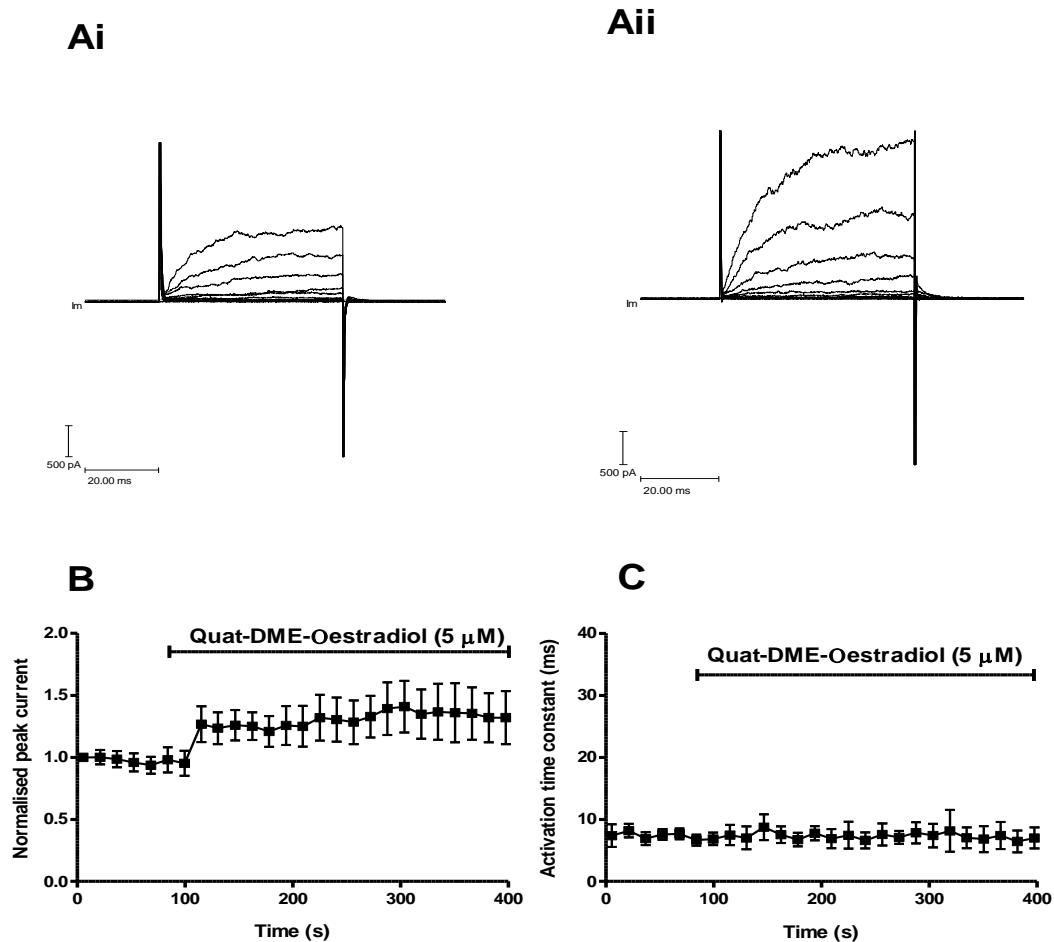


Figure 4.3.13.1 The effect of Quat-DME-Oestradiol (5 μM) on evoked currents in HEK 293 cells expressing BK α and β₁ subunits. (A) Comparison of currents evoked by stepping from -40 mV to +60 mV in 10 mV increments, before (Ai) and after (Aii) the applications of Quat-DME-Oestradiol (5 μM). (B) Mean data have been normalised and plotted against recording time. Current significantly increased during the application of Quat-DME-Oestradiol ($p < 0.01$, $r = 0.62$, $n = 5$). (C) The activation time constant did not significantly change during the application of drug.

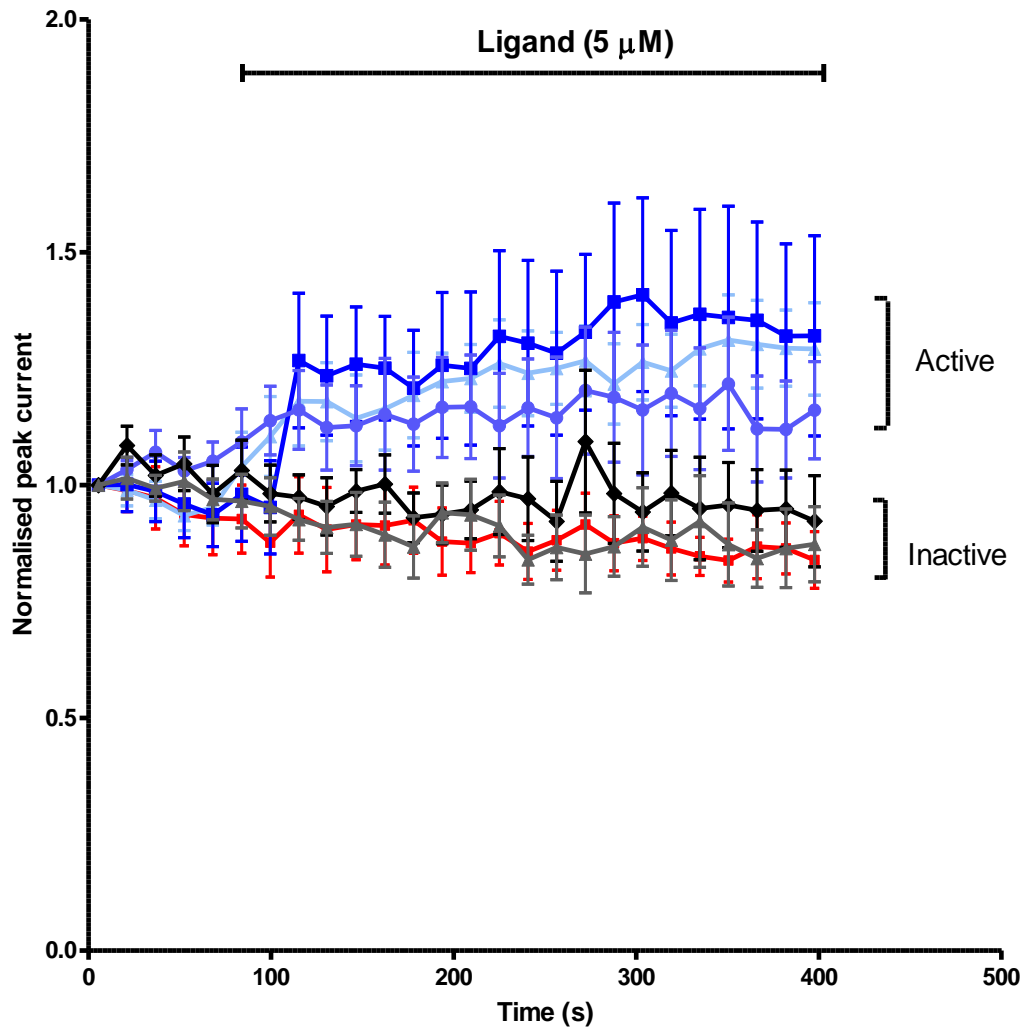
The mean activation rate was obtained by fitting a single exponential curve to the rising phase of the currents evoked at +60 mV. The activation time did not significantly change on addition of Quat-DME-Oestradiol (C).

4.3.14 Comparison of the effects of oestrogens on BK α + β_1 peak currents with control data

As can be seen from the graph (Figure 4.3.8.1 (B)), the average normalised peak current data reveal a run-down in HEK 293 cells expressing BK α and β_1 subunits. Consequently, a Kruskal-Wallis analysis followed by a Dunn's *post hoc* multi-comparison test was undertaken to assess the true significance of peak current changes in the presence of oestrogens. The statistical analyses revealed that the application of DME-Oestrone (5 μ M) or Quat-DME-Oestrone (5 μ M) had no significant effect on peak current. However, the application of Oestrone (5 μ M), Oestrone-Oxime (5 μ M) or Quat-DME-Oestradiol (5 μ M) significantly increased peak current. These statistical analyses are summarised in Table 4.3.14.1 and illustrated in Figure 4.3.14.1.

Table 4.3.14.1 *Kruskal-Wallis analysis followed by a post hoc Dunn's Multiple Comparison test, comparing control (run down) with peak current in HEK cell expressing BK α and β_1 subunits exposed to oestrogens.*

Dunn's Multiple Comparison Test	[ligand]	<i>P</i> value	Significance
Control vs Oestrone	5 μ M	$p < 0.05$	***
Control vs Quat-DME Oestradiol	5 μ M	$p < 0.05$	***
Control vs Oestrone Oxime	5 μ M	$p < 0.05$	***
Control vs DME Oestrone	5 μ M	$p > 0.05$	ns
Control vs Quat-DME Oestrone	5 μ M	$p > 0.05$	ns



- Control (run down)
- Oestrone (5 μM)
- ◆ DME-Oestrone (5 μM)
- Quat-DME-Oestrone (5 μM)
- Quat-DME-Oestradiol (5 μM)
- Oestrone-Oxime (5 μM)

Figure 4.3.14.1 *Dunn's Multiple Comparison test, comparing control (run-down) with normalised peak current in the presence of ligands in HEK 293 cells expressing BK α and β_1 subunits. Oestrone, Quat-DME-Oestradiol and Oestrone-Oxime significantly increased peak BK currents.*

4.3.15 Summary of results

The findings of this chapter are summarised as follows:-

In HEK cells only expressing BK α subunits:-

- BK currents run up with time as demonstrated by a positive regression.
- The effects of free intracellular Ca^{2+} concentrations (0.2 nM - 55 μM) on the conductance-voltage relationship was as expected, i.e. raising the $[\text{Ca}^{2+}]_i$ effected a hyperpolarising shift in the $V_{0.5}$.
- Evoked currents were rapidly inhibited by IbTX (100 nM).
- After current run-up is taken into consideration, it was found that 17 keto-oestrogens (Oestrone, DME-Oestrone, Quat-DME-Oestrone) (5 μM) had no effect on evoked BK currents. Oestrone-Oxime and the 17 β -hydroxy oestrogen - Quat-DME-Oestradiol, produced a small inhibition of BK α currents.

In HEK cells expressing both BK α and β_1 subunits:-

- BK currents run down with time.
- The effects of free intracellular Ca^{2+} concentrations (0.2 nM - 55 μM) on the conductance-voltage relationship was as expected, i.e. raising the $[\text{Ca}^{2+}]_i$ effected a hyperpolarising shift in the $V_{0.5}$. The shift was greater in HEK cells expressing a combination of α and β_1 subunits.
- As expected evoked currents were sensitive to IbTX (100 nM), and the rate of inhibition was slower than that seen in HEK cells only expressing α subunits.

- Oestrone (5 μ M) enhanced evoked BK currents in these cells; this has not been reported before and demonstrates that 17β -oestradiol is not the only endogenous oestrogen able to activate BK channels. Oestrone-Oxime and Quat-DME-Oestradiol also activated BK $\alpha+\beta_1$ channels. However, DME-Oestrone and Quat-DME-Oestrone were inactive. It was expected that Quat-DME-Oestrone would be inactive as it was completely inactive in rat aortic ring assays.

4.4 DISCUSSION

The aim of this chapter was to investigate *directly* the oestrogen derivatives as novel BK activators in a cellular expression system expressing solely α or α and β_1 subunits. The novel oestrogens synthesised for this study should show similar subunit dependence to known non-steroidal antioestrogens and steroidal oestrogens which have previously been shown to activate BK channels in a subunit-dependent manner [101, 102, 129]. Thus, the investigations in this chapter should not only demonstrate which compounds are able to modulate BK function, but also confirm the requirement of the presence of the β_1 subunit for the oestrogen derivatives to be capable of modulating BK currents.

In addition, the investigations should expand the findings and observations seen in the aortic ring experiments of the previous chapter. For example, Quat-DME-Oestrone was completely inactive in rat aortic rings and as expected, was found to be inactive against BK currents in HEK 293 cells. Additionally, Quat-DME-Oestradiol was the only compound that was sensitive to IbTX in aortic rings; therefore, one would expect it to behave in a similar fashion on BK currents in HEK cells, this proved to be correct.

To explore *directly* the effects of these compounds on BK currents, it was essential to first confirm the presence of functional BK α and BK α + β_1 channels in HEK 293 cells. This was accomplished through noise analysis and kinetic observation of the channels using the whole cell patch-clamp configuration.

To support the functional expression of these subunits, the sensitivity to the BK channel blocker, iberiotoxin, was also explored.

4.4.1 Comparison of α control data with $\alpha+\beta_1$ control data

It has been well established that for oestrogens and xenoestrogens to activate the BK channel, the association of probably two or more regulatory β_1 subunits is required [40, 102, 103]. For this research, BK channels were over-expressed in HEK 293 cells comprising both α subunits alone and α subunits with associating β_1 subunits. Using the patch-clamp technique (holding potential -40 mV stepped to +60 mV), extensive control experiments such as noise analysis, peak current flow, scorpion toxin blockade and calcium sensitivity as well as BK channel activation kinetics, were undertaken to substantiate the presence of BK channels in the chosen expression system (HEK 293 cells). These are discussed in the following sections.

4.4.1.1 Run-up/run-down

Peak currents evoked from HEK 293 cells over-expressing just α subunits increased significantly over a 400 second recording window (Figure 4.3.1.1(B)), whereas, peak currents evoked from HEK 293 cells over-expressing both α and β_1 BK subunits decreased significantly over a similar 400s recording period (Figure 4.3.7.1(B)). Currents recorded from cells can decrease/increase during data collection, regardless of the application of possible activating or inhibitory compounds [430, 436]. These time-dependent modulations in current - “run-up and run-down”, are known artefacts of the

whole cell configuration patch-clamp technique, especially in HEK 293 cells [291]. Approximately 10% of HEK cells transfected with exogenous proteins have a tendency to current instability after initial break-through of the cell membrane [291].

As yet, there is no definitive explanation as to why run-up/down occurs but Thomas and Smart (2005), in their appraisal of the HEK 293 cell line as an expression vehicle for recombinant proteins suggest that it may be agonist-induced, receptor internalisation or mobilisation of receptor proteins to the cell membrane or, simply, re-equilibration of diffusible factors leading to dephosphorylation and phosphorylation of expressed proteins [291]. There are various diffusible factors within cells that are potentially responsible for run-up/down during patch-clamp recordings, some of which are tabulated in Table 4.4.1.1.1.

Table 4.4.1.1.1 Potential diffusible factors that may be responsible for run-up/down.

Diffusible factors that affect run-up/down	α subunits	$\alpha+\beta_1$ subunits	Refs.
Mg ²⁺	Known modulator	Known modulator	[363, 437-439]
ATP, cAMP; GTP, cGMP	Potential phosphorylation site at position:- 569 serine 763 threonine 765 serine 977 serine 978 serine 1086 tyrosine 1088 threonine	Potential phosphorylation site at position:- 69 threonine	[30, 355, 427, 440, 441]
Polyamines	Pore blockers	Pore blockers	[442-444]
Antioxidants	Cysteines at position:- 14, 53, 54, 56, 141, 277, 348, 422, 430, 485, 498, 554, 557, 612, 615, 628, 630, 695, 722, 797, 800, 820, 911, 975, 995, 1001, 1011, 1028, and 1051	Cysteines at position:- 18, 26, 53, 76, 103, 135	[356, 357, 428, 445]

In whole-cell recordings, rupture of the cell membrane is necessary in order to control the intracellular pH and ionic environment of the cell and this is achieved through dialysis of the cell. However, this will inevitably invoke consequences over time, such as the dialysis of intracellular signalling factors, due to the fact that the patch-pipette will always contain a greater volume of solution than the intracellular compartment [446]. For example, Duchatelle-Gourdon *et al.*, have presented evidence that run-down of delayed rectifier currents in frog cardiac atrial cells could be explained by the amount of Mg²⁺ present in the patch electrode at the beginning of a whole cell recording [447, 448]. They postulate that this happens in three possible ways, namely, voltage-dependent block of the channel; Mg²⁺ could be affecting the surface

charge at the intracellular face of the membrane leading to an alteration of transmembrane potential; or Mg^{2+} could either be binding allosterically or itself be a regulating molecule thereby, triggering channel modulation.

Interestingly, work done by DiChiara *et al.*, [356] in patch excision preparations of *hSlo*, revealed significant run-down in current flow. They postulated that this was on account of cysteine residues, normally protected by the reduced state within the cell, becoming oxidised, a theory which was later also put forward by Tang *et al.*, [357] and confirmed by Zhang *et al.*, in inside out patches [428]. Another investigation carried out by Lin *et al.*, on inside-out patches, has suggested that run-down in $BK\alpha+\beta_1$ channels may more likely be due to dephosphorylation rather than cysteine oxidation as the run-down observed in their experiments was antagonised, in part, by a phosphatase inhibitor [427].

These observed decay and graduated increases of various intracellular responses and ionic dialysis are time-dependent and different cell types have different time-courses [449]. Indeed, the cell cytoplasm may not be in equilibrium at the time of drug perfusion. This will depend entirely on the molecular weight and time constant of the dialysing molecule, the series resistance between the patch electrode and the cell, and also the cell volume [446, 450].

Thus, it is imperative for accurate data collection that run-up/down is addressed. However, ascertaining the source of the occurrence would be

costly and lengthy, due to the myriad origins and potential causes of the phenomenon. For example, listed below is a non-exhaustive list of potential routes of experimental design optimisation, but each of these is not without issues.

1. Whole cell perforated patch could be used but there are access problems with perforated patch-clamp. Clamping the intracellular free calcium would be difficult as perforating agents, such as amphotericin, do not allow EGTA to enter the intracellular compartment and therefore, controlling intracellular free calcium is not possible. Only with whole cell patch-clamp can EGTA gain access to the cell and, thereby, control free intracellular calcium, a must in studies involving calcium-activated potassium channels. Therefore, perforated patch is inappropriate.
2. ATP, GTP, cAMP, cGMP, Mg^{2+} , to name but a few intracellular signalling pathway molecules, could have been added to the pipette but which of these signalling molecules may be responsible for the observed run-up/down in HEK cells, expressing BK α / BK α and β_1 subunits and also how much would be required to optimise experiments? Indeed, it may well be that none of the above is involved in generating the run-up/down. Evidently, to ameliorate the effects of run-up/down on the collected data by replacing possible dialysed substances would involve many individual experiments and would not be time or cost effective.
3. Polyamines, known regulators of BK channels [451], could be added to the pipette, but which - putrescine, spermidine, spermine - might be

contributing to the run-up/down in HEK cells expressing α/α and β_1 subunits? As with the previous point, investigating the possible dialysis of polyamines, again would not be time or cost effective.

4. To obviate antioxidant effects, superoxide dismutase (SOD) or catalase could be added to the pipette but are O_2^- or H_2O_2 involved in run-up/down in HEK cells over-expressing BK channels? Also, enzyme diffusion into the intracellular space *via* a patch electrode is known to be slow.

In short, to optimise time spent exploring many avenues of potential solutions to remove these artefacts, it was decided to simply measure observed run-up/down in these experiments and to take into account these phenomena when analysing the data. In these experiments run-up/down was observed over approximately 8 minutes and a Kruskal-Wallis non-parametric test followed by a multi-comparison statistical analysis (Dunn's) was used to allow for observed time-dependent changes.

4.4.1.2 Ca^{2+} sensitivity

BK currents are sensitive to internal free calcium ion concentrations. It is well-documented that increases in $[Ca^{2+}]_i$ and membrane depolarisation results in BK channel activation [38, 212, 360, 452, 453]. Work done by Meera *et al.*, has shown that intracellular calcium levels above 1 μ M causes modulation from a state of Ca^{2+} - independence to a channel with enhanced voltage sensitivity and activation kinetics [37]. And indeed, at the intracellular

concentrations of free calcium (<0.2 nM) used in this study, the functional coupling of the BK complex of α and β_1 subunits is independent of Ca^{2+} and thus, channel “switches” to a purely voltage-gated mode.

Work done by Cui *et al.*, on *mSlo* BK currents, demonstrates increasing concentrations of intracellular Ca^{2+} leads to a concomitant increase in conductance, and this occurs in conjunction with a leftward shift along the voltage axis in the G-V curve [370]. The $V_{0.5}$ depicts the necessary voltage to half activate the channel and thus, is a useful measure to assess the effects of Ca^{2+} as a BK modulator. Here, in HEK 293 cells expressing only α subunits, increasing the free $[\text{Ca}^{2+}]_i$ from 0.2 nM to 55 μM instigated a hyperpolarising shift in the $V_{0.5}$ for the voltage conductance curve by approximately 60 mV (Figure 4.3.1.2(C)). However, it is known that the association of β_1 subunits augments the channel’s sensitivity to intracellular Ca^{2+} [97] and as may be expected, increasing the free $[\text{Ca}^{2+}]_i$ from 0.2 nM to 55 μM in HEK cells expressing both α and β_1 subunits instigated a bigger hyperpolarising shift in the $V_{0.5}$ for the voltage conductance curve (100 mV) (Figure 4.3.7.2(C)). Furthermore, at all concentrations of free $[\text{Ca}^{2+}]_i$, HEK cells expressing both BK α and β_1 subunits exhibited a $V_{0.5}$ more negative than cells with only α subunits expressed. In cells expressing both BK α and BK α + β_1 subunits, the G-V relation maintained a shape which could be fitted with a single Boltzmann function, with differing $[\text{Ca}^{2+}]_i$.

These parameters display typical BK channel activity which correlates with findings of other workers [38, 212, 370], substantiating the expression of functional BK subunits in these HEK 293 cells.

4.4.1.3 Activation rates and toxin blockade

BK channels have multiple phenotypes and *hSlo* α BK channels exhibit fast-gating, toxin-sensitive characteristics, whereas in comparison, *hSlo* α + β_1 channels are slow-gating and less sensitive to some scorpion toxins [31, 41, 431]. Indeed, examination of control activation rate data and example trace recordings (Figures 4.3.1.1(Ai); (Aii) and (C) and Figure 4.3.7.1(Ai); (Aii) and (C)) uphold these findings. Recordings made from HEK 293 cells containing BK α alone subunits revealed activation rates of approximately 2.5 ms whereas, activation rates observed in recordings made from HEK 293 cells containing both α and β_1 subunits were approximately 10 ms slower. This is entirely in accordance with similar findings by other groups [34, 38, 41, 212, 454, 455] and consistent with functional BK channels.

Although BK channels comprising both α and β_1 subunits are effectively blocked with charybdotoxin (ChTX), it is promiscuous blocker and not BK channel specific (refer to Table 4.1.3.1 for details). Iberitoxin (IbTX) is a known blocker of BK channels, however, the rate of block for this toxin is slower when applied to BK α + β_1 channels than for channels comprising only α subunits [325, 392]. In line with reports by other investigators [392, 399, 432] appropriate inhibition of BK current was observed on application of IbTX (100 nM) to both HEK 293 cells expressing α alone and those comprising α plus β_1

subunits combined. As expected, current inhibition was slower in cells expressing BK α + β_1 subunits (rate of block $\equiv 2.18 \pm 0.65 \times 10^4 \text{ M}^{-1} \text{ s}^{-1}$) compared to those cells expressing just BK α channels (rate of block $\equiv 2.552 \pm 0.48 \times 10^5 \text{ M}^{-1} \text{ s}^{-1}$) (Figures 4.3.1.2(B) and 4.3.7.2(B)). This is perfectly concurrent with separate observations reported by Meera *et al.*, and Dworetzky *et al.*, whose investigations involving the sensitivity of BK currents to ChTX and IbTX demonstrated a 10 x fold slowing down of IbTX (100 nM) block in the presence of the β_1 subunit [392, 431]. Meera *et al.*, postulate that the slower blocking rate of IbTX induced by BK β subunits may be attributable to an allosteric mechanism, steric hindrance from charged residues or direct involvement of the extracellular loop of the β_1 subunits. They have demonstrated that toxin association and dissociation characteristics are determined in this region and suggest that the extracellular β_1 subunit loop not only acts as a partial toxin receptor but acts a structural barrier to the binding site for the large toxin molecules [392].

4.4.2 Effects of Oestrone and novel compounds (5 μM) on HEK 293 cells expressing BK α subunits and HEK 293 cells expressing BK α + β_1 subunits

Oestrogens have been extensively investigated as BK channel modulators, particularly in vascular smooth muscle. *In vivo*, oestrone can be readily converted to 17 β -oestradiol, which makes it a germane parent compound for the novel xenoestrogens synthesised for this study. In this chapter, the effects of Oestrone, DME-Oestrone, Quat-DME-Oestrone, Oestrone-Oxime and Quat-DME-Oestradiol on the activity of BK α or BK α + β_1 currents in HEK

293 cells were examined. A summary of the observed effects of these compounds, alongside previous findings for 17 β -oestradiol and non-steroidal antioestrogens, are tabulated in Table 4.4.2.1.

Table 4.4.2.1 Summary of effects of oestrogen and novel derivatives on BK whole cell currents in HEK 293 cell over-expressing BK channels.

Compound		BK α alone	BK $\alpha+\beta_1$	Refs
17-keto oestrogens	<u>Oestrone</u>	0	↑↑	PS [235]
	<u>DME-Oestrone</u>	0	0	PS [235]
	<u>Quat-DME-Oestrone</u>	0	0	PS [235]
17 oxime	<u>Oestrone-Oxime</u>	↓	↑	PS [235]
17 β -hydroxy oestrogens	<u>DME-Oestradiol</u>	Not tested in HEK293 cells	Not tested in HEK293 cells	PS [235]
	<u>Quat-DME-Oestradiol</u>	↓	↑↑↑	PS [235]
	<i>17 β-Oestradiol</i>	0	↑↑↑	[129, 251]
Non-steroidal anti-oestrogens	<i>Tamoxifen</i>	↓	↑↑↑	[129]
	<i>Ethylbromide tamoxifen</i>	NDA for HEK 293 cells	NDA for HEK 293 cells	[103, 104, 129]
	<ul style="list-style-type: none"> Increases BK NP_o in outside-out patches (mouse colonic smooth muscle) No effect on BK NP_o in inside-out patches (mouse colonic smooth muscle) 			

Key: Inactive compound (0); Significant activation in order of potency (↑↑↑ > ↑↑ > ↑); Significant inhibition (↓); Underlined compounds (novel findings from this study); *Italicised compounds* (known effects of non-steroidal anti-oestrogens shown by other groups); NDA (no data available); NP_o (number of channels multiplied by open probability); PS (present study).

Near zero levels of free $[Ca^{2+}]_i$ (>0.2 nM) were used for the recordings as oestrogens have been reported to be better activators of BK channels when the free $[Ca^{2+}]$ is low and the open probability for the channel is small [40]. Kruskal-Wallis followed by Dunn's multiple-comparison analyses were executed to take account of run-up/run-down, displayed in whole-cell recordings. These statistical tests established none of the compounds tested on BK α channels increased potassium peak current (Figure 4.3.7.1 and Table 4.3.7.1). Conversely, in whole cell recordings of cells expressing both subunits, a significant increase in peak current was observed in response to Oestrone, Oestrone-Oxime and Quat-DME-Oestradiol (Figure 4.3.14.1 and Table 4.3.14.1). Interestingly, two of the compounds tested, Oestrone-Oxime and Quat-DME-Oestradiol, initiated slight inhibition of peak current in cells expressing BK α channels. As predicted in Section 4.1.4 (AIMS), Quat-DME-Oestrone proved to be inactive both in the presence and absence of the β_1 subunit.

Quat-DME-Oestradiol

Quat-DME-Oestradiol has a quaternary ammonium group (Figure 4.4.2.1) and this could be responsible for the weak inhibition of peak current observed in cells expressing BK α subunits.

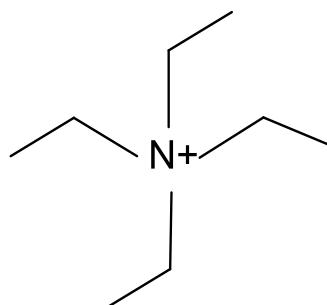
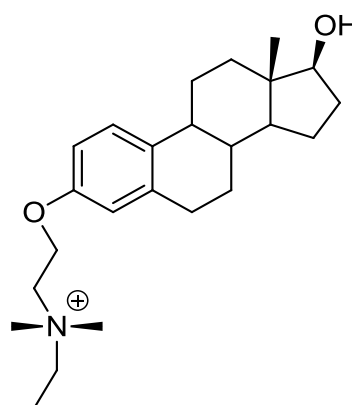
Ai**Aii**

Figure 4.4.2.1 Tetraethylammonium (TEA) is a quaternary ammonium cation consisting of a positively charged nitrogen attached to four ethyl groups (Ai). As with Quat-DME-Oestradiol (Aii), TEA exists in association with a counter-ion.

Quaternary amines such as tetraethylammonium (TEA) inhibit the flow of potassium currents by occlusion of the channel pore. Indeed, it has been demonstrated that TEA, a quaternary ammonium K^+ channel blocker, is able to block BK potassium currents with millimolar affinity for the intracellular opening of the channel pore [104, 377, 456]. In *hSlo*, BK channels have a ring of eight negatively charged glutamate residues (Glu386 and Glu389) at the intracellular opening. Moreover, in the pore-forming extracellular loop, two acidic amino residues (Asp326 and Glu329) generate a pronounced negative electrostatic potential [382, 456, 457] conducive to binding of positively-charged molecules such as TEA and Quat-DME-Oestradiol to the extracellular region of the pore. This has been further explored by Wilkens and Aldrich (2006) whose work revealed that a large quaternary ammonium compound (bbTBA) blocks the BK channel from the extracellular side of the channel near the selectivity filter even when the channel is closed. It is worth noting that

oestrogens can act as antioxidants by capturing a $\cdot\text{OH}$ hydroxyl radical to produce a phenoxyl radical. Further scavenging of a $\cdot\text{OH}$ produces a quinol which is easily converted back to its parent oestrogen compound by NADPH-dependent enzymes [458-461] (Figure 4.4.2.2).

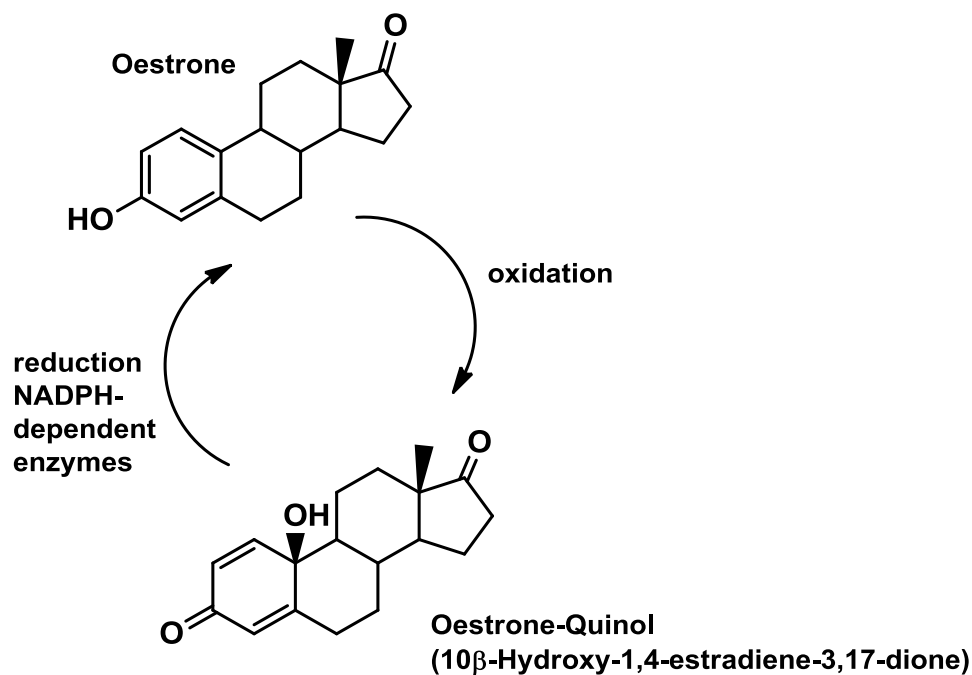


Figure 4.4.2.2 A putative pathway for redox conversion and metabolic regeneration of A ring oestrogens through quinols.

These antioxidant properties may very well account for the effects on BK currents of phenolic oestrogens such as oestrone, and 17β -oestradiol but this explanation would not be true for quaternary oestrogens such as Quat-DME-Oestradiol which are substituted in the three position and thus, are unable to form quinols.

Oestrone-Oxime

Oestrone is a high affinity ligand of oestrogen receptor (ER) and Oestrone-Oximes are known ER ligands [462]. Nevertheless, Oestrone-Oxime has weak oestrogenic activity (about x40 less than its parent compound Oestrone) [463, 464]. Previous work has identified the pharmacophore effect of the oxime functional group (N-OH) as one of a NOS-independent NO donor [257, 258]. For instance, Oximes can be converted into NO *via* cytochrome P-450 or NAD/NADP-dependent oxido-reductases [258, 259, 465]. Of course, Oestrone-Oxime is easily able to cross cell membranes and thus, the enhanced peak current observed in experiments involving both BK subunits could be due to NO-induced intracellular events. Additionally, it is possible that Oestrone-Oxime undergoes hydrolysis. If this is the case, a ketone would replace the oxime group, generating a bioactive compound with known BK activity (Figure 4.4.2.3). In addition, hydrolysis of Oestrone-Oxime generates hydroxylamine (HA) which is a putative intermediate in the conversion of L-arginine to nitric oxide and as such may be an endogenous nitric oxide donor [466, 467]. HA has also been reported to cause the relaxation of pre-contracted aortic rings [466, 468].

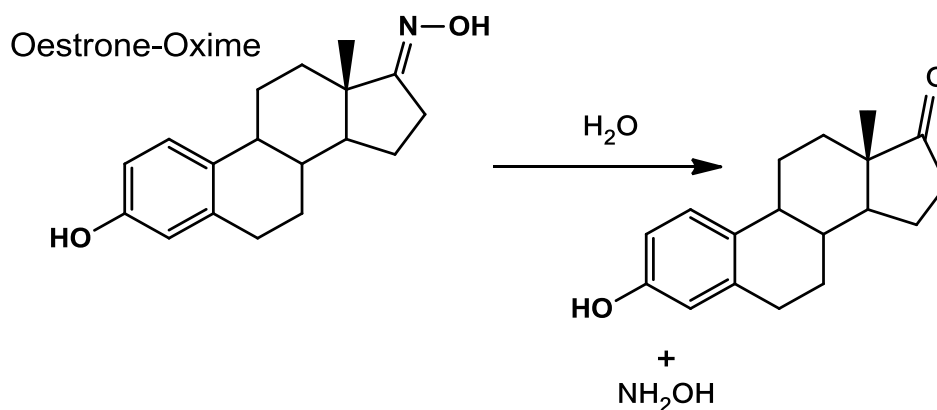


Figure 4.4.2.3 The mechanism from which Oestrone-Oxime could undergo hydrolysis and generate Oestrone (starting compound). This reaction also results in the generation of hydroxylamine (HA). NH_2OH is a precursor for nitric oxide generation.

However, this does not explain how NO generation from Oxime-Oestrone inhibits BK α currents but increases BK α + β_1 currents. Yet, this phenomenon is not unknown and work done by Cui *et al.*, demonstrates both activation and inhibition of BK α channels by novel oxime ether derivatives of the benzylic ketone of diCl-DHAA, a tested BK α modulator [256]. Additionally, Dick and Sanders have previously established xenoestrogens, such as tamoxifen along with steroidal oestrogens like 17 β -oestradiol, can elicit a decrease in unitary current by interaction with the α subunit [103].

4.5 SUMMARY

Characterisation of the evoked BK currents recorded from whole cell patch-clamp using non-stationary noise analysis, toxin blockade, activation rate and conductance-voltage relationship confirmed the expression of α and α plus β_1 subunits in HEK 293 cells. The data in this chapter demonstrate that Oestrone, Quat-DME-Oestradiol and Oestrone-Oxime were able to increase BK currents in HEK 293 cells over-expressing both α and β_1 subunits, whereas, Quat-DME-Oestrone, as anticipated, proved to be completely inactive in both types of cells. Quat-DME-Oestradiol, due to the presence of a quaternary functional group, is membrane-impermeant which may indicate an extracellular site of action. This would be in line with previous work done by Dick *et al.*, which suggests a putative binding site for xenoestrogens within the extracellular loop of the β_1 subunit [104]. However, these data cannot determine definitively, the location of a possible BK activation site or sites and it must be borne in mind that the mechanism of action of these oestrogens could very well be due to interaction *via* second messenger pathways, such as G-protein-coupled (GPE) receptors. Although HEK 293 cells do not express endogenous GPE receptors [271, 469], it cannot be ruled out that other membrane delineated receptors may have a contributory involvement in the observed augmentation of potassium current in the presence of the ligands. Thus, the observed non-genomic actions of the novel compounds could be direct or secondary to modulation of intracellular cell signalling pathways.

Although further checks on mechanisms could be done using inside out & outside out patch-clamp experiments to check for sidedness and to study the

effects of the novel compounds on single channel conductance, channel life time and open probability, it was decided to extend the investigation by exploring these considerations on BK channels reconstituted in lipid bilayers. Bilayer experiments will afford the opportunity to carry out these investigations without interference from intracellular signalling events. Thus, any channel modulation observed in bilayers containing reconstituted BK subunits would obviate an intracellular signalling mechanism and could be attributed to the applied compound.

CHAPTER 5

Single Channel Recordings

in

Lipid Bilayers

5.1 INTRODUCTION

This study, so far, has considered the effects of Oestrone and novel derivatives on vascular smooth muscle relaxation using pre-contracted rat aortic rings to appraise their ability to modulate BK channels. These whole tissue experiments, however, can only demonstrate possible BK involvement and do not provide conclusive evidence that these oestrogens and xenoestrogens act *directly* on the BK channel. Additionally, whole cell BK recordings using the patch-clamp configuration, described in Chapter 4, cannot rule out the effects of the compounds on intracellular signalling events and second messenger involvement. To this end, a simpler and more direct route was necessary to investigate the effect of these novel compounds on BK channels. Thus, this chapter will report on the effect of these oestrogens on BK channels reconstituted into planar lipid bilayers.

5.1.2 Cell membranes and the lipid bilayer

All eukaryotic cells are encased in a framework of lipids. These aggregate as a three dimensional bilayer, consisting of amphipathic phospholipids, glycolipids and sterol molecules which surround the contents of the cell in the presence of non-covalent molecular forces and physical interactions (London-van der Waals, electrostatic and hydrophobic forces) [470]. The specific arrangement of lipids is not only paramount to membrane stability, fluidity and its self-assembly properties, but at the same time, sustains critical concentration gradients by providing a tight barrier against the permeability to water-soluble ions and molecules [471]. The bilayer of a cell membrane, thus,

is a dynamic structure which, at the same time, affords a functional environment for ion channels, receptors and other integral proteins (Figure 5.1.2.1).

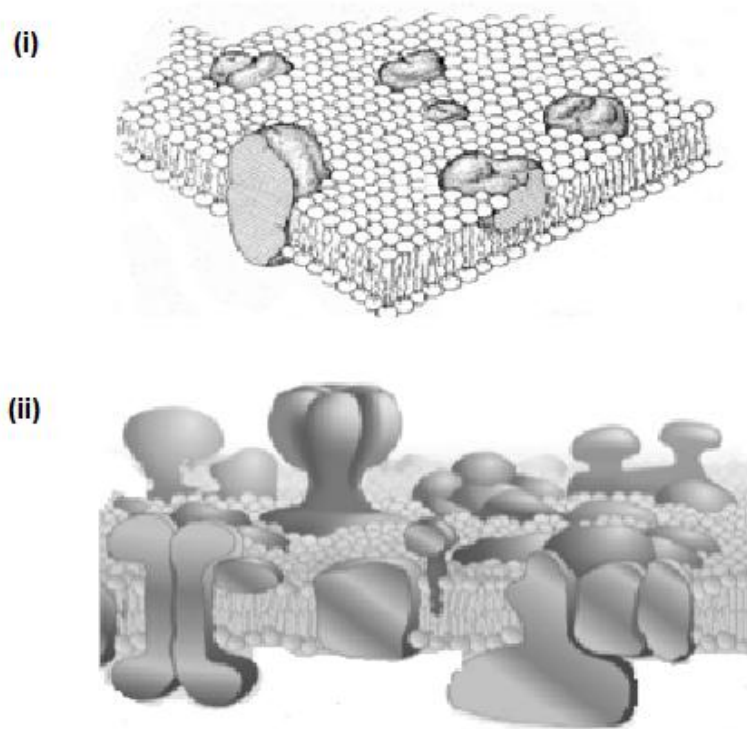


Figure 5.1.2.1 (i) Schematic of a cell membrane structure based on the Singer-Nicolson fluid mosaic model first mooted in 1972 [472]. (ii) A revised contemporary adaptation of the Singer-Nicolson model proposed by Engelman and founded on work done on putative lipid raft domains and bilayer composition, showing the bilayer as a crowded structure with varying thicknesses of bilayer [473].

Regardless of a cell's cytoskeletal structure and uniformity of bilayer thickness, biological membranes engage an array of lipids including sphingolipids, glycerophospholipids (GPLs) and cholesterol displaying differences not only in tail length (no fewer than 12 and as many as 24 carbon atoms), but also in the extent of saturation of acyl chains and head group polarity [474]. GPLs are the major lipid constituents in the cell membrane - between 50 and 80% of most mammalian cell membranes are adjudged to comprise these lipids, the

remainder of the structure being made up of various proteins. Typically, they possess one fatty acid chain containing no less than one *cis* double bond, which causes the chain to kink, whilst the other chain is saturated [475, 476]. Most commonly, the two hydrophobic acyl chains are connected to the charged headgroup by way of a common linker group or glycerol backbone (Figure 5.1.2.2). Phosphatidylethanolamine, phosphatidylserine and phosphatidylcholine are the predominant glycerol-based phospholipids present in biological mammalian membranes [474, 476]. Interestingly, the only overall charged phospholipid is phosphatidylserine which carries a net negative charge at physiological pH. All other phospholipids are neutrally charged zwitterions [475].

Other important constituents of the membranes are the sphingophospholipids, glycolipids and sterols. The sterols include cholesterol, a class of steroid, which is a vital element of the cell's lipid membrane and is essential for the organisation and integrity of the bilayer [477-479]. In mammalian cells cholesterol can be manufactured within the cell and also, received into the cell from lipoprotein uptake. The plasma membrane in mammalian cells contains approximately 30-50 mol% of cholesterol, which is randomly and unevenly distributed throughout the cell membrane in cholesterol-rich and cholesterol-impooverished sphingolipid domains [479-481]. These domains, sometimes known as lipid rafts, are purported to play an indispensable role in maintaining the structure and function of the cell membrane [482-485].

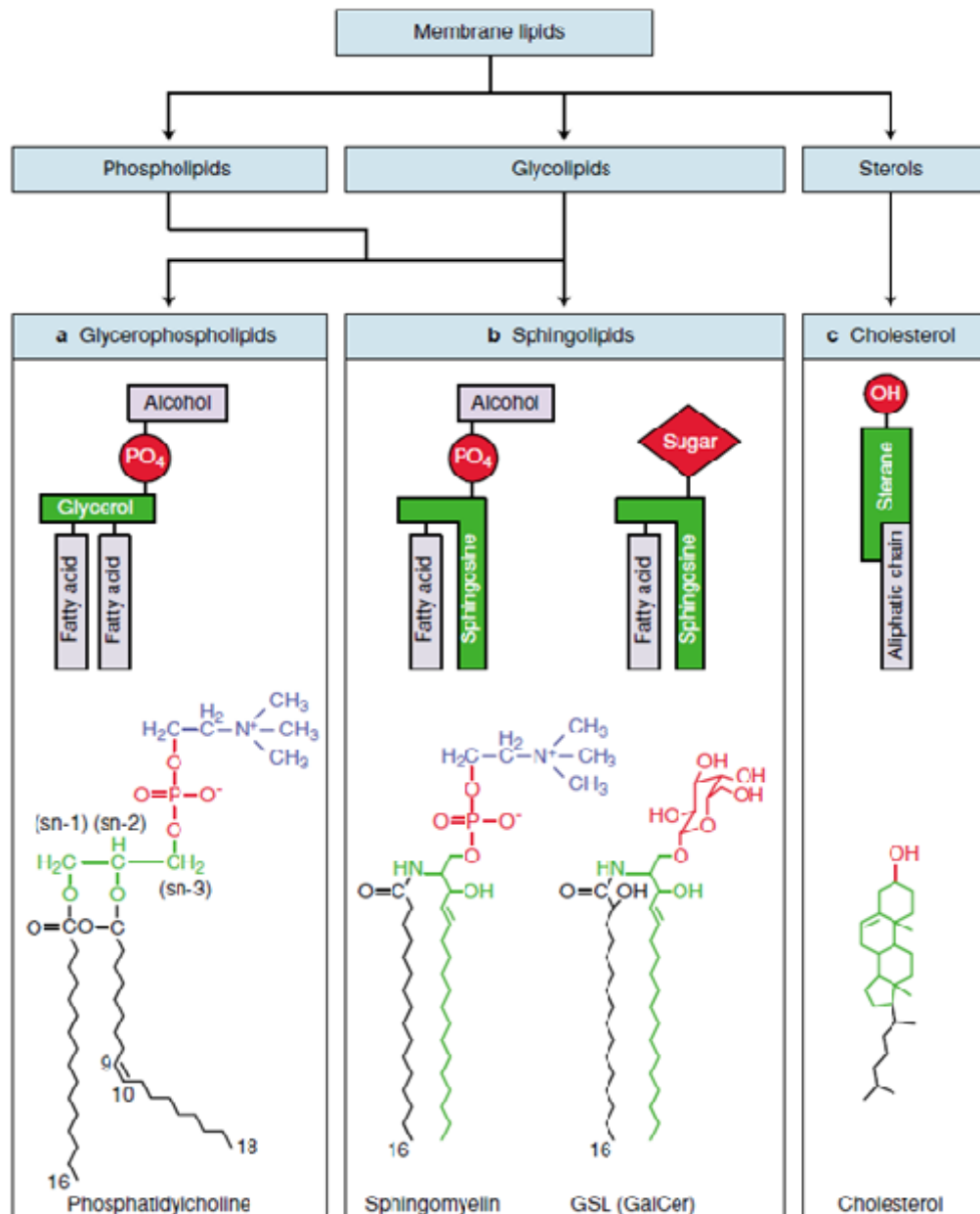


Figure 5.1.2.2 Structure and classification of mammalian cell membrane lipids. Lipids in the plasma membrane include glycerophospholipids (GPLs), sphingolipids and cholesterol.

(a) GPLs, the foremost lipid component of the bilayer. The main GPL molecules are phosphatidylcholine, phosphatidylethanolamine and phosphatidylserine.

(b) Sphingolipids include the phospholipid, sphingomyelin and the glycosphingolipids (resulting from a glycosidic bond due to linkage of a sugar or oligosaccharide to an OH group).

(c) Cholesterol is a steroid with a single OH polar head group and an hydrophobic moiety consisting of an aliphatic, iso-octyl carbon chain [476].

5.1.3 Reconstitution of a planar lipid bilayer

The two principle techniques of membrane reconstitution in current use are (i) the painted bilayer technique, devised by Mueller and co-workers over fifty years ago [486, 487] and (ii) the monolayer folding method [488] (Figure 5.1.3.1).

(i)



(ii)

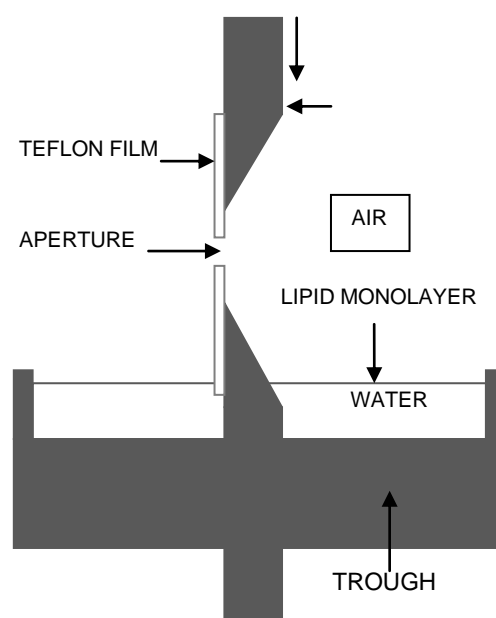


Figure 5.1.3.1 Illustrations of equipment and set-up of vertical painted bilayers. (i) The black bilayer chamber and cuvettes are milled from black and white acetyl resin (Warner Instruments) although, other materials for cuvettes e.g. polystyrene and polysulfone, are available. Polyethylene centrifuge tubes serve as wells to create electrical communication between the headstage Ag/AgCl electrodes via agar salt bridges and the cup or chamber (see Methods 5.2). (ii) Schematic showing the folded method of bilayer formation. The illustration shows two monolayer troughs which are segregated by a moveable septum with a hole which is then covered by a thin tetrafluoroethylene film which contains the aperture. The two sections are filled with a saline solution to below the aperture after which a lipid monolayer is applied to each side. The water levels are very slowly raised in turn until the aperture is submerged [488].

Both methods of membrane reconstitution involve the spread of phospholipids, dispersed in non-polar solvents, across a machined aperture on an artificial surface separating two fluid-filled chambers (Figure 5.1.3.2).

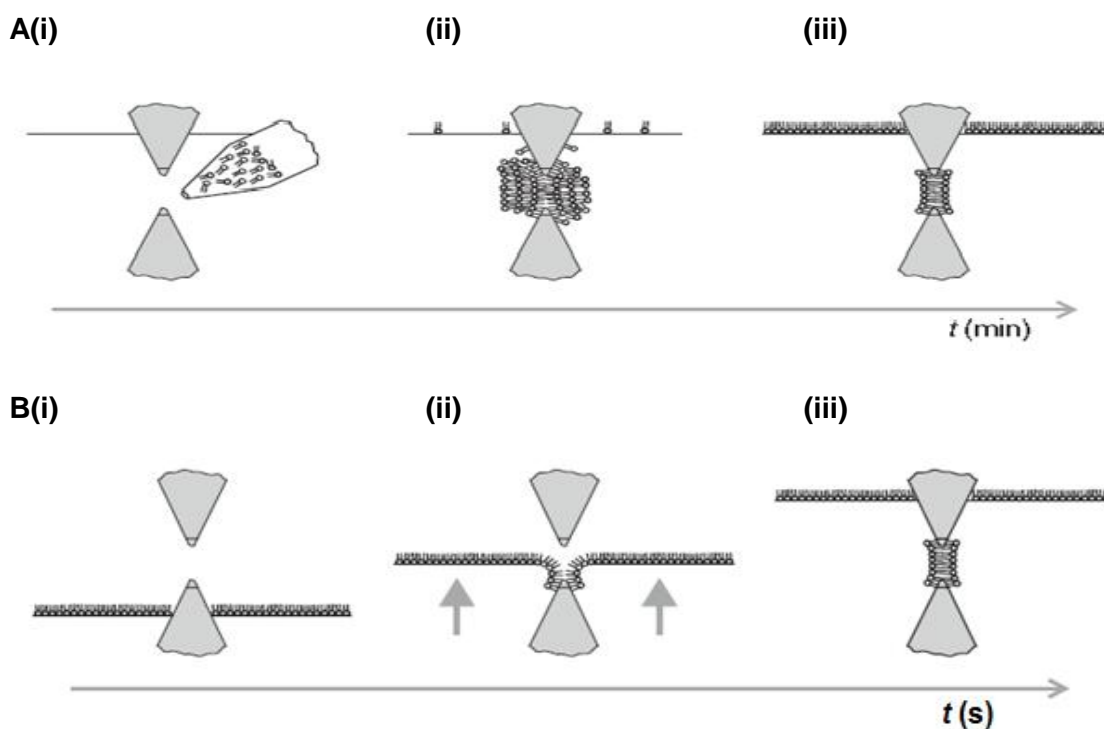


Figure 5.1.3.2 Schematic illustrating the two principle techniques for the formation of a planar lipid bilayer in current practice that is the painted bilayer and the monolayer folding technique [471]. A(i) A mixture of lipids, dispersed in a solvent such as *n*-decane, is painted onto the aperture with a glass painting stick or nib; (ii) lipid molecules cluster around the aperture to form a thick lipid film of several μm thick, while excess lipids float to surface of water based solution; (iii) the planar lipid bilayer is formed; B(i) a mixture of lipids, dispersed in a solvent *n*-pentane, is applied to the surface of the salt solution as a monolayer; (ii) the salt solution levels are gradually raised until the aperture is covered and the lipids still floating on the surface; (iii) A film of lipids cover the aperture and the bilayer is formed. Excess lipids float on surface of salt solution [471].

To aid protein fusion, choice of lipid is deemed to be important and literature indicates the use of an acidic lipid as useful. Phosphatidylserine (PS) is a popular choice and is usually mixed with one or more neutral phospholipids such as phosphatidylethanolamine or phosphatidylcholine in a variety of ratios [489].

For both techniques, thinning of the membrane is critical for the formation of a stable bilayer and the success of this is dependent on several parameters, not least the size and shape of the aperture which can vary (~100 μm to >300 μm) (Figure 5.1.3.3).

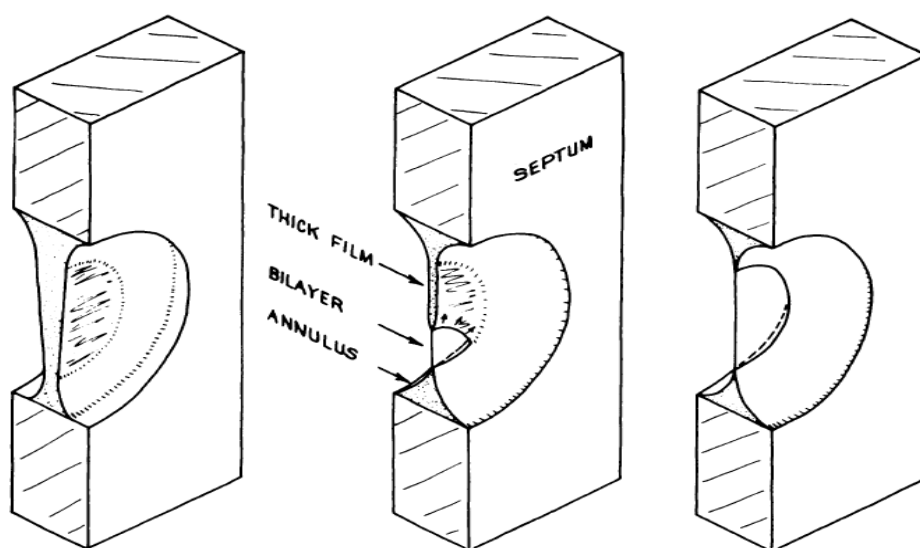


Figure 5.1.3.3 Cross-section of cup and septum illustrating the process of bilayer thinning. The lipid dispersion coats the septum as a thick film and forms an annulus at the edge of the bilayer which is known as the Plateau-Gibbs border. Formation of a planar lipid bilayer is due to the spontaneous thinning process of the film, driven in the first instance, by the Plateau-Gibbs border suction, which arises from the curvature of the annulus. The hydrocarbon drains into a Plateau-Gibbs border (which is known as a torus) and as the film thins, London-van der Waals forces between the two aqueous phases help to form a thin bilayer [471, 486, 490, 491].

The progress of bilayer formation can be followed simply by observing the thinning process under reflective light [492]. Initially, the film has a rainbow-like iridescence due to the effects of reflected white light. As the film thins and a bilayer starts to form, the appearance of the membrane gradually morphs into a black structure due to the lack of reflective light [492]. Membrane capacitance can also be monitored to indicate the state of membrane thinning and stability. The bilayer system is set up using a low frequency filter (1 kHz), low amplitude triangular waveform which, because the *cis* and *trans* chambers are electrically coupled, produces sizeable fluctuations in capacitive current through the hole. Once the aperture is painted with lipid dispersion, the orifice becomes blocked and is witness to small deflections from zero current with each voltage transition. As the thinning of the lipid film progresses, so the deflections in current amplify and membrane capacitance increases [471, 489, 490, 492]. The resultant stable bilayer has a capacitance between 0.3 and 0.6 $\mu\text{F}/\text{cm}^2$ with a conductance of <10 pS [489].

5.1.4 Planar lipid bilayers (BLMs) and ion channel reconstitution

Since its inception over fifty years ago, the planar lipid bilayer concept has been a key model for the study of biological cell membranes. Accordingly, the inert properties and high electrical resistance of these artificial lipid bilayers, alongside the advent of successful reconstitution into the bilayers of ion channel proteins, has advanced the investigation and appraisal of single channel currents. Indeed, compared with such techniques as patch-clamp or *ex vivo* tissue experiments, ion channel reconstitution into lipid bilayers has afforded many workers the opportunity to study in depth, the molecular

mechanisms of ion channels and ionic transport across a membrane, with negligible interference from other ubiquitous cellular components.

Reconstitution of ion channels into lipid bilayers requires that the channel proteins of interest must first be extracted from the cell, either by cell fractionation and insertion into native membrane vesicles, or purification *via* solubilisation using detergent [492] (see Methods 5.2). Whether contained in membrane vesicles or proteoliposomes, channel proteins insert into the planar lipid bilayer by fusion (Figure 5.1.4.1).

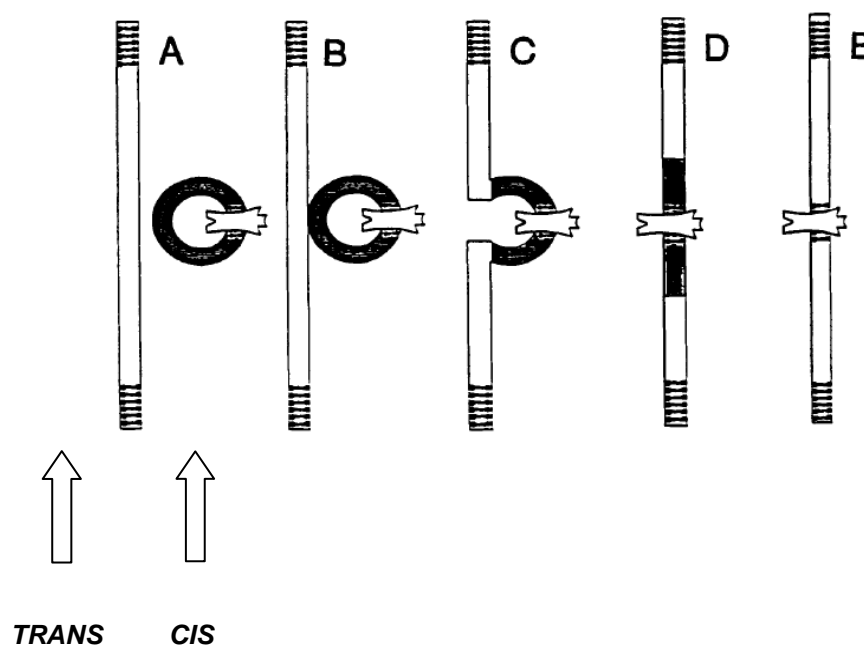


Figure 5.1.4.1 Schematic of the fusion process of ion channel protein with the planar lipid bilayer (BLM). (A) Vesicle containing ion channel protein of interest is added to the cis side of the bilayer chamber containing electrolyte solution; (B) Vesicle adheres to the BLM in a stochastic manner; (C) Illustrates the beginning of the fusion process; accommodation of vesicle into membranes; (D) Fusion of vesicle and channel protein is completed; (E) Vesicle lipids diffuse away, leaving incorporated channel protein [493].

Evidence of incorporation of channel protein into a black lipid membrane was first reported by Bean *et al.*, who recorded discrete single channel currents from bilayers with added excitability inducing material (EIM), a bacterial protein extracted from *Aerobacter cloacae* (now named *Enterobacter cloacae*) [494]. Bean and his co-workers demonstrated biophysical and kinetic characteristics strongly indicative of a long-lived polar channel [494]. Later, ion conducting gramicidin channels in bilayers were reported by Hladky and Haydon (1970). Gramicidins are pore-forming linear 15-amino acid polypeptides produced by *Bacillus brevis* from which single-channel conductances could be readily recorded [495-498].

Other workers have since recorded conductances from toxin-induced transmembrane pores in artificial membranes. For instance, Hardy and co-workers demonstrated enterotoxin (type A) (CPE), produced by *Clostridium perfringens*, forms pores in receptor-free planar lipid bilayers made up from synthetic phospholipids (phosphatidylethanolamine and phosphatidylserine) [499]. These workers established that when 10 µg CPE was added to the *cis* chamber, channels inserted in approximately 50% of all bilayers used.

More recently, McClain *et al.*, reported a toxin, secreted by *Helicobacter pylori* (VacA), forms anion-selective ion channels in lipid bilayers [500]. In addition, there have been myriad integral transmembrane channel proteins, (not least K⁺, Na⁺ Ca²⁺ and Cl⁻ channels), successfully isolated from modified expression systems and functionally reconstituted into lipid bilayers [474].

There is a plethora of literature characterising BK channel function after reconstitution into an artificial planar lipid bilayer [47, 131, 136, 501, 502]. For example, Kapicka *et al.*, carried out experiments to compare the gating, ion conduction and pharmacology of BK channels reconstituted from canine colonic smooth muscle in both artificial lipid bilayers and excised patches [503]. Interestingly, they found BK gating activity in both bilayers and excised patches, in response to changes in membrane potential and free Ca^{2+} , was identical.

5.1.5 Advantages / disadvantages of the BLM as a model for biomembranes

Ion channel reconstitution into a model bilayer system is an authoritative standard available to demonstrate ion specificity of any channel of interest [489, 504]. Undoubtedly, the lack of a cellular environment and control over the microenvironment obviating the effects of cytoplasmic miscellanea gives a clear advantage over other techniques. However, there are known limitations to a bilayer model system which are listed in Table 5.1.5.1).

Table 5.1.5.1 Advantages and disadvantages of artificial bilayer systems as a model for ion channel investigation and characterisation.

Advantages	Disadvantages	Refs
Artificial lipid bilayers can be used to investigate permeation and gating characteristics of individual ion channels in a chemically isolated environment	Planar lipid bilayers are fragile and are easily blown by electrical and / or mechanical noises	[491, 505, 506]
Ease of access to the internal and external aspect of a channel protein allows effective solution exchange in modulatory experiments	Lack of control over channel insertion causing challenge to integrity of membrane	[504, 507, 508]
Artificial bilayers can now be formed on a range of substrates which confer long-lived, stable membrane integrity, smoothing the way for advances in biotechnology	Time consuming and slow throughput - can takes hours to achieve stable, thin bilayer and/or channel insertion	[491, 505]
Total control of lipid environment	Requires a highly trained researcher	
	Lack of certainty of channel origin	
	Bacterial contamination causing porins	
	Bilayers produced in this way will contain some solvent which may affect channel performance	[492]

5.1.6 AIMS

This chapter will examine the effects of Oestrone and derivatives on the activity of BK channels expressing α subunits alone and also those expressing both $\alpha+\beta_1$ subunits reconstituted into planar lipid bilayers. In the previous chapter it was shown that Oestrone, Oestrone-Oxime and Quat-DME-Oestradiol were able to activate BK currents. This activation required the presence of the β_1 subunit. Quat-DME-Oestrone, as predicted, was inactive in aortic rings, and showed no activation of BK currents in HEK cells, whilst DME-Oestrone could relax aortic rings but seemed to have no effect on BK currents recorded in HEK cells.

Whilst Oestrone, Oestrone-Oxime and Quat-DME-Oestradiol were able to activate BK currents, it is not known if this is a direct effect on the BK channel or through other surface membrane receptors triggering cytosolic events involving second messenger systems e.g. G-protein coupled receptors and G-protein coupled oestrogen receptors (GPR30/GPER). These potential cytosolic effects can be removed if a simpler system of investigation is employed. Thus, the aim of this chapter is to investigate these compounds as novel activators of the BK channel in a planar lipid bilayer system where the consequences of cytosolic effectors and nuclear events are absent.

It has been shown previously that oestradiol and antioestrogens can increase NP_o of BK channels in lipid bilayers when the β_1 subunit is associating. It is also well-documented that oestrogens and antioestrogens can activate BK channels in a non-genomic manner. Thus, it is hypothesised that if the novel

compounds in this study are able to modulate BK currents in a direct, non-genomic manner, then they should, increase the open probability of the channel.

Objectives:–

1. To investigate the activity of the novel compounds on reconstituted BK channels consisting of α subunits alone.
2. To investigate the activity of these compounds on reconstituted BK channels consisting of α and β_1 subunits.

This approach should:-

1. confirm that Quat-DME-Oestrone, which is inactive in both aortic rings and HEK 293 cells over-expressing BK channels, is inactive in these direct assays;
2. facilitate investigation of active compounds to see if their BK modulating activity is dependent on intracellular signalling. For example, it is possible that Oestrone-Oxime modulates BK channels through enzymatic release of nitric oxide. If this is true, Oestrone-Oxime will be inactive in bilayers but may be active HEK 293 cells;
3. demonstrate which compounds require the β_1 subunit of the BK channel in order to modulate BK currents.

5.2 METHODS

5.2.1 Production of HEK 293 cells for lipid bilayer experiments

HEK 293 cells, expressing either BK α or BK α + β_1 subunits, were grown to confluency in T175 flasks (*Fisher UK*) and passaged and harvested as described previously in Chapter 4 [40, 347]. The resulting pellet was resuspended in Buffer 1 (10 mM Tris-HCl pH7.4; 250 mM sucrose; 200 mM CaCl₂) containing protease inhibitors (*Complete Protease Inhibitors, Roche, UK*). The cell suspension was loaded and sealed into a pre-cooled (4 °C) cavitation cell disruption vessel (*Parr Instrument Company, Illinois, USA*) (Figure 5.2.1.1).

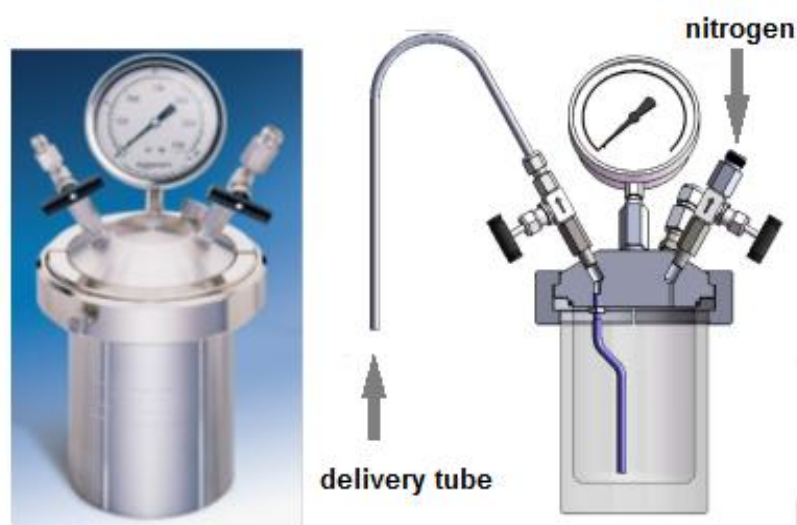


Figure 5.2.1.1 A cell disruption vessel, “cavitation bomb”, used for processing cell suspensions by the nitrogen decompression method. The apparatus has a pressure gauge; a valve for introducing nitrogen (N₂) into the “bomb” cavity; and a valve for extraction of the cell fractionate and collection through an attached delivery tube. To create fragmented cell membranes for the cell of choice, N₂ is delivered into the “bomb” cavity where it is dissolved, under high pressure, in the cell. The gas pressure is then released, allowing the N₂ to leave the cell as expanding bubbles, stretching the cell membrane in the process until the cell disrupts releasing the contents of the cell.

Nitrogen gas was delivered into the cavity (1000–1500 psi) and the apparatus was left on ice for 15 minutes (Figure 5.2.1.2).



Figure 5.2.1.2 Nitrogen cavitation device for isolating cell membranes. Nitrogen gas is delivered under pressure (1000-1500 psi) into the cavity to “bomb” the cells into membrane fragments. The cavitation device containing the fragmented cells is left on ice for 15 minutes

Cavity pressure was released gently and the fragmented cells were collected in a 50 ml Falcon tube and the bursting step repeated again. The cell lysate was diluted to 25 ml with ice-cold Buffer 2 (10 mM Tris-HCl pH7.4; 25 mM sucrose; 1 mM EDTA). The diluted suspension was centrifuged using an ultracentrifuge with fixed rotor (*Beckman L8-55*) at 500 – 1000 x g for 10 minutes to collect cell debris and unbroken cells. Using a serological pipette set, the supernatant was aspirated and gently layered into an ultracentrifuge

tube containing a sucrose cushion consisting of 10 ml of Buffer 3 (10 mM Tris-HCl pH7.4; 35% sucrose; 1 mM EDTA). The cell preparation was then centrifuged at 30 000 x g for 30 minutes at 4°C. The cloudy suspension of membrane fragments, located between the supernatant and the sucrose cushion, was retrieved using a 10 ml plastic syringe and transferred to a fresh ultracentrifuge tube. The collected interface was diluted with Buffer 4 (10 mM Tris-HCl pH7.4; 250 mM sucrose) to fill the tube and centrifuged at 100 000 x g for 45 minutes at 4°C. The supernatant was discarded and the glassy-appearing pellet was resuspended in 1.5 ml of Buffer 4 containing protease inhibitors, by triturating first with a 22G syringe needle followed by a 25G needle on a 5 ml syringe until a lump-free suspension was achieved. Aliquots (50–100 μ l) were stored at -80°C. The expression of both α and β_1 subunits in membranes were confirmed by western blotting, data not shown.

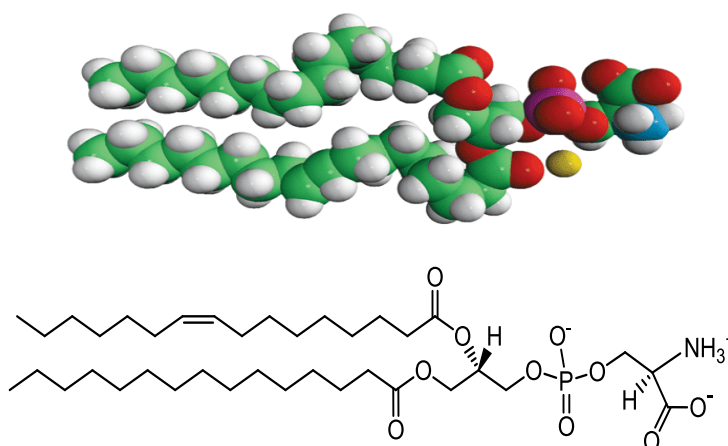
5.2.2 Planar lipid bilayer experimental methods

Lipids are fundamental constituents of cell membranes and are essential to many cell signalling processes. Biological cell membranes usually comprise bilayers composed of phospholipids and variations in the composition of these lipids may affect the function of membrane-bound proteins and other biophysical processes [507]. Planar lipid bilayers are very good models of cell membranes and are a proven methodology to explore membrane channel proteins *via* single-channel recording. Experimental bilayer systems can be set up using a single pure synthetic lipid but bilayers comprising a combination of different lipids are widely used as this is considered to more closely mimic a natural membrane [508].

5.2.2.1 Choice of lipids

Previous researchers have recommended including an acidic lipid in the lipid mixture used to form bilayers since they increase the chances of fusion [508]. The most widely used acidic lipid in many of these investigations is phosphatidylserine, which is usually mixed with a neutral lipid such as phosphatidylethanolamine in various ratios [40, 490, 499, 506]. For this investigation, a mixture of palmitoyl-oleoyl-phosphatidylserine and palmitoyl-oleoyl-phosphatidylethanolamine was used in a 1:1 ratio (Figure 5.2.2.1.1).

(i)



(ii)

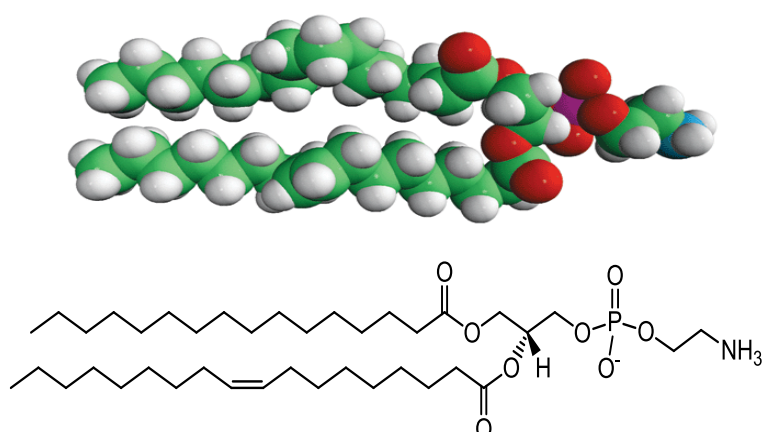


Figure 5.2.2.1.1 (i) Chemical structure of 1-palmitoyl-2-oleoyl-*sn*-glycero-3-phospho-L-serine (POPS). (ii) Chemical structure of 1-palmitoyl-2-oleoyl-*sn*-glycero-3-phosphoethanolamine (POPE)

5.2.2.2 Preparation of lipid bilayer and bilayer set-up

Pure natural lipids (*Avanti® Polar Lipids, Inc.*) were dissolved in chloroform (50 mg/ml). These lipids, comprising palmitoyl-oleoyl-phosphatidyl ethanolamine (POPE) and palmitoyl-oleoyl-phosphatidyl serine (POPS), in a 1:1 ratio were dried with nitrogen and resuspended in *n*-decane to form a final total lipid concentration of 25 mg/ml. Using a blunted glass rod, a small amount was then drawn across a 0.25 mm diameter aperture in the polysulfane cup. The cup separates two solution filled chambers, designated *cis* and *trans*, within the machined bilayer block (*Warner Instruments*). The cup was inserted into the block and 1 ml of solution was added to both sides of the aperture (Figure 5.2.2.2.1).

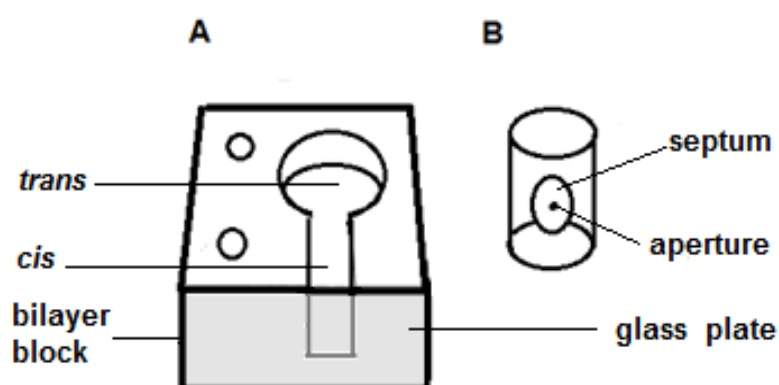


Figure 5.2.2.2.1 Schematic of chamber and cup for the formation of painted bilayers. (A) Block into which an oblong chamber is fashioned (1 ml volume) and a circular chamber into which the polysulfane is placed. The see-through front panel is made from glass to give a view of the machined hole in the bilayer cup. The two small holes hold tubes containing a 2 M solution of KCl and, via agar salt bridges and silver-silver chloride electrodes, connect the chambers to the head amplifier. (B) A polysulfane bilayer cup fits into the circular chamber and, after painting with a mixture of phospholipids, the cup is filled with 1 ml of appropriate buffer (high calcium - 53 μ M for BK α subunits or low calcium - 0.54 μ M for BK α + β_1 subunits).

The electrical connection is completed *via* two short agar salt bridges placed across each chamber into wells containing a 2 M solution of KCL. Two silver-silver chloride-coated electrodes, each immersed in one of the wells containing the salt bridges, complete the circuit by connecting the bilayer chamber to a headstage which serves as a current/voltage converter. The bilayer set-up is protected from vibrations and extraneous electromagnetic noise by being placed on a floating air table and enclosed within a Faraday cage.

The *cis* chamber was grounded and 1 ml of appropriate extracellular buffer was added to each of the chambers. Because BK channels are activated by calcium as well as voltage, and channels expressing both α and β_1 subunits are more sensitive to calcium, buffers containing “high” and “low” concentrations of free calcium were prepared. Thus, bilayers were bathed in symmetrical solutions containing 150 mM KCl, 10 mM HEPES, pH 7.2, 1 mM EGTA, 1 mM MgCl₂ and 1.05 mM CaCl₂ (resulting in 53 μ M “high” free calcium for BK channels expressing only α subunits) or 0.75 mM CaCl₂ (resulting in 0.54 μ M “low” free calcium for BK channels expressing both α and β_1 subunits) (Figure 5.2.2.2.2). Free Ca²⁺ in each solution was calculated using the web-based program *Maxchelator* (Bers *et al.*, 1994; available online at www.stanford.edu/cpatton/maxc.html).

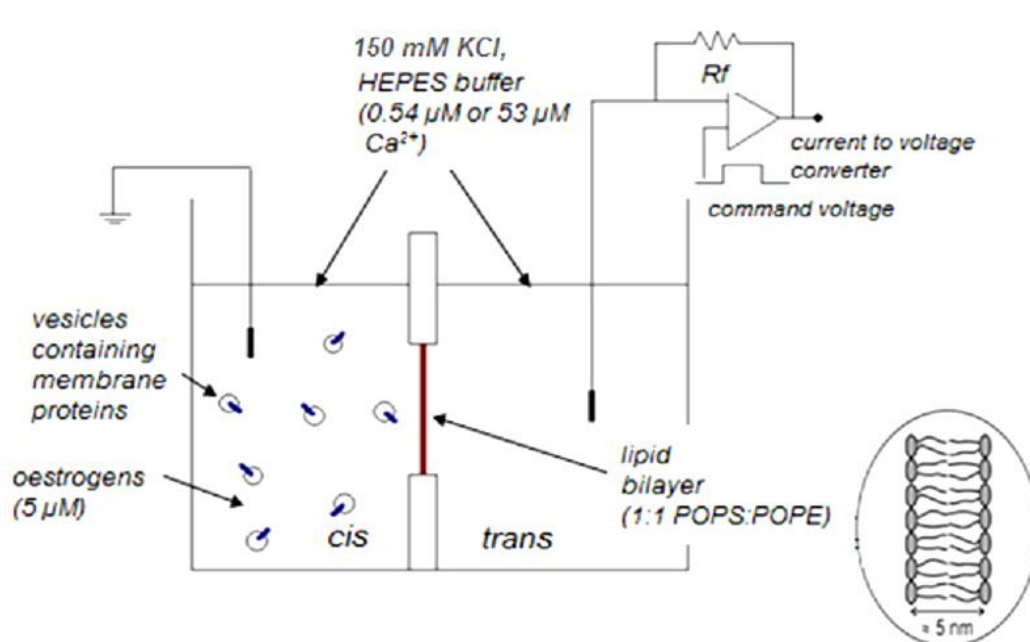


Figure 5.2.2.2 A cross-section schematic of a voltage clamped bilayer set-up depicting the two separate chambers. The grounded side is designated *cis* whilst the ungrounded side is *trans*. The chambers are bathed in symmetrical solutions of a HEPES buffer. Both fragmented membranes containing BK channel subunits and oestrogen compounds are added to the *cis* chamber.

5.2.2.3 BK channel insertion into planar lipid bilayers

Previously prepared protein suspension (see Section 5.2.1), containing BK α or BK α + β_1 subunits, was added to the *cis* side of the bilayer set-up in increments of 2 μ l up to a maximum of 8 μ l. BK channel insertion was confirmed by observation of a trace with a unitary current of ~12 - 18 pA (Figure 5.2.2.3.1).

Channel insertions were rare phenomena, with one or two insertions per day deemed to be productive. For this reason, secondary insertions during recordings are unlikely.

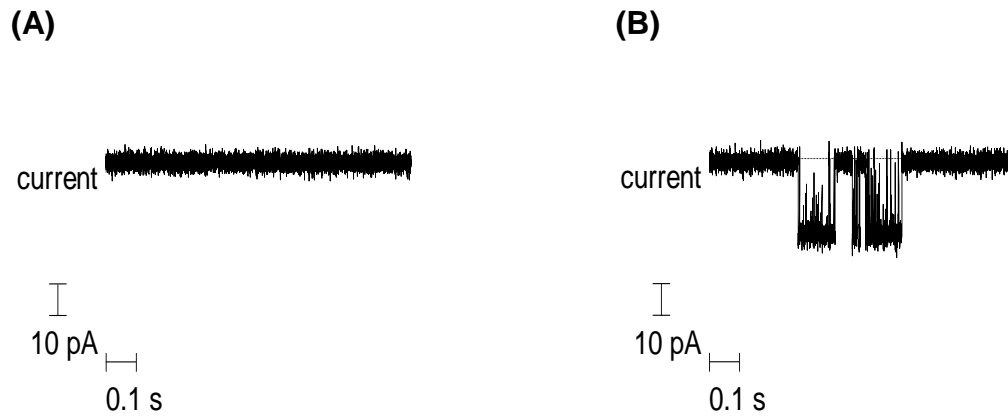


Figure 5.2.2.3.1 An example trace recording before (A) and after (B) $BK\alpha+\beta_1$ channel insertion into the prepared phospholipid bilayer. The bilayer was held at a voltage of -50 mV, and the free calcium concentration was 0.54 μM . In this recording, channel openings are characterised by downward deflections of outward current of approximately 18 pA from the current level (dashed line).

5.2.2.4 Channel orientation in the bilayer

After channel insertion, the orientation of the channel was checked. Changing the *trans* chamber to a negative voltage reduced channel openings. Changing the *trans* chamber to a positive voltage, dramatically increased channel openings demonstrating that the *trans* chamber was behaving like the intracellular compartment of a cell. Very rarely did the channels insert the wrong way round (backward orientation).

In addition, applying a positive voltage to the *trans* chamber not only makes channel opening more likely, it also gives the experimenter an idea of the number of channels in the bilayer.

5.2.2.5 Preparation and use of stock solutions

Stock solutions (1 mM or 10 mM) of each oestrogen compound were prepared in dimethylsulfoxide (DMSO). Control recordings of the single channel current were made at a holding potential of -50 mV for 150 seconds as described previously [40, 499]. After 150s of control recording was completed, 5 μ l of stock compound (5 μ M or 10 μ M final concentration) was added to the *cis* chamber of the bilayer set-up and channel activity recorded for a further 300 seconds. The *cis* chamber was stirred after application of compound at 150s and again at 300s of recording. The final DMSO concentration was less than 0.5% v/v.

Single channel current was recorded using a BLM-120 amplifier; noise was filtered at 1 kHz low pass and digitised at 25 kHz (CED, 1401 digitiser).

5.2.3 Data analysis of single channel BK current kinetics recorded in planar lipid bilayers

Single channel currents within a bilayer can provide a range of useful biophysical data. These include:-

- the unitary current size (from which, single channel conductance can be calculated),
- the average open time(s),
- the average closed time(s). However, this will be lower than the true closed time if more than one channel is present within the bilayer,

- the number of channels within the bilayer, which, in theory, can be ascertained by studying channel gating at a range of voltages. However, care needs to be exercised as apparent number can be different to the true number since :-
 - channels can be present but be existing in a long-lived closed mode and, therefore, contribute little to the recording,
 - two or more channels could be within the bilayer, but have opposite orientations. Consequently, studying channel gating at a range of voltages will underestimate the number of channels present,
 - additional channels could insert during the recording period.
- the open probability of the channels for the duration of a recording can be measured. By convention, open probability is referred to as NP_o if the number of channels is not accurately known. Here, N refers to the number of channels within the bilayer and P_o refers to the open probability for a single channel. Typically, investigators use the term NP_o because, being certain of the number of channels present is not usually possible, for the reasons given above.

5.2.3.1 Measuring open probability (NP_o)

The open probability of the BK channel or indeed, any channel of interest, is a stochastic phenomenon and the probability of the channel being in an open

state at any time point will depend on channel gating. Open probability (P_o) can be calculated from the following equation:-

$$1 - \left\{ \frac{\text{total time channel closed}}{\text{total recording time}} \right\}$$

Here, NP_o was determined rather than P_o as the number of channels in the bilayer was unknown. NP_o is calculated by dividing the total time the channel was open by the duration of the recording.

For example, if the channel opens for 1 second and, later, opens for 3 seconds with a recording lasting 10 seconds, then:-

$$NP_o = (1 \text{ s} + 3 \text{ s}) / 10 \text{ seconds}$$

$$\Rightarrow NP_o = 0.4$$

If it is certain that only one channel is present, in this example, and contributes to both openings, then the term open probability (P_o) is appropriate. However, it may be possible that two channels are present with the first opening due to channel 'A' and the second opening due to channel 'B'. If this is the case, then the most accurate term to use is NP_o . In short, P_o should only be used if the experimenter is certain of the number of channels within the bilayer.

Open times were measured by setting a transition detection threshold at 50% of the maximum current amplitude. All recordings were analysed offline using *WinEDR* v2.3.9 software.

5.2.3.2 Measuring single channel current amplitudes

The single channel current amplitude was determined in amplitude histograms fitted with a Gaussian curve. An amplitude histogram (not to be confused with a dwell time histogram) facilitates the analysis of ion channel current amplitude. This histogram can be fitted to a Gaussian curve to determine the mean current in channel open and closed states. In general, an amplitude histogram has two peaks representing channel open or closed states and the height of each histogram bin demonstrates the percentage of samples falling within the parameters of the bin. From this information, the single channel current may be calculated. Also, the area of the respective Gaussian fits can be used to calculate the NP_o .

5.2.3.3 Measuring dwell time observations

Channel open times are exponentially distributed rather than normally distributed. Dwell time histograms illustrate the distribution of channel open and closed times. Individual open times were measured by setting a transition detection threshold at 50% of the maximum current amplitude. Logarithmic dwell time histograms with variable bin widths were fitted with two exponentials for open times and three exponentials for closed times of the channels.

5.2.4 Statistical analysis of the effects of oestrogens on BK channel activity

The single channel recorded data were statistically analysed for biophysical characteristics. The volume of collected data from recordings is necessarily large; hence, analyses were undertaken using a dedicated software programme - *GraphPad Prism* version 4.00 for *Windows* (*GraphPad Software*; San Diego, California, USA).

5.2.4.1 BK channel open probability (NP_o) during 450s recordings

Statistical analysis was performed on mean NP_o data using a non-parametric Kruskal-Wallis test for one-way ANOVA with significance indicated at $p < 0.05$. Subsequently, a Dunn's *post hoc* multi comparison test for corrections was implemented. All data shown have error bars fitted according to \pm SEM. The NP_o for the first 0-150s of a recording were, thus, compared with the next 150s-300s and again with the final 300s-450s of the recording.

5.2.4.2 BK single channel current amplitude analysis

Statistical analysis was carried out on unitary currents using a one-way ANOVA followed by a *post hoc* Bonferroni correction for multiple comparisons. Significance was deemed to be significant at $p < 0.05$. Thus, the unitary current in the control period (0-150s) was compared with the unitary current recorded in the presence of oestrogens during the second 150-300s recording period and then with the final (300-450s) recording period.

5.3 RESULTS

In the previous chapter, it was shown that Oestrone, Oestrone-Oxime and Quat-DME-Oestradiol could individually enhance evoked BK currents in HEK 293 cells expressing both α and β_1 subunits. Additionally, these compounds, as well as DME-Oestrone, were able to relax pre-contracted aortic rings. In contrast, Quat-DME-Oestrone was found to be inactive in both aortic rings and patched HEK 293 cells. Examining the effects of these compounds on BK single channel currents and channel open probability (NP_o) in a planar lipid bilayer system isolates the channel from cytosolic influences and thus, will demonstrate any *direct* compound-channel association. Here, a suspension of BK channel proteins comprising α alone or $\alpha+\beta_1$ subunits was reconstituted into planar lipid bilayers to investigate directly, the effects of Oestrone and its derivatives on BK channel activity.

5.3.1 Characteristics of bilayer recording of BK α and BK $\alpha+\beta_1$ channels

Single channel currents can be recorded from bilayers after BK channels insert into the membranes. An example from a single channel recording is illustrated in Figure 5.3.1.1. An enlarged, detailed substructure of the gating events of this example trace is further illustrated in Figure 5.3.1.2.



Figure 5.3.1.1 An example of BK_{Ca} channel activity in a lipid bilayer reconstituted from synthetic phospholipids POPE and POPS (palmitoyloleoyl-phosphatidylethanolamine - and palmitoyloleoyl-phosphatidylserine, respectively, in a 1:1 ratio). The bilayer was held at a voltage of -50 mV, and the free calcium concentration was 53 μ M. The openings are characterised by a single channel current of approximately 13 pA, which corresponds to a single channel conductance of 260 pS. The channels were composed of α subunits alone.

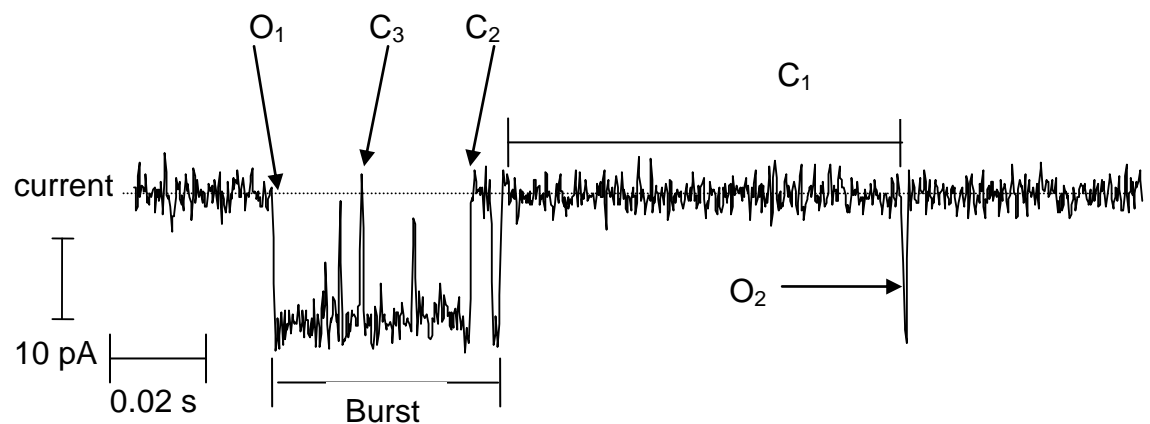


Figure 5.3.1.2 Example trace from a control recording of $BK_{\alpha+\beta_1}$ channels. The bilayer was held at a voltage of -50 mV, and the free calcium concentration was 0.54 μ M. C_1 is a long closed time after which a brief opening (O_2) is recorded. A burst, which contains a long open time (O_1) and two short closed times (C_2 , C_3), is illustrated.

The detailed substructure of the gating events illustrated in Figure 5.3.1.2 reveals a cluster of stochastic and brief open and closed states (O_1 , C_3 and

C_2), collectively known as a burst. A burst is usually separated by longer lived events, such as long closed periods, as illustrated in C_1 .

These events can be further analysed by constructing closed and open dwell time histograms illustrated in Figure 5.3.1.3 (closed dwell time) and Figure 5.3.1.4 (open dwell time). Dwell time histograms illustrate the distribution of channel open and closed times and the sequence of dwell times spent in a particular state as determined by transition detection methods.

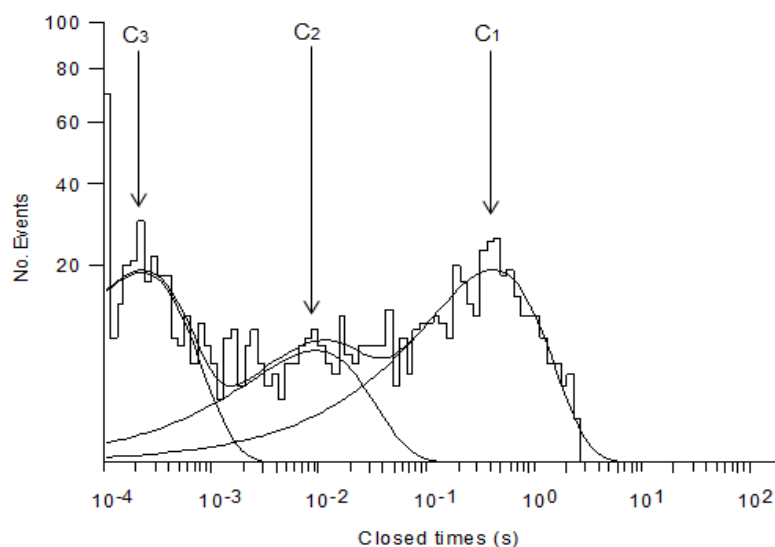


Figure 5.3.1.3 *Logarithmic closed dwell time histograms, fitted with three exponential functions, of closed time vs. number of events occurring during the control recording from BK α + β_1 channels illustrated in Figure 5.3.1.2 The recording period was 150s in duration with no added compound. The holding potential was -50 mV, and the analysis reveals 3 closed states of differing duration. The two closed times (C_3 and C_2) are within the burst duration, while the last one is consistent with the long closed state, C_1 .*

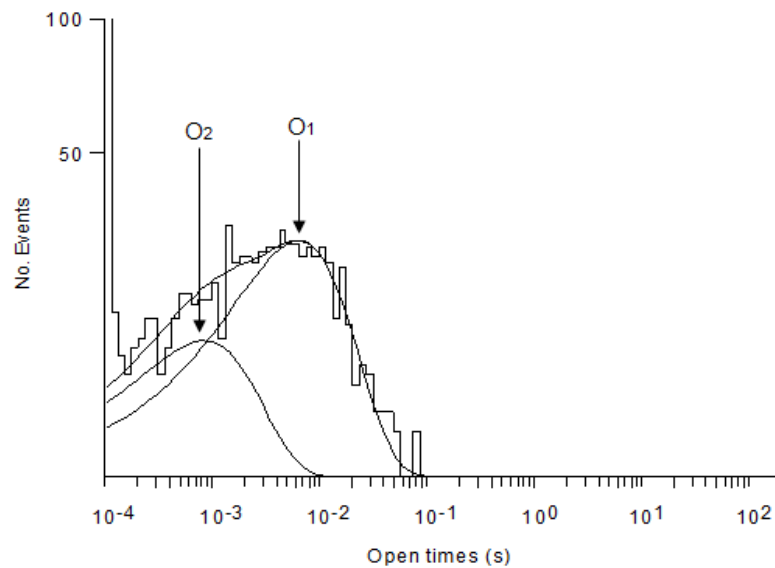


Figure 5.3.1.4 *Logarithmic open dwell time histograms, fitted with two exponential functions, of open time vs. no. of events occurring during the control recording from $BK\alpha+\beta_1$ channels illustrated in Figure 5.3.1.2. The recording period was 150s in duration with no added compound. The holding potential was -50 mV, and the analysis reveals 2 open states of differing duration within the burst. O_1 is a long open time within the burst duration and O_2 is a brief open time in the long closed time C_1 illustrated in Figures 5.3.1.2 and 5.3.1.3.*

The closed dwell time histogram in Figure 5.3.1.3 demonstrates multiple peaks corresponding to the short lived, intermediate or long lived closed events in Figure 5.3.1.2. Similarly, an open dwell time histogram relating to the two open states (O_1 and O_2) observed in Figure 5.3.1.2 is illustrated in Figure 5.3.1.4.

5.3.2 Effects of Oestrone and novel derivatives on BK channels recorded in planar lipid bilayers

Previously, Oestrone and its novel derivatives, apart from Quat-DME-Oestrone, were able to relax rat aortic rings. In whole cell recordings,

Oestrone, Quat-DME-Oestradiol and Oestrone-Oxime enhanced evoked BK currents in HEK 293 cells expressing BK α + β_1 subunits. This suggests that these Oestrogens may act through pathways involving BK α + β_1 channels. However, whole cell recordings cannot guarantee direct activation of BK channels by these compounds due to possible intracellular signalling events. Therefore, if oestrogens are able to enhance BK activity in a planar lipid bilayer system, where no intracellular cellular components can confound the data, a *direct* BK association can be inferred.

The effect of these oestrogens on the gating characteristics of BK channels in planar lipid bilayers was determined at high or low calcium, depending upon subunit configuration (54 μ M free Ca²⁺ for BK α subunits and 0.53 μ M free Ca²⁺ for BK α + β_1 subunits). All recordings were made at a holding potential of -50 mV, which is close to the resting membrane potential of smooth muscle cell (-40 mV to -50 mV) and is a potential which has been used previously to investigate BK channels reconstituted into planar lipid bilayers [40, 509, 510].

5.3.2.1 Effects of Oestrone (5 μ M) on the BK α channels in lipid bilayers

The effect of Oestrone on channel gating is illustrated in Figure 5.3.2.1.1. (Ai) and (Aii) are example traces of BK α channel activity recorded in lipid bilayers before and after the application of Oestrone (5 μ M). The average open probability of seven bilayer recordings is illustrated in (Bi) and (Bii). Each data point (Bi) represents a mean of all recordings per 30 second recording block. (Bii) compares channel activity using pooled data into larger 150 second bins.

On average the NP_o was 0.74 ± 0.24 prior to the application of Oestrone; a Kruskal-Wallis, one-way ANOVA followed by a Dunn's *post hoc* correction test for multi comparisons revealed no significant difference in NP_o after the addition of $5 \mu\text{M}$ Oestrone.

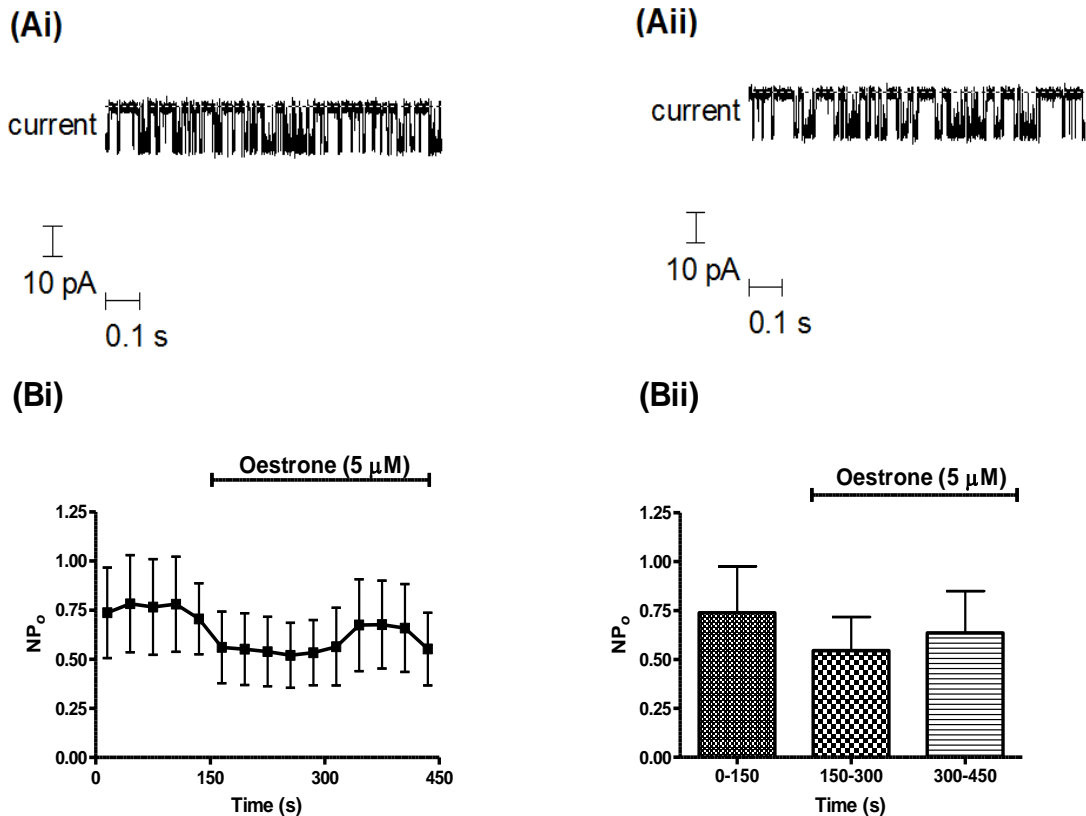


Figure 5.3.2.1.1 The effect of Oestrone ($5 \mu\text{M}$) on the NP_o of the BK channel consisting of α subunits alone. The example trace in (Ai) is taken from the first 150s of a BK α recording prior to the addition of Oestrone. Correspondingly, (Aii) shows an example trace in the presence of Oestrone. A plot of mean NP_o vs. time before (0-150 seconds), and after (150-450 seconds) the application of $5 \mu\text{M}$ Oestrone (cis side) is shown in (Bi). Subsequent grouping of the data into larger 150 second width bins is illustrated in (Bii). The application of Oestrone ($5 \mu\text{M}$) has no significant effect on BK α channel gating activity ($p > 0.05$). Recordings were made at a holding potential of -50 mV and symmetrical electrolyte solutions containing $54 \mu\text{M}$ free Ca^{2+} ($n=7$).

The effect of Oestrone (5 μM) on the unitary current of BK channels expressing only α subunits, illustrated in Figure 5.3.2.1.2, was investigated because it has been reported that xenoestrogens can affect single channel conductance [103].

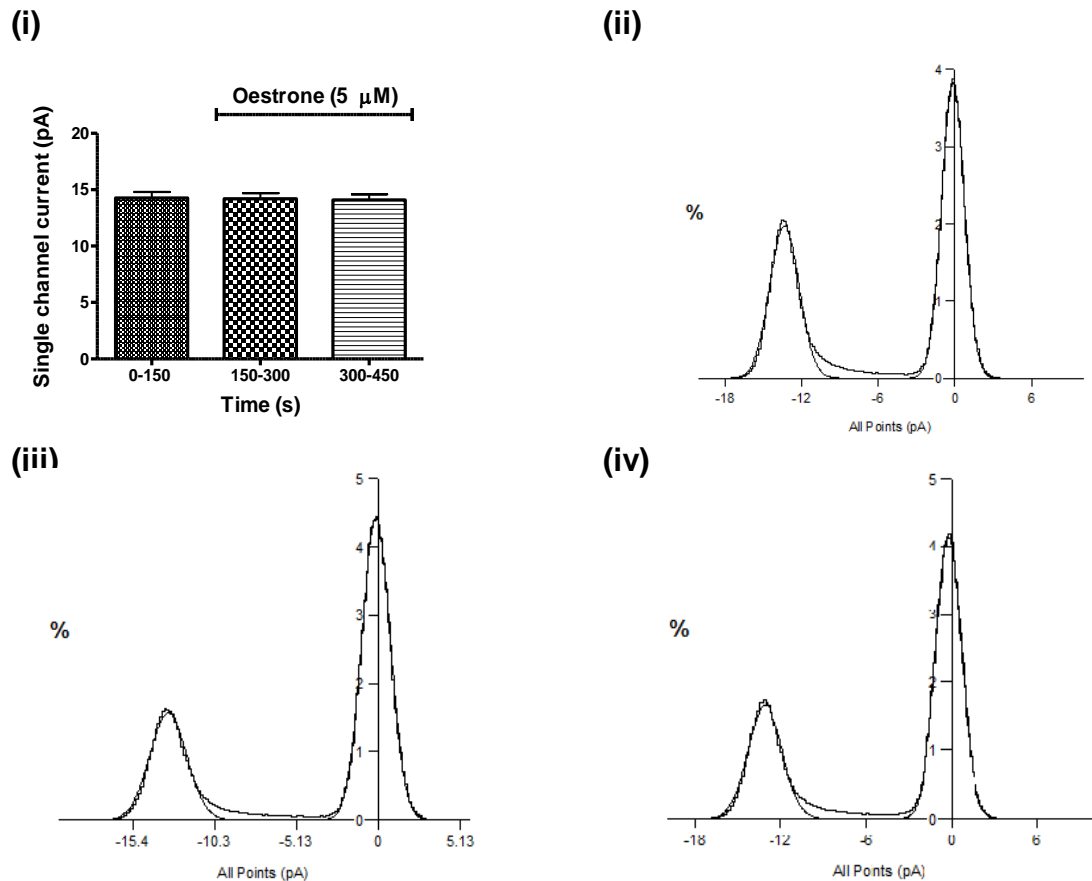


Figure 5.3.2.1.2 Graphs showing effect of Oestrone (5 μM) on the single channel current amplitude from BK α recordings. This figure demonstrates that Oestrone had no significant effect on single channel current amplitude. Plot (i) depicts a mean of single channel currents recorded in the absence or presence of Oestrone. No significant difference was observed between single channel current before and after application of compound ($p > 0.01$). The data are a mean of seven individual bilayer recordings ($n = 7$). Histograms (ii), (iii) and (iv) are constructed from a single representative bilayer recording. Plot (ii) is a representative all-points histogram of unitary currents, recorded in the absence of Oestrone (0-150 seconds) and plot (iii) in the presence of Oestrone for a further 150-300 seconds and then a further 300-450 seconds plot (iv). All recordings were held at a membrane potential of -50 mV, the free Ca^{2+} concentration was 54 μM).

Recordings could be fitted to 2 Gaussian curves and the unitary current determined. The number of Gaussian curves fitted was dependent on the number of channels within the bilayer. Figure 5.3.2.1.2 (i) shows unitary currents before (0-150s) and after (150-300s and 300-450s) application of Oestrone (5 μ M). The unitary current for the first 150 seconds prior to the addition of Oestrone was 14.25 ± 0.54 pA, which corresponds to a unitary conductance of 285 pS. There was no significant difference in unitary current after the application of Oestrone as judged by a one-way ANOVA followed by a Bonferroni *post hoc* correction test for multi comparisons ($p > 0.05$). Figure 5.3.2.1.2 (ii) (iii) and (iv) is an example of a single channel current amplitude histogram taken from a single bilayer recording of BK α channels before and after the application of Oestrone (5 μ M). The histogram examples show two peaks demonstrating at least one channel has inserted into this bilayer.

To summarise, Oestrone (5 μ M) did not alter the NP_o of the BK α channels. In addition, Oestrone did not change the single channel current and consequently, the single channel conductance. This is similar to reports for oestradiol in planar lipid bilayers which have shown that a β_1 subunit is required for BK activation [40].

5.3.2.2 Effects of Oestrone (5 μ M) on BK channels comprising α plus β_1 subunits in planar lipid bilayers

Data in Chapter 4 indicated that Oestrone was a weak activator of BK currents in whole cell recordings taken from HEK 293 cells expressing BK $\alpha + \beta_1$ subunits. Unless these effects were due to second messenger systems being

acutely activated by oestrogens, it would be reasonable to expect to record a similar activation here in a planar lipid bilayer system.

The effect of Oestrone on channel gating is illustrated in Figure 5.3.2.2.1. (Ai) and Aii are example traces of BK α + β_1 channel activity recorded in lipid bilayers before and after the application of Oestrone (5 μ M). The average open probability of six bilayer recordings is illustrated in (Bi) and (Bii). Each data point (Bi) represents a mean of all recordings per 30 second recording block. (Bii) compares channel activity using pooled data into larger 150 second bins.

On average the NP_o was 0.1 \pm 0.02 prior to the application of Oestrone. This significantly increased with the addition of 5 μ M Oestrone, increasing to 0.14 \pm 0.04 during the first 150 seconds and 0.18 \pm 0.05 for the last 150 seconds.

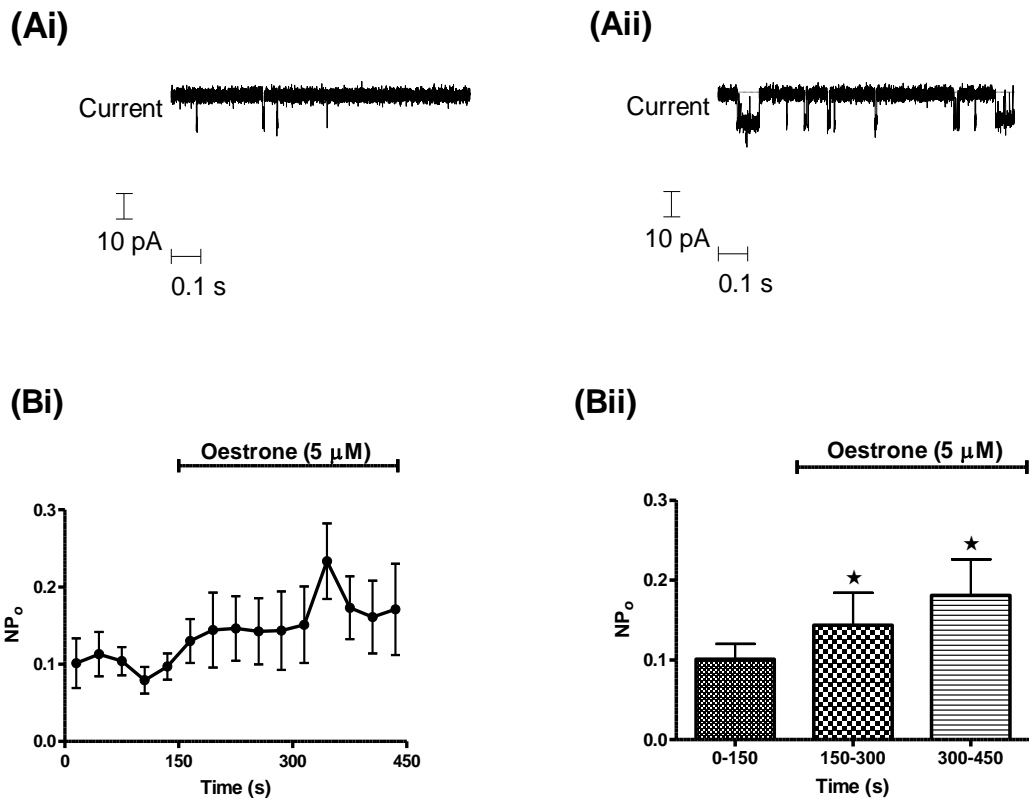


Figure 5.3.2.2.1 The effect of Oestrone (5 μM) on the NPo of the BK channel consisting of α and β_1 subunits. The example trace in (Ai) is taken from the first 150s of a $\text{BK}\alpha+\beta_1$ recording prior to the addition of Oestrone. Correspondingly, (Aii) shows an example trace in the presence of Oestrone. A plot of mean NPo vs. time before (0-150 seconds), and after (150-450 seconds) the application of 5 μM Oestrone (cis side) is shown in (Bi). Subsequent grouping of the data into larger 150 second width bins is illustrated in (Bii). The application of Oestrone (5 μM) significantly increased NPo of $\text{BK}\alpha+\beta_1$ ($p<0.05$). All recordings were made at a holding potential of -50 mV and symmetrical electrolyte solutions containing 0.53 μM free Ca^{2+} ($n=6$).

The effect of Oestrone (5 μM) on the unitary current of BK channels expressing both α and β_1 subunits, illustrated in Figure 5.3.2.2.2, was investigated to examine the possibility of increased/decreased unitary current that has been previously reported [103].

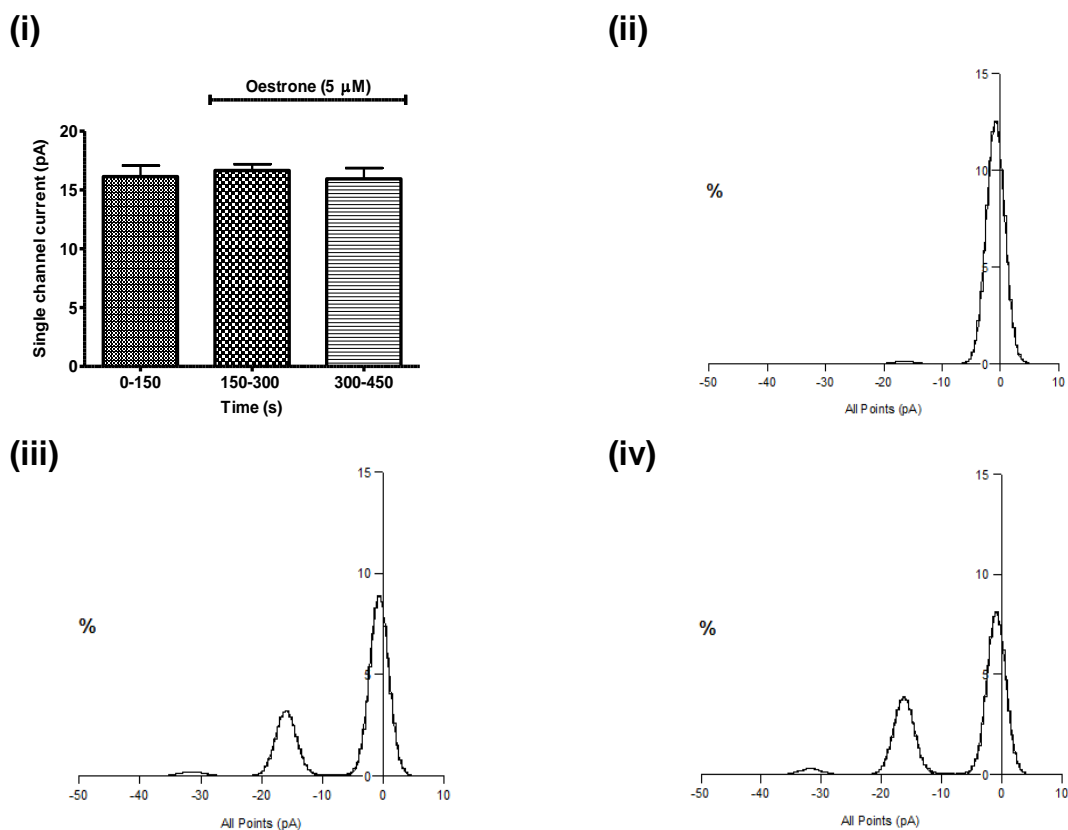


Figure 5.3.2.2 Graphs showing effect of Oestrone (5 μM) on the single channel current amplitude of $\text{BK}\alpha+\beta_1$ channels. This figure demonstrates that Oestrone had no significant effect on single channel current amplitude. Plot (i) depicts a mean of single channel currents recorded in the absence or presence of Oestrone. No significant difference was observed between single channel current before and after application of compound ($p>0.05$). The data are a mean of six individual bilayer recordings ($n=6$). Histograms (ii), (iii) and (iv) are constructed from a single representative bilayer recording. Plot (ii) is a representative all-points histogram of unitary currents, recorded in the absence of Oestrone (0-150 seconds) and plot (iii) in the presence of 5 μM Oestrone for a further 150-300 seconds and then a further 300-450 seconds plot (iv). All recordings were held at a membrane potential of -50 mV, the free Ca^{2+} concentration was 0.53 μM .

Recordings could be fitted to two or three Gaussian curves and the unitary current determined. The number of Gaussian curves fitted was dependent on the number of channels within the bilayer. Figure 5.3.2.2 (i) shows unitary currents before (0-150s) and after (150-300s and 300-450s) application of

Oestrone (5 μM). The unitary current for the first 150 seconds prior to the addition of Oestrone was 16.13 pA \pm 0.93, which corresponds to a unitary conductance of 322.6 pS. There was no significant difference in unitary current after the application of Oestrone as judged by a one-way ANOVA followed by a Bonferroni *post hoc* correction test for multi comparisons ($p > 0.05$). Figure 5.3.2.2.2 (ii) (iii) and (iv) is an example of a single channel current amplitude histogram taken from a single bilayer recording of BK α + β_1 channels before and after the application of Oestrone (5 μM).

Interestingly, although the addition of Oestrone did not affect the single channel conductance, the area of the closed example histogram plot decreases after application of compound. In addition, a second channel has become apparent in the amplitude histogram after application of Oestrone, due to channel activation.

To summarise, Oestrone (5 μM) was able to increase the open probability of BK α + β_1 channels. This novel finding concurs with other researchers who have demonstrated oestradiol-enhanced activation of BK channels in planar lipid bilayers when the β_1 subunit is present [40]. Furthermore, Oestrone did not change the single channel current and consequently, the single channel conductance.

5.3.2.3 Effects of high concentrations of Oestrone (50 μ M) on BK α channels in lipid bilayers

BK α channels did not respond to an application of 5 μ M Oestrone in bilayers and NP_o remained unchanged. To check that BK channels comprising only α subunits are indeed insensitive to Oestrone, a much higher concentration of Oestrone (50 μ M) was applied.

The effect of Oestrone (50 μ M) on channel gating is illustrated in Figure 5.3.2.3.1. Ai and Aii are example traces of BK α channel activity recorded in lipid bilayers before and after the application of Oestrone. The average NP_o of six bilayer recordings is illustrated in (Bi) and (Bii). Each data point in (Bi) represents a mean of all recordings per 30 second recording block. (Bii) compares channel activity using pooled data into larger 150 second bins.

On average the NP_o was 0.86 ± 0.40 prior to the application of Oestrone; a Kruskal-Wallis, one-way ANOVA followed by a Dunn's *post hoc* correction test for multi comparisons revealed no significant difference in NP_o after the addition of 50 μ M Oestrone in BK α channels.

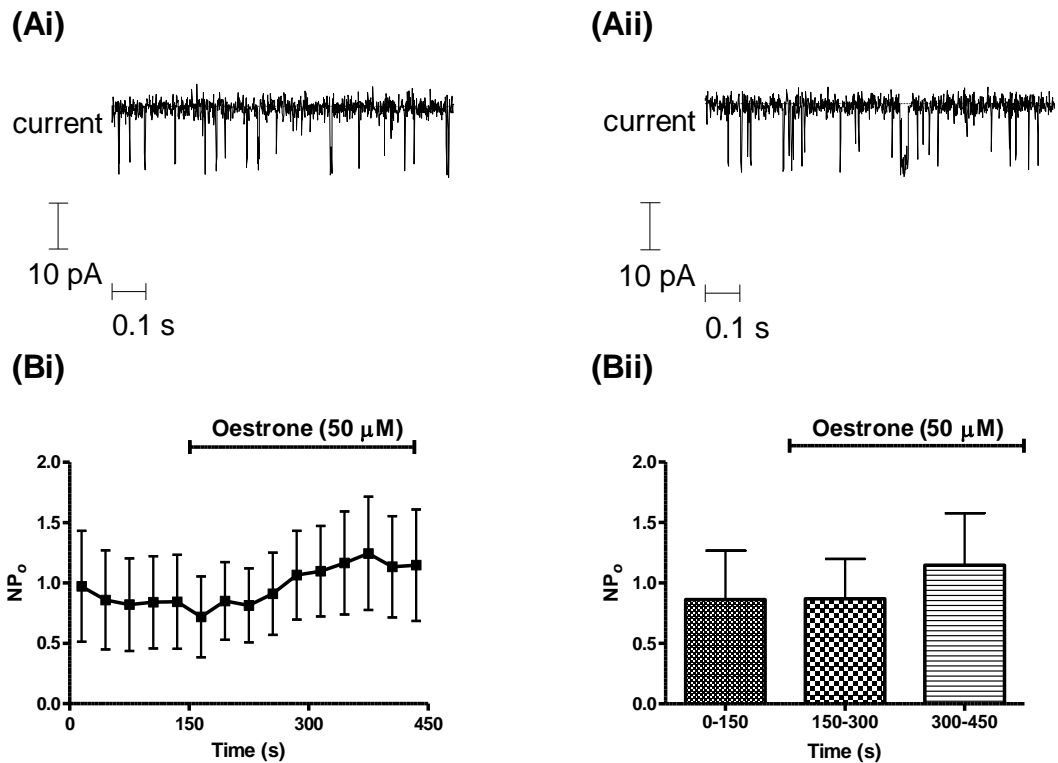


Figure 5.3.2.3.1 The effect of Oestrone (50 μM) on the NP_o of the BK channel consisting of only α subunits. The example trace in (Ai) is taken from the first 150s of a BK α recording prior to the addition of Oestrone. Correspondingly, (Aii) shows an example trace in the presence of Oestrone. A plot of mean NP_o vs. time before (0-150 seconds), and after (150-450 seconds) the application of 50 μM Oestrone (cis side) is shown in (Bi). Subsequent grouping of the data into larger 150 second width bins is illustrated in (Bii). The application of Oestrone (50 μM) has no significant effect on BK α channel gating activity ($p > 0.05$). All recordings were held at a membrane potential of -50 mV, the free Ca^{2+} concentration was 54 μM , ($n=6$).

The effect of Oestrone (50 μM) on the unitary current of BK channels expressing α subunits alone was investigated as before. Recordings could be fitted to two Gaussian curves and the unitary current determined. The number of Gaussian curves fitted was dependent on the number of channels within the bilayer.

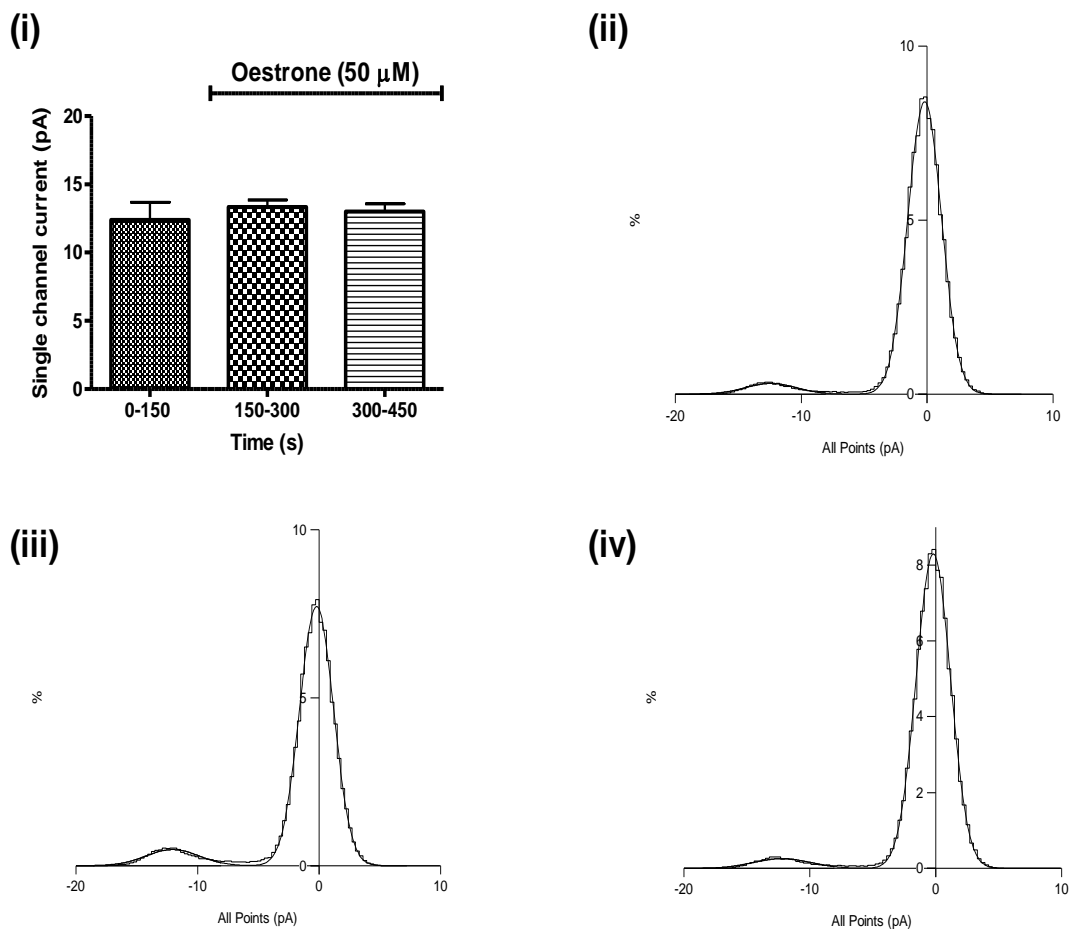


Figure 5.3.2.3.2 Graphs showing effect of Oestrone (50 μM) on the single channel current amplitude of BK α channels. This figure demonstrates that Oestrone had no significant effect on single channel current amplitude. Plot (i) depicts a mean of single channel currents recorded in the absence or presence of Oestrone. No significant difference was observed between single channel current before and after application of compound ($p > 0.05$). The data are a mean of six individual bilayer recordings ($n = 6$). Histograms (ii), (iii) and (iv) are constructed from a single representative bilayer recording. Plot (ii) is a representative all-points histogram of unitary currents, recorded in the absence of Oestrone (0-150 seconds) and plot (iii) in the presence of 50 μM Oestrone for a further 150-300 seconds and then a further 300-450 seconds plot (iv). All recordings were held at a membrane potential of -50 mV, the free Ca^{2+} concentration was 54 μM .

Figure 5.3.2.3.2 (i) shows unitary currents before (0-150s) and after (150-300s and 300-450s) application of Oestrone (50 μM). The unitary current for the first 150 seconds prior to the addition of Oestrone was 12.39 ± 1.3 pA which

corresponds to a unitary conductance of 247.8 pS. There was no significant difference in unitary current after the application of Oestrone as judged by a one-way ANOVA followed by a Bonferroni *post hoc* correction test for multi comparisons ($p>0.05$). Figure 5.3.2.3.2 (ii) (iii) and (iv) is an example of a single channel current amplitude histogram taken from a single bilayer recording of BK α channels before and after the application of Oestrone (50 μ M).

To summarise, Oestrone (50 μ M) did not alter the NP_o of the BK α channels. In addition, Oestrone did not change the single channel current and consequently, the single channel conductance.

5.3.2.4 Effects of high concentrations of Oestrone (50 μ M) on BK channels comprising both α plus β_1 subunits in lipid bilayers

To investigate whether the increase in NP_o observed in BK α + β_1 channels after application of 5 μ M Oestrone is also true for higher concentrations, a 50 μ M concentration of Oestrone was examined.

The effect of Oestrone (50 μ M) on channel gating is illustrated in Figure 5.3.2.4.1. (Ai) and (Aii) are example traces of BK α + β_1 channel activity recorded in lipid bilayers before and after the application of Oestrone. The average NP_o of five bilayer recordings is illustrated in (Bi) and (Bii). Each data point in (Bi) represents a mean of all recordings per 30 second recording block. (Bii) compares channel activity using pooled data into larger 150 second bins.

On average, the NP_o was 0.09 ± 0.03 prior to the application of Oestrone; although gating activity appears to decrease after the addition of $50 \mu\text{M}$ oestrone at 150 seconds, a Kruskal-Wallis, one-way ANOVA followed by a *post hoc* Dunn's correction test for multi comparisons revealed no significant difference in NP_o post application of Oestrone.

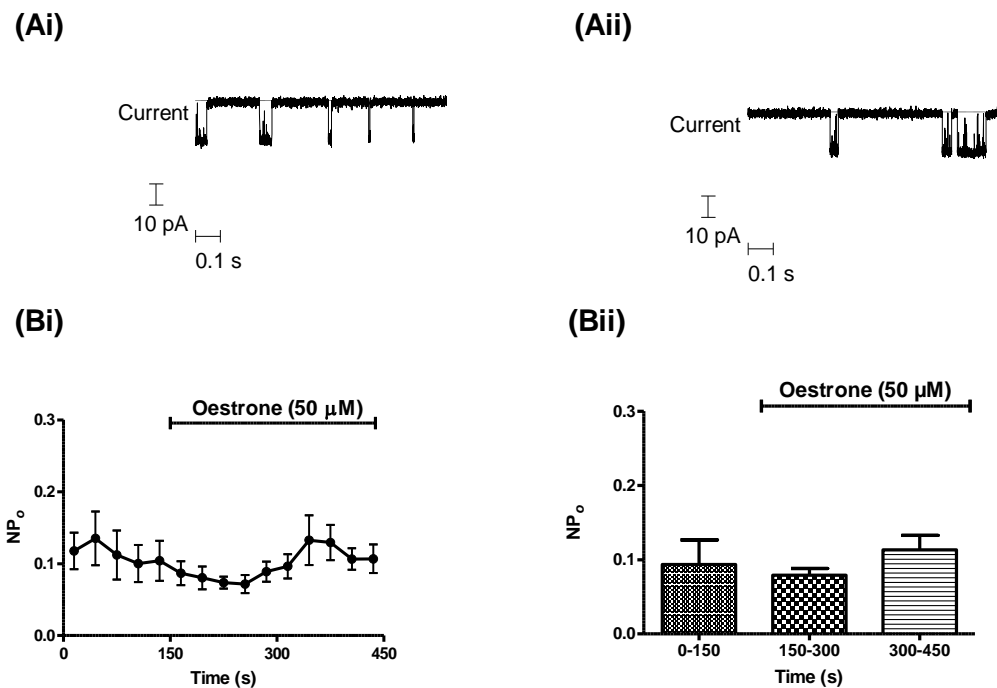


Figure 5.3.2.4.1 The effect of Oestrone ($50 \mu\text{M}$) on the NP_o of the BK channel consisting of α plus β_1 subunits. The example trace in (Ai) is taken from the first 150s of a $BK\alpha+\beta_1$ recording prior to the addition of Oestrone. Correspondingly, (Aii) shows an example trace in the presence of Oestrone ($50 \mu\text{M}$). A plot of mean NP_o vs. time before (0-150 seconds), and after (150-450 seconds) the application of $50 \mu\text{M}$ Oestrone (*cis side*) is shown in (Bi). Subsequent grouping of the data into larger 150 second width bins is illustrated in (Bii). The application of Oestrone ($50 \mu\text{M}$) has no significant effect on $BK\alpha+\beta_1$ channel gating activity ($p>0.05$). Recordings were made at a holding potential of -50 mV and symmetrical electrolyte solutions containing $0.53 \mu\text{M}$ free Ca^{2+} ($n=5$).

The effect of Oestrone ($50 \mu\text{M}$) on the unitary current of BK channels expressing both α and β_1 subunits was investigated (Figure 5.3.2.4.2).

Recordings could be fitted to two Gaussian curves and the unitary current determined. The number of Gaussian curves fitted was dependent on the number of channels within the bilayer.

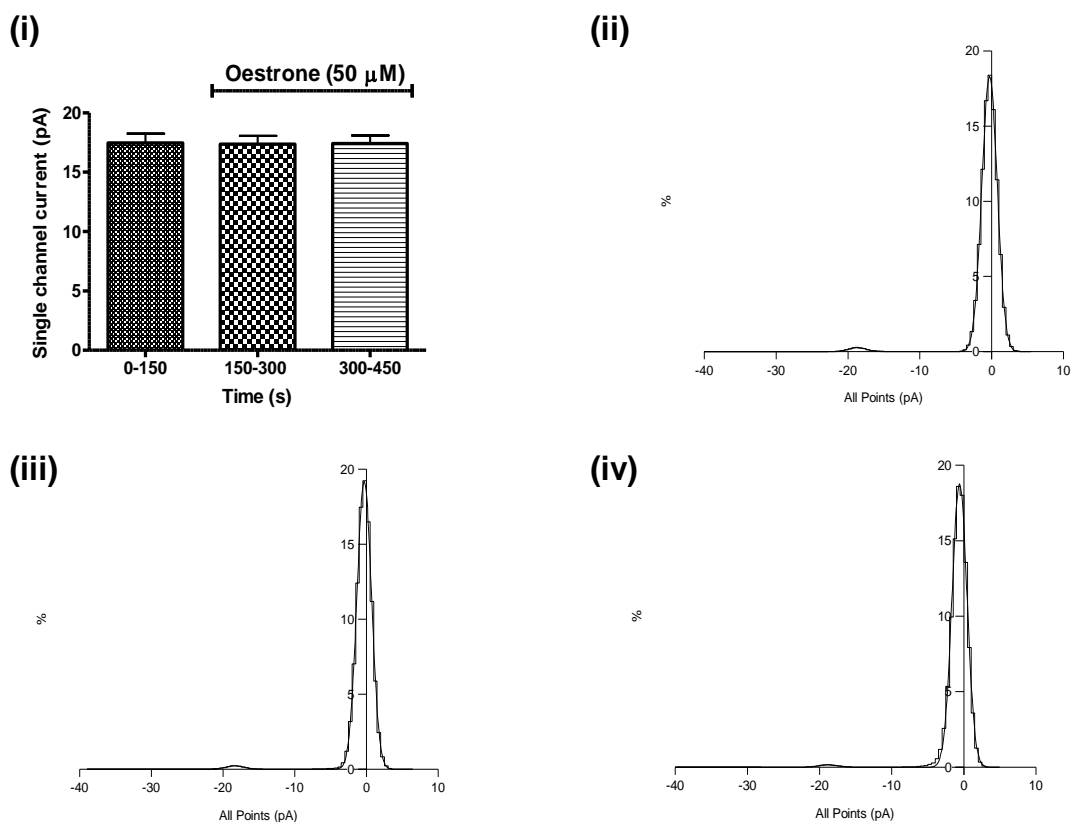


Figure 5.3.2.4.2 *Graphs showing effect of Oestrone (50 μM) on the single channel current of the BK channel consisting of α plus β_1 subunits. This figure demonstrates that Oestrone had no significant effect on single channel current amplitude. Plot (i) depicts a mean of single channel currents recorded in the absence or presence of Oestrone. No significant difference was observed between single channel current before and after application of compound ($p > 0.05$). The data are a mean of five individual bilayer recordings ($n=5$). Histograms (ii), (iii) and (iv) are constructed from a single representative bilayer recording. Plot (ii) is a representative all-points histogram of unitary currents, recorded in the absence of Oestrone (0-150 seconds) and plot (iii) in the presence of 50 μM Oestrone for a further 150-300 seconds and then a further 300-450 seconds plot (iv). All recordings were held at a membrane potential of -50 mV, the free Ca^{2+} concentration was 0.53 μM.*

Figure 5.3.2.4.2 (i) shows unitary currents before (0-150s) and after (150-300s and 300-450s) application of Oestrone (50 μM). The unitary current for the

first 150 seconds prior to the addition of Oestrone was $17.46 \text{ pA} \pm 0.78$, which corresponds to a unitary conductance of 349.2 pS . There was no significant difference in unitary current after the application of Oestrone as judged by a one-way ANOVA followed by a Bonferroni *post hoc* correction test for multi comparisons ($p > 0.05$). Figure 5.3.2.4.2 (ii) (iii) and (iv) is an example of a single channel current amplitude histogram taken from a single bilayer recording of BK α + β_1 channels before and after the application of Oestrone ($50 \text{ }\mu\text{M}$).

To summarise, unlike experiments applying $5 \text{ }\mu\text{M}$ Oestrone, a higher concentration of Oestrone ($50 \text{ }\mu\text{M}$) did not alter the NP_o of the BK α + β_1 channels. Also, the single channel current and consequently, the single channel conductance remained unaltered.

5.3.3 Effects of DME-Oestrone on BK channels recorded in lipid bilayers

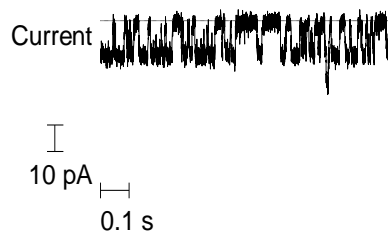
This section characterises the BK channel reconstituted into planar lipid bilayers, in the presence of different concentrations of DME-Oestrone. Previous chapters have determined DME-Oestrone was able to relax rat aortic rings but was inactive in cells expressing BK channels, suggesting this compound may act through a second messenger pathway or other intracellular mechanism. If this is the case, it would be reasonable to expect the compound to be inactive in planar lipid bilayer experiments where no cellular components can confound the data. Recordings were carried out, as before, at high or low calcium, depending upon subunit configuration ($54 \text{ }\mu\text{M}$ free Ca^{2+}

for BK α subunits and 0.53 μM free Ca²⁺ for BK $\alpha+\beta_1$ subunits) and at a holding potential of -50 mV.

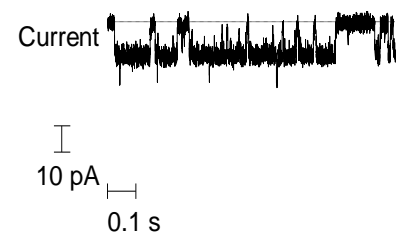
5.3.3.1 Effects of DME-Oestrone (5 μM) on BK α channels in lipid bilayers

The effect of DME-Oestrone on channel gating is illustrated in Figure 5.3.3.1.1. (Ai) and (Aii) are example traces of BK α channel activity recorded in lipid bilayers before and after the application of DME-Oestrone (5 μM). The average open probability of five bilayer recordings is illustrated in (Bi) and (Bii). Each data point in (Bi) represents a mean of all recordings per 30 second recording block. (Bii) compares channel activity using pooled data into larger 150 second bins.

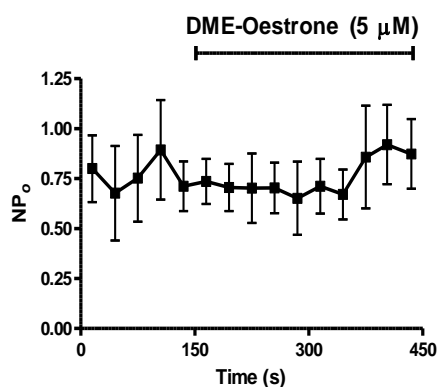
(Ai)



(Aii)



(Bi)



(Bii)

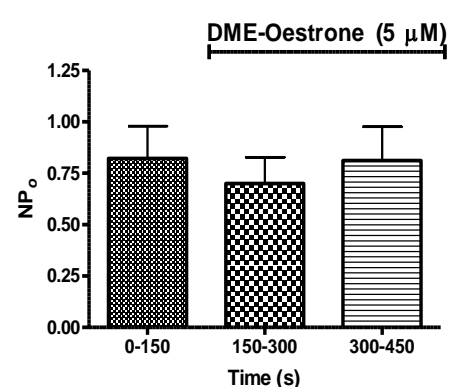


Figure 5.3.3.1.1 The effect of DME-Oestrone (5 μ M) on the NP_o of the BK channel consisting of α subunits alone. The example trace in (Ai) is taken from the first 150s of a BK α recording prior to the addition of DME-Oestrone. Correspondingly, (Aii) shows an example trace in the presence of DME-Oestrone (5 μ M). A plot of mean NP_o vs. time before (0-150 seconds), and after (150-450 seconds) the application of 5 μ M DME-Oestrone (cis side) is shown in (Bi). Subsequent grouping of the data into larger 150 second width bins is illustrated in (Bii). The application of DME-Oestrone (5 μ M) has no significant effect on BK α channel gating activity ($p > 0.05$). Recordings were made at a holding potential of -50 mV and symmetrical electrolyte solutions containing 54 μ M free Ca²⁺ ($n=5$).

On average the NP_o was 0.82 ± 0.16 prior to the application of DME-Oestrone; a Kruskal-Wallis, one-way ANOVA followed by a Dunn's *post hoc* correction test for multi comparisons revealed no significant difference in NP_o after the addition of 5 μ M DME-Oestrone ($p > 0.05$).

The effect of DME-Oestrone ($5 \mu\text{M}$) on the unitary current of BK channels expressing only α subunits was investigated (Figure 5.3.3.1.2). Recordings could be fitted to three Gaussian curves and the unitary current determined. The number of Gaussian curves fitted was dependent on the number of channels within the bilayer.

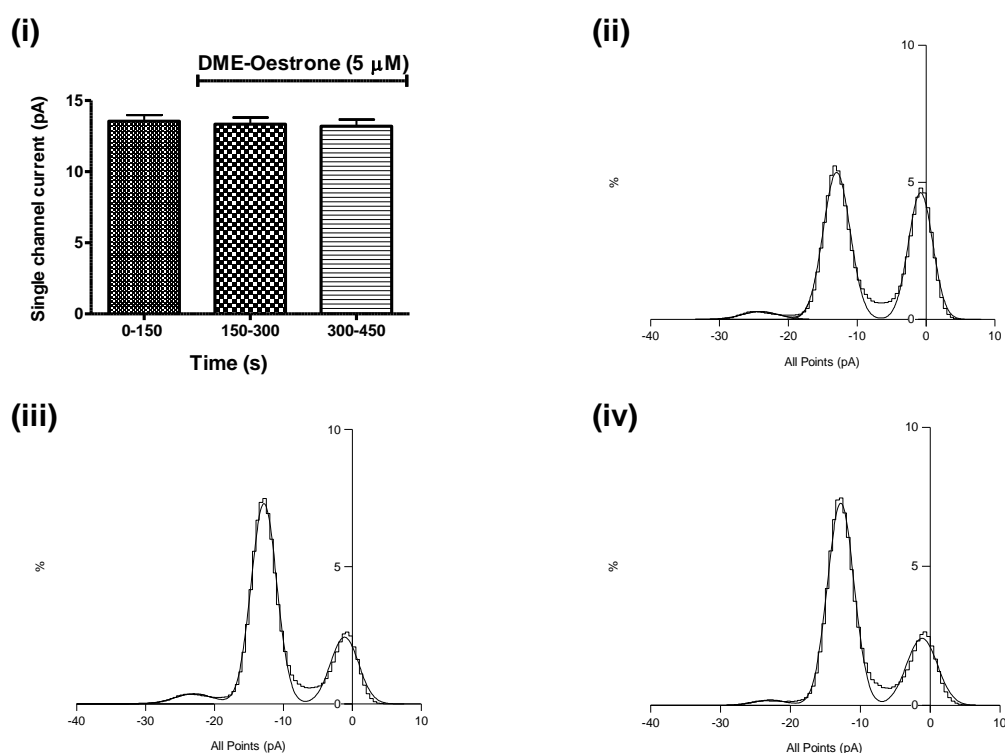


Figure 5.3.3.1.2 Graphs showing effect of DME-Oestrone ($5 \mu\text{M}$) on the single channel current of the BK channel consisting of α subunits alone. This figure demonstrates that DME-Oestrone had no significant effect on single channel current amplitude. Plot (i) depicts a mean of single channel currents recorded in the absence or presence of DME-Oestrone. No significant difference was observed between single channel current before and after application of compound ($p > 0.05$). The data are a mean of five individual bilayer recordings ($n=5$). Histograms (ii), (iii) and (iv) are constructed from a single representative bilayer recording. Plot (ii) is a representative all-points histogram of unitary currents, recorded in the absence of DME-Oestrone (0-150 seconds) and plot (iii) in the presence of $5 \mu\text{M}$ DME-Oestrone for a further 150-300 seconds and then a further 300-450 seconds plot (iv). All recordings were held at a membrane potential of -50 mV , the free Ca^{2+} concentration was $54 \mu\text{M}$.

Figure 5.3.3.1.2 (i) shows unitary currents before (0-150s) and after (150-300s and 300-450s) application of DME-Oestrone (5 μ M). The unitary current for the first 150 seconds prior to the addition of DME-Oestrone was $13.55 \text{ pA} \pm 0.43$, which corresponds to a unitary conductance of 271 pS. There was no significant difference in unitary current after the application of DME-Oestrone as judged by a one-way ANOVA followed by a Bonferroni *post hoc* correction test for multi comparisons ($p > 0.05$). Figure 5.3.3.1.2 (ii) (iii) and (iv) is an example of a single channel current amplitude histogram taken from a single bilayer recording of BK α channels before and after the application of DME-Oestrone (5 μ M). With three Gaussian curves, two channels or more have inserted into this bilayer.

To summarise, as expected, DME-Oestrone (5 μ M) did not alter the NP_o of the BK α channels. In addition, the single channel current and consequently, the single channel conductance remained unaltered.

5.3.3.2 Effects of DME-Oestrone (5 μ M) on the NP_o of BK α + β ₁ channels in lipid bilayers

The effect of DME-Oestrone on channel gating is illustrated in Figure 5.3.3.2.1. (Ai) and (Aii) are example traces of BK α + β ₁ channel activity recorded in lipid bilayers before and after the application of DME-Oestrone (5 μ M). These traces illustrate that there are at least two channels present in the bilayer. The average open probability of eight bilayer recordings is illustrated in (Bi) and (Bii). Each data point in (Bi) represents a mean of all recordings

per 30 second recording block. (Bii) compares channel activity using pooled data into larger 150 second bins.

On average the NP_o was 0.38 ± 0.08 prior to the application of DME-Oestrone; a Kruskal-Wallis, one-way ANOVA followed by a Dunn's *post hoc* correction test for multi comparisons revealed no significant difference in NP_o after the addition of $5 \mu\text{M}$ DME-Oestrone in $\text{BK}\alpha+\beta_1$ channels ($p>0.05$).

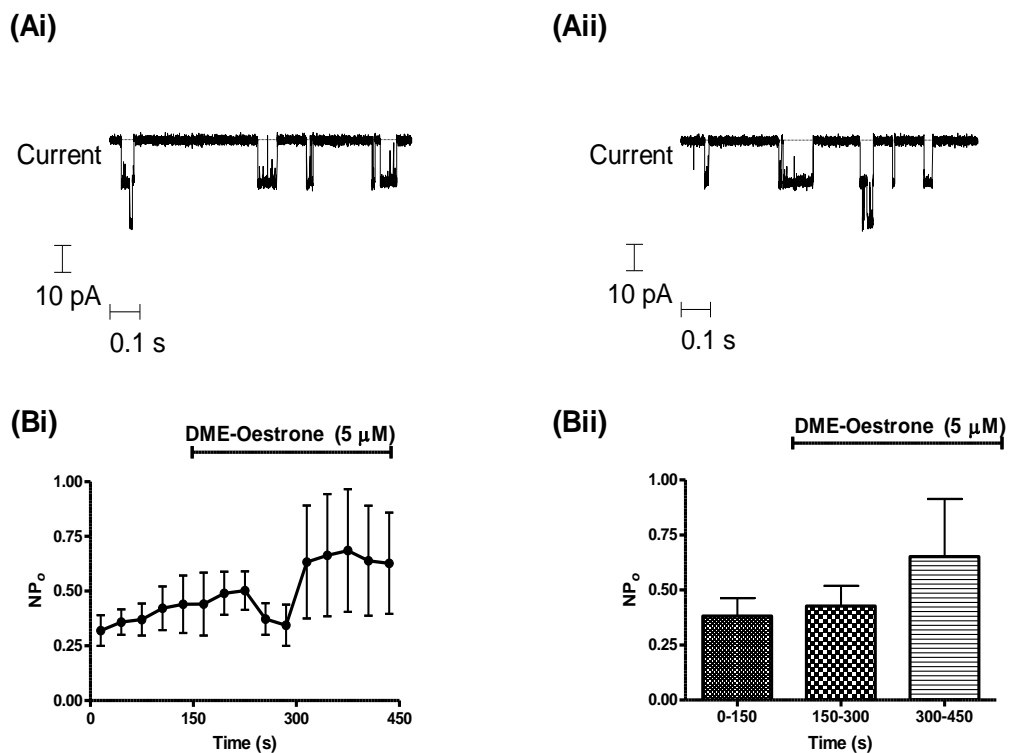


Figure 5.3.3.2.1 The effect of DME-Oestrone ($5 \mu\text{M}$) on the NP_o of the BK channel consisting of α and β_1 subunits. The example trace in (Ai) is taken from the first 150s of a $\text{BK}\alpha+\beta_1$ recording prior to the addition of DME-Oestrone. Correspondingly, (Aii) shows an example trace in the presence of DME-Oestrone ($5 \mu\text{M}$). A plot of mean NP_o vs. time before (0-150 seconds), and after (150-450 seconds) the application of $5 \mu\text{M}$ DME-Oestrone (*cis side*) is shown in (Bi). Subsequent grouping of the data into larger 150 second width bins is illustrated in (Bii). The application of DME-Oestrone ($5 \mu\text{M}$) has no significant effect on $\text{BK}\alpha+\beta_1$ channel gating activity ($p>0.05$). All recordings were made at a holding potential of -50 mV and symmetrical electrolyte solutions containing $0.53 \mu\text{M}$ free Ca^{2+} ($n=8$).

The effect of DME-Oestrone ($5 \mu\text{M}$) on the unitary current of BK channels expressing both α and β_1 subunits was investigated. Recordings could be fitted to two or three Gaussian curves and the unitary current determined. The number of Gaussian curves fitted was dependent on the number of channels within the bilayer.

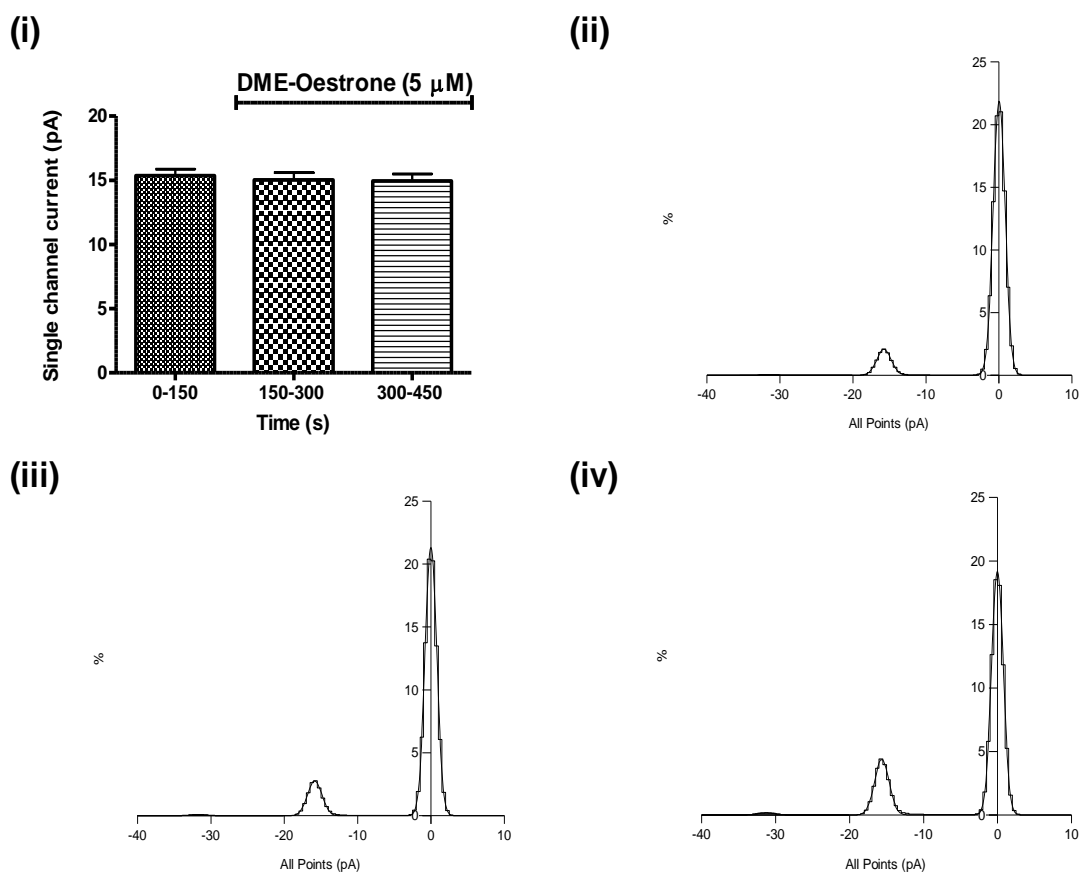


Figure 5.3.3.2.2 Graphs showing effect of DME-Oestrone ($5 \mu\text{M}$) on the single channel current amplitude of $\text{BK}\alpha+\beta_1$ channels. This figure demonstrates that DME-Oestrone had no significant effect on single channel current amplitude. Plot (i) depicts a mean of single channel currents recorded in the absence or presence of DME-Oestrone. No significant difference was observed between single channel current before and after application of compound ($p>0.05$). The data are a mean of eight individual bilayer recordings ($n=8$). Histograms (ii), (iii) and (iv) are constructed from a single representative bilayer recording. Plot (ii) is a representative all-points histogram of unitary currents, recorded in the absence of DME-Oestrone (0-150 seconds) and plot (iii) in the presence of $5 \mu\text{M}$ DME-Oestrone for a further 150-300 seconds and then a further 300-450 seconds plot (iv). All recordings were held at a membrane potential of -50 mV , the free Ca^{2+} concentration was $0.53 \mu\text{M}$.

Figure 5.3.3.2.2 (i) shows unitary currents before (0-150s) and after (150-300s and 300-450s) application of DME-Oestrone (5 μ M). The unitary current for the first 150 seconds prior to the addition of DME-Oestrone was 15.35 pA \pm 0.52 which corresponds to a unitary conductance of 307 pS. There was no significant difference in unitary current after the application of DME-Oestrone as judged by a one-way ANOVA followed by a Bonferroni *post hoc* correction test for multi comparisons ($p > 0.05$). Figure 5.3.3.2.2 (ii) (iii) and (iv) is an example of a single channel current amplitude histogram taken from a single bilayer recording of BK α + β_1 channels before and after the application of DME-Oestrone (5 μ M). Although two BK channels are clearly demonstrated in the control period in the example amplitude histogram (ii), after the application of compound the channel goes quiet and appears to have switched to a long closed period (iii) only to reactivate during the last 150s recording period (iv).

To summarise, unlike Oestrone, DME-Oestrone (5 μ M) did not alter the NP_o of the BK α + β_1 channels. In addition, the single channel current and consequently, the single channel conductance remained unaltered.

5.3.3.3 Effects of high concentrations of DME-Oestrone (50 μ M) on BK α channels in lipid bilayers

Previously, BK α channels did not respond to an application of 5 μ M DME-Oestrone in bilayers and NP_o remained unchanged. To further check that BK α channels are indeed insensitive to DME-Oestrone, a much higher concentration of DME-Oestrone (50 μ M) was applied.

The effect of DME-Oestrone (50 μ M) on channel gating is illustrated in Figure 5.3.3.3.1. (Ai) and (Aii) are example traces of BK α channel activity recorded in lipid bilayers before and after the application of DME-Oestrone. The traces reveal, during this recording, at least two or three BK channels have inserted into the bilayer. The average NP_o of six bilayer recordings is illustrated in (Bi) and (Bii). Each data point in (Bi) represents a mean of all recordings per 30 second recording block. (Bii) compares channel activity using pooled data into larger 150 second bins.

On average the NP_o was 0.31 ± 0.15 prior to the application of DME-Oestrone; a Kruskal-Wallis, one-way ANOVA followed by a Dunn's *post hoc* correction test for multi comparisons revealed no significant difference in NP_o after the addition of 50 μ M DME- Oestrone in BK α channels.

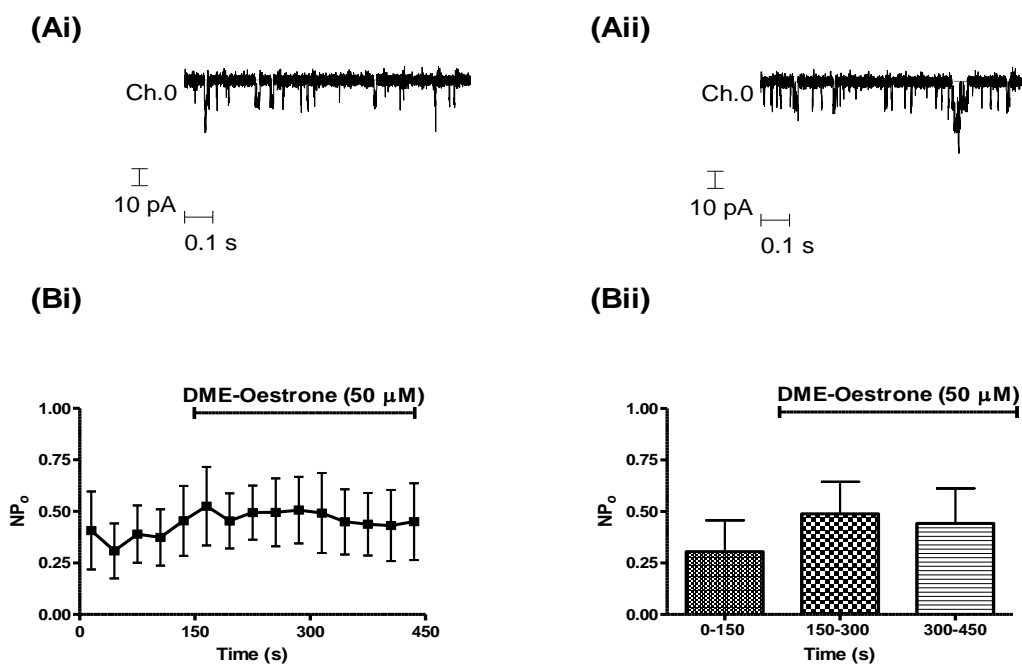


Figure 5.3.3.1 The effect of DME-Oestrone (50 μM) on the NP_o of the BK channel consisting of only α subunits. The example trace in (Ai) is taken from the first 150s of a BKα recording prior to the addition of DME-Oestrone. Correspondingly, (Aii) shows an example trace in the presence of DME-Oestrone (50 μM). A plot of mean NP_o vs. time before (0-150 seconds), and after (150-450 seconds) the application of 50 μM DME-Oestrone (cis side) is shown in (Bi). Subsequent grouping of the data into larger 150 second width bins is illustrated in (Bii). The application of DME-Oestrone (50 μM) has no significant effect on BKα channel gating activity ($p>0.05$). All recordings were held at a membrane potential of -50 mV, the free Ca²⁺ concentration was 54 μM, (n=6).

The effect of DME-Oestrone (50 μM), illustrated in Figure 5.3.3.2, on the unitary current of BKα channels was investigated. Recordings could be fitted to three or four Gaussian curves and the unitary current determined. The number of Gaussian curves fitted was dependent on the number of channels within the bilayer.

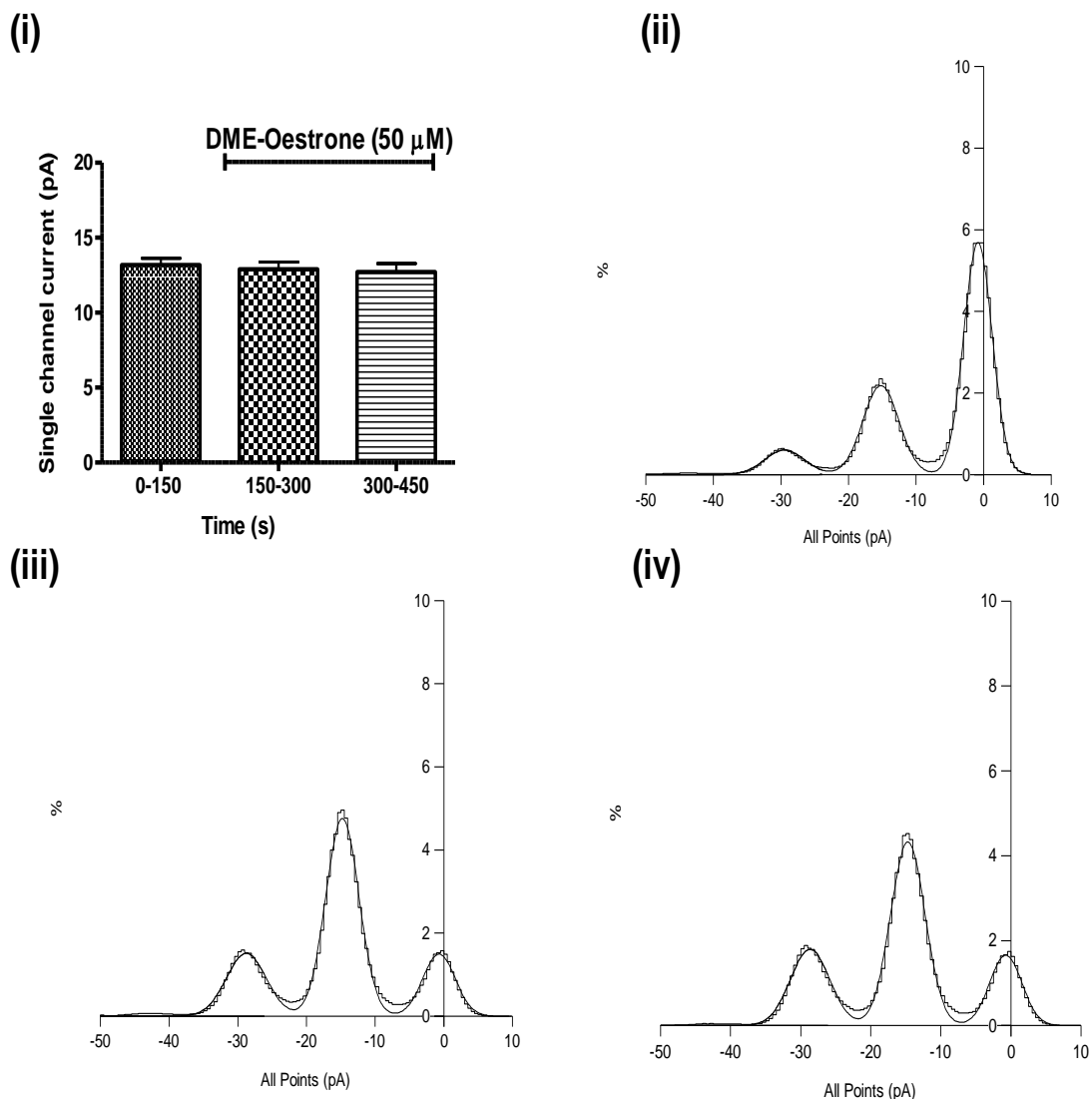


Figure 5.3.3.2 Graphs showing effect of DME-Oestrone (50 μM) on the single channel current amplitude of $\text{BK}\alpha$ channels. This figure demonstrates that Oestrone had no significant effect on single channel current amplitude. Plot (i) depicts a mean of single channel currents recorded in the absence or presence of DME-Oestrone. No significant difference was observed between single channel current before and after application of compound ($p > 0.05$). The data are a mean of six individual bilayer recordings ($n=6$). Histograms (ii), (iii) and (iv) are constructed from a single representative bilayer recording. Plot (ii) is a representative all-points histogram of unitary currents, recorded in the absence of DME-Oestrone (0-150 seconds) and plot (iii) in the presence of 50 μM DME-Oestrone for a further 150-300 seconds and then a further 300-450 seconds plot (iv). All recordings were held at a membrane potential of -50 mV, the free Ca^{2+} concentration was 54 μM .

Figure 5.3.3.3.2 (i) shows unitary currents before (0-150s) and after (150-300s and 300-450s) application of DME-Oestrone (50 μ M). The unitary current for the first 150 seconds prior to the addition of Oestrone was 13.18 pA \pm 0.44 prior to the addition of DME-Oestrone (50 μ M), which corresponds to a unitary conductance of 263.6 pS. There was no significant difference in unitary current after the application of DME-Oestrone as judged by a one-way ANOVA followed by a Bonferroni *post hoc* correction test for multi comparisons ($p > 0.05$). Figure 5.3.3.3.2 (ii) (iii) and (iv) is an example of a single channel current amplitude histogram taken from a single bilayer recording of BK α channels before and after the application of DME-Oestrone (50 μ M). After the application of compound, four amplitude peaks can be seen in plot (iii and (iv) which indicates another channel has appeared in the bilayer during this part of the recording. This also corresponds to a decrease in the area of the closed example histogram plot after application of compound.

To summarise, DME-Oestrone (50 μ M) did not alter the NP_o of the BK α channels. In addition, the single channel current and consequently, the single channel conductance remained unaltered.

5.3.4 Effects of Quaternary-DME-Oestrone on BK channels recorded in lipid bilayers

Previously, Quat-DME-Oestrone was found to be inactive in HEK 293 cells expressing BK channels and, additionally, was unable to relax pre-contracted rat aortic rings. It might be reasonable to expect, therefore, that Quat-DME-Oestrone will have no effect on BK channel activity in planar lipid bilayers. To

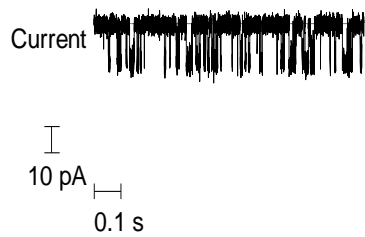
establish that Quat-DME-Oestrone is, in fact, inactive against BK activity, different concentrations of Quat-DME-Oestrone were examined.

5.3.4.1 Effects of Quaternary-DME-Oestrone (5 μ M) on BK α channels in lipid bilayers

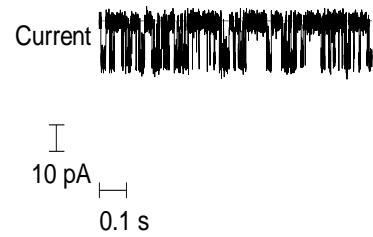
The effect of Quat-DME-Oestrone on channel gating is illustrated in Figure 5.3.4.1.1. (Ai) and (Aii) are example traces of BK α channel activity recorded in lipid bilayers before and after the application of Quat-DME-Oestrone (5 μ M). The average open probability of eight bilayer recordings is illustrated in (Bi) and (Bii). Each data point in (Bi) represents a mean of all recordings per 30 second recording block. (Bii) compares channel activity using pooled data into larger 150 second bins.

On average the NP_o was 0.67 ± 0.12 prior to the application of Quat-DME-Oestrone; a Kruskal-Wallis, one-way ANOVA followed by a Dunn's *post hoc* correction test for multi comparisons revealed no significant difference in NP_o after the addition of 5 μ M Quat-DME-Oestrone ($p > 0,05$).

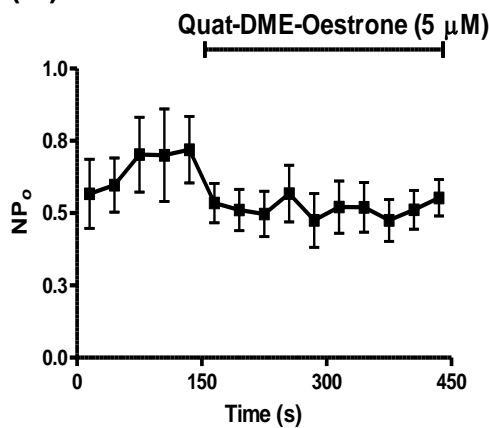
(Ai)



(Aii)



(Bi)



(Bii)

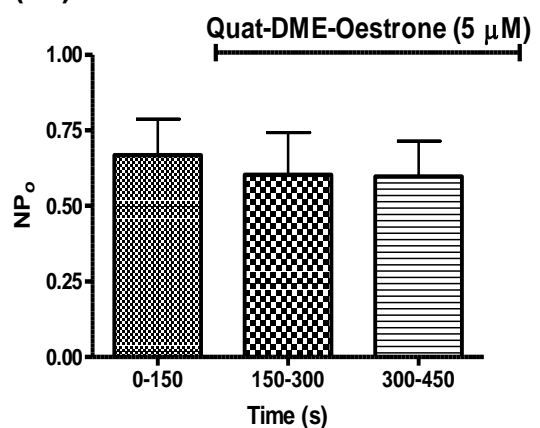


Figure 5.3.4.1.1 The effect of Quaternary-DME-Oestrone (5 μ M) on the NP_o of the BK channel consisting of α subunits alone. The example trace in (Ai) is taken from the first 150s of a BK α recording prior to the addition of Quaternary-DME-Oestrone. Correspondingly, (Aii) shows an example trace in the presence of Quaternary-DME-Oestrone (5 μ M). A plot of mean NP_o vs. time before (0-150 seconds), and after (150-450 seconds) the application of 5 μ M Quaternary-DME-Oestrone (cis side) is shown in (Bi). Subsequent grouping of the data into larger 150 second width bins is illustrated in (Bii). The application of Quaternary-DME-Oestrone (5 μ M) has no significant effect on BK α channel gating activity ($p > 0.05$). Recordings were made at a holding potential of -50 mV and symmetrical electrolyte solutions containing 54 μ M free Ca²⁺ ($n=8$).

The effect of Quat-DME-Oestrone (5 μ M) on the unitary current of BK channels expressing only α subunits was investigated. Recordings could be fitted to two Gaussian curves and the unitary current determined. The number

of Gaussian curves fitted was dependent on the number of channels within the bilayer.

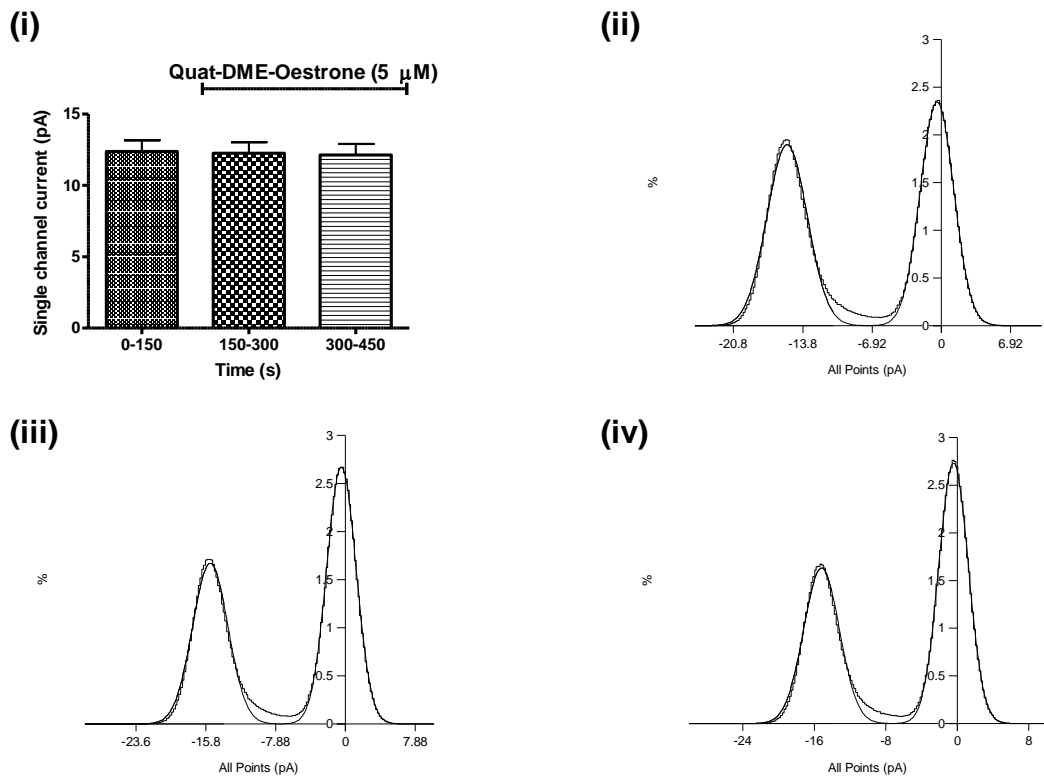


Figure 5.3.4.1.2 Graphs showing effect of Quat-DME-Oestrone (5 μM) on the single channel current of the BK channel consisting of α subunits alone. This figure demonstrates that Quat-DME-Oestrone had no significant effect on single channel current amplitude. Plot (i) depicts a mean of single channel currents recorded in the absence or presence of Quat-DME-Oestrone. No significant difference was observed between single channel current before and after application of compound ($p > 0.05$). The data are a mean of eight individual bilayer recordings ($n=8$). Histograms (ii), (iii) and (iv) are constructed from a single representative bilayer recording. Plot (ii) is a representative all-points histogram of unitary currents, recorded in the absence of Quat-DME-Oestrone (0-150 seconds) and plot (iii) in the presence of 5 μM Quat-DME-Oestrone for a further 150-300 seconds and then a further 300-450 seconds plot (iv). All recordings were held at a membrane potential of -50 mV, the free Ca^{2+} concentration was 54 μM .

Figure 5.3.4.1.2 (i) shows unitary currents before (0-150s) and after (150-300s and 300-450s) application of Quat-DME-Oestrone (5 μM). The unitary current for the first 150 seconds prior to the addition of Quat-DME-Oestrone was

12.37 pA \pm 0.79, which corresponds to a unitary conductance of 247.4 pS. There was no significant difference in unitary current after the application of Quat-DME-Oestrone as judged by a one-way ANOVA followed by a Bonferroni *post hoc* correction test for multi comparisons ($p > 0.05$). Figure 5.3.4.1.2 (ii) (iii) and (iv) is an example of a single channel current amplitude histogram taken from a single bilayer recording of BK α channels before and after the application of Quat-DME-Oestrone (5 μ M).

As expected, Quat-DME-Oestrone (5 μ M) did not change the NP_o of the BK α channels. Neither the single channel current altered nor, as a result, the single channel conductance.

5.3.4.2 Effects of Quaternary-DME-Oestrone (5 μ M) on BK channels comprising α plus β_1 subunits in lipid bilayers

The effect of Quat-DME-Oestrone on channel gating is illustrated in Figure 5.3.4.2.1. (Ai) and (Aii) are example traces of BK α + β_1 activity in a single channel, recorded in lipid bilayers before and after the application of Quat-DME-Oestrone (5 μ M). The average open probability of eight bilayer recordings is illustrated in (Bi) and (Bii). Each data point in (Bi) represents a mean of all recordings per 30 second recording block. (Bii) compares channel activity using pooled data into larger 150 second bins.

On average the NP_o was 0.25 \pm 0.09 prior to the application of Quat-DME-Oestrone; a Kruskal-Wallis, one-way ANOVA followed by a Dunn's *post hoc*

correction test for multi comparisons revealed no significant difference in NP_o after the addition of 5 μM Quat-DME-Oestrone in $\text{BK}\alpha+\beta_1$ channels ($p>0.05$).

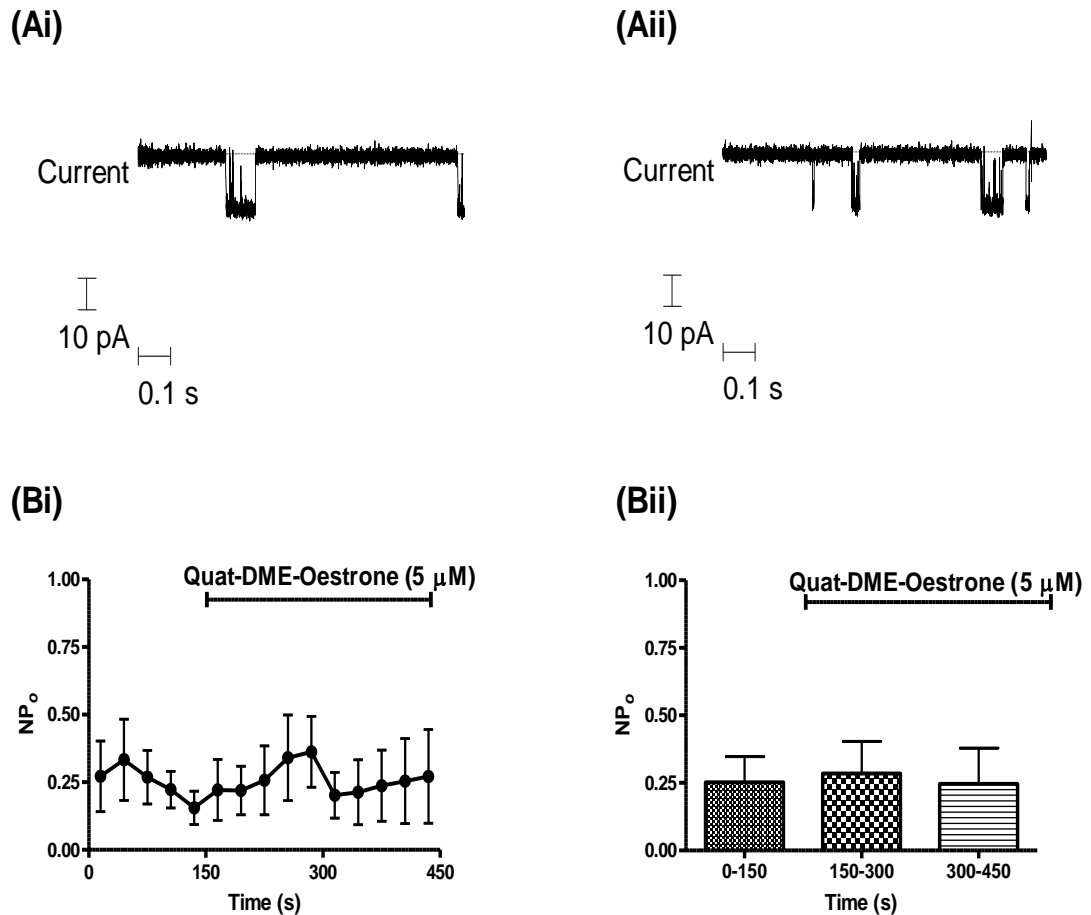


Figure 5.3.4.2.1 The effects of Quat-DME-Oestrone (5 μM) on the NP_o of the BK channel consisting of α and β_1 subunits. The example trace in (Ai) is taken from the first 150s of a $\text{BK}\alpha+\beta_1$ recording prior to the addition of Quat-DME-Oestrone. Correspondingly, (Aii) shows an example trace in the presence of Quat-DME-Oestrone (5 μM). A plot of mean NP_o vs. time before (0-150 seconds), and after (150-450 seconds) the application of 5 μM Quat-DME-Oestrone (cis side) is shown in (Bi). Subsequent grouping of the data into larger 150 second width bins is illustrated in (Bii). The application of Quat-DME-Oestrone (5 μM) has no significant effect on $\text{BK}\alpha+\beta_1$ channel gating activity ($p>0.05$). All recordings were made at a holding potential of -50 mV and symmetrical electrolyte solutions containing 0.53 μM free Ca^{2+} ($n=8$).

The effect of Quat-DME-Oestrone (5 μM) on the unitary current of BK channels expressing both α and β_1 subunits was investigated (Figure

5.3.4.2.2). Recordings could be fitted to two or three Gaussian curves and the unitary current determined. The number of Gaussian curves fitted was dependent on the number of channels within the bilayer.

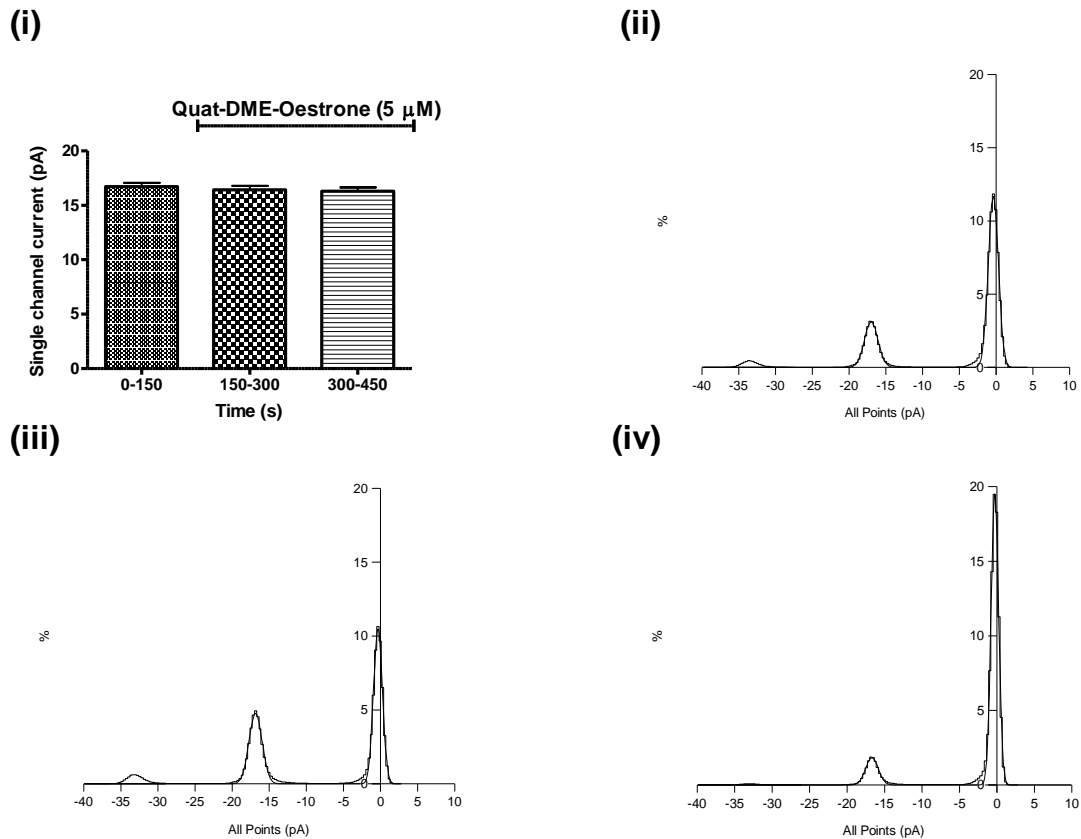


Figure 5.3.4.2.2 Graphs showing effect of Quat-DME-Oestrone (5 μM) on the single channel current amplitude of $\text{BK}\alpha+\beta_1$ channels. This figure demonstrates that Quat DME-Oestrone had no significant effect on single channel current amplitude. Plot (i) depicts a mean of single channel currents recorded in the absence or presence of Quat DME-Oestrone. No significant difference was observed between single channel current before and after application of compound ($p>0.05$). The data are a mean of eight individual bilayer recordings ($n=8$). Histograms (ii), (iii) and (iv) are constructed from a single representative bilayer recording. Plot (ii) is a representative all-points histogram of unitary currents, recorded in the absence of Quat DME-Oestrone (0-150 seconds) and plot (iii) in the presence of 5 μM Quat DME-Oestrone for a further 150-300 seconds and then a further 300-450 seconds plot (iv). All recordings were held at a membrane potential of -50 mV, the free Ca^{2+} concentration was 0.53 μM .

Figure 5.3.4.2.2 (i) shows unitary currents before (0-150s) and after (150-300s and 300-450s) application of Quat-DME-Oestrone (5 μM). The unitary current for the first 150 seconds prior to the addition of Quat-DME-Oestrone was 16.72 ± 0.35 pA, which corresponds to 334.4 pS. There was no significant difference in unitary current after the application of Quat-DME-Oestrone as judged by a one-way ANOVA followed by a Bonferroni *post hoc* correction test for multi comparisons ($p > 0.05$). Figure 5.3.4.2.2 (ii) (iii) and (iv) is an example of a single channel current amplitude histogram taken from a single bilayer recording of BK α + β_1 channels before and after the application of Quat-DME-Oestrone (5 μM). Three peaks seen in (ii) and (iii) denotes at least two BK channel insertions in this recording. However, during the last 150s of recording the channel seems to have disappeared (iv). This could be that the channel has switched to a long closed period, mirrored in the increase in area of the closed peak.

Again, Quat-DME-Oestrone (5 μM) was neither able to modify the NP_o of BK α + β_1 channels, nor alter the single channel current and consequently, the single channel conductance.

5.3.4.3 Effects of high concentrations of Quaternary-DME-Oestrone (50 μM) on the NP_o of BK α channels in lipid bilayers

As expected, BK channel gating activity did not respond to an application of 5 μM Quat-DME-Oestrone and NP_o remained unaffected. To determine whether a higher concentration of compound might influence BK gating kinetics, a 50 μM solution of Quat-DME-Oestrone was investigated.

The effect of Quat-DME-Oestrone (50 μ M) on channel gating is illustrated in Figure 5.3.4.3.1. (Ai) and (Aii) are example traces of BK α channel activity recorded in lipid bilayers before and after the application of Quat-DME-Oestrone. The average NP_o of six bilayer recordings is illustrated in (Bi) and (Bii). Each data point in (Bi) represents a mean of all recordings per 30 second recording block. (Bii) compares channel activity using pooled data into larger 150 second bins.

On average the NP_o was 0.62 ± 0.1 prior to the application of Quat-DME-Oestrone; a Kruskal-Wallis, one-way ANOVA followed by a Dunn's *post hoc* correction test for multi comparisons revealed no significant difference in NP_o after the addition of 50 μ M Quat-DME- Oestrone in BK α channels.

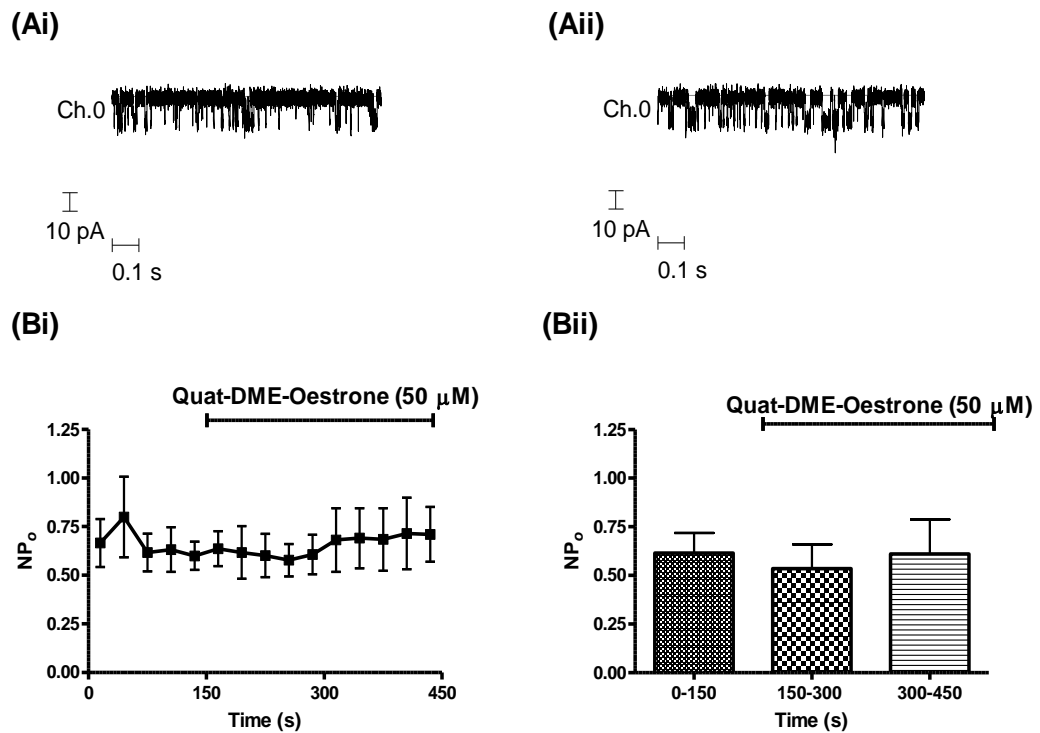


Figure 5.3.4.3.1 The effects of Quat-DME-Oestrone (50 μM) on the NP_o of the BK channel consisting of only α subunits. The example trace in (Ai) is taken from the first 150s of a $\text{BK}\alpha$ recording prior to the addition of Quat-DME-Oestrone. Correspondingly, (Aii) shows an example trace in the presence of Quat-DME-Oestrone (50 μM). A plot of mean NP_o vs. time before (0-150 seconds), and after (150-450 seconds) the application of 50 μM Quat-DME-Oestrone (cis side) is shown in (Bi). Subsequent grouping of the data into larger 150 second width bins is illustrated in (Bii). The application of Quat-DME-Oestrone (50 μM) has no significant effect on $\text{BK}\alpha$ channel gating activity ($p > 0.05$). All recordings were held at a membrane potential of -50 mV, the free Ca^{2+} concentration was 54 μM , ($n=6$).

The effect of Quat-DME-Oestrone (50 μM), illustrated in Figure 5.3.4.3.2, on the unitary current of $\text{BK}\alpha$ channels was investigated. Recordings could be fitted by two Gaussian curves and the unitary current determined. The number of Gaussian curves fitted was dependent on the number of channels within the bilayer.

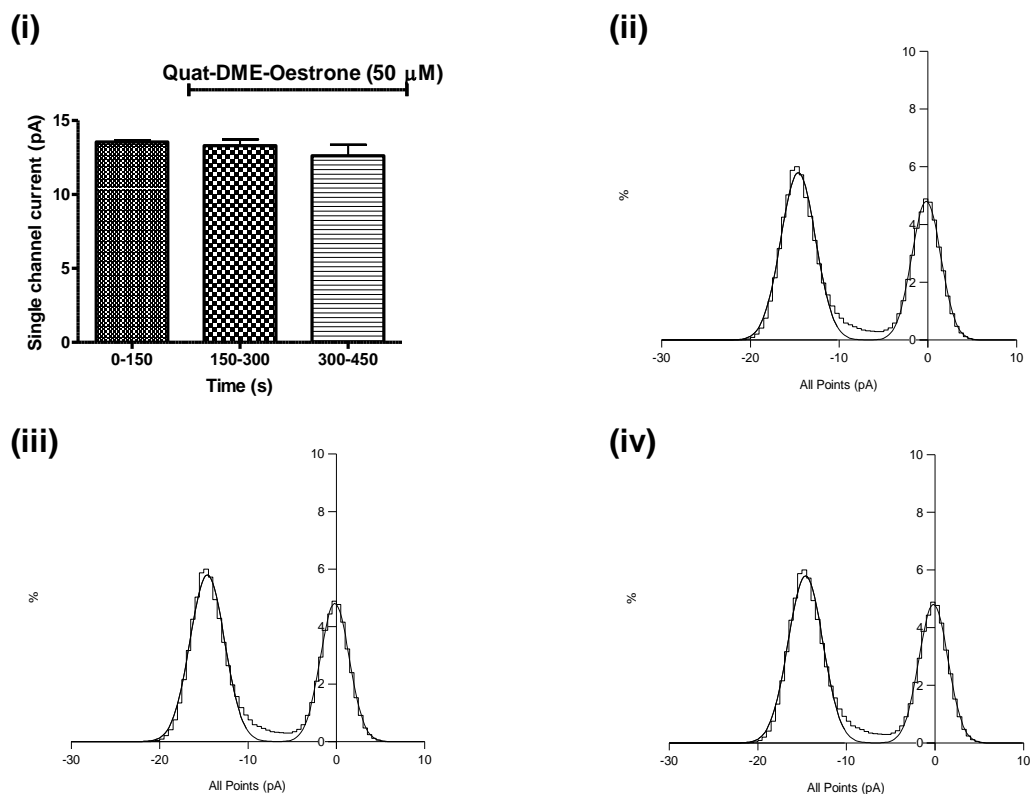


Figure 5.3.4.3.2 Graphs showing effects of Quat-DME-Oestrone (50 μM) on the single channel current amplitude of BKα channels. This figure demonstrates that Quat-DME-Oestrone had no significant effect on single channel current amplitude. Plot (i) depicts a mean of single channel currents recorded in the absence or presence of Quat-DME-Oestrone. No significant difference was observed between single channel current before and after application of compound ($p>0.05$). The data are a mean of six individual bilayer recordings ($n=6$). Histograms (ii), (iii) and (iv) are constructed from a single representative bilayer recording. Plot (ii) is a representative all-points histogram of unitary currents, recorded in the absence of Quat-DME-Oestrone (0-150 seconds) and plot (iii) in the presence of 50 μM Quat-DME-Oestrone for a further 150-300 seconds and then a further 300-450 seconds plot (iv). All recordings were held at a membrane potential of -50 mV, the free Ca^{2+} concentration was 54 μM.

Figure 5.3.4.3.2 (i) shows unitary currents before (0-150s) and after (150-300s and 300-450s) application of Quat-DME-Oestrone (50 μM). The unitary current for the first 150 seconds prior to the addition of Quat-DME-Oestrone (50 μM) was 13.54 ± 0.12 pA which corresponds to a unitary conductance of 270.8 pS. There was no significant difference in unitary current after the

application of Quat-DME-Oestrone as judged by a one-way ANOVA followed by a Bonferroni *post hoc* correction test for multi comparisons ($p > 0.05$). Figure 5.3.4.3.2 (ii) (iii) and (iv) is an example of a single channel current amplitude histogram taken from a single bilayer recording of BK α channels before and after the application of Quat-DME-Oestrone (50 μ M).

As anticipated, high concentrations of Quat-DME-Oestrone (50 μ M) did not alter the NP_o of the BK α channels. Also, the single channel current and consequently, the single channel conductance remained unaltered.

5.3.5 Effects of Oestrone-Oxime on BK channels recorded in lipid bilayers

This section characterises the BK channel consisting of α subunits alone or α plus β_1 subunits, reconstituted into planar lipid bilayers, in the presence and absence of Oestrone-Oxime. In Chapter 3, Oestrone-Oxime was shown to relax pre-contracted rat aortic rings and furthermore, in Chapter 4, whole cell patch-clamp experiments established that a perfusion of 5 μ M Oestrone-Oxime could enhance BK $\alpha + \beta_1$ currents evoked from HEK 293 cells. However, Oestrone-Oxime is easily able to cross cell membranes and thus, the enhanced peak current observed in these experiments and, indeed, the relaxation in pre-contracted rat aortic rings, may be a consequence of intracellular 2nd messenger involvement. If Oestrone-Oxime is, indeed, able to increase BK activity in planar lipid bilayers, then this would suggest direct BK involvement. Conversely, if Oestrone-Oxime is unable to enhance BK

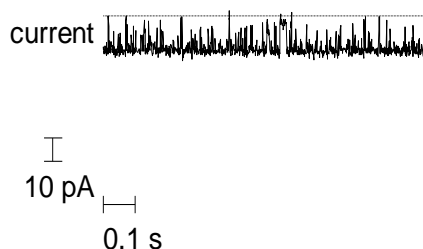
gating activity in bilayers, then this would strengthen the concept of Oestrone-Oxime working through a 2nd messenger such as nitric oxide.

5.3.5.1 Effects of Oestrone-Oxime (5 μ M) on BK α channels in lipid bilayers

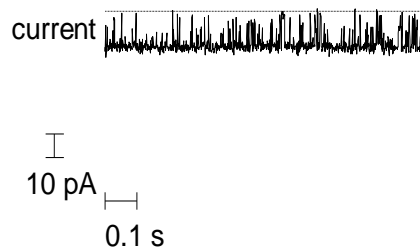
The effect of Oestrone-Oxime on channel gating is illustrated in Figure 5.3.5.1.1. (Ai) and (Aii) are example traces of BK α channel activity recorded in lipid bilayers before and after the application of Oestrone-Oxime (5 μ M). The average open probability of four bilayer recordings is illustrated in (Bi) and (Bii). Each data point in (Bi) represents a mean of all recordings per 30 second recording block. (Bii) compares channel activity using pooled data into larger 150 second bins.

On average the NP_o was 0.53 ± 0.12 prior to the application of Oestrone-Oxime; a Kruskal-Wallis, one-way ANOVA followed by a Dunn's *post hoc* correction test for multi comparisons revealed no significant difference in NP_o after the addition of 5 μ M Oestrone-Oxime ($p > 0.05$).

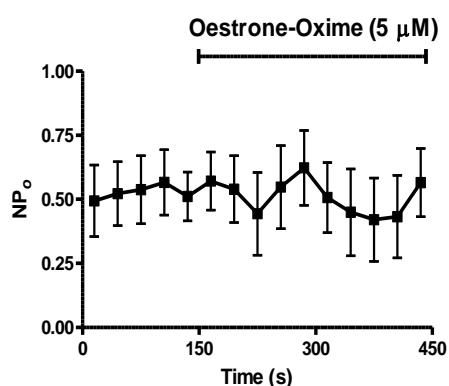
(Ai)



(Aii)



(Bi)



(Bii)

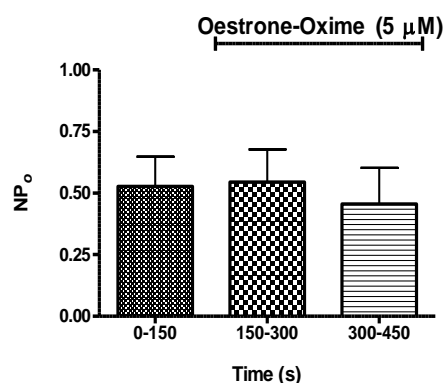


Figure 5.3.5.1.1 The effect of Oestrone-Oxime (5 μ M) on the NP_o of the BK channel consisting of α subunits alone. The example trace in (Ai) is taken from the first 150s of a BK α recording prior to the addition of Oestrone-Oxime. Correspondingly, (Aii) shows an example trace in the presence of Oestrone-Oxime (5 μ M). A plot of mean NP_o vs. time before (0-150 seconds), and after (150-450 seconds) the application of 5 μ M Oestrone-Oxime (cis side) is shown in (Bi). Subsequent grouping of the data into larger 150 second width bins is illustrated in (Bii). The application of Oestrone-Oxime (5 μ M) has no significant effect on BK α channel gating activity ($p > 0.05$). Recordings were made at a holding potential of -50 mV and symmetrical electrolyte solutions containing 54 μ M free Ca²⁺ (n=4).

The effect of Oestrone-Oxime (5 μ M) on the unitary current of BK channels expressing α subunits alone was investigated as before. Recordings could be fitted to two Gaussian curves and the unitary current determined. The number

of Gaussian curves fitted was dependent on the number of channels within the bilayer.

Figure 5.3.5.1.2 (i) shows unitary currents before (0-150s) and after (150-300s and 300-450s) application of Oestrone-Oxime (5 μM).

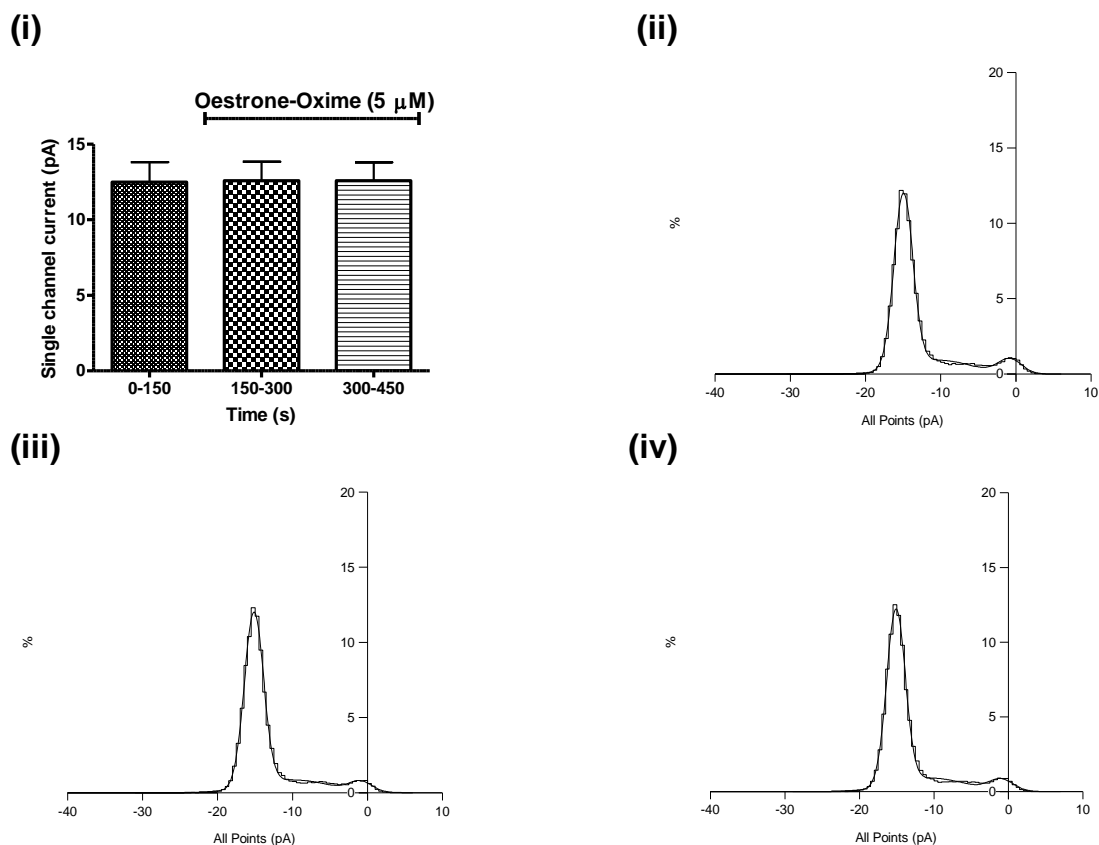


Figure 5.3.5.1.2 Graphs showing effect of Oestrone-Oxime (5 μM) on the single channel current of the BK channel consisting of α subunits alone. This figure demonstrates that Oestrone-Oxime had no significant effect on single channel current amplitude. Plot (i) depicts a mean of single channel currents recorded in the absence or presence of Oestrone-Oxime. No significant difference was observed between single channel current before and after application of compound ($p > 0.05$). The data are a mean of four individual bilayer recordings ($n=4$). Histograms (ii), (iii) and (iv) are constructed from a single representative bilayer recording. Plot (ii) is a representative all-points histogram of unitary currents, recorded in the absence of Oestrone-Oxime (0-150 seconds) and plot (iii) in the presence of 5 μM Oestrone-Oxime for a further 150-300 seconds and then a further 300-450 seconds plot (iv). All recordings were held at a membrane potential of -50 mV, the free Ca^{2+} concentration was 54 μM .

The unitary current for the first 150 seconds prior to the addition of Oestrone-Oxime (5 μ M) was 12.50 pA \pm 1.32 pA which corresponds to a unitary conductance of 250 pS. There was no significant difference in unitary current after the application of Oestrone-Oxime as judged by a one-way ANOVA followed by a Bonferroni *post hoc* correction test for multi comparisons ($p > 0.05$). Figure 5.3.5.1.2 (ii) (iii) and (iv) is an example of a single channel current amplitude histogram taken from a single bilayer recording of BK α channels before and after the application of Oestrone-Oxime (5 μ M).

To summarise, Oestrone-Oxime (5 μ M) did not alter the NP_o of the BK α channels. In addition, Oestrone-Oxime did not change the single channel current and consequently, the single channel conductance. However, as with oestradiol, if Oestrone-Oxime interacts directly with BK channels, it may be that, the presence of β_1 subunits may be required for BK modulation.

5.3.5.2 Effects of Oestrone-Oxime (5 μ M) on BK channels comprising α plus β_1 subunits in lipid bilayers

This study has established Oestrone-Oxime activates BK $\alpha + \beta_1$ currents in whole cell recordings. Unless these effects are a consequence of intracellular mechanisms, it would be not unreasonable to record a similar activation here in a planar lipid bilayer system.

The effect of Oestrone-Oxime on channel gating is illustrated in Figure 5.3.5.2.1. (Ai) and (Aii) are example traces of BK $\alpha + \beta_1$ channel activity recorded in lipid bilayers before and after the application of Oestrone-Oxime (5

μM). Figure (Aii) illustrates the long closed periods that were observed after the application of Oestrone-Oxime.

The average open probability of eight bilayer recordings is illustrated in (Bi) and (Bii). Each data point in (Bi) represents a mean of all recordings per 30 second recording block. (Bii) compares channel activity using pooled data into larger 150 second bins. On average the NP_o was 0.44 ± 0.18 prior to the application of Oestrone-Oxime.

Initially, BK channel activity appeared to gradually decrease after the addition of Oestrone-Oxime; however, a Kruskal-Wallis, one-way ANOVA followed by a Dunn's *post hoc* correction test for multi comparisons revealed no significant difference in NP_o after the addition of $5 \mu\text{M}$ Oestrone-Oxime in $\text{BK}\alpha+\beta_1$ channels ($p>0.05$).

(Ai)

current

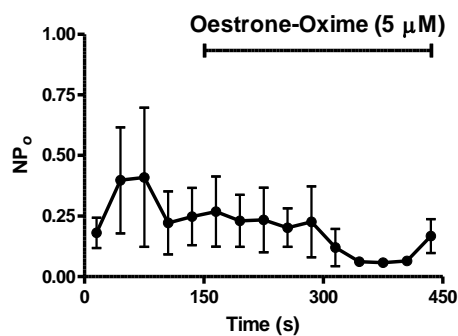
10 pA
0.1 s

(Aii)

current

10 pA
0.1 s

(Bi)



(Bii)

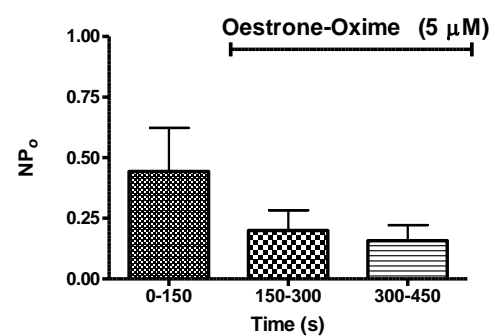


Figure 5.3.5.2.1 The effects of Oestrone-Oxime ($5 \mu\text{M}$) on the NP_o of the BK channel consisting of α and β_1 subunits. The example trace in (Ai) is taken from the first 150s of a $\text{BK}\alpha+\beta_1$ recording prior to the addition of Oestrone-Oxime. Correspondingly, (Aii) shows an example trace in the presence of Oestrone-Oxime ($5 \mu\text{M}$). A plot of mean NP_o vs. time before (0-150 seconds), and after (150-450 seconds) the application of $5 \mu\text{M}$ Oestrone-Oxime (cis side) is shown in (Bi). Subsequent grouping of the data into larger 150 second width bins is illustrated in (Bii). The application of Oestrone-Oxime ($5 \mu\text{M}$) has no significant effect on $\text{BK}\alpha+\beta_1$ channel gating activity ($p>0.05$). All recordings were made at a holding potential of -50 mV and symmetrical electrolyte solutions containing $0.53 \mu\text{M}$ free Ca^{2+} ($n=8$).

The effect of Oestrone-Oxime ($5 \mu\text{M}$) on the unitary current of BK channels expressing both α and β_1 subunits was investigated. Recordings could be fitted to two or three Gaussian curves and the unitary current determined. The

number of Gaussian curves fitted was dependent on the number of channels within the bilayer

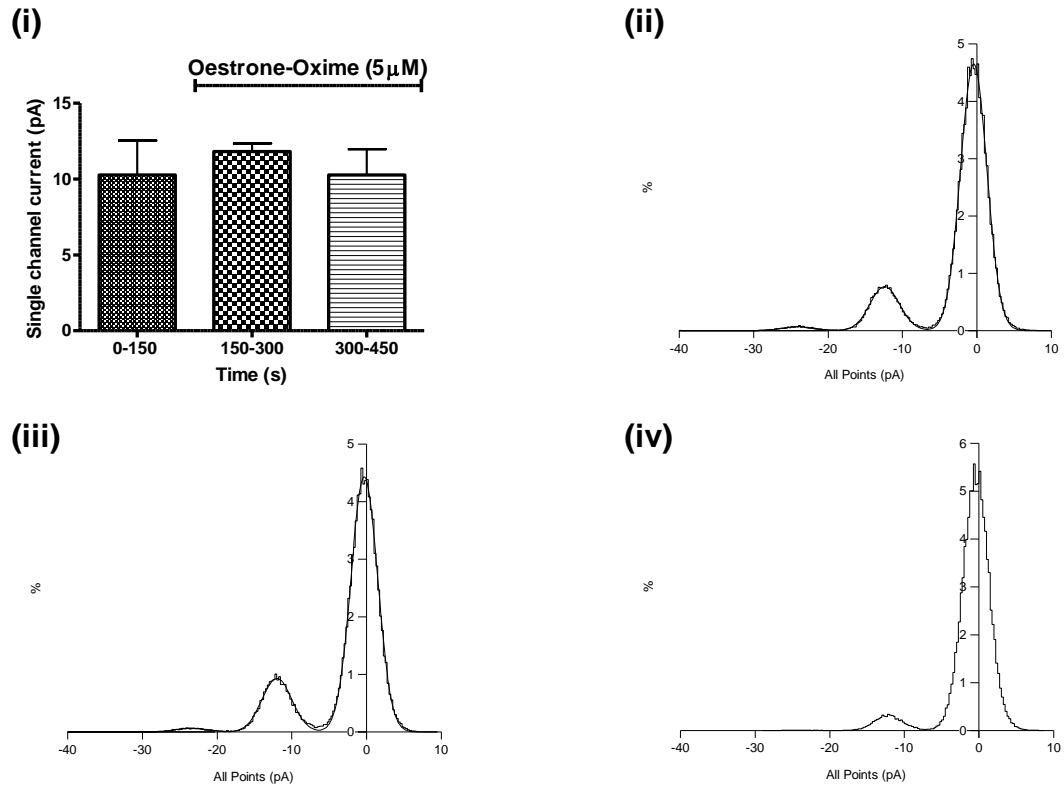


Figure 5.3.5.2.2 Graphs showing effect of Oestrone-Oxime (5 μM) on the single channel current amplitude of $BK\alpha+\beta_1$ channels. This figure demonstrates that Oestrone-Oxime had no significant effect on single channel current amplitude. Plot (i) depicts a mean of single channel currents recorded in the absence or presence of Oestrone-Oxime. No significant difference was observed between single channel current before and after application of compound ($p>0.05$). The data are a mean of eight individual bilayer recordings ($n=8$). Histograms (ii), (iii) and (iv) are constructed from a single representative bilayer recording. Plot (ii) is a representative all-points histogram of unitary currents, recorded in the absence of Oestrone-Oxime (0-150 seconds) and plot (iii) in the presence of 5 μM Oestrone-Oxime for a further 150-300 seconds and then a further 300-450 seconds plot (iv). All recordings were held at a membrane potential of -50 mV, the free Ca^{2+} concentration was 0.53 μM.

Figure 5.3.5.2.2 (i) shows unitary currents before (0-150s) and after (150-300s and 300-450s) application of Oestrone-Oxime (5 μM). The unitary current for

the first 150 seconds prior to the addition of Oestrone-Oxime was $10.29 \text{ pA} \pm 1.32$, which corresponds to a unitary conductance of 205.8 pS . There was no significant difference in unitary current after the application of Oestrone-Oxime as judged by a one-way ANOVA followed by a Bonferroni *post hoc* correction test for multi comparisons ($p > 0.05$). Figure 5.3.5.2.2 (ii) (iii) and (iv) is an example of a single channel current amplitude histogram taken from a single bilayer recording of $\text{BK}\alpha + \beta_1$ channels before and after the application of Oestrone-Oxime ($5 \text{ }\mu\text{M}$). Three peaks can be seen in this recording representing two conducting BK channels.

After application of Oestrone-Oxime, long closed periods were observed and channel activity appeared to be inhibiting over time. This is exemplified very effectively in plot (iv) which clearly shows the area of the open histograms to have decreased substantially after 150s of exposure to Oestrone-Oxime. However, a statistical analysis revealed no significant change to unitary current after application of compound.

In brief, the presence of the β_1 subunit made no significant difference to the NP_o of the BK channels after application of Oestrone-Oxime ($5 \text{ }\mu\text{M}$). In addition, Oestrone-Oxime did not change the single channel current and consequently, the single channel conductance.

5.3.6 Results summary

In planar lipid bilayer experiments, none of the oestrogens tested were able to modulate reconstituted BK channels when only α subunits were present.

However, NP_o was significantly enhanced when Oestrone (5 μM) was added to bilayers containing $\text{BK}\alpha+\beta_1$ channels. Application of a higher concentration (50 μM) of Oestrone, DME-Oestrone or Quat-DME-Oestrone had no effect on BK channel kinetic activity regardless of BK subunit configuration.

All observations are summarised in Table 5.3.6.1, alongside findings from similar studies using 17β -oestradiol, tamoxifen and its quaternary derivative, ethylbromide tamoxifen demonstrated by other workers.

Due to time constraints, bilayer experiments could not be completed. As a consequence data could not be recorded for DME-Oestradiol or Quat-DME-Oestradiol. For the same reason, a high concentration of Oestrone-Oxime (50 μM) could not be tested on either $\text{BK}\alpha$ or $\text{BK}\alpha+\beta_1$ channels. Similarly, data for the effect on $\text{BK}\alpha+\beta_1$ channels of DME-Oestrone (50 μM) and Quat-DME-Oestrone (50 μM) could not be recorded.

Table 5.3.6.1 Effects of oestrogens and novel derivatives on BK channels reconstituted in lipid bilayers.

COMPOUND		BK α alone		BK $\alpha+\beta_1$		REFS
		NP _o	γ	NP _o	γ	
17-keto oestrogens	OESTRONE	0	0	↑	0	PS
	<u>DME-OESTRONE</u>	0	0	0	0	PS
	<u>QUAT-DME-OESTRONE</u>	0	0	0	0	PS
17 oxime	<u>OESTRONE-OXIME</u>	0	0	0	0	PS
17 β -hydroxy oestrogens	<u>DME-OESTRADIOL</u>	NDA	NDA	NDA	NDA	PS
	<u>QUAT-DME-OESTRADIOL</u>	NDA	NDA	NDA	NDA	PS
	17 β -OESTRADIOL	0	0	↑↑↑	0	[40] UD
Non-steroidal antioestrogens	TAMOXIFEN	NDA	0	↑	0	UD
	ETHYLBROMIDE TAMOXIFEN	↓	0	↑↑	0	UD

Key: 0 = compound inactive;

↑ < ↑↑ < ↑↑↑ = significant activation in order of potency;

↓ = significant inhibition;

NP_o = open probability of channel x the number of channels;

γ = single channel conductance;

NDA (no data available in bilayers); PS (present study); UD (Allen et al., unpublished data)

(xenoestrogen) = novel compound synthesised for the purpose of this study

5.4 DISCUSSION

The patch clamping technique is considered by many to be the gold standard in ion channel analysis [511-513]. However, acute activation of BK channels by any potential ligand may be influenced by various intracellular signalling processes. Subsequently, this raises the question of whether BK activation, observed in whole cell recordings, is purely a consequence of direct BK involvement or possibly a result of other membrane receptor-induced events. For instance, second messenger pathways involving G-proteins, cAMP-mediated phosphorylation, GMP, cGMP-mediated phosphorylation and NOS are all known routes to BK activation *in vivo* and *in vitro*, while inhibition of BK conductance may sometimes be attributable to redox changes and cysteine oxidation [118, 213, 215, 354-357, 514]. In view of this, consideration must be given to the fact that HEK 293 cells, though well-tailored for use as a stable expression system, are nonetheless, human cells with an attendant capacity to respond to normal cellular signalling. Accordingly, the patch clamping data amassed for this study (Chapter 4) have raised some unanswered questions, about how and where oestrogens and their novel derivatives influence BK channels. Resolution of some of these questions was attempted by examining the effects of oestrogens on reconstituted BK channels in planar lipid bilayers.

The planar lipid bilayer technique is an elegant, alternative investigative methodology in ion channel behaviour, not least because it can be used to explore permeation and gating characteristics of individual ion channels in a chemically isolated environment. It also affords the opportunity to preclude or at least ameliorate the effects of unwanted intracellular protein signalling

brought about by the many endogenous signalling molecules and receptors present in whole cells. Using purified membrane vesicles, reconstituted from cells over-expressing the channel of interest, ensures that the resultant membrane vesicles used for bilayer insertion will contain an over-abundance of the wanted protein with less likelihood of interference from any residual, less numerous, endogenous channels.

Whilst previous work in patched whole cell recordings has established the prerequisite co-association of auxiliary β_1 subunits with their companion α subunits in order for oestrogens and xenoestrogens to modulate BK channels [102, 129, 515, 516], it was work done by de Wet *et al.*, using the planar lipid bilayer technique, which established mandatory association of multiple auxiliary β_1 subunits with the core channel for optimum oestrogen-induced activation [40, 517]. Here, bilayer experiments suggest that Oestrone, like its metabolite 17 β -oestradiol, activates BK channels provided α subunits are expressed with the β_1 subunit.

5.4.1 Effects of Oestrone and novel derivative xenoestrogens on NP_o of BK channels recorded in lipid bilayers

Given the body of evidence provided by many previous studies, it was not anticipated that Oestrone, readily converted to 17 β -oestradiol *in vivo*, would affect the gating or permeation kinetics of BK α alone channels inserted into lipid bilayers. Here indeed, the open probability (NP_o) of these channels after application of 5 μ M Oestrone (150-450s) did not significantly alter from the control period (0-150s) (Figure 5.3.2.1.1). Similarly, DME-Oestrone, Quat-

DME-Oestrone and Oestrone-Oxime, followed the same pattern when applied to BK α channels (Figures 5.3.3.1.1; 5.3.4.1.1; 5.3.5.1.1 respectively). This was expected and parallels findings previously proposed by Valverde *et al.*, (1999), that β_1 subunit association is required for oestrogen-induced BK α activation. Additionally, the outcome was no different for higher concentrations of oestrogens. Application of Oestrone, DME-Oestrone and Quat-DME-Oestrone (50 μ M) to the *cis* side of the bilayer had little or no effect on BK α NP $_o$ (Figures 5.3.2.3.1; 5.3.3.3.1; and 5.3.4.3.1 respectively).

Predictably, there was a sustained and significant increase over time in NP $_o$ of BK α + β_1 channels after treatment with Oestrone (5 μ M) but interestingly, treatment of these channels with a high concentration of Oestrone (50 μ M), had no significant effect on NP $_o$ (Figures 5.3.2.2.1 and 5.3.2.4.1 respectively). Nevertheless, 50 μ M is a high concentration of Oestrone, close to saturation and, with a danger of precipitation, the need for a complete concentration response analysis is essential.

None of the novel xenoestrogens tested - DME-Oestrone; Quat-DME-Oestrone nor Oestrone-Oxime mirrored previous published reports of other xenoestrogen-BK activation in the presence of β_1 subunits [103, 129, 518]. All of the synthesised compounds in this study proved to be inactive when applied to BK α + β_1 channels reconstituted in lipid bilayers. However, studies using other techniques, including this study, have shown oxime compounds to be possible nitric oxide donors. For example, work done by Chalupsky *et al* demonstrated that some oxime derivatives increase NO levels in human

smooth muscle cells which exert significant vasorelaxant effects. They deduced that this was due to NO formation in the smooth muscle cells triggering subsequent activation of soluble guanylyl cyclase and cyclic GMP-dependent protein kinases [261]. If this is true for Oestrone-Oxime, then the bilayer technique will not record such events, due to the absence of intracellular enzymes and would explain the lack of any observed BK channel activity here.

5.4.2 Effects of Oestrone and novel derivative xenoestrogens on single channel current of BK channels recorded in lipid bilayers

The effect of Oestrone, DME-Oestrone, Quat-DME-Oestrone and Oestrone-Oxime on the unitary current of BK channels was investigated. Previous researchers have reported some xenoestrogens have been found to effect unitary current of BK channels in a β_1 subunit-independent way. This is suggestive of a possible alternative interaction between the ligand and the pore-forming α subunit. Dick *et al.*, have reported such effects from tamoxifen and its quaternary derivative ethylbromide tamoxifen [103, 104, 129]. According to Dick *et al.*, both steroidal oestrogens and non-steroidal xenoestrogens are able to reduce the unitary conductance of BK channels when expressing only α subunits [103, 104, 129]. Interestingly, this would imply that such compounds may interact with the channel independently of any associating β_1 subunits. Reduced single channel currents are often thought to be due to a rapid association of the drug with the open pore of the channel inducing a rapid form of flicker block. However, this study found no evidence of a significant alteration in unitary current in bilayers, before or after

application of Oestrone or the xenoestrogens DME-Oestrone, Quat-DME-Oestrone and Oestrone-Oxime.

5.4.3 The planar bilayer as a system for investigating direct activation of BK channels

The planar lipid bilayer system has the advantage that it is a cell free system free of the complications arising from back ground cellular process such as changes in second messenger systems, redox changes and receptor mediated cellular events. However, there are deficiencies in the system which can make it problematic as a tool for investigating drug actions at the single channel level. For example:-

- The lipid constituents of the artificial bilayer are determined by the experimenter but usually have different constituents to real cell membranes. For example, cell membranes also contain cholesterol which helps to create more stable artificial bilayers. However, several workers have reported cholesterol-induced modulation of BK channels in artificial bilayers [519-521]. Indeed, BK channels are known to cluster in cholesterol-rich membranes which affords the opportunity to investigate cholesterol-BK channel interactions as possible therapeutic and pharmacological targets [521].
- Cell membranes are asymmetric, having different lipids on the inner leaflet to the outer leaflet; with the painted bilayer system, it is difficult to produce asymmetric bilayers.
- It is still possible that the BK channel subunits, reconstituted from purified HEK cell membrane vesicles, could be associated with

unknown accessory integral proteins. For example, BK channels associate with β subunits but are also known to associate with voltage-gated Ca^{2+} channels. The only real way of studying BK channels in isolation is to purify the BK protein away from all other proteins and reconstitute with an excess of β_1 subunits into proteoliposomes. These proteoliposomes could then be used in planar lipid bilayers. In this study, purified membranes not purified proteins are used; consequently, unknown proteins could be associating with the BK channel. However, this is unlikely as the α and β_1 subunits have been over-expressed and hence, should be the dominant proteins in the purified membrane vesicles.

- The experimenter does not know how many β_1 subunits are associating with the BK channel under investigation. This is important, especially when investigating the effects of oestrogens on the channel. It has been documented that for oestrogens to modulate gating activity of BK channels, at least two β_1 subunits need to be associating with the core channel [40].
- Bilayers are fragile, easily blown by electrical and / or mechanical noises and have low success rates.
- The experimenter has no control over channel insertion. For example, in these experiments, one recording a day was exceptional. Channel activity is also difficult to record when more than three channels are conducting in concert as the traces go off scale.
- Small residual pockets of solvent, trapped in the bilayer, may cause denaturing / disruption of the channel proteins. Setting up the bilayer,

the solvent is initially allowed to evaporate, but to generate a perfect working bilayer, the cup may need re-painting with lipids, thus, re-introducing solvent.

However, the painted lipid bilayer is, indeed, an invaluable technique when used in juxtaposition with other investigative methodologies such as whole cell patch-clamp experiments, as it can rule out any oestrogenic effects on BK gating characteristics which may be attributable to genomic origins. Also, because this technique allows for easy access to the internal and external surface of the channel protein in a chemically isolated environment, drug delivery is effectively achieved.

5.5 SUMMARY

These bilayer data have successfully demonstrated that Oestrone can activate the BK channel in a non-genomic way, provided β_1 subunits are co-expressed with α subunit tetramers. This was expected and concurs with previous evidence documenting the ability of steroidal oestrogens to activate the BK channel *via* a non-genomic pathway. However, single channel analysis in bilayers confirmed the novel xenoestrogens - DME-Oestrone, Quat-DME-Oestrone are inactive on BK channels. In addition, Oestrone-Oxime was unable to activate the channel at membrane level, regardless of subunit composition.

Unfortunately, time constraints prevented investigation of the effects of DME-Oestradiol or Quat-DME-Oestradiol on BK channels reconstituted in artificial lipid bilayers. Experiments using high concentrations of oestrogens (50 μ M) could not be completed.

CHAPTER 6

General Discussion

6.1 GENERAL DISCUSSION

There is a wealth of evidence claiming oestrogens promote vasorelaxant effects in vascular smooth muscle which are rapid in onset and are mediated by an endothelium-independent, non-genomic pathway [82, 522] and the aim of this investigation was to explore the acute effects and underlying mechanisms of novel oestrogen derivatives as vasorelaxants and activators of the large conductance BK potassium channel.

6.1.1 Synthesis of novel xenoestrogens from known BK activators

It was intended to design and synthesise compounds that could activate the BK channel *via* a non-genomic pathway by incorporating some of the structural motifs of recognized xenoestrogens with proven vasorelaxant capabilities. Previously, oestradiol-BSA conjugates as direct BK activators have been synthesised [102]. These membrane-impermeant oestrogen derivatives were reported to activate BK channels directly. However, the efficacy of these molecules has since been queried as it has been demonstrated that these conjugates easily disassociate, resulting in leaching of free oestrogen [151, 152]. Additionally, because of steric hindrance, the relative binding efficiency of these conjugates is low and consequently these molecules do not compete for oestradiol binding to oestrogen receptors *in vitro*. Thus, in experiments using conjugates, it may indeed be possible that the observed activity is attributable to leached oestradiol. It is clear that there is a need for a new experimental approach to non-permeable oestrogens.

To achieve the objectives of this study then, the initial task was to successfully synthesise suitable novel oestrogen derivatives. The compounds were designed to:-

- retain the four-ringed backbone of steroidal oestrogens
- incorporate the amine side chain of tamoxifen
- incorporate the positively charged side chain of ethyl bromide tamoxifen, a membrane-impermeable quaternary analogue of tamoxifen [143], which would offer an elegant alternative to oestradiol-BSA conjugate compounds.

Five novel xenoestrogens, DME-Oestrone, Quat-DME-Oestrone, DME-Oestradiol, Quat-DME-Oestradiol and Oestrone-Oxime were synthesised using Oestrone as the parent compound. A pure crystal structure of DME-Oestrone was achieved which informed the successful synthesis of other derivatives. Although, this was the only crystal structure to be realised, it was not totally unexpected due to the deliquescence of the other compounds, especially true of those compounds with a quaternary ammonium tail. However, the purity of each of these compounds was fully confirmed using a series of analytical techniques before evaluation of their pharmacological response on BK channels was undertaken.

Pharmacologic appraisal of the novel compounds was undertaken using the following methodologies:-

- *ex vivo* whole tissue isolated organ bath assays using rat aortic rings, to investigate selectivity for BK channels and other potential oestrogen targets of these novel compounds
- *in vitro*, whole cell patch-clamp recordings of BK currents from HEK 293 cells expressing either α or $\alpha+\beta_1$ subunits, to investigate novel oestrogens and subunit dependence of BK activation
- planar lipid bilayers to investigate the molecular and functional effects of novel oestrogens on reconstituted BK channels.

DME-Oestrone, Quat-DME-Oestrone, DME-Oestradiol and Quat-DME-Oestradiol are all novel compounds. Furthermore, this study is the first time that these compounds have been synthesised and pharmacologically tested, all of which were carried out by the author. Oestrone is an endogenous hormone and Oestrone-Oxime has been reported to have been synthesised [464]. However, to the best of the author's knowledge, there has been no pharmacological assessment of its activity on BK channels.

6.1.2 *Ex vivo* vascular studies

An isolated organ bath is the classical pharmacological screening tool used to assess concentration-response relationships in contractile tissue. In contrast to molecular assays, the effects of compounds with unknown molecular targets can be studied and aortic ring assays bridge the gap between *in vivo* and *in vitro* models. The assay was implemented in this study primarily to investigate selectivity of the synthesised compounds for BK channels and other potential oestrogen targets.

If the compounds synthesised for this study are indeed novel BK activators, then smooth muscle relaxant activity in arterial smooth muscle would be apparent in the presence of the compounds. In addition, the relaxation would not be dependent on nitric oxide release from an intact endothelium, while relaxation would be reversed by specific BK channel blockers such as iberiotoxin. It would be necessary to examine the effects of the compounds in endothelium-intact and denuded aortic rings in order to investigate effects on smooth muscle directly and rule out endothelium-dependent mechanisms of action.

This present study has successfully demonstrated that Oestrone and the novel oestrogens, except Quat-DME-Oestrone, were able to relax smooth muscle in a concentration-dependent manner (Refer to Table 3.3.9.1). Previously, oestrogens have been reported to produce rapid vasorelaxation in smooth muscle over a range of concentrations, from as little as 5 pM to as much as 1 mM [225], and this investigation was no exception. Here, the novel oestrogen derivatives could promote relaxation of pre-contracted aorta with and without an intact endothelium within an increasing and cumulative range of concentrations (0.3 μ M to 30 μ M). These concentrations were in accord with previous studies [219, 234, 523]. However, relaxation was instigated through different mechanisms. In particular, Oestrone-Oxime required the presence of the endothelium to exert much of its effect. This suggests the relaxant properties of this xenoestrogen may not necessarily involve BK activation. Indeed, the oxime functional group (N=OH) of this steroid confers NO donor status because it is susceptible to oxidative-cleavage [258, 261]. Furthermore,

some oximes are metabolised to NO by cytochrome P450 [259] or NAD/NADP-dependent oxido-reductases [258, 465, 524].

Quat-DME-Oestradiol depended both on nitric oxide and BK channel activation. This was demonstrated by significant endothelium-dependent and endothelium-independent relaxation in the pre-contracted aorta as well as IbTX sensitivity. This implies that BK channels are important in its mode of action.

Reversal of tissue relaxation by iberiotoxin, however, is only an indication of BK channel involvement and is not proof of direct binding of the compound to the BK channel. It is possible that compounds that are capable of relaxing whole tissue could be activating the BK channel indirectly *via* various membrane receptors, some of which are listed in Table 3.4.1, or indeed, through mechanisms independent of the BK activation.

As this technique is at best an assessment of the relaxant properties of the novel oestrogens in aortic smooth muscle and not a test for direct activation of the BK channel in isolation, it was necessary to examine their effectiveness in a more defined *in vitro* system using the whole cell patch-clamp method.

6.1.3 Whole cell patch-clamp studies

The patch-clamp technique was employed to record whole cell BK currents in an appropriate cellular expression system. Cloned BK genes have been successfully expressed in HEK 293 cells facilitating single-channel analysis of

BK currents [307, 525]. HEK 293 cells, over-expressing either *hSlo* α or both *hSlo* α and *hSlo* β_1 subunits, were used for this purpose as these cells:-

- have no constitutively expressed BK channels [292]
- do not express ER α , ER β [269, 270] or
- do not express GPR30/GPER receptors [271, 469]
- have little or no NOS activity [253, 526, 527].

HEK 293 cells over expressing the α and $\alpha+\beta_1$ subunits of the BK channel were capable of generating robust BK currents. Before evaluating the effects of the compounds on these evoked currents, it was essential to establish the successful expression of BK α and β_1 subunits, therein. Characterisation of evoked BK currents recorded from whole cell patch-clamp using non-stationary noise analysis, toxin blockade, activation rate and conductance-voltage relationship confirmed the expression of α and α plus β_1 subunits in the HEK 293 cells.

In this study, it was hypothesised that whole cell patch-clamp experiments would provide some answers as to which, if any, of the compounds are able to modulate BK channel function. For instance, if relaxation of the rings in the presence of DME-Oestrone is independent of BK channels, one would expect this compound to be inactive against BK currents in HEK cells over-expressing BK channels. Likewise, Quat-DME-Oestrone, inactive in rings, would be unable to modulate BK channels in an expression system. Because Quat-DME-Oestradiol produced IbTX-sensitive relaxation in aortic rings, it was hypothesised that this compound would be able to enhance evoked BK currents in HEK 293 cells.

It was anticipated that whole cell recordings of BK currents would demonstrate a β_1 subunit-dependence of any compounds that were able to enhance evoked BK currents. Previously, it has been shown that non-steroidal antioestrogens and steroidal oestrogens activate BK channels in a subunit-dependent manner [101, 102, 129] and it was hypothesised that if the oestrogen compounds in this study are BK activators then they will show similar subunit-dependence. The collected data demonstrated that Oestrone, Quat-DME-Oestradiol and Oestrone-Oxime could, indeed, enhance BK currents when both α and β_1 subunits were expressed in HEK 293 cells (refer to Table 4.4.2.1). Furthermore, the macroscopic gating kinetics of the channel remained unaltered in the presence of these compounds. These data agree with the investigation by Morrow *et al.*, who postulated that the β_1 subunit ability to confer oestrogen sensitivity is separate from its ability to alter the macroscopic gating kinetics of BK currents [251].

Although the experiments in this study have illuminated which of the tested compounds are BK activators, these data alone cannot determine definitively, the location of a possible BK activation site or sites. For instance, HEK 293 cells lack endogenous GPE receptors [271, 469], but this does not preclude direct or secondary modulation of other membrane receptors. Previous investigations, using xenoestrogens such as tamoxifen plus membrane-impermeable isoforms such as ethylbromide tamoxifen [143] and have put forward compelling evidence that the site of action for these compounds, is located extracellularly [137, 143, 515]. This study also supports a proposed extracellular site of action and these findings have been published in a peer

reviewed journal [235]. Quat-DME-Oestradiol, due to the presence of a quaternary functional group, is the only active synthesised compound that is membrane-impermeable. This indicates an extracellular site of action for this compound and corroborates previous work done by Dick *et al.*, which suggests a putative binding site for ethylbromide tamoxifen within the extracellular loop of the β_1 subunit [104].

To further explore the mechanism of action of these compounds on BK currents, single channel conductance, channel lifetime and channel open probability were investigated. These effects can be considered from inside-out and outside-out patches, however, it was decided to extend the investigation in a reductionist system where recombinant BK protein is studied in artificial lipid bilayers. HEK 293 cell membranes, over-expressing BK α and BK α plus β_1 subunits, were purified and reconstituted in planar lipid bilayers. An over-abundance of these subunits ameliorates interference from any residual, less numerous, endogenous channels.

6.1.4 Planar lipid bilayer studies

Whole cell experiments in patched HEK 293 cells, although confirming which of the compounds were able to enhance evoked BK currents, raised other questions about how and where they interact with BK channels. To investigate whether these observed phenomena are a result of direct BK involvement or other cellular events, the effects of the oestrogens on reconstituted BK channels in planar lipid bilayers was explored. Although considerations such as single channel conductance, channel lifetime and

channel open probability can easily be accomplished using outside-out and inside-out patch-clamp configurations, the planar lipid bilayer system furnishes the opportunity to control lipid content in the artificial reconstituted bilayer.

Cell membranes consist of a combination of sphingophospholipids, glycolipids and sterols. The sterols include cholesterol, a class of steroid, which is a vital element of the cell's lipid membrane and is essential for the organisation and integrity of the bilayer [477-479]. The plasma membrane in mammalian cells contains approximately 30-50 mol% of cholesterol, which is randomly and unevenly distributed throughout the cell membrane in cholesterol-rich and cholesterol-impooverished sphingolipid domains [479-481, 528, 529]. HEK 293 cells are mammalian cells with typical mammalian cell membrane composition which will include areas rich in cholesterol. BK channels are known to cluster in cholesterol-rich membrane microdomains and functional BK-cholesterol interactions have been reported [521]. It has been hypothesised that depletion of membrane cholesterol leads to potentiation of BK currents, while the presence of cholesterol in a mixture of phospholipids within an artificial bilayer depresses BK single channel activity [519, 521]. It has also been proposed that cholesterol may even interact with a protein surface that resides at the BK α subunit itself, leading to BK channel function modification including decreased channel open probability [520]. In this study, the bilayers were made up from a 1:1 ratio of phospholipids (POPS and POPE). Cholesterol was not added to the phospholipid mixture in order to obviate the possibility of BK subunit and sterol interaction.

The results of this study, so far, support investigations, which have demonstrated that co-association of auxiliary β_1 subunits is a pre-requisite for modulation of BK channels by oestrogens [102, 129, 515, 516]. As anticipated, planar lipid bilayer experiments substantiated oestrogens and xenoestrogens are inactive when only α subunits were present. Moreover, Oestrone, like its metabolite 17β -oestradiol, significantly enhanced the open probability of channels associating with accessory β_1 subunits. This also demonstrates that oestrogens, unlike ethanol - a cholesterol antagonist [519], do not require cholesterol-BK interaction for channel modulation. Oestrone-Oxime was found to be inactive in bilayers even in the presence of the β_1 subunit. This was anticipated, as other techniques have demonstrated the mechanism of action for oximes involves nitric oxide. Due to the absence of intracellular signalling enzymes in a reductionist bilayer system, Oestrone-Oxime was, predictably, inactive.

As with the other techniques used in this study, Quat-DME-Oestrone could not modify BK channel kinetics and remained inactive. DME-Oestrone, similarly, was inactive in bilayers as in HEK 293 cells. Unfortunately, the opportunity to test DME-Oestradiol and Quat-DME-Oestradiol was denied due to time constraints.

6.2 SUMMARY

The main findings of this thesis are summarised below in Table 6.2.1

Table 6.2.1 Summary of main findings of compounds on smooth muscle relaxation and BK channel currents.

Compound	Effects on pre-contracted intact aortic rings	Effects on pre-contracted denuded aortic rings	Effects on BK α currents HEK 293 cells	Effects on BK α + β_1 currents HEK 293 cells	Effects on BK α currents planar lipid bilayers	Effects on BK α + β_1 currents planar lipid bilayers
Oestrone	Relaxes	Relaxes	Inactive (5 μ M)	Activates (5 μ M)	Inactive (5 μ M, 50 μ M)	Activates (5 μ M) Inactive (50 μ M)
DME-Oestrone	Relaxes	Relaxes	Inactive (5 μ M)	Inactive (5 μ M)	Inactive (5 μ M)	Inactive (5 μ M)
Quat-DME-Oestrone	Inactive	Inactive	Inactive	Inactive	Inactive	Inactive
Oestrone-Oxime	Relaxes	Relaxes	Inhibited	Activates	Inactive	Inactive
DME-Oestradiol	Relaxes	Relaxes	Not tested	Not tested	Not tested	Not tested
Quat-DME-Oestradiol	Relaxes	Relaxes	Inhibited	Activates	Not tested	Not tested

These novel compounds showed a range of activity - from the completely inactive (Quat-DME-Oestradiol) to relaxant activity independent of BK involvement and relaxant activity dependent on BK activation. All BK activation in the presence of oestrogens required the presence of the β_1 subunit.

6.3 FURTHER WORK

Because Quat-DME-Oestradiol was able to relax pre-contracted smooth muscle aortic tissue and enhance evoked BK currents in HEK 293 cells, for the sake of completeness, this novel compound should be considered as a BK activator in a planar lipid bilayer system.

In smooth muscle, relaxation of pre-contracted tissue induced by Quat-DME-Oestradiol may involve other mechanisms in addition to direct BK activation (e.g. *via* nitric oxide or other second messengers). In these whole tissue studies, Quat-DME-Oestradiol-induced relaxation was reversed by application of the BK blocker IbTX but this only indicates BK involvement and not a direct effect of the compound on the channel. Recent work done by Royal *et al.*, [250] has proposed that oestrogens can regulate nNOS within arterial smooth muscle.

Since this present study was completed, further experiments outside the remit and time-frame of this thesis and published by the author, support this hypothesis [235]. It was found that the relaxant effects of Quat-DME-Oestradiol were partially reduced by L-NAME, a non-specific NOS inhibitor. Because this novel oestrogen is membrane impermeant, these data suggest the compound may be targeting unknown membrane receptors that modulate nNOS within aortic smooth muscle. However, in HEK 293 cells, although enhancement of BK currents by Oestrone and novel oestrogens may still involve second messengers, it is highly improbable that nitric oxide is involved due to lack of NOS (refer to Chapter 4 Section 4.1.1.2) [526]. This all

illustrates the need to apply a reductionist approach to investigate direct actions on the channel.

The planar lipid bilayer system provides this reductionist approach, removing all possibility of nitric oxide and second messenger interference, and would be the next logical step to investigate direct effects of Quat-DME-Oestradiol on BK channel kinetics.

Following on from this for comparison, a series of BK single channel kinetics experiments could be carried out exploring ionic activity from different surfaces of the cell membrane on inside-out and outside-out patches using HEK 293 cells (refer to Chapter 4.1.2; Figure 4.1.2.1; and Table 4.1.2.1). These experiments may also add to evidence of a possible site of action.

The acute effects of 17β -oestradiol have been studied on vascular smooth muscle [9-12], and a vasorelaxant effect over a large range of concentrations (10 pM–1 mM) was demonstrated [225]. In this study, cumulative additions of Oestrone and the novel oestrogens (ranging through 0.1 μ M to 30 μ M) were used on pre-contracted aortic smooth muscle to assess their ability to induce tissue relaxation. In whole cell patch-clamp experiments a 5 μ M concentration of compound was used to treat HEK 293 cells and in planar lipid bilayer experiments, both 5 μ M and a high concentration (50 μ M) were applied to BK channels. In bilayers, it was shown that 5 μ M Oestrone enhanced BK α + β ₁ channels, while 50 μ M had no effect. Although, the concentrations used in this study are pharmacologically compatible and are within the range that have

been used by previous workers [40, 102, 104], for a complete insight into mechanisms of action, it would be edifying to plot complete concentration-response curves for the compounds used in both HEK 293 cells and planar lipid bilayers.

Investigation of the effects of the novel compounds on other β subunits to determine subunit specificity should be carried out. There are at least 4 known BK β subunits and a full list of these along with their tissue expression and kinetic properties is reported in Table 4.1.3.4.1. Oestrogens are well documented to activate BK α channels when there are β_1 subunits present and this study supports this. However, although β_2 subunits are sensitive to some steroids e.g. dehydroepiandrosterone (DHEA) - a stress-related adrenal androgen, they are not sensitive to oestrogens [530, 531].

Following on from this, it is possible that studies using chimeric constructs between different BK β subunits might provide valuable information as to the site of action for the novel oestrogens. Chimeric exchange of the different regions of the β_1 and β_2 , β_3 or β_4 subunits have been used previously to demonstrate behaviour of BK subunits [39]. This study supports other workers' reports of an extracellular site of action for oestrogens and their β_1 subunit-dependence [532]. The use of chimeric constructs of BK subunits could pinpoint such sites to particular residues within the β_1 subunit. For instance, it has been documented that co-association of β_2 or β_3 subunits with BK α tetramers induces rapid and complete inactivation (refer to Sections 4.1.3.(4)(5) and Table 4.1.3.4.1). Therefore, examining the effects of

oestrogens on a β_1 - β_2 subunit chimeric construct (replacement of the extracellular loop of the β_1 subunit with the extracellular loop of a β_2 subunit) (Figure 6.3.1), could reveal if the site of action resides at the extracellular loop of the β_1 subunit.

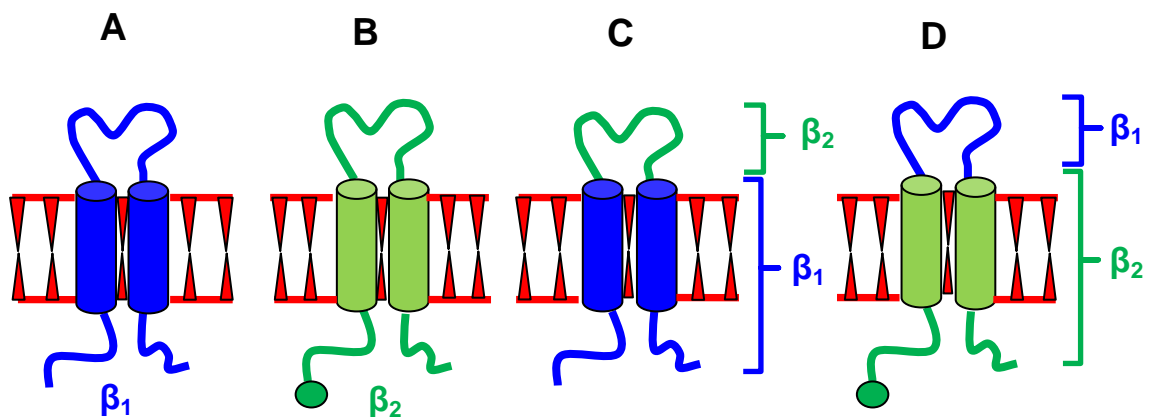


Figure 6.3.1 Schematic description of a BK β_1 subunit (A); a BK β_2 subunit (B); a potential β_1 - β_2 chimera (C); and a potential β_2 - β_1 subunit chimera (D). If the extracellular loop of the β_1 subunit confers oestrogen sensitivity, then construct C would not respond to oestrogen, whereas, the construct D would respond to oestrogen as well as showing rapid inactivation of BK currents.

Liu *et al.*, have suggested that the S0 domain of the α subunit is in close proximity to the transmembrane domain 2 of the β_1 subunit, and the transmembrane domain 1 of the β_1 subunit is associated with S1 and S2 domains of the α subunit [367]. Additionally, work done by Morrow *et al.*, demonstrated that deletion of the extracellular N-terminal of the murine α subunit did not prevent the α and β_1 subunits interacting kinetically but did affect BK modulation by 17 β -oestradiol [251]. This suggests a putative site of

action for oestrogens at the interface between the β_1 subunit extracellular loop and the α subunit extracellular N-terminal. To expand on this, deletion of groups or individual amino acid(s) within the extracellular loop of the β_1 subunit could isolate salient residues that may be involved in oestrogen-induced BK modulation.

Finally, the effects of Quat-DME-Oestradiol on BK channels in other smooth muscle tissue should be explored. In airway smooth muscle, BK channel function also requires the β_1 subunit to enhance BK channel opening and knockout β_1 BK channels increase airway contractions commensurate with pharmacological blockade of BK channels [422]. Quat-DME-Oestradiol, active in vascular smooth muscle, does not cross cell membranes, thus, examining its relaxant properties on bronchial smooth muscle as a therapeutic screen to determine whether the compound could be developed as an inhaled smooth muscle relaxant. In fact, other quaternary antimuscarinics are currently used clinically as bronchodilators e.g. tiotropium bromide and ipratropium - a non-selective muscarinic antagonist.

In the urinary bladder smooth muscle, BK channels have been demonstrated to play an important role in regulating contraction and relaxation [533]. Indeed, BK^{-/-} mice display urinary bladder dysfunction leading to an overactive bladder [534]. BK channels, then, would be considered a suitable therapeutic target for urinary bladder dysfunction. Tanaka *et al.*, reported that the novel BK opener NS-8, a pyrrole derivative, suppresses the rat micturition reflex (refer to Figure 2.1.2.1) [114, 115]. This compound was selected for clinical trials but

withdrawn soon after. Therefore, to examine the effects of the novel oestrogens synthesised in this study on bladder smooth muscle would make a valuable contribution to this field of research.

6.4 CONCLUSIONS

In the introduction three hypotheses were suggested and they were:-

(i) Oestrogens and xenoestrogens can relax vascular smooth muscle by directly activating BK channels.

(ii) BK activation by oestrogens and xenoestrogens requires the presence of the β_1 subunit.

(iii) The site of action for oestrogens and xenoestrogens on the BK channel is located on the external interface between α and β_1 subunits.

Concerning the first hypothesis, the work on aortic rings described in Chapter 3, demonstrates that oestrogen can relax vasculature, but suggests that in many incidences this relaxation is multifactorial and may involve more than just BK direct activation. For example Oestrone-Oxime demonstrates both endothelial and non-endothelial dependent relaxation but marginal activation of BK channels when expressed in HEK 293 cells.

Concerning the second hypothesis, compounds were either active e.g. Oestrone or devoid of activity e.g. Quat-DME-Oestrone. However, active compounds were only able to activate BK currents in the presence of the β_1 subunit, thus, the second hypothesis, currently stands.

With regards to the third hypothesis, the data from this study are consistent with an external site of action for oestrogens, as quaternary ammonium oestrogens such as Quat-DME-Oestradiol and Ethylbromide tamoxifen are

able to activate BK currents only when the β_1 subunit is present [104, 235]. As these compounds are membrane-impermeant, these data suggest a site of action on the external interface between α and β_1 subunits and thus, the third hypothesis to date is supported by the literature [235].

To examine these hypotheses, the initial aims, outlined within the introduction (Section 1.3) of this investigation, proposed to develop novel BK activators incorporating key features of steroidal and non-steroidal antioestrogens. To this aim, pure xenoestrogens were successfully synthesised (two of which were cell-impermeant quaternary amine derivatives) and thus, fulfilled the first part of the investigation objectives. The cell-impermeant quaternary derivatives, Quat-DME-Oestrone and Quat-DME-Oestradiol, proved to be the most interesting compounds - Quat-DME-Oestrone provided a perfect control as it remained inactive in all techniques and conversely, Quat-DME-Oestradiol, in possession of a 17β hydroxyl group, demonstrated direct BK activation in HEK cells when the β_1 subunit is present, and was able to relax smooth muscle in a BK channel dependent manner.

The findings described within this thesis have since been presented at three international scientific conferences by the author and published (and cited) as a full paper in a peer-reviewed journal. These publications are listed in the appendix. These data and results represent a genuine and novel contribution to the scientific literature, and a library of knowledge relevant to BK channels as potential pharmacological targets.

REFERENCES
and
BIBLIOGRAPHY

1. Nardi, A., V. Calderone, and S.P. Olesen, *Potassium channel openers: The case of BK channel activators*. *Letters in Drug Design & Discovery*, 2006. **3**(4): p. 210-218.
2. Seebohm, G., *Activators of Cation Channels: Potential in Treatment of Channelopathies*. *Molecular Pharmacology*, 2005. **67**(3): p. 585-588.
3. Shieh, C.C., et al., *Potassium channels: Molecular defects, diseases, and therapeutic opportunities*. *Pharmacological Reviews*, 2000. **52**(4): p. 557-593.
4. Gopalakrishnan, M. and C.C. Shieh, *Potassium channel subtypes as molecular targets for overactive bladder and other urological disorders*. *Expert Opinion on Therapeutic Targets*, 2004. **8**(5): p. 437-458.
5. Du, W., et al., *Calcium-sensitive potassium channelopathy in human epilepsy and paroxysmal movement disorder*. *Nat Genet*, 2005. **37**(7): p. 733-738.
6. Garcia, M.L., D.-M. Shen, and G.J. Kaczorowski, *High-conductance calcium-activated potassium channels: validated targets for smooth muscle relaxants?* *Expert Opinion on Therapeutic Patents*, 2007. **17**(7): p. 831-842.
7. Ponte, C.G., et al., *Selective, Direct Activation of High-Conductance, Calcium-Activated Potassium Channels Causes Smooth Muscle Relaxation*. *Molecular Pharmacology*, 2012. **81**(4): p. 567-577.
8. Haynes, M.P., et al., *Rapid vascular cell responses to estrogen and membrane receptors*. *Vascular Pharmacology*, 2002. **38**(2): p. 99-108.

9. Ruehlmann, D.O. and G.E. Mann, *Rapid non-genomic vasodilator actions of oestrogens and sex steroids*. Current Medicinal Chemistry, 2000. **7**(5): p. 533-541.
10. Ruehlmann, D.O., et al., *Environmental estrogenic pollutants induce acute vascular relaxation by inhibiting L-type Ca^{2+} channels in smooth muscle cells*. The FASEB Journal, 1998. **12**(7): p. 613-619.
11. Asano, S., J.D. Tune, and G.M. Dick, *Bisphenol A activates Maxi-K ($K(Ca)1.1$) channels in coronary smooth muscle*. British Journal of Pharmacology, 2010. **160**(1): p. 160-170.
12. Zhang, H.-T., et al., *Daidzein relaxes rat cerebral basilar artery via activation of large-conductance Ca^{2+} -activated K^+ channels in vascular smooth muscle cells*. European Journal of Pharmacology, 2010. **630**(1–3): p. 100-106.
13. Abou-Mohamed, G., et al., *Estradiol relaxes rat aorta via endothelium-dependent and -independent mechanisms*. Pharmacology, 2003. **69**(1): p. 20-26.
14. Cignarella, A., R. Paoletti, and L. Puglisi, *Direct effects of estrogen on the vessel wall*. Medicinal Research Reviews, 2001. **21**(2): p. 171-184.
15. Wu, R.S. and S.O. Marx, *The BK potassium channel in the vascular smooth muscle and kidney: alpha- and beta-subunits*. Kidney International, 2010. **78**(10): p. 963-974.
16. Elkins, T., B. Ganetzky, and C.F. Wu, *A Drosophila Mutation That Eliminates a Calcium-Dependent Potassium Current*. Proceedings of the National Academy of Sciences of the United States of America, 1986. **83**(21): p. 8415-8419.

17. Atkinson, N.S., G.A. Robertson, and B. Ganetzky, *A Component of Calcium-Activated Potassium Channels Encoded by the Drosophila-Slo Locus*. Science, 1991. **253**(5019): p. 551-555.
18. Adelman, J.P., *Calcium-activated potassium channels expressed from cloned complementary DNAs*. Neuron, 1992. **9**: p. 206-216.
19. Butler, A., et al., *Mslo, a Complex Mouse Gene Encoding Maxi Calcium-Activated Potassium Channels*. Science, 1993. **261**(5118): p. 221-224.
20. Pallanck, L. and B. Ganetzky, *Cloning and characterization of human and mouse homologs of the Drosophila calcium-activated potassium channel gene, slowpoke*. Hum. Mol. Genet., 1994. **3**(8): p. 1239-1243.
21. Diaz, L., et al., *Role of the S4 segment in a voltage-dependent calcium-sensitive potassium (hSlo) channel*. Journal of Biological Chemistry, 1998. **273**(49): p. 32430-32436.
22. Quirk, J.C. and P.H. Reinhart, *Identification of a novel tetramerization domain in large conductance K-Ca channels*. Neuron, 2001. **32**(1): p. 13-23.
23. Meera, P., et al., *Large conductance voltage- and calcium-dependent K⁺ channel, a distinct member of voltage-dependent ion channels with seven N-terminal transmembrane segments (S0-S6), an extracellular N terminus, and an intracellular (S9-S10) C terminus*. Proceedings of the National Academy of Sciences of the United States of America, 1997. **94**(25): p. 14066-14071.
24. Wallner, M., P. Meera, and L. Toro, *Determinant for beta-subunit regulation in high-conductance voltage-activated and Ca²⁺-sensitive K⁺*

- channels: An additional transmembrane region at the N terminus.* Proceedings of the National Academy of Sciences of the United States of America, 1996. **93**(25): p. 14922-14927.
25. Ledoux, J., et al., *Calcium-activated potassium channels and the regulation of vascular tone.* Physiology, 2006. **21**: p. 69-78.
 26. Knaus, H.G., et al., *Subunit Composition of the High-Conductance Calcium-Activated Potassium Channel from Smooth-Muscle, a Representative of the Mslo and Slowpoke Family of Potassium Channels.* Journal of Biological Chemistry, 1994. **269**(6): p. 3921-3924.
 27. Knaus, H.G., et al., *Primary Sequence and Immunological Characterization of Beta-Subunit of High-Conductance Ca²⁺-Activated K⁺ Channel from Smooth-Muscle.* Journal of Biological Chemistry, 1994. **269**(25): p. 17274-17278.
 28. Garcia-Calvo, M., et al., *Characterization of the solubilized charybdotoxin receptor from bovine aortic smooth muscle.* Biochemistry, 1991. **30**(46): p. 11157-11164.
 29. Garcia-Calvo, M., et al., *Purification and reconstitution of the high-conductance, calcium- activated potassium channel from tracheal smooth muscle.* J. Biol. Chem., 1994. **269**(1): p. 676-682.
 30. Schubert, R. and M.T. Nelson, *Protein kinases: tuners of the BKCa channel in smooth muscle.* Trends in Pharmacological Sciences, 2001. **22**(10): p. 505-512.
 31. Brenner, R., et al., *Cloning and functional characterization of novel large conductance calcium-activated potassium channel beta subunits,*

- hKCNMB3 and hKCNMB4*. Journal of Biological Chemistry, 2000. **275**(9): p. 6453-6461.
32. Uebele, V.N., et al., *Cloning and functional expression of two families of beta-subunits of the large conductance calcium-activated K⁺ channel*. Journal of Biological Chemistry, 2000. **275**(30): p. 23211-23218.
33. Weiger, T.M., et al., *A novel nervous system beta subunit that downregulates human large conductance calcium-dependent potassium channels*. Journal of Neuroscience, 2000. **20**(10): p. 3563-3570.
34. Dworetzky, S.I., et al., *Phenotypic alteration of a human BK (hSlo) channel by hSlo beta subunit coexpression: Changes in blocker sensitivity, activation/relaxation and inactivation kinetics, and protein kinase A modulation*. Journal of Neuroscience, 1996. **16**(15): p. 4543-4550.
35. Orio, P., et al., *New disguises for an old channel: MaxiK channel beta-subunits*. News in Physiological Sciences, 2002. **17**: p. 156-161.
36. McManus, O.B., et al., *Functional-Role of the Beta-Subunit of High-Conductance Calcium-Activated Potassium Channels*. Neuron, 1995. **14**(3): p. 645-650.
37. Meera, P., et al., *A calcium switch for the functional coupling between a (hslo) and beta subunits (K-v,K-Ca beta) of maxi K channels*. FEBS Letters, 1996. **382**(1-2): p. 84-88.
38. Meera, P., et al., *A calcium switch for the functional coupling between alpha (hslo) and beta subunits (K-v,K-ca beta) of maxi K channels (vol 382, pg 84, 1996)*. FEBS Letters, 1996b. **385**(1-2): p. 127-128.

39. Orio, P., et al., *Structural determinants for functional coupling between the beta and alpha subunits in the Ca²⁺-activated K⁺ (BK) channel*. Journal of General Physiology, 2006. **127**(2): p. 191-204.
40. De Wet, H., et al., *Modulation of the BK channel by oestrogens: examination at single channel level*. Molecular Membrane Biology, 2006. **23**(5): p. 420-429.
41. Cox, D.H. and R.W. Aldrich, *Role of the beta 1 subunit in large-conductance Ca²⁺-activated K⁺ channel gating energetics - Mechanisms of enhanced Ca²⁺ sensitivity*. Journal of General Physiology, 2000. **116**(3): p. 411-432.
42. Xia, X.M., J.P. Ding, and C.J. Lingle, *Molecular basis for the inactivation of Ca²⁺- and voltage-dependent BK channels in adrenal chromaffin cells and rat insulinoma tumor cells*. Journal of Neuroscience, 1999. **19**(13): p. 5255-5264.
43. Brenner, R., et al., *Vasoregulation by the beta 1 subunit of the calcium-activated potassium channel*. Nature, 2000. **407**(6806): p. 870-876.
44. Brayden, J.E. and M.T. Nelson, *Regulation of arterial tone by activation of calcium-dependent potassium channels*. Science, 1992. **256**(5056): p. 532-535.
45. Nelson, M.T., et al., *Calcium channels, potassium channels, and voltage dependence of arterial smooth muscle tone*. American Journal of Physiology - Cell Physiology, 1990. **259**(1): p. C3-C18.
46. Nelson, M.T. and A.D. Bonev, *The beta(1) subunit of the Ca²⁺-sensitive K⁺ channel protects against hypertension*. Journal of Clinical Investigation, 2004. **113**(7): p. 955-957.

47. Garciacalvo, M., et al., *Purification and Reconstitution of the High-Conductance, Calcium-Activated Potassium Channel from Tracheal Smooth-Muscle*. Journal of Biological Chemistry, 1994. **269**(1): p. 676-682.
48. Navarro-Antolin, J., et al., *Decreased expression of maxi-K⁺ channel beta(1)-subunit and altered vasoregulation in hypoxia*. Circulation, 2005. **112**(9): p. 1309-1315.
49. Jackson, W.F., *Potassium channels in the peripheral microcirculation*. Microcirculation, 2005. **12**(1): p. 113-127.
50. Dick, G.M. and K.M. Sanders, *(Xeno)estrogen sensitivity of smooth muscle BK channels conferred by the regulatory beta1 subunit: a study of beta1 knockout mice*. J Biol Chem, 2001. **276**(48): p. 44835-40.
51. Pluger, S., et al., *Mice with disrupted BK channel beta 1 subunit gene feature abnormal Ca²⁺ spark/STOC coupling and elevated blood pressure*. Circulation Research, 2000. **87**(11): p. E53-E60.
52. Fernandez-Fernandez, J.M., et al., *Gain-of-function mutation in the KCNMB1 potassium channel subunit is associated with low prevalence of diastolic hypertension*. Journal of Clinical Investigation, 2004. **113**(7): p. 1032-1039.
53. Amberg, G.C. and L.F. Santana, *Downregulation of the BK channel beta 1 subunit in genetic hypertension*. Circulation Research, 2003. **93**(10): p. 965-971.
54. Allender, S., et al., *Patterns of coronary heart disease mortality over the 20(th) century in England and Wales: Possible plateaus in the rate of decline*. BMC Public Health, 2008. **8**.

55. Rayner, M., et al., *Cardiovascular disease in Europe*. European Journal of Cardiovascular Prevention & Rehabilitation, 2009. **16**: p. S43-S47.
56. Allender, S., et al., *European cardiovascular disease statistics (3rd Ed.)*. 2008, European Heart Network
57. Scarborough, P., et al., *Coronary heart disease statistics 2010 (16th Ed.)*. 2010, British Heart Foundation Statistics Database www.heartstats.org.
58. Stampfer, M.J., et al., *Postmenopausal estrogen therapy and cardiovascular disease - 10-year follow-up from the nurses health study*. New England Journal of Medicine, 1991. **325**(11): p. 756-762.
59. Coylewright, M., J.F. Reckelhoff, and P. Ouyang, *Menopause and Hypertension*. Hypertension, 2008. **51**(4): p. 952-959.
60. Muller, R.E., et al., *Studies on the mechanism of estradiol uptake by rat uterine cells and on estradiol binding to uterine plasma membranes*. Advances in Experimental Medicine and Biology, 1979. **117**: p. 401-21.
61. Prossnitz, E.R. and M. Maggiolini, *Mechanisms of estrogen signaling and gene expression via GPR30*. Molecular and Cellular Endocrinology, 2009. **308**(1-2): p. 32-38.
62. Kelly, M.J. and E.R. Levin, *Rapid actions of plasma membrane estrogen receptors*. Trends in Endocrinology and Metabolism, 2001. **12**(4): p. 152-156.
63. Tostes, R.C., et al., *Effects of estrogen on the vascular system*. Brazilian Journal of Medical and Biological Research, 2003. **36**(9): p. 1143-1158.

64. Beato, M. and A. SanchezPacheco, *Interaction of steroid hormone receptors with the transcription initiation complex*. *Endocrine Reviews*, 1996. **17**(6): p. 587-609.
65. Russell, K.S., et al., *Human vascular endothelial cells contain membrane binding sites for estradiol, which mediate rapid intracellular signaling*. *Proceedings of the National Academy of Sciences of the United States of America*, 2000. **97**(11): p. 5930-5.
66. Klinge, C.M., *Estrogen receptor interaction with estrogen response elements*. *Nucleic Acids Research*, 2001. **29**(14): p. 2905-2919.
67. Mendelsohn, M.E., *Genomic and nongenomic effects of estrogen in the vasculature*. *The American Journal of Cardiology*, 2002. **90**(1, Supplement 1): p. F3-F4.
68. Green, S., et al., *Human oestrogen receptor cDNA: sequence, expression and homology to v-erb-A*. *Nature*, 1986. **320**(6058): p. 134-139.
69. Greene, G.L., et al., *Sequence and expression of human estrogen-receptor complementary-DNA*. *Science*, 1986. **231**(4742): p. 1150-1154.
70. Mosselman, S., J. Polman, and R. Dijkema, *ER beta: Identification and characterization of a novel human estrogen receptor*. *Febs Letters*, 1996. **392**(1): p. 49-53.
71. Falkenstein, E., et al., *Multiple Actions of Steroid Hormones—A Focus on Rapid, Nongenomic Effects*. *Pharmacological Reviews*, 2000. **52**(4): p. 513-556.

72. Wehling, M., A. Schultz, and R. Lösel, *Nongenomic actions of estrogens: Exciting opportunities for pharmacology*. *Maturitas*, 2006. **54**(4): p. 321-326.
73. Gilligan, D.M., et al., *Acute vascular effects of estrogen in postmenopausal women*. *Circulation*, 1994. **90**(2): p. 786-791.
74. Lefkowitz, R.J., . *Seven transmembrane receptors—A brief personal retrospective*. *Biochimica et Biophysica Acta (BBA) - Biomembranes*, 2007. **1768**(4): p. 748-755.
75. Revankar, C.M., et al., *A transmembrane intracellular estrogen receptor mediates rapid cell signaling*. *Science*, 2005. **307**(5715): p. 1625-1630.
76. Carmeci, C., et al., *Identification of a Gene (GPR30) with Homology to the G-Protein-Coupled Receptor Superfamily Associated with Estrogen Receptor Expression in Breast Cancer*. *Genomics*, 1997. **45**(3): p. 607-617.
77. O'Dowd, B.F., et al., *Discovery of Three Novel G-Protein-Coupled Receptor Genes*. *Genomics*, 1998. **47**(2): p. 310-313.
78. Prossnitz, E.R., J.B. Arterburn, and L.A. Sklar, *GPR30: A G protein-coupled receptor for estrogen*. *Molecular and Cellular Endocrinology*, 2007. **265**: p. 138-142.
79. Gilligan, D., A. Quyyumi, and R. Cannon, *Effects of physiological levels of estrogen on coronary vasomotor function in postmenopausal women*. *Circulation*, 1994. **89**(6): p. 2545-2551.
80. Fu, X.D. and T. Simoncini, *Extra-nuclear signaling of estrogen receptors*. *IUBMB Life*, 2008. **60**(8): p. 502-510.

81. Fu, X.D. and T. Simoncini, *Non-genomic sex steroid actions in the vascular system*. Seminars in Reproductive Medicine, 2007. **25**(3): p. 178-186.
82. Salom, J.B., et al., *Acute relaxant effects of 17-[beta]-estradiol through non-genomic mechanisms in rabbit carotid artery*. Steroids, 2002. **67**(5): p. 339-346.
83. Nakajima, T., et al., *17 β -Estradiol inhibits the voltage-dependent L-type Ca²⁺ currents in aortic smooth muscle cells*. European Journal of Pharmacology, 1995. **294**(2-3): p. 625-635.
84. Ullrich, N.D., A. Koschak, and K.T. MacLeod, *Oestrogen directly inhibits the cardiovascular L-type Ca²⁺ channel Ca(v)1.2*. Biochemical and Biophysical Research Communications, 2007. **361**(2): p. 522-527.
85. Rubio-Gayosso, I., et al., *17[beta]-Estradiol Increases Intracellular Calcium Concentration Through a Short-Term and Nongenomic Mechanism in Rat Vascular Endothelium in Culture*. Journal of Cardiovascular Pharmacology, 2000. **36**(2): p. 196-202.
86. Geng, Y.J., M. Almqvist, and G.K. Hansson, *cDNA cloning and expression of inducible nitric-oxide synthase from rat vascular smooth-muscle cells*. Biochimica Et Biophysica Acta-Gene Structure and Expression, 1994. **1218**(3): p. 421-424.
87. Kaku, Y., et al., *Differential induction of constitutive and inducible nitric oxide synthases by distinct inflammatory stimuli in bovine aortic endothelial cells*. Biochimica et Biophysica Acta (BBA) - Molecular Cell Research, 1997. **1356**(1): p. 43-52.

88. Mershon, J.L., R.S. Baker, and K.E. Clark, *Estrogen increases iNOS expression in the ovine coronary artery*. American Journal of Physiology - Heart and Circulatory Physiology, 2002. **283**(3): p. H1169-H1180.
89. Schubert, R., T. Noack, and V.N. Serebryakov, *Protein kinase C reduces the K(Ca) current of rat tail artery smooth muscle cells*. American Journal of Physiology-Cell Physiology, 1999. **276**(3): p. C648-C658.
90. Nelson, M.T. and J.M. Quayle, *Physiological roles and properties of potassium channels in arterial smooth muscle*. American Journal of Physiology - Cell Physiology, 1995. **268**(4): p. C799-C822.
91. Zhou, X.B., et al., *A molecular switch for specific stimulation of the BKCa channel by cGMP and cAMP kinase*. Journal of Biological Chemistry, 2001. **276**(46): p. 43239-43245.
92. Zhou, X.B., et al., *Dual role of protein kinase C on BK channel regulation*. Proceedings of the National Academy of Sciences of the United States of America, 2010. **107**(17): p. 8005-8010.
93. Nelson, M.T. and J.M. Quayle, *Physiological roles and properties of potassium channels in arterial smooth muscle*. American Journal of Physiology-Cell Physiology, 1995. **268**(4): p. C799-C822.
94. Jaggar, J.H., et al., *Calcium sparks in smooth muscle*. American Journal of Physiology-Cell Physiology, 2000. **278**(2): p. C235-C256.
95. Peng, W., J.R. Hoidal, and I.S. Farrukh, *Regulation of Ca²⁺-activated K⁺ channels in pulmonary vascular smooth muscle cells: Role of nitric oxide*. Journal of Applied Physiology, 1996. **81**(3): p. 1264-1272.

96. White, R.E., D.J. Darkow, and J.L.F. Lang, *Estrogen relaxes coronary arteries by opening BKCa channels through a cGMP-dependent mechanism*. *Circulation Research*, 1995. **77**(5): p. 936-942.
97. Toro, L., et al., *Maxi-KCa, a Unique Member of the Voltage-Gated K Channel Superfamily*. *News Physiol Sci*, 1998. **13**(3): p. 112-117.
98. Tsengcrank, J., et al., *Cloning, expression, and distribution of functionally distinct Ca²⁺-activated K⁺ channel isoforms from human brain*. *Neuron*, 1994. **13**(6): p. 1315-1330.
99. Saito, M., et al., *A cysteine-rich domain defined by a novel exon in a slo variant in rat adrenal chromaffin cells and PC12 cells*. *J. Biol. Chem.*, 1997. **272**: p. 11710-11717.
100. Taniguchi, J., K. Furukawa, and M. Shigekawa, *Maxi K⁺ channels are stimulated by cyclic guanosine monophosphate-dependent protein kinase in canine coronary artery smooth muscle cells*. *Pflugers Archiv-European Journal of Physiology*, 1993. **423**(3-4): p. 167-172.
101. Valverde, M.A., et al., *Activation of Maxi-K channel (hslo) by 17 beta-estradiol requires coexpression of alpha and beta subunits*. *Biophysical Journal*, 1999. **76**(1): p. A186-A186.
102. Valverde, M.A., et al., *Acute activation of Maxi-K channels (hSlo) by estradiol binding to the beta subunit*. *Science*, 1999. **285**(5435): p. 1929-1931.
103. Dick, G.M. and K.M. Sanders, *(Xeno)estrogen sensitivity of smooth muscle BK channels conferred by the regulatory beta 1 subunit - A study of beta 1 knockout mice*. *Journal of Biological Chemistry*, 2001. **276**(48): p. 44835-44840.

104. Dick, G.M., A.C. Hunter, and K.M. Sanders, *Ethylbromide tamoxifen, a membrane-impermeant antiestrogen, activates smooth muscle calcium-activated large-conductance potassium channels from the extracellular side*. *Molecular Pharmacology*, 2002. **61**(5): p. 1105-1113.
105. Tomas, M., et al., *Genetic variation in the KCNMA1 potassium channel alpha subunit as risk factor for severe essential hypertension and myocardial infarction*. *Journal of Hypertension*, 2008. **26**(11): p. 2147-2153.
106. Hu, S., et al., *Variants of the KCNMB3 regulatory subunit of maxi BK channels affect channel inactivation*. *Physiological Genomics*, 2003. **15**(3): p. 191-198.
107. Yang, J.Q., et al., *An Epilepsy/Dyskinesia-Associated Mutation Enhances BK Channel Activation by Potentiating Ca²⁺ Sensing*. *Neuron*, 2010. **66**(6): p. 871-883.
108. Lorenz, S., et al., *Allelic association of a truncation mutation of the KCNMB3 gene with idiopathic generalized epilepsy*. *American Journal of Medical Genetics Part B: Neuropsychiatric Genetics*, 2007. **144B**(1): p. 10-13.
109. Siemer, C., et al., *Effects of NS1608 on MaxiK Channels in Smooth Muscle Cells from Urinary Bladder*. *Journal of Membrane Biology*, 2000. **173**(1): p. 57-66.
110. Olesen, S.-P., et al., *Selective activation of Ca²⁺-dependent K⁺ channels by novel benzimidazolone*. *European Journal of Pharmacology*, 1994. **251**(1): p. 53-59.

111. McManus, O.B., et al., *An activator of calcium-dependent potassium channels isolated from a medicinal herb*. *Biochemistry*, 1993. **32**(24): p. 6128-6133.
112. Olesen, S.P., F. Watjen, and A.G. Hayes, *A novel benzimidazolone, NS004, activates large-conductance Ca²⁺-dependent K⁺ channels in aortic smooth muscle*. *British Journal of Pharmacology*, 1993. **110**: p. 25.
113. Nardi, A. and S.P. Olesen, *BK channel modulators: A comprehensive overview*. *Current Medicinal Chemistry*, 2008. **15**(11): p. 1126-1146.
114. Tanaka, M., et al., *A novel pyrrole derivative, NS-8, activated the Ca²⁺-sensitive K⁺-channels and suppresses micturition reflex in rats*. *Journal of Urology*, 1998. **159**(5): p. 21.
115. Tanaka, M., et al., *A novel pyrrole derivative, NS-8, suppresses the rat micturition reflex by inhibiting afferent pelvic nerve activity*. *BJU International*, 2003. **92**(9): p. 1031-1036.
116. Hewawasam, P., et al., *The synthesis and characterization of BMS-204352 (MaxiPost(TM)) and related 3-fluorooxindoles as openers of maxi-K potassium channels*. *Bioorganic & Medicinal Chemistry Letters*, 2002. **12**(7): p. 1023-1026.
117. Cheney, J.A., et al., *The Maxi-K Channel Opener BMS-204352 Attenuates Regional Cerebral Edema and Neurologic Motor Impairment After Experimental Brain Injury*. *J. Cereb. Blood Flow Metab.*, 2001. **21**(4): p. 396-403.

118. Calderone, V., *Large-conductance, Ca²⁺-activated K⁺ channels: Function, pharmacology and drugs*. *Current Medicinal Chemistry*, 2002. **9**(14): p. 1385-1395.
119. Arshad, S.H., et al., *Andolast, a Novel Calcium-activated Potassium-channel Opener, Inhibits AMP+Exercise Induced Bronchoconstriction in Asthma*. *Journal of Allergy and Clinical Immunology*, 2007. **119**(1, Supplement 1): p. S307.
120. McKay, M.C., et al., *Opening of large-conductance calcium-activated potassium channels by the substituted benzimidazolone NS004*. *Journal of Neurophysiology*, 1994. **71**(5): p. 1873-1882.
121. Imaizumi, Y., et al., *Molecular Basis of Pimarane Compounds as Novel Activators of Large-Conductance Ca²⁺-Activated K⁺ Channel α -Subunit*. *Molecular Pharmacology*, 2002. **62**(4): p. 836-846.
122. Singh, S.B., et al., *MaxiKdiol - a novel dihydroxyisoprimane as an agonist of maxi-K channels*. *Journal of the Chemical Society-Perkin Transactions 1*, 1994(22): p. 3349-3352.
123. Garcia, M.L., et al., *Potassium channels: from scorpion venoms to high-resolution structure*. *Toxicon*, 2001. **39**(6): p. 739-748.
124. Calderone, V., et al., *Vasorelaxing effects of flavonoids: investigation on the possible involvement of potassium channels*. *Naunyn-Schmiedebergs Archives of Pharmacology*, 2004. **370**(4): p. 290-298.
125. Bukiya, A.N., et al., *Channel beta 2-4 subunits fail to substitute for beta 1 in sensitizing BK channels to lithocholate*. *Biochemical and Biophysical Research Communications*, 2009. **390**(3): p. 995-1000.

126. Bukiya, A.N., et al., *beta(1) (KCNMB1) subunits mediate lithocholate activation of large-conductance Ca²⁺-activated K⁺ channels and dilation in small, resistance-size arteries*. *Molecular Pharmacology*, 2007. **72**(2): p. 359-369.
127. Dick, G.M., *The pure anti-oestrogen ICI 182,780 (Faslodex (TM)) activates large conductance Ca²⁺-activated K⁺ channels in smooth muscle*. *British Journal of Pharmacology*, 2002. **136**(7): p. 961-964.
128. Sha, Y., et al., *Compounds Structurally Related to Tamoxifen as Openers of Large-Conductance Calcium-Activated K⁺ Channel*. *Chemical & Pharmaceutical Bulletin*, 2005. **53**(10): p. 1372-1373.
129. Dick, G.M., et al., *Tamoxifen activates smooth muscle BK channels through the regulatory beta 1 subunit*. *Journal of Biological Chemistry*, 2001. **276**(37): p. 34594-34599.
130. Hu, S. and H.S. Kim, *On the mechanism of the differential effects of NS004 and NS1608 in smooth muscle cells from guinea pig bladder*. *European Journal of Pharmacology*, 1996. **318**(2-3): p. 461-468.
131. Giangiacomo, K.M., et al., *Mechanism of Maxi-K Channel Activation by Dehydrosoyasaponin-I*. *The Journal of General Physiology*, 1998. **112**(4): p. 485-501.
132. Li, Y., et al., *The discovery of novel openers of Ca²⁺-dependent large-conductance potassium channels: Pharmacophore search and physiological evaluation of flavonoids*. *Bioorganic & Medicinal Chemistry Letters*, 1997. **7**(7): p. 759-762.

133. Dong, K., et al., *Endothelium-independent vasorelaxant effect of puerarin on rat thoracic aorta*. *Zhongguo Zhongyao Zazhi (Journal of Chinese Material Medical)*, 2004. **29**(10): p. 981-984.
134. Sun, X.-H., et al., *Activation of Large-Conductance Calcium-Activated Potassium Channels by Puerarin: The Underlying Mechanism of Puerarin-Mediated Vasodilation*. *Journal of Pharmacology and Experimental Therapeutics*, 2007. **323**(1): p. 391-397.
135. Dopico, A.M., J.V. Walsh, and J.J. Singer, *Natural bile acids and synthetic analogues modulate large conductance Ca^{2+} -activated K^+ (BKCa) channel activity in smooth muscle cells*. *Journal of General Physiology*, 2002. **119**(3): p. 251-273.
136. de Wet, H., J.D. Lippiat, and M. Allen, *Analysing Steroid Modulation of BKCa Channels Reconstituted into Planar Lipid Bilayers*, in *Methods in Molecular Biology*, J.D. Lippiat, Editor. 2008. p. 177-186.
137. Allen, M.C., C. Newland, and S.P. Hardy, *Inhibition of ligand-gated cation-selective channels by nonsteroidal antioestrogens*. *European Journal of Neuroscience*, 1998. **10**: p. 66.
138. Valverde, M.A., G.M. Mintenig, and F.V. Sepulveda, *Differential-Effects of Tamoxifen and the halide, I⁻, on 3 Distinguishable Chloride Currents Activated in T84 Intestinal-Cells*. *Pflugers Archiv-European Journal of Physiology*, 1993. **425**(5-6): p. 552-554.
139. Hardy, S.P., C. Defelipe, and M.A. Valverde, *Effect of Tamoxifen on Cationic and Anionic Conductances in C1300 Neuroblastoma-Cells and Isolated Embryonic Rat Hypothalamic Neurons in-Vitro*. *Journal of Physiology-London*, 1995. **487P**: p. P194-P194.

140. Sahebgharani, M., et al., *Volume-activated chloride currents in HeLa cells are blocked by tamoxifen but not by a membrane impermeant quaternary analogue*. Cellular Physiology and Biochemistry, 2001. **11**(2): p. 99-104.
141. Zhang, J.J., et al., *Tamoxifen blocks chloride channels - A possible mechanism for cataract formation*. Journal of Clinical Investigation, 1994. **94**(4): p. 1690-1697.
142. Zhang, J.J., et al., *Lens opacification by antiestrogens - tamoxifen vs ICI-182,780*. British Journal of Pharmacology, 1995. **115**(8): p. 1347-1348.
143. Allen, M.C., et al., *Membrane impermeant antioestrogens discriminate between ligand- and voltage-gated cation channels in NG108-15 cells*. Biochimica Et Biophysica Acta-Biomembranes, 2000. **1509**(1-2): p. 229-236.
144. Dick, G.M., I.D. Kong, and K.M. Sanders, *Effects of anion channel antagonists in canine colonic myocytes: comparative pharmacology of Cl⁻, Ca²⁺ and K⁺ currents*. British Journal of Pharmacology, 1999. **127**(8): p. 1819-1831.
145. Nadal, A., et al., *Nongenomic actions of estrogens and xenoestrogens by binding at a plasma membrane receptor unrelated to estrogen receptor alpha and estrogen receptor beta*. Proceedings of the National Academy of Sciences of the United States of America, 2000. **97**(21): p. 11603-11608.
146. Liu, Y.C., et al., *Inhibitory action of ICI-182,780, an estrogen receptor antagonist, on BKCa channel activity in cultured endothelial cells of*

- human coronary artery*. *Biochemical Pharmacology*, 2003. **66**(10): p. 2053-2063.
147. Auger, S., et al., *Synthesis and Biological-Activities of Thioether Derivatives Related to the Antiestrogens Tamoxifen and ICI-164384*. *Journal of Steroid Biochemistry and Molecular Biology*, 1995. **52**(6): p. 547-565.
148. Frazier, D.T., Narahash.T, and M. Yamada, *Site of action and active form of local anesthetics .2. Experiments with quaternary compounds*. *Journal of Pharmacology and Experimental Therapeutics*, 1970. **171**(1): p. 45-51.
149. Blunt, J.W. and J.B. Stothers, *C-13 NMR-studies. C-13 NMR-spectra of steroids - Survey and commentary*. *Organic Magnetic Resonance*, 1977. **9**(8): p. 439-464.
150. Kirk, D.N., et al., *A survey of the high-field H-1-NMR spectra of the steroid hormones, their hydroxylated derivatives, and related compounds*. *Journal of the Chemical Society-Perkin Transactions 2*, 1990(9): p. 1567-1594.
151. Stevis, P.E., et al., *Differential effects of estradiol and estradiol-BSA conjugates*. *Endocrinology*, 1999. **140**(11): p. 5455-5458.
152. Taguchi, K.M.L.D.Y., *Binding of estrogen receptor with estrogen conjugated to bovine serum albumin (BSA)* *Nucl Recept*;, 2004. **2**(5).
153. Lafleur, M.A., M.M. Handsley, and D.R. Edwards, *Metalloproteinases and their inhibitors in angiogenesis*. *Expert Reviews in Molecular Medicine*, 2003. **5**(03006628 Cited December 12, 2003).

154. Webb, R.C., *Smooth muscle contraction and relaxation*. Advances in Physiology Education, 2003. **27**(4): p. 201-206.
155. Ganitkevich, V.Y. and G. Isenberg, *Contribution of Ca²⁺-induced Ca²⁺ release to the [Ca²⁺]_i transients in myocytes from guinea-pig urinary-bladder*. Journal of Physiology-London, 1992. **458**: p. 119-137.
156. Wellner, M.C. and G. Isenberg, *Properties of stretch-activated channels in myocytes from the guinea-pig urinary bladder*. Journal of Physiology-London, 1993. **466**: p. 213-227.
157. Loewenstein, W.R., *Junctional inter-cellular communication - The cell-to-cell membrane channel*. Physiological Reviews, 1981. **61**(4): p. 829-913.
158. Davies, P.F., et al., *Endothelial communication. State of the art lecture*. Hypertension, 1988. **11**(6): p. 563a-572.
159. Rozental, R., M. Srinivas, and D.C. Spray, *How to close a gap junction channel. Efficacies and potencies of uncoupling agents*. Methods Mol. Biol., 2001. **154**: p. 447-76.
160. Kameritsch, P., et al., *Nitric oxide specifically reduces the permeability of Cx37-containing gap junctions to small molecules*. Journal of Cellular Physiology, 2005. **203**(1): p. 233-242.
161. Yao, J., et al., *Nitric oxide-mediated regulation of connexin43 expression and gap junctional intercellular communication in mesangial cells*. J. Am. Soc. Nephrol., 2005. **16**(1): p. 58-67.
162. Figueroa, X.F. and B.R. Duling, *Gap Junctions in the Control of Vascular Function*. Antioxidants & Redox Signaling, 2009. **11**(2): p. 251-266.

163. Figueroa, X.F., B.E. Isakson, and B.R. Duling, *Vascular gap junctions in hypertension*. *Hypertension*, 2006. **48**(5): p. 804-811.
164. Brink, P.R., *Gap junctions in vascular smooth muscle*. *Acta Physiologica Scandinavica*, 1998. **164**(4): p. 349-356.
165. van Kempen, M.J.A. and H.J. Jongsma, *Distribution of connexin37, connexin40 and connexin43 in the aorta and coronary artery of several mammals*. *Histochemistry and Cell Biology*, 1999. **112**(6): p. 479-486.
166. Hill, C.E., et al., *Heterogeneity in the distribution of vascular gap junctions and connexins: Implications for function*. *Clinical and Experimental Pharmacology and Physiology*, 2002. **29**(7): p. 620-625.
167. Rummery, N.M., et al., *Connexin37 is the major connexin expressed in the media of caudal artery*. *Arteriosclerosis Thrombosis and Vascular Biology*, 2002. **22**(9): p. 1427-1432.
168. Busse, R., et al., *EDHF: bringing the concepts together*. *Trends in Pharmacological Sciences*, 2002. **23**(8): p. 374-380.
169. Sandow, S.L. and C.E. Hill, *Incidence of myoendothelial gap junctions in the proximal and distal mesenteric arteries of the rat is suggestive of a role in endothelium-derived hyperpolarizing factor-mediated responses*. *Circulation Research*, 2000. **86**(3): p. 341-346.
170. Griffith, T.M., *Endothelium-dependent smooth muscle hyperpolarization: do gap junctions provide a unifying hypothesis?* *British Journal of Pharmacology*, 2004. **141**(6): p. 881-903.
171. Sandow, S.L., et al., *What's where and why at a vascular myoendothelial microdomain signalling complex*. *Clinical and Experimental Pharmacology and Physiology*, 2009. **36**(1): p. 67-76.

172. Dora, K.A., J. Xia, and B.R. Duling, *Endothelial cell signaling during conducted vasomotor responses*. American Journal of Physiology-Heart and Circulatory Physiology, 2003. **285**(1): p. H119-H126.
173. Emerson, G.G. and S.S. Segal, *Electrical coupling between endothelial cells and smooth muscle cells in hamster feed arteries - Role in vasomotor control*. Circulation Research, 2000. **87**(6): p. 474-479.
174. Xia, J. and B.R. Duling, *Electromechanical coupling and the conducted vasomotor response*. American Journal of Physiology-Heart and Circulatory Physiology, 1995. **269**(6): p. H2022-H2030.
175. Xia, J., T.L. Little, and B.R. Duling, *Cellular pathways of the conducted electrical response in arterioles of hamster cheek pouch in vitro*. American Journal of Physiology-Heart and Circulatory Physiology, 1995. **269**(6): p. H2031-H2038.
176. Dora, K.A., M.P. Doyle, and B.R. Duling, *Elevation of intracellular calcium in smooth muscle causes endothelial cell generation of NO in arterioles*. Proceedings of the National Academy of Sciences of the United States of America, 1997. **94**(12): p. 6529-6534.
177. Christ, G.J., et al., *Gap junctions in vascular tissues - Evaluating the role of intercellular communication in the modulation of vasomotor tone*. Circulation Research, 1996. **79**(4): p. 631-646.
178. Kamm, K.E. and J.T. Stull, *Myosin phosphorylation, force, and maximal shortening velocity in neurally stimulated tracheal smooth muscle*. American Journal of Physiology, 1985. **249**(3): p. C238-C247.

179. Kamm, K.E. and J.T. Stull, *The function of myosin and myosin light chain kinase phosphorylation in smooth muscle*. Annual Review of Pharmacology and Toxicology, 1985. **25**: p. 593-620.
180. Woodrum, D.A. and C.M. Brophy, *The paradox of smooth muscle physiology*. Molecular and Cellular Endocrinology, 2001. **177**(1-2): p. 135-143.
181. Kimura, K., et al., *Regulation of myosin phosphatase by Rho and Rho-Associated kinase (Rho-kinase)*. Science, 1996. **273**(5272): p. 245-248.
182. Noda, M., et al., *Involvement of rho in GTP-gamma S-induced enhancement of phosphorylation of 20 kDa myosin light chain in vascular smooth muscle cells*. Japanese Journal of Physiology, 1995. **45**(SUPPL. 1): p. S18.
183. Furchgott, R.F. and J.V. Zawadzki, *The obligatory role of endothelial-cells in the relaxation of arterial smooth-muscle by acetylcholine*. Nature, 1980. **288**(5789): p. 373-376.
184. Ignarro, L.J., et al., *Endothelium-derived relaxing factor from pulmonary-artery and vein possesses pharmacological and chemical-properties identical to those of nitric oxide radical*. Circulation Research, 1987. **61**(6): p. 866-879.
185. Palmer, R.M.J., A.G. Ferrige, and S. Moncada, *Nitric oxide release accounts for the biological activity of endothelium-derived relaxing factor*. Nature, 1987. **327**(6122): p. 524-526.
186. Nilius, B., *Signaltransduction in vascular endothelium: the role of intracellular calcium and ion channels*. Verh K Acad Geneesk Belg, 1998. **60**(3): p. 215-50.

187. Nilius, B. and G. Droogmans, *Ion channels and their functional role in vascular endothelium*. *Physiological Reviews*, 2001. **81**(4): p. 1415-1459.
188. Caramori, P.R. and A.J. Zago, *Endothelial dysfunction and coronary artery disease*. *Arq. Bras. Cardiol.*, 2000. **75**(2): p. 163-82.
189. Furchgott, R.F. and P.M. Vanhoutte, *Endothelium-derived relaxing and contracting factors*. *FASEB Journal*, 1989. **3**(9): p. 2007-2018.
190. Moncada, S., et al., *The L-arginine - nitric oxide pathway*. *Journal of Cardiovascular Pharmacology*, 1991. **17**: p. S1-S9.
191. Moncada, S., R.M.J. Palmer, and E.A. Higgs, *The discovery of nitric oxide as the endogenous nitrovasodilator*. *Hypertension*, 1988. **12**(4): p. 365-372.
192. Alderton, W.K., C.E. Cooper, and R.G. Knowles, *Nitric oxide synthases: structure, function and inhibition*. *Biochemical Journal*, 2001. **357**: p. 593-615.
193. Moncada, S. and E.A. Higgs, *The discovery of nitric oxide and its role in vascular biology*. *British Journal of Pharmacology*, 2006. **147**: p. S193-S201.
194. Moncada, S. and A. Higgs, *Mechanisms of disease - The L-arginine nitric oxide pathway*. *New England Journal of Medicine*, 1993. **329**(27): p. 2002-2012.
195. Vanhoutte, P.M., *Other endothelium-derived vasoactive factors*. *Circulation*, 1993. **87**(5 SUPPL. 5): p. V9-V17.

196. Feletou, M. and Vanhoute, P.M., *Endothelium-dependent hyperpolarization of vascular smooth muscle cells*. Acta Pharmacologica Sinica, 2000. **21**(1): p. 1-18.
197. Feletou, M. and P.M. Vanhoutte, *Third pathway: Endothelium-dependent hyperpolarization*. Drug Development Research, 2003. **58**(1): p. 18-22.
198. Vanhoutte, P.M., *Say NO to ET*. Journal of the Autonomic Nervous System, 2000. **81**(1-3): p. 271-277.
199. Kapela, A., S. Nagaraja, and N.M. Tsoukias, *A mathematical model of vasoreactivity in rat mesenteric arterioles. II. Conducted vasoreactivity*. American Journal of Physiology-Heart and Circulatory Physiology. **298**(1): p. H52-H65.
200. Taylor, M.S., et al., *Altered expression of small-conductance Ca^{2+} -activated K^+ (SK3) channels modulates arterial tone and blood pressure*. Circulation Research, 2003. **93**(2): p. 124-131.
201. Feletou, M., *Calcium-activated potassium channels and endothelial dysfunction: therapeutic options?* British Journal of Pharmacology, 2009. **156**(4): p. 545-562.
202. Brakemeier, S., et al., *Modulation of Ca^{2+} -activated K^+ channel in renal artery endothelium in situ by nitric oxide and reactive oxygen species*. Kidney International, 2003. **64**(1): p. 199-207.
203. Kohler, R., et al., *Expression and function of endothelial Ca^{2+} -activated K^+ channels in human mesenteric artery - A single-cell reverse transcriptase-polymerase chain reaction and electrophysiological study in situ*. Circulation Research, 2000. **87**(6): p. 496-503.

204. Neylon, C.B., et al., *Molecular cloning and characterization of the intermediate-conductance Ca^{2+} -activated K^+ channel in vascular smooth muscle - Relationship between K-Ca channel diversity and smooth muscle cell function*. *Circulation Research*, 1999. **85**(9): p. E33-E43.
205. Feletou, M. and P.M. Vanhoutte, *Endothelium-derived hyperpolarizing factor - Where are we now?* *Arteriosclerosis Thrombosis and Vascular Biology*, 2006. **26**(6): p. 1215-1225.
206. Gutterman, D.D., H. Miura, and Y.P. Liu, *Redox modulation of vascular tone - Focus of potassium channel mechanisms of dilation*. *Arteriosclerosis Thrombosis and Vascular Biology*, 2005. **25**(4): p. 671-678.
207. Burnham, M.P., et al., *Characterization of an apamin-sensitive small-conductance Ca^{2+} -activated K^+ channel in porcine coronary artery endothelium: relevance to EDHF*. *British Journal of Pharmacology*, 2002. **135**(5): p. 1133-1143.
208. Papassotiriou, J., et al., *Endothelial K^+ channel lacks the Ca^{2+} sensitivity-regulating beta subunit*. *FASEB Journal*, 2000. **14**(7): p. 885-894.
209. Tanaka, Y., et al., *Molecular constituents of maxi K-Ca channels in human coronary smooth muscle: predominant alpha+beta subunit complexes*. *Journal of Physiology-London*, 1997. **502**(3): p. 545-557.
210. Kamouchi, M., et al., *Functional effects of expression of hsl α Ca^{2+} activated K^+ channels in cultured macrovascular endothelial cells*. *Cell Calcium*, 1997. **22**(6): p. 497-506.

211. Nimigean, C.M. and K.L. Magleby, *The beta Subunit Increases the Ca^{2+} Sensitivity of Large Conductance Ca^{2+} -activated Potassium Channels by Retaining the Gating in the Bursting States*. J. Gen. Physiol., 1999. **113**(3): p. 425-440.
212. Nimigean, C.M. and K.L. Magleby, *Functional coupling of the beta(1) subunit to the large conductance Ca^{2+} -activated K^+ channel in the absence of Ca^{2+} - Increased Ca^{2+} sensitivity from a Ca^{2+} -independent mechanism*. Journal of General Physiology, 2000. **115**(6): p. 719-734.
213. Sobey, C.G., D.D. Heistad, and F.M. Faraci, *Potassium channels mediate dilatation of cerebral arterioles in response to arachidonate*. American Journal of Physiology-Heart and Circulatory Physiology, 1998. **275**(5): p. H1606-H1612.
214. Sobey, C.G. and F.M. Faraci, *Effect of nitric oxide and potassium channel agonists and inhibitors on basilar artery diameter*. Am. J. Physiol. Heart Circ. Physiol., 1997. **272**(1): p. H256-262.
215. Sobey, C.G., D.D. Heistad, and F.M. Faraci, *Mechanisms of Bradykinin-Induced Cerebral Vasodilatation in Rats : Evidence That Reactive Oxygen Species Activate K^+ Channels*. Stroke, 1997. **28**(11): p. 2290-2295.
216. Lu, T., et al., *Dihydroxyeicosatrienoic acids are potent activators of Ca^{2+} -activated K^+ channels in isolated rat coronary arterial myocytes*. Journal of Physiology-London, 2001. **534**(3): p. 651-667.
217. Calderone, V., et al., *Functional contribution of the endothelial component to the vasorelaxing effect of resveratrol and NS 1619, activators of the large-conductance calcium-activated potassium*

- channels*. Naunyn-Schmiedeberg's Archives of Pharmacology, 2007. **375**(1): p. 73-80.
218. Jiang, C.W., et al., *Endothelium-independent relaxation of rabbit coronary artery by 17beta-estradiol in vitro*. British Journal of Pharmacology, 1991. **104**(4): p. 1033-1037.
219. Freay, A.D., et al., *Mechanism of Vascular Smooth Muscle Relaxation by Estrogen in Depolarized Rat and Mouse Aorta : Role of Nuclear Estrogen Receptor and Ca²⁺ Uptake*. Circ. Res., 1997. **81**(2): p. 242-248.
220. Gilligan, D.M., et al., *Effects of estrogen replacement therapy on peripheral vasomotor function in postmenopausal women*. American Journal of Cardiology, 1995. **75**(4): p. 264-268.
221. White, R.E., et al., *Endothelium-independent effect of estrogen on Ca²⁺-activated K⁺ channels in human coronary artery smooth muscle cells*. Cardiovascular Research, 2002. **53**(3): p. 650-661.
222. Lydrup, M.L. and B.O. Nilsson, *Acute and long-term effects of 17 beta-oestradiol on agonist-stimulated force in rat tail artery*. Acta Physiologica Scandinavica, 1996. **158**(3): p. 253-259.
223. Ma, L.M., et al., *Effect of 17-beta estradiol in the rabbit: Endothelium-dependent and -independent mechanisms of vascular relaxation*. Journal of Cardiovascular Pharmacology, 1997. **30**(1): p. 130-135.
224. Zhang, F., et al., *17beta-estradiol attenuates voltage-dependent Ca²⁺ currents in A7R5 vascular smooth muscle cell line*. American Journal of Physiology, 1994. **266**(4): p. C975-C980.

225. Tep-areenan, P., D.A. Kendall, and M.D. Randall, *Mechanisms of vasorelaxation to 17 beta-oestradiol in rat arteries*. European Journal of Pharmacology, 2003. **476**(1-2): p. 139-149.
226. Kitazawa, T., et al., *Non-genomic mechanism of 17 beta-oestradiol-induced inhibition of contraction in mammalian vascular smooth muscle*. Journal of Physiology-London, 1997. **499**(2): p. 497-511.
227. Park, S., et al., *Tamoxifen induces vasorelaxation via inhibition of mitogen-activated protein kinase in rat aortic smooth muscle*. Journal of Veterinary Medical Science, 2003. **65**(11): p. 1155-1160.
228. Leung, H.S., et al., *Endothelium-independent relaxation to raloxifene in porcine coronary artery*. European Journal of Pharmacology, 2007. **555**(2-3): p. 178-184.
229. Wellman, G.C., et al., *Gender differences in coronary artery diameter involve estrogen, nitric oxide, and Ca²⁺-dependent K⁺ channels*. Circulation Research, 1996. **79**(5): p. 1024-1030.
230. Mugge, A., et al., *Endothelium-independent relaxation of human coronary arteries by 17beta-estradiol in vitro*. Cardiovascular Research, 1993. **27**(11): p. 1939-1942.
231. Jiang, C., et al., *Effect of 17beta-estradiol on contraction, Ca²⁺ current and intracellular free Ca-2+ in guinea-pig isolated cardiac myocytes*. British Journal of Pharmacology, 1992. **106**(3): p. 739-745.
232. Node, K., et al., *Roles of NO and Ca²⁺-activated K⁺ channels in coronary vasodilation induced by 17 beta-estradiol in ischemic heart failure*. FASEB Journal, 1997. **11**(10): p. 793-799.

233. Ru, X.-c., et al., *Ethanol induced relaxation of rat thoracic aorta at different resting tension and its possible mechanism*. FASEB Journal, 2007. **21**(6): p. A1164.
234. Rubanyi, G.M., et al., *Vascular estrogen receptors and endothelium-derived nitric oxide production in the mouse aorta - Gender difference and effect of estrogen receptor gene disruption*. Journal of Clinical Investigation, 1997. **99**(10): p. 2429-2437.
235. Maher, J., et al., *Smooth muscle relaxation and activation of the large conductance Ca^{2+} – activated K^+ (BKCa) channel by novel oestrogens*. British Journal of Pharmacology, 2013. **169**(5): p. 1153-1165.
236. Batenburg, W.W., et al., *Angiotensin II aldosterone interaction in human coronary microarteries involves GPR30, EGFR, and endothelial NO synthase*. Cardiovascular Research, 2012. **94**(1): p. 136-143.
237. Broughton, B.R.S., A.A. Miller, and C.G. Sobey, *Endothelium-dependent relaxation by G protein-coupled receptor 30 agonists in rat carotid arteries*. American Journal of Physiology-Heart and Circulatory Physiology, 2010. **298**(3): p. H1055-H1061.
238. Haynes, M.P., et al., *Membrane estrogen receptor engagement activates endothelial nitric oxide synthase via the PI3-kinase-Akt pathway in human endothelial cells*. Circulation Research, 2000. **87**(8): p. 677-682.
239. Russell, K.S., et al., *Human vascular endothelial cells contain membrane binding sites for estradiol, which mediate rapid intracellular signaling*. Proceedings of the National Academy of Sciences, 2000. **97**(11): p. 5930-5935.

240. Kannel, W.B., et al., *Menopause and risk of cardiovascular-disease - Framingham study*. Annals of Internal Medicine, 1976. **85**(4): p. 447-452.
241. Gordon, T., et al., *Menopause and coronary heart-disease-Framingham study*. Annals of Internal Medicine, 1978. **89**(2): p. 157-161.
242. Harrington, W.R., et al., *Estrogen Dendrimer Conjugates that Preferentially Activate Extranuclear, Nongenomic Versus Genomic Pathways of Estrogen Action*. Molecular Endocrinology, 2006. **20**(3): p. 491-502.
243. Mendelsohn, M.E., *Mechanisms of estrogen action in the cardiovascular system*. The Journal of Steroid Biochemistry and Molecular Biology, 2000. **74**(5): p. 337-343.
244. Li, L., M.P. Haynes, and J.R. Bender, *Plasma membrane localization and function of the estrogen receptor alpha variant (ER46) in human endothelial cells*. Proceedings of the National Academy of Sciences of the United States of America, 2003. **100**(8): p. 4807-4812.
245. Sribnick, E.A., et al., *Estrogen attenuates glutamate-induced cell death by inhibiting Ca^{2+} influx through L-type voltage-gated Ca^{2+} channels*. Brain Research, 2009. **1276**: p. 159-170.
246. Cairrao, E., et al., *Non-genomic vasorelaxant effects of 17 beta-estradiol and progesterone on rat aorta are mediated by L-type Ca^{2+} current inhibition*. Acta Pharmacologica Sinica, 2012. **33**(5): p. 615-624.

247. Prossnitz, E.R., et al., *GPR30: a novel therapeutic target in estrogen-related disease*. Trends in Pharmacological Sciences, 2008. **29**(3): p. 116-123.
248. Han, G.C., et al., *Nongenomic, endothelium-independent effects of estrogen on human coronary smooth muscle are mediated by type I (neuronal) NOS and PI3-kinase-Akt signaling*. American Journal of Physiology-Heart and Circulatory Physiology, 2007. **293**(1): p. H314-H321.
249. Lekontseva, O., et al., *Role of Neuronal Nitric-Oxide Synthase in Estrogen-Induced Relaxation in Rat Resistance Arteries*. Journal of Pharmacology and Experimental Therapeutics, 2011. **339**(2): p. 367-375.
250. Royal, C.R., et al., *Estrogen signaling in microvascular arteries: Parturition reduces vasodilation by reducing 17 β -estradiol and nNOS*. Steroids, 2011. **76**(10–11): p. 991-997.
251. Morrow, J.P., et al., *Defining the BK channel domains required for beta 1-subunit modulation*. Proceedings of the National Academy of Sciences of the United States of America, 2006. **103**(13): p. 5096-5101.
252. Figtree, G.A., C.M. Webb, and P. Collins, *Tamoxifen acutely relaxes coronary arteries by an endothelium-, nitric oxide-, and estrogen receptor-dependent mechanism*. Journal of Pharmacology and Experimental Therapeutics, 2000. **295**(2): p. 519-523.
253. Leung, H.S., et al., *Tamoxifen dilates porcine coronary arteries: roles for nitric oxide and ouabain-sensitive mechanisms*. British Journal of Pharmacology, 2006. **149**(6): p. 703-711.

254. Wickman, G. and B. Vollrath, *Effects of tamoxifen on oxyhemoglobin-induced cerebral vasoconstriction*. European Journal of Pharmacology, 2000. **390**(1-2): p. 181-184.
255. Hutchison, S.J., et al., *Tamoxifen is an acute, estrogen-like, coronary vasodilator of porcine coronary arteries in vitro*. Journal of Cardiovascular Pharmacology, 2001. **38**(5): p. 657-665.
256. Cui, Y.-M., et al., *Novel oxime and oxime ether derivatives of 12,14-dichlorodehydroabiatic acid: Design, synthesis, and BK channel-opening activity*. Bioorganic & Medicinal Chemistry Letters, 2008. **18**(24): p. 6386-6389.
257. Bartik, P., et al., *Diaphorase can metabolize some vasorelaxants to NO and eliminate NO scavenging effect of 2-phenyl-4,4,5,5-tetramethylimidazoline-1-oxyl-3-oxide (PTIO)*. Physiological Research, 2004. **53**(6): p. 615-620.
258. Vetrovsky, P., et al., *Involvement of NO in the Endothelium-Independent Relaxing Effects of N ω-Hydroxy-l-arginine and Other Compounds Bearing a C=NOH Function in the Rat Aorta*. Journal of Pharmacology and Experimental Therapeutics, 2002. **303**(2): p. 823-830.
259. Jousserandot, A., et al., *Microsomal Cytochrome P450 Dependent Oxidation of N-Hydroxyguanidines, Amidoximes, and Ketoximes: Mechanism of the Oxidative Cleavage of Their CN(OH) Bond with Formation of Nitrogen Oxides*. Biochemistry, 1998. **37**(49): p. 17179-17191.

260. Mansuy, D., J.L. Boucher, and B. Clement, *On the mechanism of nitric oxide formation upon oxidative cleavage of C-N(OH) bonds by NO-synthases and cytochromes P450*. *Biochimie*, 1995. **77**(7-8): p. 661-667.
261. Chalupsky, K., et al., *Relaxant effect of oxime derivatives in isolated rat aorta: role of nitric oxide (NO) formation in smooth muscle*. *Biochemical Pharmacology*, 2004. **67**(6): p. 1203-1214.
262. Fernandes, V., et al., *Mechanisms involved in the nitric oxide-induced vasorelaxation in porcine prostatic small arteries*. *Naunyn-Schmiedeberg's Archives of Pharmacology*, 2011. **384**(3): p. 245-253.
263. Ahern, G.P., S.-F. Hsu, and M.B. Jackson, *Direct actions of nitric oxide on rat neurohypophysial K⁺ channels*. *The Journal of Physiology*, 1999. **520**(1): p. 165-176.
264. Zhou, X.B., et al., *Regulation of stably expressed and native BK channels from human myometrium by cGMP- and cAMP-dependent protein kinase*. *Pflugers Archiv-European Journal of Physiology*, 1998. **436**(5): p. 725-734.
265. Daneshtalab, N. and J.S. Smeda, *Alterations in the modulation of cerebrovascular tone and blood flow by nitric oxide synthases in SHRsp with stroke*. *Cardiovascular Research*, 2010. **86**(1): p. 160-168.
266. Seddon, M.D., et al., *Neuronal Nitric Oxide Synthase Regulates Basal Microvascular Tone in Humans In Vivo*. *Circulation*, 2008. **117**(15): p. 1991-1996.
267. Capettini, L.S.A., et al., *Neuronal nitric oxide synthase-derived hydrogen peroxide is a major endothelium-dependent relaxing factor*.

- American Journal of Physiology - Heart and Circulatory Physiology, 2008. **295**(6): p. H2503-H2511.
268. Han, G.C., et al., *Essential Role of the 90-Kilodalton Heat Shock Protein in Mediating Nongenomic Estrogen Signaling in Coronary Artery Smooth Muscle*. Journal of Pharmacology and Experimental Therapeutics, 2009. **329**(3): p. 850-855.
269. Leung, Y.-K., et al., *Estrogen receptor (ER)- β isoforms: A key to understanding ER- β signaling*. Proceedings of the National Academy of Sciences, 2006. **103**(35): p. 13162-13167.
270. Chantzi, N.I., et al., *Insights into ectopic estrogen receptor expression, nucleocytoplasmic distribution and interaction with chromatin obtained with new antibodies to estrogen receptors α and β* . Steroids, 2011. **76**(10–11): p. 974-985.
271. Filardo, E., et al., *Activation of the Novel Estrogen Receptor G Protein-Coupled Receptor 30 (GPR30) at the Plasma Membrane*. Endocrinology, 2007. **148**(7): p. 3236-3245.
272. Rai, M. and H. Padh, *Expression systems for production of heterologous proteins*. Current Science, 2001. **80**(9): p. 1121-1128.
273. Theodoulou, F.L. and A.J. Miller, *Xenopus oocytes as a heterologous expression system*, in *Methods in Molecular Biology; Plant gene transfer and expression protocols*, H. Jones, Editor. 1995, Humana Press Inc. {a}. p. 317-340.
274. Tammaro, P., K. Shimomura, and P. Proks, *Xenopus oocytes as a heterologous expression system for studying ion channels with the patch-clamp technique*. Methods Mol. Biol., 2008. **491**: p. 127-39.

275. Sigel, E., *Use of xenopus oocytes for the functional expression of plasma membrane proteins*. Journal of Membrane Biology, 1990. **117**(3): p. 201-221.
276. Sigel, E. and F. Minier, *The Xenopus oocyte: System for the study of functional expression and modulation of proteins*. Molecular Nutrition & Food Research, 2005. **49**(3): p. 228-234.
277. Hediger, M.A., et al., *Expression of size-selected messenger-rna encoding the intestinal na/glucose co-transporter in Xenopus-laevis oocytes*. Proceedings of the National Academy of Sciences of the United States of America, 1987. **84**(9): p. 2634-2637.
278. Miledi, R., I. Parker, and K. Sumikawa, *Properties of acetylcholine receptors translated by cat muscle messenger-rna in Xenopus oocytes*. Embo Journal, 1982. **1**(11): p. 1307-1312.
279. Miledi, R., I. Parker, and K. Sumikawa, *Synthesis of chick brain GABA receptors by frog oocytes*. Proceedings of the Royal Society of London Series B-Biological Sciences, 1982. **216**(1205): p. 509-515.
280. Goldin, A.L., *Expression of Ion Channels in Xenopus Oocytes*. Expression and Analysis of Recombinant Ion Channels. 2006: Wiley-VCH Verlag GmbH & Co. KGaA. 1-25.
281. Sanguinetti, M.C., et al., *Coassembly of K(v)LQT1 and minK (IsK) proteins to form cardiac I-Ks potassium channel*. Nature, 1996. **384**(6604): p. 80-83.
282. Shcherbatko, A., et al., *Voltage-dependent sodium channel function is regulated through membrane mechanics*. Biophysical Journal, 1999. **77**(4): p. 1945-1959.

283. Wagner, C.A., et al., *The use of Xenopus laevis oocytes for the functional characterization of heterologously expressed membrane proteins*. Cellular Physiology and Biochemistry, 2000. **10**(1-2): p. 1-12.
284. Jiang, B., et al., *Endogenous K-V channels in human embryonic kidney (HEK-293) cells*. Molecular and Cellular Biochemistry, 2002. **238**(1-2): p. 69-79.
285. Petersen, K.R. and J.M. Nerbonne, *Expression environment determines K⁺ current properties: Kv1 and Kv4 alpha-subunit-induced K⁺ currents in mammalian cell lines and cardiac myocytes*. Pflugers Archiv-European Journal of Physiology, 1999. **437**(3): p. 381-392.
286. Seebohm, G., et al., *Dependence of I-Ks biophysical properties on the expression system*. Pflugers Archiv-European Journal of Physiology, 2001. **442**(6): p. 891-895.
287. Zhang, Z.M., Y.F. Tang, and M.X. Zhu, *Increased inwardly rectifying potassium currents in HEK-293 cells expressing murine transient receptor potential 4*. Biochemical Journal, 2001. **354**: p. 717-725.
288. Uebele, V.N., et al., *Functional differences in Kv1.5 currents expressed in mammalian cell lines are due to the presence of endogenous Kv beta 2.1 subunits*. Journal of Biological Chemistry, 1996. **271**(5): p. 2406-2412.
289. Graham, F.L., et al., *Characteristics of a human cell line transformed by DNA from human adenovirus type-5*. Journal of General Virology, 1977. **36**(JUL): p. 59-72.

290. Shaw, G., et al., *Preferential transformation of human neuronal cells by human adenoviruses and the origin of HEK 293 cells*. FASEB Journal, 2002. **16**(6): p. 869-871.
291. Thomas, P. and T.G. Smart, *HEK293 cell line: A vehicle for the expression of recombinant proteins*. Journal of Pharmacological and Toxicological Methods, 2005. **51**(3): p. 187-200.
292. Yu, S.P. and G.A. Kerchner, *Endogenous voltage-gated potassium channels in human embryonic kidney (HEK293) cells*. Journal of Neuroscience Research, 1998. **52**(5): p. 612-617.
293. Avila, G., A. Sandoval, and R. Felix, *Intramembrane charge movement associated with endogenous K⁺ channel activity in HEK-293 cells*. Cellular and Molecular Neurobiology, 2004. **24**(3): p. 317-330.
294. Ukomadu, C., et al., *MU-1 NA⁺ channels expressed transiently in human embryonic kidney-cells - biochemical and biophysical properties*. Neuron, 1992. **8**(4): p. 663-676.
295. Moran, O., M. Nizzari, and F. Conti, *Endogenous expression of the beta 1A sodium channel subunit in HEK-293 cells*. FEBS Letters, 2000. **473**(2): p. 132-134.
296. Berjukow, S., et al., *Endogenous calcium channels in human embryonic kidney (HEK293) cells*. British Journal of Pharmacology, 1996. **118**(3): p. 748-754.
297. Gunthorpe, N.J., et al., *Characterisation of a human acid-sensing ion channel (hASIC1a) endogenously expressed in HEK293 cells*. Pflugers Archiv-European Journal of Physiology, 2001. **442**(5): p. 668-674.

298. Mignen, O. and T.J. Shuttleworth, *Permeation of monovalent cations through the non-capacitative arachidonate-regulated Ca²⁺ Channels in HEK293 cells - Comparison with endogenous store-operated channels.* Journal of Biological Chemistry, 2001. **276**(24): p. 21365-21374.
299. Zhu, G.Y., et al., *Identification of endogenous outward currents in the human embryonic kidney (HEK 293) cell line.* Journal of Neuroscience Methods, 1998. **81**(1-2): p. 73-83.
300. Fukao, M., et al., *Cyclic GMP-dependent protein kinase activates cloned BKCa channels expressed in mammalian cells by direct phosphorylation at serine 1072.* Journal of Biological Chemistry, 1999. **274**(16): p. 10927-10935.
301. Ndubuka, C., Y. Li, and C.S. Rubin, *Expression of a kinase anchor protein-75 depletes type-II camp-dependent protein kinases from the cytoplasm and sequesters the kinases in a particulate pool.* Journal of Biological Chemistry, 1993. **268**(11): p. 7621-7624.
302. Li, Y., C. Ndubuka, and C.S. Rubin, *A Kinase Anchor Protein 75 Targets Regulatory (RII) Subunits of cAMP-dependent Protein Kinase II to the Cortical Actin Cytoskeleton in Non-neuronal Cells.* Journal of Biological Chemistry, 1996. **271**(28): p. 16862-16869.
303. Zagranichnaya, T.K., X.Y. Wu, and M.L. Villereal, *Endogenous TRPC1, TRPC3, and TRPC7 proteins combine to form native store-operated channels in HEK-293 cells.* Journal of Biological Chemistry, 2005. **280**(33): p. 29559-29569.
304. Querfurth, H.W., et al., *Expression of ryanodine receptors in human embryonic kidney (HEK293) cells.* Biochem. J., 1998. **334**(1): p. 79-86.

305. Iwata, K., et al., *Bimodal Regulation of the Human H1 Histamine Receptor by G Protein-coupled Receptor Kinase 2*. Journal of Biological Chemistry, 2005. **280**(3): p. 2197-2204.
306. Varghese, A., et al., *Endogenous channels in HEK cells and potential roles in HCN ionic current measurements*. Progress in Biophysics & Molecular Biology, 2006. **90**(1-3): p. 26-37.
307. Ahring, P.K., et al., *Stable expression of the human large-conductance Ca^{2+} -activated K^+ channel alpha- and beta-subunits in HEK293 cells*. FEBS Letters, 1997. **415**(1): p. 67-70.
308. Latorre, R., C. Vergara, and C. Hidalgo, *Reconstitution in Planar Lipid Bilayers of a Ca^{2+} -Dependent K^+ Channel from Transverse Tubule Membranes Isolated from Rabbit Skeletal Muscle*. PNAS, 1982. **79**(3): p. 805-809.
309. Tang, Q.Y., et al., *Characterization of a Functionally Expressed Stretch-activated BKca Channel Cloned from Chick Ventricular Myocytes*. Journal of Membrane Biology, 2003. **196**(3): p. 185.
310. Fedida, D., R. Bouchard, and F.S.P. Chen, *Slow gating charge immobilization in the human potassium channel Kv1.5 and its prevention by 4-aminopyridine*. Journal of Physiology-London, 1996. **494**(2): p. 377-387.
311. Fedida, D., *Gating charge and ionic currents associated with quinidine block of human Kv1.5 delayed rectifier channels*. Journal of Physiology-London, 1997. **499**(3): p. 661-675.

312. Lindsey, S.H., et al., *Chronic Treatment with the G Protein-Coupled Receptor 30 Agonist G-1 Decreases Blood Pressure in Ovariectomized mRen2.Lewis Rats*. *Endocrinology*, 2009. **150**(8): p. 3753-3758.
313. Eissa, N.T., et al., *Identification of Residues Critical for Enzymatic Activity in the Domain Encoded by Exons 8 and 9 of the Human Inducible Nitric Oxide Synthase*. *American Journal of Respiratory Cell and Molecular Biology*, 2001. **24**(5): p. 616-620.
314. Kolodziejcki, P.J., M.B. Rashid, and N.T. Eissa, *Intracellular formation of "undisruptable" dimers of inducible nitric oxide synthase*. *Proceedings of the National Academy of Sciences*, 2003. **100**(24): p. 14263-14268.
315. Kolodziejcka, K.E., et al., *Regulation of inducible nitric oxide synthase by aggresome formation*. *Proceedings of the National Academy of Sciences of the United States of America*, 2005. **102**(13): p. 4854-4859.
316. Schmidt, K., et al., *Comparison of neuronal and endothelial isoforms of nitric oxide synthase in stably transfected HEK 293 cells*. *American Journal of Physiology - Heart and Circulatory Physiology*, 2001. **281**(5): p. H2053-H2061.
317. Sessa, W.C., et al., *The golgi association of endothelial nitric oxide synthase is necessary for the efficient synthesis of nitric oxide*. *Journal of Biological Chemistry*, 1995. **270**(30): p. 17641-17644.
318. Bischof, G., T.F. Serwold, and T.E. Machen, *Does nitric oxide regulate capacitative Ca influx in HEK 293 cells?* *Cell Calcium*, 1997. **21**(2): p. 135-142.

319. Hamill, O.P., et al., *Improved patch-clamp techniques for high-resolution current recording from cells and cell-free membrane patches*. Pflugers Archiv-European Journal of Physiology, 1981. **391**(2): p. 85-100.
320. Schreiber, M., et al., *Slo3, a novel pH-sensitive K⁺ channel from mammalian spermatocytes*. Journal of Biological Chemistry, 1998. **273**(6): p. 3509-3516.
321. Yuan, A., et al., *SLO-2, a K⁺ channel with an unusual Cl⁻ dependence*. Nature Neuroscience, 2000. **3**(8): p. 771-779.
322. Yuan, A., et al., *The sodium-activated potassium channel is encoded by a member of the Slo gene family*. Neuron, 2003. **37**(5): p. 765-773.
323. Bhattacharjee, A., W.J. Joiner, and L.K. Kaczmarek, *Slick and Slack: Chloride and sodium-activated potassium channels in neurons and other excitable cells*. Journal of General Physiology, 2003. **122**(1): p. 26.
324. Salkoff, L., et al., *High-conductance potassium channels of the SLO family*. Nature Reviews Neuroscience, 2006. **7**(12): p. 921-931.
325. Garcia-Valdes, J., et al., *Slotoxin, [α]KTx1.11, a new scorpion peptide blocker of MaxiK channels that differentiates between [α] and [α]+[β] ([β]1 or [β]4) complexes*. FEBS Letters, 2001. **505**(3): p. 369-373.
326. Candia, S., M.L. Garcia, and R. Latorre, *Mode of Action of Iberiotoxin, a potent blocker of the large conductance Ca²⁺-activated K⁺ channel*. Biophysical Journal, 1992. **63**(2): p. 583-590.

327. Reinhart, P.H., S. Chung, and I.B. Levitan, *A family of calcium-dependent potassium channels from rat brain*. *Neuron*, 1989. **2**: p. 1031-1041.
328. Knaus, H.G., et al., *Covalent attachment of charybdotoxin to the beta-subunit of the high-conductance Ca^{2+} -activated K^+ channel - Identification of the site of incorporation and implications for channel topology*. *Journal of Biological Chemistry*, 1994. **269**(37): p. 23336-23341.
329. Anderson, C., et al., *Charybdotoxin block of single Ca^{2+} -activated K^+ channels. Effects of channel gating, voltage, and ionic strength*. *J. Gen. Physiol.*, 1988. **91**(3): p. 317-333.
330. Mackinnon, R. and C. Miller, *Mechanism of charybdotoxin block of the high-conductance, Ca^{2+} -activated K^+ channel*. *Journal of General Physiology*, 1988. **91**(3): p. 335-349.
331. Egan, T.M., D. Dagan, and I.B. Levitan, *Properties and modulation of a calcium-activated potassium channel in rat olfactory-bulb neurons*. *Journal of Neurophysiology*, 1993. **69**(5): p. 1433-1442.
332. Dun, N.J., Z.G. Jiang, and N. Mo, *Tubocurarine suppresses slow calcium-dependent after-hyperpolarization in guinea-pig inferior mesenteric ganglion-cells*. *Journal of Physiology-London*, 1986. **375**: p. 499-514.
333. Nohmi, M. and K. Kuba, *(+)-Tubocurarine blocks the Ca^{2+} -dependent K^+ channel of the bullfrog sympathetic ganglion cell*. *Brain Research*, 1984. **301**(1): p. 146-148.

334. Smart, T.G., *Single Ca²⁺-activated K⁺ channels recorded from cultured rat sympathetic neurons*. Journal of Physiology-London, 1987. **389**(AUG): p. 337-360.
335. Crest, M., et al., *Kaliotoxin, a novel peptidyl inhibitor of neuronal BK-type Ca²⁺-activated K⁺ channels characterized from Androctonus mauretanicus mauretanicus venom*. J. Biol. Chem., 1992. **267**(3): p. 1640-1647.
336. Knaus, H.-G., et al., *Tremorgenic Indole Alkaloids Potently Inhibit Smooth Muscle High-Conductance Calcium-Activated Potassium Channels*. Biochemistry, 1994. **33**(19): p. 5819-5828.
337. Yellen, G., *Ionic permeation and blockade in Ca²⁺-activated K⁺ channels of bovine chromaffin cells*. Journal of General Physiology, 1984. **84**(2): p. 157-186.
338. Tagliatela, M., et al., *Patterns of internal and external tetraethylammonium block in 4 homologous K⁺ channels*. Molecular Pharmacology, 1991. **40**(2): p. 299-307.
339. Villarroel, A., et al., *Probing a Ca²⁺-activated K⁺ channel with quaternary ammonium ions*. Pflugers Archiv-European Journal of Physiology, 1988. **413**(2): p. 118-126.
340. Li, W. and R.W. Aldrich, *Unique Inner Pore Properties of BK Channels Revealed by Quaternary Ammonium Block*. The Journal of General Physiology, 2004. **124**(1): p. 43-57.
341. Holland, M., et al., *Effects of the BKCa channel activator, NS1619, on rat cerebral artery smooth muscle*. British Journal of Pharmacology, 1996. **117**(1): p. 119-129.

342. Dai, L., V. Garg, and M.C. Sanguinetti, *Activation of Slo2.1 channels by niflumic acid*. Journal of General Physiology, 2010. **135**(3): p. 275-295.
343. Yang, B., et al., *Pharmacological activation and inhibition of Slack (Slo2.2) channels*. Neuropharmacology, 2006. **51**(4): p. 896-906.
344. Biton, B., et al., *The antipsychotic drug loxapine is an opener of the Na⁺-activated potassium channel Slack (slo2.2)*. Journal of Pharmacology and Experimental Therapeutics, 2012. **340**(3): p.706-715.
345. Leonetti, M.D., et al., *Functional and structural analysis of the human SLO3 pH- and voltage-gated K⁺ channel*. Proceedings of the National Academy of Sciences of the United States of America, 2012. **109**(47): p. 19274-19279.
346. Adelman, J.P., et al., *Calcium-activated potassium channels expressed from cloned complementary DNAs*. Neuron, 1992. **9**(2): p. 209-216.
347. Saito, M. and C.F. Wu, *Expression of Ion Channels and Mutational Effects in Giant Drosophila Neurons Differentiated from Cell-Division Arrested Embryonic Neuroblasts*. Journal of Neuroscience, 1991. **11**(7): p. 2135-2150.
348. Dworetzky, S.I., J.T. Trojnacki, and V.K. Gribkoff, *Cloning and expression of a human large-conductance calcium-activated potassium channel*. Molecular Brain Research, 1994. **27**(1): p. 189-193.
349. Rittenhouse, A.R., *PIP2 PIP2 hooray for maxi K⁺*. The Journal of General Physiology, 2008. **132**(1): p. 5-8.

350. Lagrutta, A., et al., *Functional differences among alternatively spliced variants of Slowpoke, a Drosophila calcium-activated potassium channel*. J. Biol. Chem., 1994. **269**(32): p. 20347-20351.
351. Navaratnam, D.S., et al., *Differential distribution of Ca²⁺-activated K⁺ channel splice variants among hair cells along the tonotopic axis of the chick cochlea*. Neuron, 1997. **19**(5): p. 1077-1085.
352. Lagrutta, A., et al., *Structural studies of unitary conductance in maxi-K (slowpoke) channels*. Biophysical Journal, 1994. **66**(2): p. A108-A108.
353. Joiner, W.J., et al., *Formation of intermediate-conductance calcium-activated potassium channels by interaction of Slack and Slo subunits*. Nature Neuroscience, 1998. **1**(6): p. 462-469.
354. Reinhart, P. and I. Levitan, *Kinase and phosphatase activities intimately associated with a reconstituted calcium-dependent potassium channel*. J. Neurosci., 1995. **15**(6): p. 4572-4579.
355. Sansom, S.C., et al., *Regulation of large calcium-activated potassium channels by protein phosphatase 2A*. J. Biol. Chem., 1997. **272**: p. 9902-9906.
356. DiChiara, T.J. and P.H. Reinhart, *Redox Modulation of hslo Ca²⁺-Activated K⁺ Channels*. J. Neurosci., 1997. **17**(13): p. 4942-4955.
357. Tang, X.D., et al., *Oxidative Regulation of Large Conductance Calcium-Activated Potassium Channels*. The Journal of General Physiology, 2001. **117**(3): p. 253-274.
358. Shen, K.Z., *Tetraethylammonium block of Slowpoke calcium-activated potassium channels expressed in Xenopus oocytes: evidence for tetrameric channel formation*. Pflugers Arch., 1994. **426**: p. 440-445.

359. Meera, P., et al., *Large conductance voltage- and calcium-dependent K⁺ channel, a distinct member of voltage-dependent ion channels with seven N-terminal transmembrane segments (S0-S6), an extracellular N terminus, and an intracellular (S9-S10) C terminus*. Proc. Natl Acad. Sci. USA, 1997. **94**: p. 14066-14071.
360. Magleby, K.L., *Gating Mechanism of BK (Slo1) Channels*. The Journal of General Physiology, 2003. **121**(2): p. 81-96.
361. Marty, A., *Ca²⁺-dependent K⁺ channels with large unitary conductance in chromaffin cell membranes*. Nature, 1981. **291**: p. 497-500.
362. Latorre, R. and S. Brauchi, *Large conductance Ca²⁺-activated K⁺ (BK) channel: Activation by Ca²⁺ and voltage*. Biological Research, 2006. **39**(3): p. 385-401.
363. Cui, J., H. Yang, and U.S. Lee, *Molecular mechanisms of BK channel activation*. Cellular and Molecular Life Sciences, 2009. **66**(5): p. 852-875.
364. Latorre, R., F.J. Morera, and C. Zaelzer, *Allosteric interactions and the modular nature of the voltage- and Ca²⁺-activated (BK) channel*. Journal of Physiology-London, 2010. **588**(17): p. 3141-3148.
365. Niu, X. and K.L. Magleby, *Stepwise contribution of each subunit to the cooperative activation of BK channels by Ca²⁺*. Proc. Natl Acad. Sci. USA, 2002. **99**: p. 11441-11446.
366. Liu, G., et al., *Position and role of the BK channel alpha subunit S0 helix inferred from disulfide crosslinking*. Journal of General Physiology, 2008. **131**(6): p. 537-548.

367. Liu, G., et al., *Location of modulatory β subunits in BK potassium channels*. The Journal of General Physiology, 2010. **135**(5): p. 449-459.
368. Koval, O.M., Y. Fan, and B.S. Rothberg, *A role for the SO transmembrane segment in voltage-dependent Gating of BK channels*. Journal of General Physiology, 2007. **129**(3): p. 209-220.
369. Semenova, N.P., et al., *Bimane Fluorescence Scanning Suggests Secondary Structure near the S3-S4 Linker of BK Channels*. Journal of Biological Chemistry, 2009. **284**(16): p. 10684-10693.
370. Cui, J., D.H. Cox, and R.W. Aldrich, *Intrinsic voltage dependence and Ca^{2+} regulation of mslo large conductance Ca-activated K^+ channels*. Journal of General Physiology, 1997. **109**(5): p. 647-673.
371. Ma, Z., X.J. Lou, and F.T. Horrigan, *Role of Charged Residues in the S1–S4 Voltage Sensor of BK Channels*. The Journal of General Physiology, 2006. **127**(3): p. 309-328.
372. Cui, J.M. and R.W. Aldrich, *Allosteric linkage between voltage and Ca^{2+} -dependent activation of BK-type mslo1 K^+ channels*. Biochemistry, 2000. **39**(50): p. 15612-15619.
373. Heginbotham, L., et al., *Mutations in the K^+ channel signature sequence*. Biophys.J., 1994. **66**: p. 1061-1067.
374. Giangiacomo, K.M., et al., *Novel alpha-KTx sites in the BK channel and comparative sequence analysis reveal distinguishing features of the BK and KV channel outer pore*. Cell Biochemistry and Biophysics, 2008. **52**(1): p. 47-58.

375. MacKinnon, R. and C. Miller, *Mechanism of charybdotoxin block of the high-conductance, Ca²⁺- activated K⁺ channel*. J. Gen. Physiol., 1988. **91**(3): p. 335-349.
376. Mackinnon, R., P.H. Reinhart, and M.M. White, *Charybdotoxin block of shaker K⁺ channels suggests that different types of K⁺ channels share common structural features*. Neuron, 1988. **1**(10): p. 997-1001.
377. Yellen, G., et al., *Mutations affecting internal tea blockade identify the probable pore-forming region of a K⁺ channel*. Science, 1991. **251**(4996): p. 939-942.
378. Gross, A., T. Abramson, and R. Mackinnon, *Transfer of the scorpion toxin receptor to an insensitive potassium channel*. Neuron, 1994. **13**(4): p. 961-966.
379. Mackinnon, R. and C. Miller, *Mutant potassium channels with altered binding of charybdotoxin, a pore-blocking peptide inhibitor*. Science, 1989. **245**(4924): p. 1382-1385.
380. Vergara, C., E. Moczydlowski, and R. Latorre, *Conduction, blockade and gating in a Ca²⁺-activated K⁺ channel incorporated into planar lipid bilayers*. Biophysical Journal, 1984. **45**(1): p. 73-76.
381. Miller, C., et al., *Charybdotoxin, a protein inhibitor of single Ca²⁺-activated K⁺ channels from mammalian skeletal muscle*. Nature, 1985. **313**(6000): p. 316-318.
382. Carvacho, I., et al., *Intrinsic electrostatic potential in the BK channel pore: Role in determining single channel conductance and block*. Journal of General Physiology, 2008. **131**(2): p. 147-161.

383. Jiang, Y.X., et al., *Structure of the RCK domain from the E. coli K⁺ channel and demonstration of its presence in the human BK channel*. *Neuron*, 2001. **29**(3): p. 593-601.
384. Wu, Y.K., et al., *Structure of the gating ring from the human large-conductance Ca²⁺-gated K⁺ channel*. *Nature*, 2010. **466**(7304): p. 393-U148.
385. Schreiber, M. and L. Salkoff, *A novel calcium-sensing domain in the BK channel*. *Biophys. J.*, 1997. **73**: p. 1355-1363.
386. Yusifov, T., et al., *The RCK1 domain of the human BKCa channel transduces Ca²⁺ binding into structural rearrangements*. *Journal of General Physiology*, 2010. **136**(2): p. 189-202.
387. Schreiber, M. and L. Salkoff, *A novel calcium-sensing domain in the BK channel*. *Biophys J*, 1997. **73**(3): p. 1355-63.
388. Bian, S., I. Favre, and E. Moczydlowski, *Ca²⁺-binding activity of a COOH-terminal fragment of the Drosophila BK channel involved in Ca²⁺-dependent activation*. *Proc. Natl. Acad. Sci. USA*, 2001. **98**: p. 4776-4781.
389. Bao, L., et al., *Mapping the BKCa channel's "Ca²⁺ bowl": Side-chains essential for Ca²⁺ sensing*. *Journal of General Physiology*, 2004. **123**(5): p. 475-489.
390. Wallner, M., P. Meera, and L. Toro, *Molecular basis of fast inactivation in voltage and Ca²⁺-activated K⁺ channels: A transmembrane β -subunit homolog*. *Proceedings of the National Academy of Sciences of the United States of America*, 1999. **96**(7): p. 4137-4142.

391. Xia, X.-M., et al., *Rectification and rapid activation at low Ca^{2+} of Ca^{2+} -activated, voltage-dependent BK currents: consequences of rapid inactivation by a novel beta subunit*. J. Neurosci., 2000. **20**(13): p. 4890-4903.
392. Meera, P., M. Wallner, and L. Toro, *A neuronal beta subunit (KCNMB4) makes the large conductance, voltage- and Ca^{2+} -activated K^+ channel resistant to charybdotoxin and iberiotoxin*. Proceedings of the National Academy of Sciences of the United States of America, 2000. **97**(10): p. 5562-5567.
393. Wei, A., et al., *Calcium sensitivity of BK-type KCa channels determined by a separable domain*. Neuron, 1994. **13**: p. 671-681.
394. Cox, D.H., J. Cui, and R.W. Aldrich, *Allosteric gating of a large conductance Ca^{2+} -activated K^+ channel*. J. Gen. Physiol., 1997. **110**: p. 257-281.
395. Horrigan, F.T., J. Cui, and R.W. Aldrich, *Allosteric voltage gating of potassium channels I. Mslo ionic currents in the absence of Ca^{2+}* . J. Gen. Physiol., 1999. **114**: p. 277-304.
396. Rothberg, B.S. and K.L. Magleby, *Voltage and Ca^{2+} activation of single large-conductance Ca^{2+} -activated K^+ channels described by a two-tiered allosteric gating mechanism*. J. Gen. Physiol., 2000. **116**: p. 75-99.
397. DiChiara, T.J. and P.H. Reinhart, *Distinct effects of Ca^{2+} and voltage on the activation and deactivation of cloned Ca^{2+} -activated K^+ channels*. J. Physiol., 1995. **489**(Pt_2): p. 403-418.

398. Knaus, H.G., et al., *The beta subunit of the high-conductance Ca²⁺-activated K⁺ channel from smooth muscle*. Biophysical Journal, 1994. **66**(2): p. A108.
399. Torres, Y.P., et al., *A marriage of convenience: beta-subunits and voltage-dependent K⁺ channels*. Journal of Biological Chemistry, 2007. **282**: p. 24485-24489.
400. Lu, R., et al., *MaxiK channel partners: physiological impact*. Journal of Physiology-London, 2006. **570**(1): p. 65-72.
401. Pongs, O. and J.R. Schwarz, *Ancillary Subunits Associated With Voltage-Dependent K⁺ Channels*. Physiological Reviews, 2010. **90**(2): p. 755-796.
402. Oberst, C., et al., *Suppression in transformed avian fibroblasts of a gene (CO6) encoding a membrane protein related to mammalian potassium channel regulatory subunits*. Oncogene, 1997. **14**(9): p. 1109-1116.
403. Chang, C.P., et al., *Differential expression of the alpha and beta subunits of the large-conductance calcium-activated potassium channel: Implication for channel diversity*. Molecular Brain Research, 1997. **45**(1): p. 33-40.
404. Lippiat, J.D., et al., *Properties of BKCa channels formed by bicistronic expression of hSlo alpha and beta 1-4 subunits in HEK293 cells*. Journal of Membrane Biology, 2003. **192**(2): p. 141-148.
405. Li, J., et al., *Coexpression and characterization of the human large-conductance Ca²⁺-activated K⁺ channel alpha + beta 1 subunits in*

- HEK293 cells*. *Molecular and Cellular Biochemistry*, 2009. **331**(1-2): p. 117-126.
406. Orio, P. and R. Latorre, *Differential Effects of $\beta 1$ and $\beta 2$ Subunits on BK Channel Activity*. *The Journal of General Physiology*, 2005. **125**(4): p. 395-411.
407. Wang, B., B.S. Rothberg, and R. Brenner, *Mechanism of beta 4 subunit modulation of BK channels*. *Journal of General Physiology*, 2006. **127**(4): p. 449-465.
408. Petrik, D. and R. Brenner, *Regulation of stretch-activated large conductance, calcium-activated potassium channels by the beta 4 accessory subunit*. *Neuroscience*, 2007. **149**(4): p. 789-803.
409. Hanner, M., et al., *The beta subunit of the high conductance calcium-activated potassium channel - Identification of residues involved in charybdotoxin binding*. *Journal of Biological Chemistry*, 1998. **273**(26): p. 16289-16296.
410. Knaus, H.-G., et al., *Characterization of Tissue-expressed alpha Subunits of the High Conductance Ca²⁺-activated K⁺ Channel*. *J. Biol. Chem.*, 1995. **270**(38): p. 22434-22439.
411. Bentrop, D., et al., *NMR structure of the "ball-and-chain" domain of KCNMB2, the beta(2)-subunit of large conductance Ca²⁺ and voltage-activated potassium channels*. *Journal of Biological Chemistry*, 2001. **276**(45): p. 42116-42121.
412. Wang, Y.-W., et al., *Consequences of the stoichiometry of slo1alpha and auxiliary beta subunits on functional properties of large-*

- conductance Ca²⁺-activated K⁺ channels*. J. Neurosci., 2002. **22**(5): p. 1550-1561.
413. Li, W., et al., *Characterization of voltage- and Ca²⁺-activated K⁺ channels in rat dorsal root ganglion neurons*. Journal of Cellular Physiology, 2007. **212**: p. 348-357.
414. Jones, E.M.C., M. Gray-Keller, and R. Fettiplace, *The role of Ca²⁺-activated K⁺ channel spliced variants in the tonotopic organization of the turtle cochlea*. J. Physiol., 1999. **518**(3): p. 653-665.
415. Jiang, Z., et al., *Human and rodent MaxiK channel beta-subunit genes: Cloning and characterization*. Genomics, 1999. **55**(1): p. 57-67.
416. Vogalis, F., et al., *Cloning and expression of the large-conductance Ca²⁺-activated K⁺ channel from colonic smooth muscle*. American Journal of Physiology-Gastrointestinal and Liver Physiology, 1996. **271**(4): p. G629-G639.
417. Bao, L. and D.H. Cox, *Gating and ionic currents reveal how the BKCa channel's Ca²⁺ sensitivity is enhanced by its beta 1 subunit*. Journal of General Physiology, 2005. **126**(4): p. 393-412.
418. Nelson, M.T., *Relaxation of arterial smooth muscle by calcium sparks*. Science, 1995. **270**: p. 633-637.
419. Koide, M., et al., *Reduced Ca²⁺ spark activity after subarachnoid hemorrhage disables BK channel control of cerebral artery tone*. Journal of Cerebral Blood Flow and Metabolism, 2011. **31**(1): p. 3-16.
420. Grimm, P.R., et al., *Hypertension of Kcnmb1(-/-) is linked to deficient K secretion and aldosteronism*. Proceedings of the National Academy of

- Sciences of the United States of America, 2009. **106**(28): p. 11800-11805.
421. Petkov, G.V., et al., *{beta}1-Subunit of the Ca^{2+} - activated K^+ channel regulates contractile activity of mouse urinary bladder smooth muscle*. J. Physiol., 2001. **537**(2): p. 443-452.
422. Semenov, I., et al., *BK channel beta(1)-subunit regulation of calcium handling and constriction in tracheal smooth muscle*. American Journal of Physiology-Lung Cellular and Molecular Physiology, 2006. **291**(4): p. L802-L810.
423. Toro, B., et al., *KCNMB1 regulates surface expression of a voltage and Ca^{2+} -activated K^+ channel via endocytic trafficking signals*. Neuroscience, 2006. **142**(3): p. 661-669.
424. Lippiat, J.D., N.B. Standen, and N.W. Davies, *A residue in the intracellular vestibule of the pore is critical for gating and permeation in Ca^{2+} -activated K^+ (BKCa) channels*. Journal of Physiology-London, 2000. **529**(1): p. 131-138.
425. De Wet, H., et al., *Modulation of the BK channel by estrogens: examination at single channel level*. Mol. Membr. Bio., 2006. **23**(5): p. 420-9.
426. Allen, M.C., et al., *Membrane impermeant antioestrogens discriminate between ligand- and voltage-gated cation channels in NG108-15 cells*. Biochim. Biophys. Acta, 2000. **1509**(1-2): p. 229-36.
427. Lin, M.T., et al., *Ca^{2+} -activated K^+ channel-associated phosphatase and kinase activities during development*. American Journal of Physiology - Heart and Circulatory Physiology, 2005. **289**(1): p. H414-H425.

428. Zhang, G.P., et al., *Cysteine oxidation and rundown of large-conductance Ca^{2+} -dependent K^+ channels*. Biochemical and Biophysical Research Communications, 2006. **342**(4): p. 1389-1395.
429. Alvarez, O., C. Gonzalez, and R. Latorre, *Counting channels: A tutorial guide on ion channel fluctuation analysis*. Advances in Physiology Education, 2002. **26**(4): p. 327-341.
430. Chung, S.H. and G. Pulford, *Fluctuation analysis of patch-clamp or whole cell recordings containing many single channels*. Journal of Neuroscience Methods, 1993. **50**(3): p. 369-384.
431. Dworetzky, S.I., *Phenotypic alteration of a human BK (hSlo) channel by hSlobeta subunit coexpression: Changes in blocker sensitivity, activation/relaxation and inactivation kinetics, and protein kinase A modulation*. J. Neurosci., 1996. **16**: p. 4543-4550.
432. Candia, S., M.L. Garcia, and R. Latorre, *Mode of action of iberiotoxin, a potent blocker of the large conductance Ca^{2+} -activated K^+ channel*. Biophysical Journal, 1992. **63**(2): p. 583-590.
433. Giangiacomo, K.M., M.L. Garcia, and O.B. McManus, *Mechanism of iberiotoxin block of the large-conductance calcium-activated potassium channel from bovine aortic smooth muscle*. Biochemistry, 1992. **31**(29): p. 6719-6727.
434. Galvez, A., et al., *Purification and characterization of a unique, potent, peptidyl probe for the high conductance calcium-activated potassium channel from venom of the scorpion *Buthus-tamulus**. Journal of Biological Chemistry, 1990. **265**(19): p. 11083-11090.

435. Toth, G.K., et al., *Synthesis of 2 peptide scorpion toxins and their use to investigate the aortic tissue regulation*. *Peptides*, 1995. **16**(7): p. 1167-1172.
436. Alvarez, O., C. Gonzalez, and R. Latorre, *Counting channels: a tutorial guide on ion channel fluctuation analysis*. *Advances in physiology education*, 2002. **26**(1-4): p. 327-41.
437. Hu, L., et al., *Participation of the S4 voltage sensor in the Mg²⁺-dependent activation of large conductance (BK) K⁺ channels*. *Proceedings of the National Academy of Sciences of the United States of America*, 2003. **100**(18): p. 10488-10493.
438. Horrigan, F.T. and Z.M. Ma, *Mg²⁺ enhances voltage sensor/gate coupling in BK channels*. *Journal of General Physiology*, 2008. **131**(1): p. 13-32.
439. Shi, J. and J. Cui, *Intracellular Mg²⁺ Enhances the Function of Bk-Type Ca²⁺-Activated K⁺ Channels*. *The Journal of General Physiology*, 2001. **118**(5): p. 589-606.
440. Tian, L., et al., *Palmitoylation gates phosphorylation-dependent regulation of BK potassium channels*. *PNAS*, 2008. **105**(52): p. 21006-21011.
441. Zhou, X.-B., et al., *Dual role of protein kinase C on BK channel regulation*. *Proceedings of the National Academy of Sciences*, 2010. **107**(17): p. 8005-8010.
442. Weiger, T. and A. Hermann, *Polyamines block Ca(2+)-activated K⁺ channels in pituitary tumor cells (GH3)*. *Journal of Membrane Biology*, 1994. **140**(2): p. 133-142.

443. Zhang, Y., et al., *Ring of Negative Charge in BK Channels Facilitates Block by Intracellular Mg^{2+} and Polyamines through Electrostatics*. The Journal of General Physiology, 2006. **128**(2): p. 185-202.
444. Li, M., et al., *Augmented bladder urothelial polyamine signaling and block of BK channel in the pathophysiology of overactive bladder syndrome*. American Journal of Physiology - Cell Physiology, 2009. **297**(6): p. C1445-C1451.
445. Tang, X.D., et al., *Reactive oxygen species impair Slo1 BK channel function by altering cysteine-mediated calcium sensing*. Nature Structural & Molecular Biology, 2004. **11**(2): p. 171-178.
446. D'Ambrosio, R., *Perforated Patch Clamp Technique*, in *Patch Clamping Analysis ; Advanced Techniques*, W. WALZ, Editor. 2007, Humana Press: Totowa, USA.
447. Duchatellegourdon, I., A.A. Lagrutta, and H.C. Hartzell, *Effects of Mg^{2+} on basal and beta-adrenergic-stimulated delayed rectifier potassium current in frog atrial myocytes*. Journal of Physiology-London, 1991. **435**: p. 333-347.
448. Duchatellegourdon, I., H.C. Hartzell, and A.A. Lagrutta, *Modulation of the delayed rectifier potassium current in frog cardiomyocytes by beta-adrenergic agonists and magnesium*. Journal of Physiology-London, 1989. **415**: p. 251-274.
449. Stansfield, A.M.C., ed. *Membrane currents of peripheral neurones in short-term culture*. 1st ed. Electrophysiology - A practical approach, ed. R.D.a.H.B. D. 1993, IRL: New York. 293.

450. Beech, D.J., et al., *Intracellular Ca²⁺ buffers disrupt muscarinic suppression of Ca²⁺ current and M-current in rat sympathetic neurons*. Proceedings of the National Academy of Sciences of the United States of America, 1991. **88**(2): p. 652-656.
451. Drouin, H. and A. Hermann, *Intracellular action of spermine on neuronal Ca²⁺ and K⁺ currents*. European Journal of Neuroscience, 1994. **6**(3): p. 412-419.
452. Barrett, J.N., K.L. Magleby, and B.S. Pallotta, *Properties of single calcium-activated potassium channels in cultured rat muscle*. J. Physiol., 1982. **331**(1): p. 211-230.
453. Pallotta, B.S., K.L. Magleby, and J.N. Barrett, *Single channel recordings of Ca²⁺-activated K⁺ currents in rat muscle cell culture*. Nature, 1981. **293**: p. 471-474.
454. McManus, O.B., *Functional role of the beta subunit of high conductance calcium-activated potassium channels*. Neuron, 1995. **14**: p. 645-650.
455. Wallner, M., *Characterization of and modulation by a beta-subunit of a human maxi KCa channel cloned from myometrium*. Receptors Channels, 1995. **3**: p. 185-199.
456. Blatz, A.L. and K.L. Magleby, *Ion conductance and selectivity of single calcium-activated potassium channels in cultured rat muscle*. Journal of General Physiology, 1984. **84**(1): p. 1-23.
457. Brelidze, T.I., X. Niu, and K.L. Magleby, *A ring of eight conserved negatively charged amino acids doubles the conductance of BK channels and prevents inward rectification*. Proceedings of the National

- Academy of Sciences of the United States of America, 2003. **100**(15): p. 9017-9022.
458. Prokai, L., et al., *Mechanistic insights into the direct antioxidant effects of estrogens*. Drug Development Research, 2005. **66**(2): p. 118-125.
459. Prokai-Tatrai, K., et al., *Mechanistic investigations on the antioxidant action of a neuroprotective estrogen derivative*. Steroids, 2008. **73**(3): p. 280-288.
460. Ohe, T., M. Hirobe, and T. Mashino, *Novel metabolic pathway of estrone and 17 beta-estradiol catalyzed by cytochrome P-450*. Drug Metabolism and Disposition, 2000. **28**(2): p. 110-112.
461. Prokai, L., et al., *Quinol-based metabolic cycle for estrogens in rat liver microsomes*. Drug Metabolism and Disposition, 2003. **31**(6): p. 701-704.
462. Muddana, S.S. and B.R. Peterson, *Facile synthesis of CIDs: Biotinylated estrone Oximes efficiently heterodimerize estrogen receptor and streptavidin proteins in yeast three hybrid systems*. Organic Letters, 2004. **6**(9): p. 1409-1412.
463. Peters, R.H., et al., *17-desoxy estrogen analogs*. Journal of Medicinal Chemistry, 1989. **32**(7): p. 1642-1652.
464. Hejaz, H.A.M., et al., *Synthesis and Biological Activity of the Superestrogen (E)-17-Oximino-3-O-sulfamoyl-1,3,5(10)-estratriene: X-ray Crystal Structure of (E)-17-Oximino-3-hydroxy-1,3,5(10)-estratriene*. Journal of Medicinal Chemistry, 1999. **42**(16): p. 3188-3192.

465. Caro, A.A., A.I. Cederbaum, and D.A. Stoyanovsky, *Oxidation of the Ketoxime Acetoxime to Nitric Oxide by Oxygen Radical-Generating Systems*. Nitric Oxide, 2001. **5**(4): p. 413-424.
466. Huang, Y., *Hydroxylamine-induced relaxation inhibited by K⁺ channel blockers in rat aortic rings*. European Journal of Pharmacology, 1998. **349**(1): p. 53-60.
467. Demaster, E.G., et al., *Hydroxylamine is a vasorelaxant and a possible intermediate in the oxidative conversion of L-arginine to nitric oxide*. Biochemical and Biophysical Research Communications, 1989. **163**(1): p. 527-533.
468. Kruszyna, H., R. Kruszyna, and R.P. Smith, *Nitroprusside increases cyclic guanylate monophosphate concentrations during relaxation of rabbit aortic strips and both effects are antagonized by cyanidel*. Anesthesiology, 1982. **57**(4): p. 303-308.
469. Thomas, P., et al., *Identity of an estrogen membrane receptor coupled to a G protein in human breast cancer cells*. Endocrinology, 2005. **146**(2): p. 624-632.
470. Bagatolli, L.A., et al., *An outlook on organization of lipids in membranes: Searching for a realistic connection with the organization of biological membranes*. Progress in Lipid Research, 2010. **49**(4): p. 378-389.
471. Kramar, P., D. Miklavcic, and A.M. Lebar, *Determination of the lipid bilayer breakdown voltage by means of linear rising signal*. Bioelectrochemistry, 2007. **70**(1): p. 23-27.

472. Singer, S.J. and G.L. Nicolson, *Fluid mosaic model of structure of cell membranes*. Science, 1972. **175**(4023): p. 720.
473. Engelman, D.M., *Membranes are more mosaic than fluid*. Nature, 2005. **438**(7068): p. 578-580.
474. Ottova, A. and H.T. Tien, *The Lipid Bilayer Principle: A Historic Perspective and Some Highlights*, in *Advances in Planar Lipid Bilayers and Liposomes*, H.T. Tien and A. Ottova-Leitmannova, Editors. 2005, Academic Press. p. 1-76.
475. Tien, H.T. and A.L. Ottova, *The lipid bilayer concept and its experimental realization: from soap bubbles, kitchen sink, to bilayer lipid membranes*. Journal of Membrane Science, 2001. **189**(1): p. 83-117.
476. Fantini, J., et al., *Lipid rafts: structure, function and role in HIV, Alzheimer's and prion diseases*. Expert Reviews in Molecular Medicine, 2002. **4**(27): p. 1-22.
477. Simons, K. and E. Ikonen, *How cells handle cholesterol*. Science, 2000. **290**(5497): p.1721-6.
478. Yeagle, P., *Lipid regulation of cell membrane structure and function*. The FASEB Journal, 1989. **3**(7): p. 1833-1842.
479. Hao, M., S. Mukherjee, and F.R. Maxfield, *Cholesterol depletion induces large scale domain segregation in living cell membranes*. Proceedings of the National Academy of Sciences, 2001. **98**(23): p. 13072-13077.
480. Mondal, M., et al., *Sterols Are Mainly in the Cytoplasmic Leaflet of the Plasma Membrane and the Endocytic Recycling Compartment in CHO Cells*. Molecular Biology of the Cell, 2009. **20**(2): p. 581-588.

481. Brown, D.A. and E. London, *Structure and function of sphingolipid- and cholesterol-rich membrane rafts*. Journal of Biological Chemistry, 2000. **275**(23): p. 17221-17224.
482. Mukherjee, S. and A. Chattopadhyay, *Monitoring cholesterol organization in membranes at low concentrations utilizing the wavelength-selective fluorescence approach*. Chemistry and Physics of Lipids, 2005. **134**(1): p. 79-84.
483. Eggeling, C., et al., *Direct observation of the nanoscale dynamics of membrane lipids in a living cell*. Nature, 2009. **457**(7233): p. 1159-62.
484. Wenger, J., et al., *Diffusion Analysis within Single Nanometric Apertures Reveals the Ultrafine Cell Membrane Organization*. Biophysical Journal, 2007. **92**(3): p. 913-919.
485. Gaus, K., et al., *Visualizing lipid structure and raft domains in living cells with two-photon microscopy*. Proceedings of the National Academy of Sciences of the United States of America, 2003. **100**(26): p. 15554-15559.
486. Mueller, P., et al., *Methods for the formation of single bimolecular lipid membranes in aqueous solution*. The Journal of Physical Chemistry, 1963. **67**(2): p. 534-535.
487. Mueller, P., et al., *Reconstitution of Excitable Cell Membrane Structure in Vitro*. Circulation, 1962. **26**(5): p. 1167-1171.
488. Montal, M. and P. Mueller, *Formation of bimolecular membranes from lipid monolayers and a study of their electrical properties*. Proceedings of the National Academy of Sciences of the United States of America, 1972. **69**(12): p. 3561-3566.

489. Labarca, P. and R. Latorre, *Insertion of ion channels into planar lipid bilayers by vesicle fusion*, in *Methods in Enzymology*, R. Bernardo, Editor. 1992, Academic Press. p. 447-463.
490. White, S.H., et al., *Formation of planar bilayer membranes from lipid monolayers - Critique*. *Biophysical Journal*, 1976. **16**(5): p. 481-489.
491. Niles, W.D., R.A. Levis, and F.S. Cohen, *Planar bilayer membranes made from phospholipid monolayers form by a thinning process*. *Biophysical Journal*, 1988. **53**(3): p. 327-335.
492. Williams, A.J., *Chapter 5 An introduction to the methods available for ion channel reconstitution (Microelectrode techniques : the Plymouth Workshop handbook)*. 2nd ed., D. Ogden. 1994: Cambridge : Company of Biologists. p. 448.
493. Frenkel, C. and B.W. Urban, *A Molecular Target Site for Propofol: Voltage-Clamp Studies on Human CNS Sodium Channels in Bilayers*. *Anesthesiology*, 1989. **71**(3A): p. A590.
494. Bean, R.C., et al., *Discrete Conductance Fluctuations in Lipid Bilayer Protein Membranes*. *The Journal of General Physiology*, 1969. **53**(6): p. 741-757.
495. Sarges, R. and B. Witkop, *Gramicidin A .V. Structure of valine-and isoleucine-gramicidin A*. *Journal of the American Chemical Society*, 1965. **87**(9): p. 2011..
496. Hladky, S.B. and D.A. Haydon, *Discreteness of conductance change in bimolecular lipid membranes in presence of certain antibiotics*. *Nature*, 1970. **225**(5231): p. 451..

497. Hladky, S.B. and D.A. Haydon, *Ion Movements in Gramicidin Channels*, in *Current Topics in Membranes and Transport*, B. Felix, Editor. 1984, Academic Press. p. 327.
498. McLaughlin, S. and M. Eisenberg, *Antibiotics and membrane biology*. Annual Review of Biophysics and Bioengineering, 1975. **4**: p. 335-366.
499. Hardy, S.P., et al., *Clostridium perfringens type A enterotoxin forms mepacrine-sensitive pores in pure phospholipid bilayers in the absence of putative receptor proteins*. Biochimica Et Biophysica Acta-Biomembranes, 2001. **1515**(1): p. 38-43.
500. McClain, M.S., et al., *Essential Role of a GXXXG Motif for Membrane Channel Formation by Helicobacter pylori Vacuolating Toxin*. Journal of Biological Chemistry, 2003. **278**(14): p. 12101-12108.
501. Dalziel, J.E., et al., *Expression of human BK ion channels in Sf9 cells, their purification using metal affinity chromatography, and functional reconstitution into planar lipid bilayers*. Journal of Chromatography B, 2007. **857**(2): p. 315-321.
502. Giangiacomo, K.M., et al., *Functional reconstitution of the large-conductance, calcium-activated potassium channel purified from bovine aortic smooth-muscle*. Biochemistry, 1995. **34**(48): p. 15849-15862.
503. Kapicka, C.L., et al., *Comparison of large-conductance Ca²⁺-activated K⁺ channels in artificial bilayer and patch-clamp experiments*. American Journal of Physiology, 1994. **266**(3): p. C601-C610.
504. Pérez, G., et al., *Reconstitution of expressed KCa channels from Xenopus oocytes to lipid bilayers*. Biophysical Journal, 1994. **66**(4): p. 1022-1027.

505. Alvarez, O., D. Benos, and R. Latorre, *The study of ion channels in planar lipid bilayer-membranes*. Journal of Electrophysiological Techniques, 1985. **12**(3): p. 159-177.
506. Labarca, P. and R. Latorre, *Insertion of ion channels into planar lipid bilayers by vesicle fusion*, in *Methods in Enzymology; Ion channels*, B. Rudy and L.E. Iverson, Editors. 1992, Academic Press, Inc., 1250 Sixth Ave., San Diego, California 92101, USA; Academic Press Ltd., 14 Belgrave Square, 24-28 Oval Road, London NW1 70X, England, UK. p. 447-463.
507. Cantor, R.S., *Lipid composition and the lateral pressure profile in bilayers*. Biophysical Journal, 1999. **76**(5): p. 2625-2639.
508. Sharom, F.J. and P.D.W. Eckford, *Reconstitution of membrane transporters*. Methods in molecular biology (Clifton, N.J.), 2003. **227**: p. 129-54.
509. Yuan, C.B., et al., *Bilayer thickness modulates the conductance of the BK channel in model membranes*. Biophysical Journal, 2004. **86**(6): p. 3620-3633.
510. Yuan, C.B., et al., *Regulation of the gating of BKCa channel by lipid bilayer thickness*. Journal of Biological Chemistry, 2007. **282**(10): p. 7276-7286.
511. Farre, C., et al., *Automated ion channel screening: patch clamping made easy*. Expert Opinion on Therapeutic Targets, 2007. **11**(4): p. 557-565.

512. Brueggemann, A., et al., *Planar Patch Clamp: Advances in Electrophysiology*, in *Methods in Molecular Biology*, J.D. Lippiat, Editor. 2008. p. 165-176.
513. Stoelzle, S., et al., *Automated patch clamp for ion channel screening*. *Journal of Physiological Sciences*, 2009. **59**: p. 402.
514. Toro, L., J. Ramos-Franco, and E. Stefani, *GTP-dependent regulation of myometrial K_{Ca} channels incorporated into lipid bilayers*. *The Journal of General Physiology*, 1990. **96**(2): p. 373-394.
515. Coiret, G., et al., *The antiestrogen tamoxifen activates BK channels and stimulates proliferation of MCF-7 breast cancer cells*. *Molecular Pharmacology*, 2007. **71**(3): p. 843-851.
516. Coiret, G., et al., *17-beta-estradiol activates maxi-K channels through a non-genomic pathway in human breast cancer cells*. *FEBS Letters*, 2005. **579**(14): p. 2995-3000.
517. De Wet, H., J.D. Lippiat, and M. Allen, *Analysing Steroid Modulation of BK_{Ca} Channels Reconstituted into Planar Lipid Bilayers*. *Methods in Molecular Biology*, ed. J.D. Lippiat. Vol. 491. 2009. p. 177-186.
518. Duncan, R.K., *Tamoxifen alters gating of the BK [alpha] subunit and mediates enhanced interactions with the avian [beta] subunit*. *Biochemical Pharmacology*, 2005. **70**(1): p. 47-58.
519. Crowley, J.J., S.N. Treistman, and A.M. Dopico, *Cholesterol antagonizes ethanol potentiation of human brain BK_{Ca} channels reconstituted into phospholipid bilayers*. *Molecular Pharmacology*, 2003. **64**(2): p. 365-372.

520. Bukiya, A.N., et al., *Specificity of cholesterol and analogs to modulate BK channels points to direct sterol-channel protein interactions*. Journal of General Physiology, 2011. **137**(1): p. 93-110.
521. Dopico, A.M., A.N. Bukiya, and A.K. Singh, *Large conductance, calcium- and voltage-gated potassium (BK) channels: Regulation by cholesterol*. Pharmacology & Therapeutics, 2012. **135**(2): p. 133-150.
522. Naderali, E.K., et al., *Comparable vasorelaxant effects of 17 alpha- and 17 beta-oestradiol on rat mesenteric resistance arteries: an action independent of the oestrogen receptor*. Clinical Science, 1999. **97**(6): p. 649-655.
523. Rubanyi, G.M., K. Kauser, and A. Johns, *Role of estrogen receptors in the vascular system*. Vascular Pharmacology, 2002. **38**(2): p. 81-88.
524. MohazzabH, K.M., et al., *Potential role of a membrane-bound NADH oxidoreductase in nitric oxide release and arterial relaxation to nitroprusside*. Circulation Research, 1999. **84**(2): p. 220-228.
525. Moczydlowski, E.G., *BK Channel News*. The Journal of General Physiology, 2004. **123**(5): p. 471-473.
526. Schmidt, K., et al., *Comparison of neuronal and endothelial isoforms of nitric oxide synthase in stably transfected HEK 293 cells*. American Journal of Physiology-Heart and Circulatory Physiology, 2001. **281**(5): p. H2053-H2061.
527. Fang, J. and R.B. Silverman, *A cellular model for screening neuronal nitric oxide synthase inhibitors*. Analytical Biochemistry, 2009. **390**(1): p. 74-78.

528. Epand, R.M., *Cholesterol and the interaction of proteins with membrane domains*. Progress in Lipid Research, 2006. **45**(4): p. 279-294.
529. Levitan, I., et al., *Cholesterol and Ion Channels*, in *Cholesterol Binding and Cholesterol Transport Proteins: Structure and Function in Health and Disease*, J.R. Harris, Editor. 2010. p. 509-549.
530. Rojas, P., et al., *Molecular basis of BK modulation by beta subunits and channel activation by estrogens*. Biophysical Journal, 2003. **84**(2): p. 541A.
531. King, J.T., et al., *$\beta 2$ and $\beta 4$ Subunits of BK Channels Confer Differential Sensitivity to Acute Modulation by Steroid Hormones*. Journal of Neurophysiology, 2006. **95**(5): p. 2878-2888.
532. Latorre, R. and G. Contreras, *Keeping you healthy: BK channel activation by omega-3 fatty acids*. The Journal of General Physiology, 2013.
533. Zakoji, H., et al., *The expression and role of large conductance, voltage- and Ca^{2+} - activated K^+ (BK) channels in the urinary bladder: The alteration of subunit expression profile in association with bladder outlet obstruction, and the affect of BK channel on the afferent ex*. Journal of Urology, 2007. **177**(4): p. 325-325.
534. Meredith, A.L., et al., *Overactive bladder and incontinence in the absence of the BK large conductance Ca^{2+} - activated K^+ channel*. Journal of Biological Chemistry, 2004. **279**(35): p. 36746-36752.
535. WorldPharma, *Posters*. Basic & Clinical Pharmacology & Toxicology, 2010. **107**: p. 162-692.

APPENDICES

1 to 3

APPENDIX 1

This investigation forms the basis of a peer-reviewed full paper, “*Smooth muscle relaxation and activation of the large conductance Ca^{2+} – activated K^+ (BKCa) channel by novel oestrogens*”, published in the *British Journal of Pharmacology* (BJP) in July 2013 [235]. The paper was also recently cited in a commentary published in the *Journal of General Physiology* (JGP) by Latorre *et al*; [532]

APPENDIX 2

The following abstracts relevant to this thesis have been peer-reviewed and published as follows:-

1) The Effect of Novel Xenooestrogens on The Maxi-K Potassium Channel

Jacqueline Maher¹, Natasha Tisovszky¹, Christy Hunter¹, Heidi de Wet², Jonathan Lippiat³, Marcus Allen¹

¹University of Brighton, Sussex, United Kingdom, ²University of Oxford, Oxford, United Kingdom, ³University of Leeds, Yorkshire, United Kingdom

Peer-reviewed and published by the *British Pharmacological Society* Winter Meeting Brighton, UK December 2007

2) Non-genomic effects of oestrogens and xenoestrogens on voltage gated ion channels

Maher J¹., Allen M¹., & Hunter A¹.

¹Univ of Brighton, Brighton, UK
Publication ref.: *FENS Abstr.*, vol.4, 078.2, 2008

Peer-reviewed and published by the *Federation of European Neurosciences (FENS) Forum* 2008 Geneva, SWITZERLAND July 2008

3) Non-genomic effects of oestrogen derivatives on BK channels

Jacqueline Maher¹, A Hunter¹, J Mabley¹, M Allen¹

¹University of Brighton, School of Pharmacy & Biomolecular Sciences, Brighton, UK

Peer-reviewed and published by the WorldPharma 16th World Congress of Basic Clinical Pharmacology (Copenhagen) DENMARK July 2010

APPENDIX 3

The following poster presentations, relevant to this thesis, have been peer-reviewed and presented by the candidate at the following international and national conferences as follows:-

1) The Effect of Novel Xenooestrogens on The Maxi-K Potassium Channel

Jacqueline Maher¹, Natasha Tisovszky¹, Christy Hunter¹, Heidi de Wet², Jonathan Lippiat³, Marcus Allen¹

¹University of Brighton, Sussex, United Kingdom, ²University of Oxford, Oxford, United Kingdom, ³University of Leeds, Yorkshire, United Kingdom

Presented at and peer-reviewed by the *British Pharmacological Society Winter Meeting Brighton, UK December 2007*

2) Non-genomic effects of oestrogens and xenoestrogens on voltage gated ion channels

Maher J¹., Allen M¹., & Hunter A¹.

¹Univ of Brighton, Brighton, UK

Presented at and peer-reviewed by the *Federation of European Neurosciences (FENS) Forum 2008 Geneva, SWITZERLAND July 2008*

3) Non-genomic effects of oestrogen derivatives on BK channels

Jacqueline Maher¹, A Hunter¹, J Mabley¹, M Allen¹

¹University of Brighton, School of Pharmacy & Biomolecular Sciences, Brighton, UK

P12 - ION CHANNELOPATHIES: NEW WINDOWS ON COMPLEX DISEASE AND THERAPY

Presented at and peer-reviewed by the *WorldPharma 16th World Congress of Basic Clinical Pharmacology 2010 Copenhagen DENMARK July 2010 [535]*.